Deposit & Copying of Dissertation Declaration

UNIVERSITY OF CAMBRIDGE

Board of Graduate Studies

Please note that you will also need to bind a copy of this Declaration into your final, hardbound copy of thesis - this has to be the very first page of the hardbound thesis.

1 Surname (Family Name)	Forenames(s)	Title
Anžiček	Nika	Miss

2 Title of Dissertation as approved by the Degree Committee

Studies Towards a Second-Generation Synthesis of the Aplyronines

In accordance with the University Regulations in *Statutes and Ordinances* for the PhD, MSc and MLitt Degrees, I agree to deposit one print copy of my dissertation entitled above and one print copy of the summary with the Secretary of the Board of Graduate Studies who shall deposit the dissertation and summary in the University Library under the following terms and conditions:

1. Dissertation Author Declaration

I am the author of this dissertation and hereby give the University the right to make my dissertation available in print form as described in 2. below.

My dissertation is my original work and a product of my own research endeavours and includes nothing which is the outcome of work done in collaboration with others except as declared in the Preface and specified in the text. I hereby assert my moral right to be identified as the author of the dissertation.

The deposit and dissemination of my dissertation by the University does not constitute a breach of any other agreement, publishing or otherwise, including any confidentiality or publication restriction provisions in sponsorship or collaboration agreements governing my research or work at the University or elsewhere.

2. Access to Dissertation

I understand that one print copy of my dissertation will be deposited in the University Library for archival and preservation purposes, and that, unless upon my application restricted access to my dissertation for a specified period of time has been granted by the Board of Graduate Studies prior to this deposit, the dissertation will be made available by the University Library for consultation by readers in accordance with University Library Regulations and copies of my dissertation may be provided to readers in accordance with applicable legislation.

3 Signature	Date
	19 Sep 2017

Corresponding Regulation

Before being admitted to a degree, a student shall deposit with the Secretary of the Board one copy of his or her hard-bound dissertation and one copy of the summary (bearing student's name and thesis title), both the dissertation and the summary in a form approved by the Board. The Secretary shall deposit the copy of the dissertation together with the copy of the summary in the University Library where, subject to restricted access to the dissertation for a specified period of time having been granted by the Board of Graduate Studies, they shall be made available for consultation by readers in accordance with University Library Regulations and copies of the dissertation provided to readers in accordance with applicable legislation.

Studies Towards a Second-Generation Synthesis of the Aplyronines

A dissertation submitted for the degree of Doctor of Philosophy

Nika Anžiček

Downing College

August 2017

Declaration

This dissertation is the result of my own work and includes nothing which is the outcome of work done in collaboration except where specified in the text. It is not substantially the same as any that I have submitted or will submit for such degree or other qualification at the University of Cambridge or any other institution. It does not exceed the 60,000 word limit (excluding experimental data) as prescribed by the Board of Graduate Studies.

Nika Anžiček

August 2017

Acknowledgements

My journey through the past four years of research was anything but steady progress. I am grateful to everybody who contributed towards my project and my time in Cambridge as a whole, making the steep PhD learning curve a rewarding experience I will fondly look back upon.

Above all, I thank Prof. Ian Paterson for the opportunity to pursue chemistry to such a high level with valuable guidance yet the freedom to explore my own ideas. I appreciate his continuous support, trust and encouragement, not only with regards to research but also professional development.

Lab 122 has been a very fun and stimulating place to work and I thank everyone who has lent me reagents, ran NMR spectra or looked after my experiments on occasion. Previous and current members of team aplyronine (Mike Woodrow, Cam Cowden, Simon Blakey, Lydia Lee, Steve Atkinson, Sarah Fink, Simon Williams, Mike Housden, Talia Pettigrew and Rachel Porter) had laid excellent foundations of the project and generously shared stocks of material with me. A special thanks goes to Simon Williams who was an outstanding role model, patiently answered countless questions and made time for discussions which taught me a great deal about organic chemistry. I am also grateful to Phil Murray for doing the chiral GC analyses for me.

Melvyn Orriss, Matt Pond, Nic Davies and Naomi Hobbs have provided invaluable technical support.

I am grateful to Bing Yuan Han, Callum MacGregor and Simon Williams for their critical proofreading of this document on short notice as well as Matt Grayson and Nelson Lam for their input.

I must credit the Public Scholarship, Development, Disability and Maintenance Fund of the Republic of Slovenia for their financial support since my undergraduate studies.

To my family: Thank for you the endless help, love and support you have provided during my time abroad. I promise I am now very proficient at drawing hexagons.

On a personal note I thank the members of the Cambridge University Olympic Gymnastics Club who I have crossed paths with and who helped create many of my favourite memories of Cambridge.

Finally, I would like to acknowledge Mateja Strnad Zorec who recognised my eagerness for chemistry and perseverence. Without her encouragment to always reach further I would not have ended up studying at Cambridge.

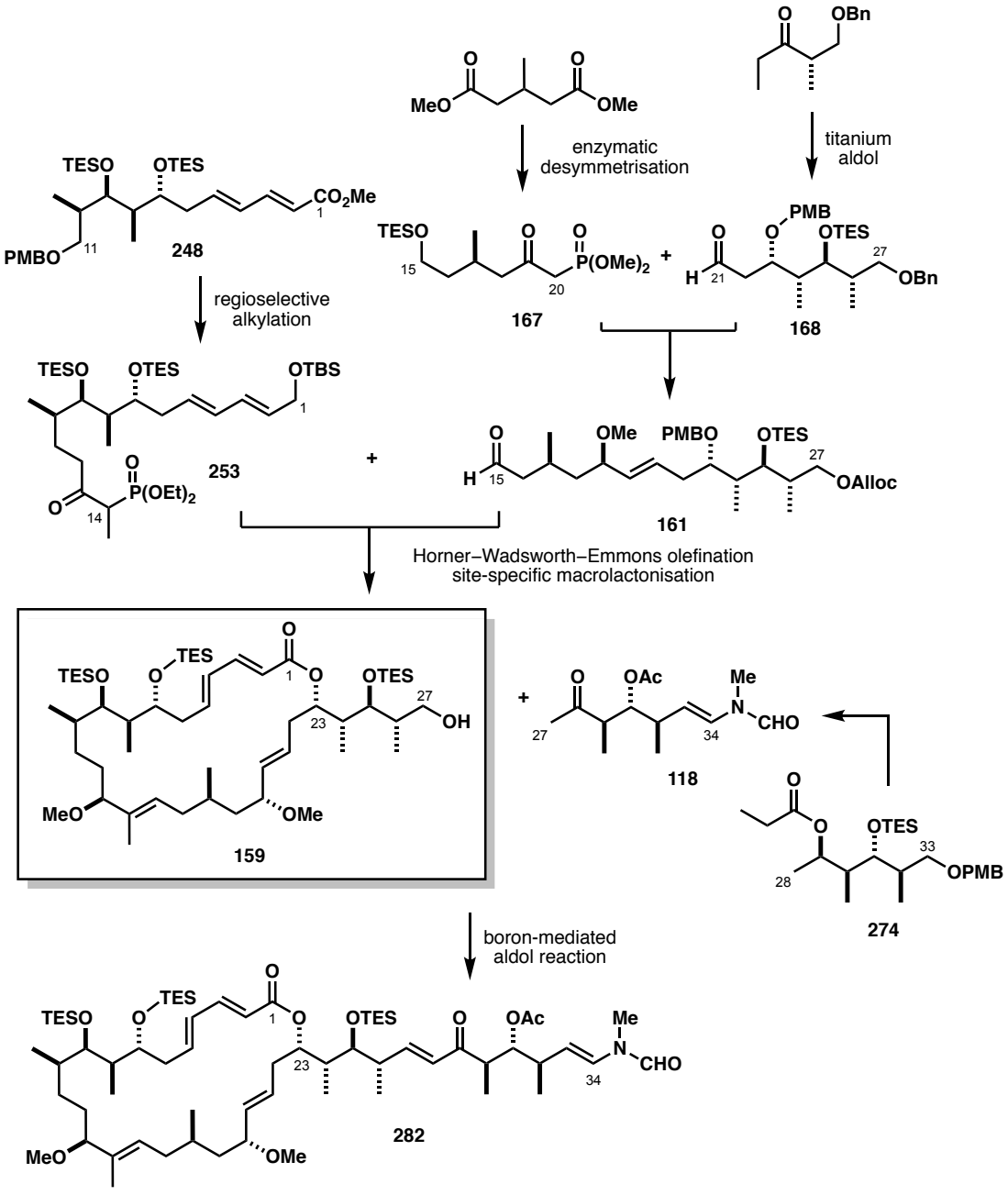
enzymatic desymmetrisation
titanium aldol
regioselective alkylation
Horner–Wadsworth–Emmons olefination
site-specific macrolactonisation
boron-mediated aldol reaction
248
167
168
253
161
159
118
274
282

Studies Towards a Second-Generation Synthesis of the Aplyronines

Nika Anžiček

Summary

The aplyronines are a family of 24-membered macrolides of polyketide origin, isolated from the Japanese sea hare *Aplysia kurodai*. They exhibit an exceptional biological activity profile, acting through an actin and tubulin dual-targeting mechanism, with subnanomolar growth inhibitory potency against a diverse range of cancer cell lines. These characteristics render the aplyronines ideal payloads for antibody-drug conjugates but their prohibitively low natural abundance calls for an efficient total synthesis to overcome the supply issue. This dissertation describes the efforts towards developing a second-generation Paterson synthesis of the macrocyclic core of the aplyronines, focused on improving the scalability and selectivity of key transformations.

Chapter 1 details the isolation, biological background and previous synthetic efforts towards the aplyronines to illustrate their therapeutic potential and the challenges associated with material sourcing by chemical synthesis. Chapter 2 presents the existing body of work on the aplyronine project within the Paterson group, highlighting the lessons learned over the past two decades and shortcomings to be addressed.

Chapter 3 discusses a revised protecting group strategy towards the C_1–C_{27} macrocyclic alcohol **159** with fewer manipulation steps. A refined reaction sequence featuring titanium aldol methodology and an enzymatic desymmetrisation process delivered multigram stocks of the C_{15}–C_{27} aldehyde **161** upon scale-up, testifying to the robustness of the devised route. Synthesis of the C_1–C_{14} northern fragment **253** closely followed the existing boron aldol approach with optimisation of the C_{11}–C_{12} alkylation step, geared towards enhancing the regioselectivity.

Chapter 4 describes the coupling of the two major fragments using an Horner–Wadsworth–Emmons reaction to assemble the C_1–C_{27} backbone of the cyclic aplyronine core and suitably adjusted endgame steps to enable a one-step oxidative unmasking of the macrolactonisation sites. The first-generation intermediate **159** was accessed *via* site-specific Yamaguchi esterification and orthogonal deprotection of the C_{27} allyl carbonate. Discussion in Chapter 5 includes the appendage of the C_{28}–C_{34} side chain **118**, prepared by the known sequence, and suggestions for the future direction of the second-generation route with the outlook of linker appendage for the purposes of antibody-drug conjugate development.

Contents

Nomenclature

Double Bond Stereochemistry

In accordance to the established convention, the two metal enolates **A** and **B** are referred to as (*E*)- and (*Z*)-enolates, respectively (**Figure 1**). The metal-oxygen substituent has a higher priority than the R^1 substituent designated in all cases.

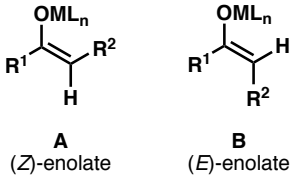

Figure 1

Syn- and *Anti*-Diastereomers

Assignments of relative configuration of vicinal stereocentres as *syn* or *anti* follows the convention introducted by Masamune.[1] A *syn* relationship is defined by the two substituents (R^1 and R^2) both pointing into or out of a plane with the main chain drawn in a zig-zag conformation as shown in **Figure 2**. An *anti* relationship refers to the substituents on opposite sides of the plane. Hence, diastereomers **C** and **D** are regarded as *syn* and *anti*, respectively.

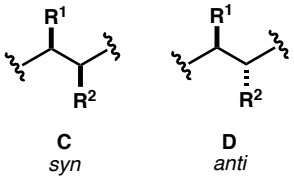

Figure 2

Aldol Adduct Stereochemistry

Products of aldol reactions in which the stereochemical outcome is governed by the α-chiral centre of the ketone are referred to as shown in **Figure 3**. The pre-existing ketone stereocentre is assigned the label "1" as a point of reference for the relative configuration between substituents.

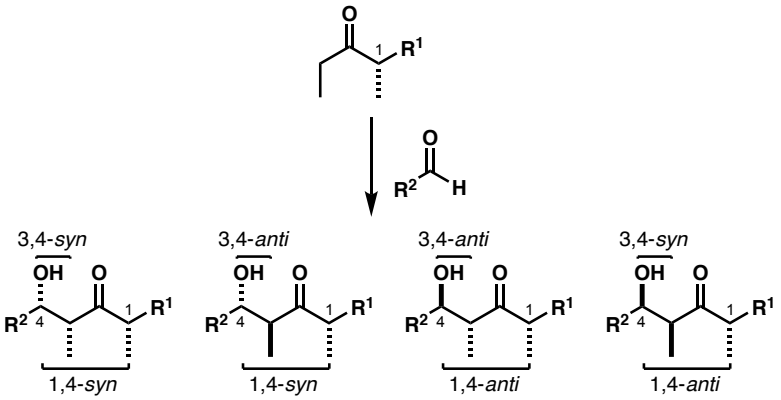

Figure 3

Compound and Atom Numbering

The naming and numbering of compounds in this dissertation is done in accordance to the priorities set out by IUPAC. The numbering system adopted for aplyronine intermediates follows that proposed by Yamada and co-workers in their original publication on aplyronine isolation and characterisation.[2] It is used in assignments of ^{1}H NMR data and follows that shown in **Figure 4**.

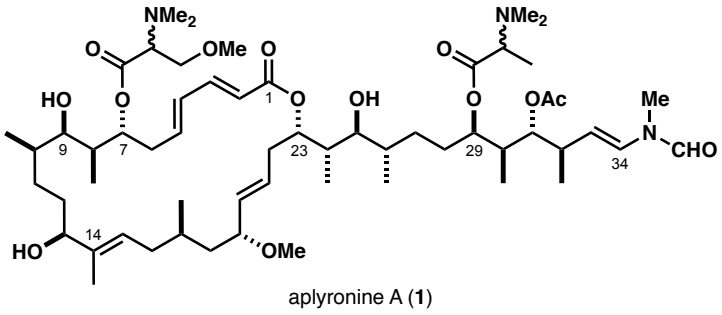

Figure 4 Atom numbering for the aplyronines

Abbreviations

Ac	Acetyl
ADC	Antibody-drug conjugate
ADP	Adenosine diphosphate
Alloc	Allyloxycarbonyl
ApA, ApB etc.	Aplyronine A, B etc.
app	Apparent
Ar	Generic aromatic group
ATP	Adenosine triphosphate
aq.	Aqueous
BBN	9-Borabicyclo[3.3.1]nonyl
Bn	Benzyl
BOM	Benzyloxymethyl acetal
br	Broad
BRSM	Based on recovered starting material
^{n}Bu	*n*-Butyl
^{t}Bu	*tert*-Butyl
cat.	Catalytic
δ	Chemical shift
c	Concentration
ca.	Circa
Cy	Cyclohexyl
CBS	Corey−Bakshi−Shibata
cm^{-1}	Wavenumber(s)
COSY	^{1}H–^{1}H Correlation spectroscopy
15-crown-5	1,4,7,10,13-pentaoxacyclopentadecane
CSA	10-Camphorsulfonic acid
DAR	Drug to antibody ratio
DBU	1,8-Diazabicyclo[5.4.0]undec-7-ene
DCC	*N*,*N'*-Dicyclohexylcarbodiimide
DDQ	2,3-Dichloro-5,6-dicyano-1,4-benzoquinone
DET	Diethyltartrate

DIAD	Di*iso*propyl azodicarboxylate
DIBALH	Di*iso*butylaluminium hydride
DMAla	*N*,*N*-Dimethylalanine
DMAP	*N*,*N*-Dimethylaminopyridine
DMB	3,4-Dimethoxybenzyl
DMF	*N*,*N*-Dimethylformamide
DMGly	*N*,*N*-Dimethylglycine
DMP	Dess−Martin periodinane
DMSer	*N*,*O*-Dimethylserine
DMSO	Dimethylsulfoxide
dppp	1,3-*bis*(Diphenylphosphino)propane
dppf	1,1-*bis*(Diphenylphosphino)ferrocene
dr	Diastereomeric ratio
ee	Enantiomeric excess
eq.	Equivalents
ESI	Electrospray ionisation method
Et	Ethyl
FABMS	Fast atom bombardment mass spectrometry
FDA	Food and Drug Administration (USA)
g	Gram(s)
GC	Gas chromatography
GI_{50}	Half maximal growth inhibitory concentration
h	Hour(s)
HeLa	Human cervical adenocarcinoma cell line
HMDS	Hexamethyldisilazane
HMPA	Hexamethylphosphoramide
HRMS	High resolution mass spectrometry
HTS	High throughput screening
HWE	Horner−Wadsworth−Emmons
Hz	Hertz
IBX	2-Iodoxybenzoic acid
IC_{50}	Half maximal inhibitory concentration
IgG	Human immunoglobulin G

imid.	Imidazole
IR	Infrared spectroscopy
J	$^{1}H-^{1}H$ coupling constant
L	Unspecified ligand
LLS	Longest linear sequence
K_d	Dissociation constant
LDA	Lithium diisopropylamide
LiDBB	Lithium 4,4'-di-*tert*-butylbiphenyl
2,6-lut.	2,6-Lutidine
*m*CPBA	*meta*-Chloroperoxybenzoic acid
MHz	Megahertz
Me	Methyl
µg	Microgram(s)
µL	Microlitre(s)
µmol	Micromole(s)
µM	Micromolar
mg	Milligram(s)
mL	Millilitre(s)
mM	Millimolar
mmol	Millimole(s)
min	Minute(s)
mol	Mole(s)
mAb	Monoclonal antibody
m	Multiplet
MMAla	*N*-Monomethylalanine
MNBA	2-Methyl-6-nitrobenzoic acid
MOM	Methoxymethyl ether
m.p.	Melting point
Ms	Methanesulfonyl
MS	Molecular sieves
MTM	Methylthiomethyl ether
MTPA	Methoxy(trifluoromethyl)phenyl acetic acid
NCI	National Cancer Institute

nM	Nanomolar
NMO	*N*-Methylmorpholine-*N*-oxide
NHK	Nozaki–Hiyama–Kishi
NMR	Nuclear magnetic resonance
nOe	Nuclear Overhauser effect
obs	Obscured
α_D	Optical rotation
OTf	Trifluoromethanesulfonate
P	Unspecified protecting group
PABC	*para*-Aminobenzyl carbamate
PCC	Pyridinium chlorochromate
30–40 PE	Petroleum ether, boiling point 30–40 °C
40–60 PE	Petroleum ether, boiling point 40–60 °C
Ph	Phenyl
pM	Picomolar
Piv	Pivaloyl
PMB	*Para*-methoxybenzyl
PMP	*Para*-methoxyphenyl
ppm	Part per million
PEG	Polyethyleneglycol
^{i}Pr	*iso*-Propyl
^{n}Pr	*n*-Propyl
py	Pyridine
PPTS	Pyridinium *para*-toluenesulfonate
R	Unspecified substituent
Red-Al	Sodium *bis*-(2-methoxyethoxy)-aluminium hydride
R_f	Thin layer chromatography retention factor
rt	Room temperature
s	Second(s)
SAR	Structure-activity relationship
salen	*N*,*N*'-ethylenebis(salicylideneiminato)
SET	Single electron transfer
SPR	Surface plasmon resonance

TAMRA	Tetramethylrhodamine
TBAF	Tetrabutylammonium fluoride
TBAI	Tetrabutylammonium iodide
^{t}Bu	*tert*-Butyl
TBDPS	*tert*-Butyldiphenylsilyl
TBS	*tert*-Butyldimethylsilyl
TCA	2,2,2-Trichloroacetimidate
TCBC	2,4,6-Trichlorobenzoyl chloride
TES	Triethylsilyl
Tf	Trifluoromethanesulfonyl
THF	Tetrahydrofuran
TIPS	Triisopropylsilyl
TLC	Thin layer chromatography
TMS	Trimethylsilyl
TMSer	*N*,*N*,*O*-trimethylserine
TMSQ	Trimethylsilylquinine
TMSQD	Trimethylsilylquinidine
Tr	Triphenylmethyl
Ts	*para*-Toluenesulfonyl
TS	Transition state
UV	Ultraviolet

Chapter 1

Introduction – Part I

Marine Natural Products in Targeted Anticancer Therapy

1.1. Natural Products and Chemical Synthesis in Drug Development

1.1.1. Natural Products as Early Cures

Natural products are secondary metabolites, produced by living organisms for functions not directly related to survival such as signalling, transport, excretion, chemical warfare or others.[3] They are thought to confer a competitive advantage to the organism that produces them or to their host in case of a symbiotic relationship. The variety of processes they enable is linked to the vast array of intricate structures they display, each with their own specific purpose. If their primary intention is to immobolise prey or as a form of chemical defence against predators, they often exhibit exceptional potency against a well-defined molecular target. A combination of the two is a desirable trait with respect to increasing the species' chance of survival and can thus be selected for in evolution.

Owing to the same principles, natural products also play a central part in the history of medicine. Before the 20th century the only cures available to treat illnesses were crude or semi-pure extracts of plants, microbes and minerals. Scientific progress in pharmacology and other related fields has since enabled the isolation and characterisation of pure, active ingredients of many traditional remedies, e.g. artemisinin from *Artemisia annua* or morphine from *Papaver somniferum*. Eliciting a biological response in humans is merely a side effect of the inherent function of secondary metabolites in the organisms which produce them. However, having a better understanding of the relationship between their function, structure and molecular target can provide the tools to evaluate and harness their potential for the benefit of mankind.

The early harvesting of bioactive compounds was limited to specimens from terrestrial organisms. Advances in diving and submarine technologies have permitted sampling the underwater enviroment, opening the opportunity to explore the sea habitat as well. This marks a major step forward in natural product discovery as the oceans represent 95% of the biosphere with greater biodiversity due to harsh conditions which are encountered within the oceans.[4,5] It is therefore unsurprising that metabolites isolated from marine organisms often display a wider structural variation and complexity than their terrestrial counterparts. In addition, many marine cytotoxins have been found to display exceptionally potent biological activity, possibly to offset the rapid dilution effect upon release into the environment. Further discoveries are ongoing in parallel with improving sampling and isolation techniques which may yield many more molecules of interest to modern medicine.[6,7]

1.1.2. Sourcing and Supply of Bioactive Compounds

Marine-derived natural products are often isolated from the source organism in minute amounts. In such cases, direct harvesting to obtain even very humble supplies of material would leave a devastating environmental impact. Fortunately, the recent advances in bioengineering have made it possible to edit the genetic sequence of plants or certain strains of microbes to synthesise the desired compounds, which can then be extracted and purified as necessary. However, in many cases this process is not achievable as it is not trivial to pinpoint the exact biosynthetic origin of the natural product or it is difficult to create a suitable cultivation environment as these compounds are often produced under extreme conditions.[8] Another reason pertaining specifically to highly potent metabolites may be the fatal toxicity to the parent organism at the concentrations required for a practical production.

A commercially more significant strategy is semi-synthesis, which involves the chemical modification of an appropriate advanced intermediate obtained from plant or bacterial sources.[9] For example, paclitaxel (**2**) is a cytotoxic agent isolated from the bark of the Pacific yew tree and is currently used in the treatment of a variety of cancers. Large-scale commercial manufacture route currently employs plant tissue culture and fermentation,[10] though the preceding process was a four-step synthetic transformation from 10-deacetylbaccatin (**3**) (**Scheme 1**).[11]

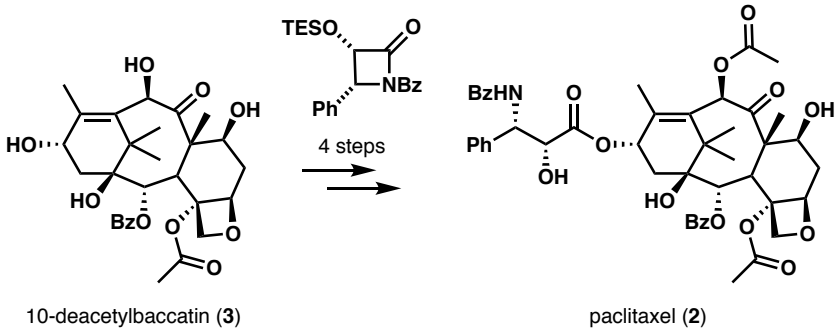

Scheme 1 Semi-synthesis of paclitaxel (**2**) from 10-deacetylbaccatin (**3**)[11]

The ultimate option is *de novo* synthesis.[12] While this seems like a daunting and laborious task for compounds with complex architectures, remarkable progress has been made by process chemists in translating research laboratory discoveries to natural product-derived commercial items.[13] Several notable partnerships with the industry so far have made bold statements by demonstrating that with a collaborative approach total synthesis can indeed meet supply demands to facilitate clinical trials or even the market needs.

An illustrative example is the story of discodermolide (**4**), a microtubule-stabilising agent originally isolated from a deep-sea sponge *Discodermia dissolute* (**Figure 5**). Drawing from the total syntheses of Smith[14] and Paterson,[15] Novartis devised a 33-step process chemistry route suitable for the pilot plant. Discodermolide was prepared in an overall yield of 0.65%, resulting in 60 g of material at the end of the scale-up campaign.[16–20] Novartis' commendable synthetic achievement enabled the Phase I clinical trials of discodermolide for treatment of pancreatic cancer.

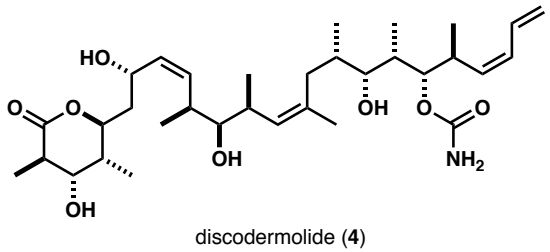

Figure 5 Structure of discodermolide (**4**)

Another hallmark venture is the development of eribulin mesylate (**5**, Halaven®), a derivative of the natural product halichondrin B (**Figure 6**).[21] The first total synthesis of this marine antiproliferative agent was completed by Kishi[22] and served as a starting point for structure-activity-relationship (SAR) studies. Subsequent biological screening of numerous analogues revealed that the active pharmacophore of the natural product resides in the right-hand portion of the structure highlighted in red.[23] The truncated skeleton retains the activity of the parent compound while the synthetic sequence is greatly simplified by

the omission of the seven polyether rings. It is marketed as a breast cancer drug and is produced by Eisai in a 37-step commercial manufacturing process.[24]

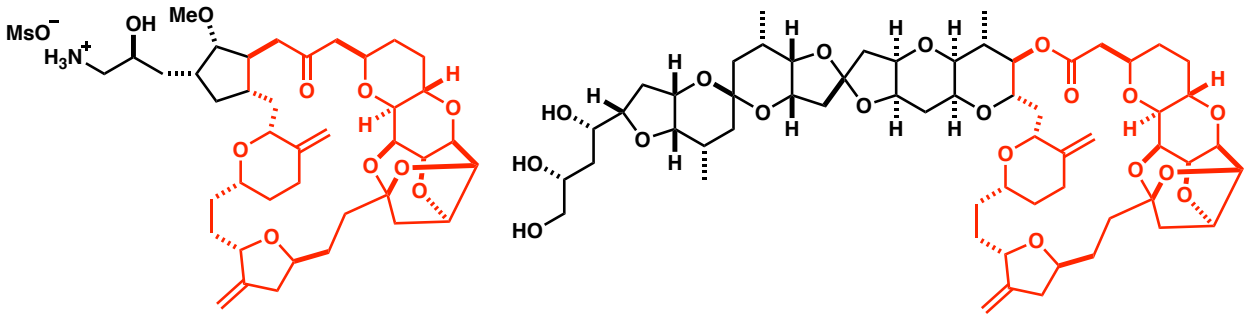

Figure 6 Halichondrin B (**6**) and eribulin mesylate (**5**, Halaven®) with highlighted structural similarity

Both projects are success stories of the combined efforts of academia and industry which resulted in a viable solution to the supply problem purely by synthesis. In addition, they provide a test of robustness (and selectivity, where applicable) for any chemical reaction performed on structurally complex late-stage intermediates in the sequence. If no suitable conditions are available, receptive organic chemists will seek inspiration in these challenges and devise novel methodologies or optimise existing ones to carry out the necessary steps. In the context of Halaven (**5**), the commercial synthesis underscored the power of the Nozaki–Hiyama–Kishi reaction,[25,26] implementing this macrocycle formation step on more than a kilogram scale. Other related work contributes towards dispelling the prejudice against total synthesis in scale-up and creating a positive outlook for the field in future.

1.1.3. Natural Products as Drug Leads

Natural products represent the optimal starting point for drug development through chemical modifications. Design of mimics and analogues based on compounds which already interact with their biological targets in a highly selective manner offers the means of biological pathway determination and probing *in vivo* pharmacology. Ultimately, the results of these studies lead to a better understanding of what makes a good drug for the specific purpose and synthesis provides the tools to produce them.

Unfortunately, over the past 20 years, the pharmaceutical industry has largely neglected natural products as lead molecules. This is partially due to expensive failures of numerous late-stage clinical candidates and comparatively long development timelines relative to other types of small molecule drugs. The rise of alternative compound screening tools such as high-throughput screening (HTS) for small molecule hits held great promise for the industry with the ability to rapidly produce and screen thousands of compounds. Once an active skeleton has been identified, the capacity of combinatorial chemistry for

structural optimisation is without par. However, this approach merely scratched the surface of available chemical space and after years of effort, only two approved drugs from this pipeline fall under the *de novo* category of discovery.[27]

Despite the recent trends, natural products have clearly retained their dominant status in many areas of medicine. For example, chemotherapy still represents an essential pillar in the treatment of various forms of cancer. Of 136 small-molecule antineoplastic drugs which gained Food and Drug Administration (FDA) approval between 1940 and 2014 only 17% are fully synthetic candidates while others are derived from bioactive compounds isolated from nature (**Figure 7**).[28]

Great promise comes from the search for secondary metabolites with novel cellular mechanisms of action to overcome the rising issue of drug resistance or development of targeted delivery systems. The latter would allow for previously abandoned projects, such as discodermolide, to be revisited and given a new chance at success with reduced toxicity.[29] This is particularly relevant as the search for novel targets and natural product therapeutics is undeniably becoming increasingly difficult as demonstrated by the recent decline in FDA approval of new chemical entities.[30]

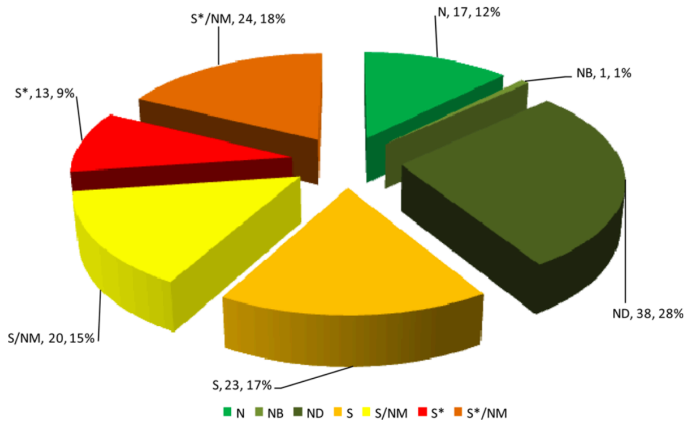

Figure 7 Small-molecule anticancer drugs 1940–2014. N = unaltered natural product, NB = botanical drug, ND = natural product derivative, S = synthetic drug, S* = synthetic drug with a natural product pharmacophore, NM = natural product mimic[28]

The above discussion aims to put the role of natural products and chemical synthesis in the context of pharmaceutical drug discovery. The groundwork for a greater impact of basic total synthesis research on future endeavours in the industry had been laid by establishing ambitious but ultimately fruitful collaborations. It is no longer a challenge to simply complete the synthesis of a complex target but to execute it in an elegant, concise, green, high yielding and scalable manner which provides a truly sustainable supply.[31]

1.2. The Aplyronines

1.2.1. Isolation and Structural Determination

The aplyronine natural products were first isolated in 1993 by Yamada and co-workers from the sea hare *Aplysia kurodai*, a mollusk collected off the coast of the Mie prefecture in Japan.[2] This marine species has been an abundant source of biologically active natural products such as aplysin (**7**),[32] aplaminal (**8**),[33] aplysiasecosterols (**9**–**11**)[34,35] and others (**Figure 8**). Aplyronines A (**1**), B (**12**) and C (**13**) were characterised in an *in vitro* cytotoxicity-guided assay against HeLa-S_3 cervical adenocarcinoma cells following extraction of natural specimens and laborious chromatographic separation. In 2000, the Yamada group developed a refined isolation protocol involving solvent partitioning and five-step chromatography which enabled the identification of five further minor congeners D–H (**14**–**18**).[36,37] While this had also facilitated a more efficient harvest of aplyronines A–C (**1**, **12**–**13**), the yield remained extremely low (10^{-5} to 10^{-7} based on wet weight); 300 kg of the wet mollusk provided just 75 mg of the most abundant congener, aplyronine A and less than 1 mg of most others.

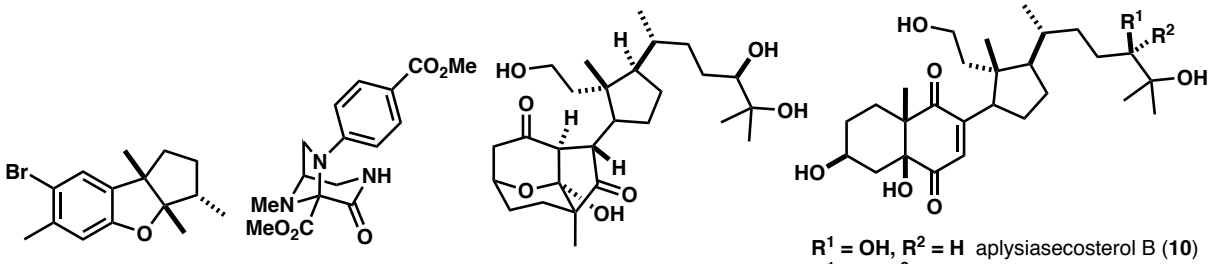

Figure 8 Selected bioactive natural products isolated from *Aplysia kurodai*

The gross structure of aplyronine A was determined through detailed 1D and 2D NMR analysis and degradation studies (**Scheme 2**), followed by enantioselective synthesis of the resulting fragments.[2,38–41] Yamada designed a flexible strategy to access all possible permutations of the stereocentres which asserted the structures of congeners A–C through total synthesis.[41–43]

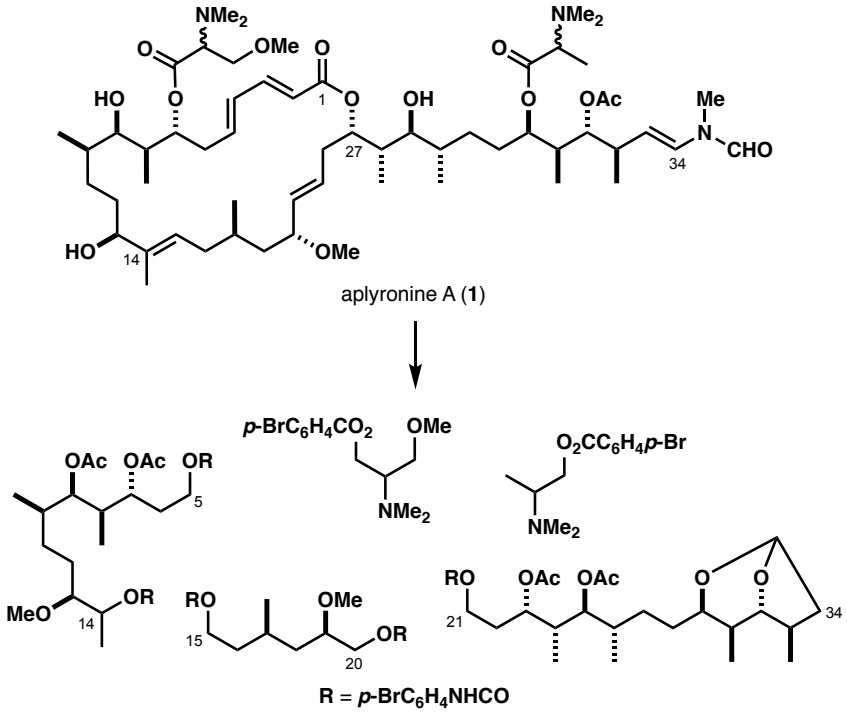

Scheme 2 Degradation fragments from aplyronine A (**1**)

Table 1 Structure of aplyronines A–H (**1**, **12**–**18**) and their biological activity in HeLa-S_3 cell line assay

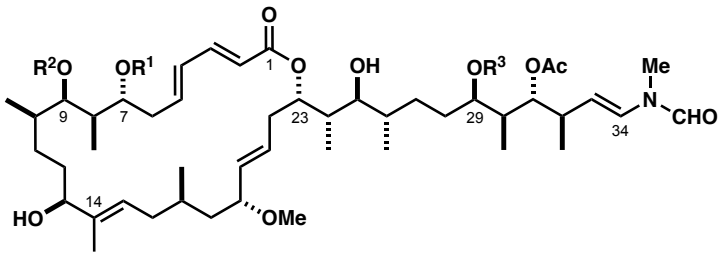

Aplyronine congener	R^1	R^2	R^3	IC_{50} / nM
A (**1**)	TMSer	H	DMAla	0.450
B (**12**)	H	TMSer	DMAla	2.89
C (**13**)	H	H	DMAla	22.4
D (**14**)	TMSer	H	DMGly	0.071
E (**15**)	= 22-methylaplyronine A			0.184
F (**16**)	TMSer	H	MMAla	0.189
G (**17**)	DMSer	H	DMAla	0.120
H (**18**)	H	DMSer	DMAla	9.80

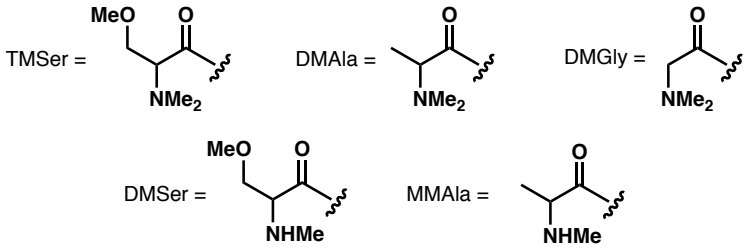

The aplyronines are comprised of a highly decorated 34-carbon backbone. The two most prominent features are the 24-membered macrolactone and a polyketide side chain, terminating in an *N*-methyl-*N*-vinylformamide moiety. Other notable structural elements are the three stereotetrads (C_7–C_{10}, C_{23}–C_{26} and C_{29}–C_{32}), three isolated chiral centres (C_{13}, C_{17} and C_{19}), an (*E*,*E*)-dienoate and two additional olefins. The variation between the congeners is seen in the identity and positioning of amino acid residues at the C_7, C_9 or C_{29} hydroxyls. This is true for the entire family except aplyronine E (**15**), which was deduced to be 22-methylaplyronine A (**Table 1**). Interestingly, the amino acids are present as scalemic mixtures of (*R*) and (*S*)-epimers, where the ratio is always in favour of the latter though not identical between different samples of *Aplysia kurodai*.[2] This observation suggests that the naturally occurring (*S*)-configuration may be subject to epimerisation in the aplyronines' biosynthesis or the isolation process.[36] Aplyronine A obtained from the sea hare is thus a mixture of four diastereomers and the rotamers at the *N*-vinylformamide terminus (2:1 ratio) which further complicates the NMR spectra.

The stereochemistry of aplyronines B–H (**12**–**18**) was determined by fast atom bombardment mass spectrometry (FABMS) and NMR comparison to the known structure of aplyronine A. The large discrepancies in their biological activities suggest that small variations in the amino acid structure play an important role in the binding to the cellular target which constitutes an early qualitative insight into the structure-activity relationships (SAR). A seemingly insignificant disparity of a single methyl group on the C_{29} amino acid between congeners A and D translates into a remarkable six-fold difference in potency (IC_{50} = 0.45 nM and 0.071 nM). Yamada's investigations into this phenomenon as well as further biological studies are presented below.

1.2.2. Biological Activity

The prohibitively low availability of most congeners has prevented significant biological studies of the entire aplyronine family apart from the *in vitro* assay against the HeLa-S_3 cells in the isolation process. However, even the limited data acquired so far shows that the anticancer activity is nothing short of exceptional with the IC_{50} values for all congeners in the low- to subnanomolar range) for that particular cell line (**Table 1**).

The most abundant congener, aplyronine A, was also studied by Yamada on a selection of mouse cancer xenografts *in vivo*, which is arguably a better indicator of the true therapeutic potential. Mice receiving intraperitoneal treatment with the natural product showed a longer median survival rates against the control group over a period of 60 days with the highest success rate for the P388 leukaemia and Lewis lung carcinoma (**Table 2**).[2,36,44]

Table 2 *In vivo* antitumour activity of aplyronine A in mouse cancer xenografts[44]

Tumour	Test group	Dose / mg/kg/day	Median survival time / days	Survivors after 60 days
P388 leukaemia	treatment	0.08	59.9	4/6
	control	/	11.0	0/7
colon C26 carcinoma	treatment	0.08	40.0	0/6
	control	/	15.7	0/10
Lewis lung carcinoma	treatment	0.04	60.1	6/6
	control	/	10.8	0/8
B16 melanoma	treatment	0.04	46.8	0/6
	control	/	23.3	1/9
Ehrlich carcinoma	treatment	0.04	59.7	2/6
	control	/	15.0	0/8

Subsequently, Kigoshi reported revised IC_{50} values for aplyronine A, namely 10 pM for the activity in the HeLa-S_3 cell line[45] and 2.9 pM against HL60.[46] There is clearly a degree of variation compared to Yamada's data, which must be taken into account when trying to rationalise the discrepancy in activities between the congeners. Nevertheless, on testing in the US National Cancer Institute (NCI) primary screen,[47] aplyronine A (NSC687160) displayed exquisite potency against 60 cancer cell lines where the GI_{50} values for the vast majority fell below the minimum measurement threshold (mean GI_{50} = 0.2 nM).[48] Interestingly, aplyronine A does not inhibit growth in a homogeneous manner and does not behave *in vitro* as a non-specific poisonous agent but rather displays some selectivity though not toward any given histopathological group. This data puts the aplyronines into serious contention for potential preclinical drug development, which is further supported by its unique mechanism of action and will be discussed in detail in **Section 1.2.4.**

1.2.3. Studies on Actin Binding

In 1996, Karaki and co-workers identified actin as the target biomacromolecule of aplyronine A.[49] Actin is a highly abundant protein, present in nearly all eukaryotic cells, structurally conserved among the organisms and it is one of the main classes of cytoskeletal proteins within the cytoplasm (**Figure 9**).[50] It participates in a number of fundamental cell processes such as motility,[51] division, signalling, cytokinesis and establishment of cell junctions.[52]

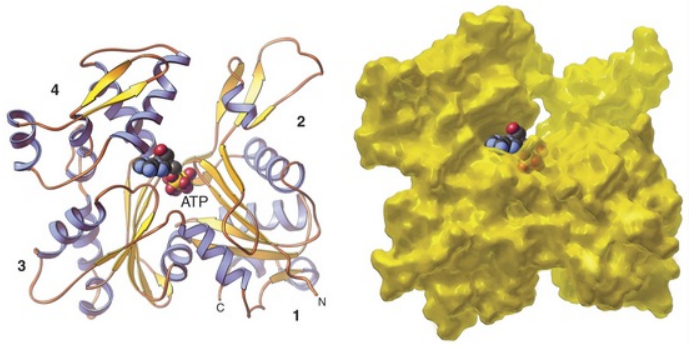

Figure 9 Ribbon and space-filling models of ATP-bound actin with subdomains 1–4 indicated[53]

These mechanisms are facilitated by the interconversion between the two distinct forms of the protein. The core constituent of the actin skeleton is the monomeric globular (G-) actin, which can polymerise into double-stranded helical microfilaments (F-actin) under physiological conditions, involving head-to-tail interactions (**Figure 10**). Elongation primarily takes place at the barbed (+) end of the filament, starting with the incorporation of the adenosine triphosphate (ATP)-bound G-actin monomer. This event activates the ATPase which allows F-actin to carry out stoichiometric hydrolysis of ATP, causing a conformational change and weakening of the intermolecular interactions at the pointed (–) end. This leads to increased dissociation of the adenosine diphosphate (ADP)-bound G-actin, which is able to undergo phosphorylation to ATP and repolymerisation at the barbed end. The overall process is known as treadmilling and provides the means for unidirectional growth, which contributes to the spatial organisation of the actin cytoskeleton.

Regulation of actin filament dynamics is affected by an array of actin-binding proteins through a variety of mechanisms. These include trapping free G-actin monomers to render them unavailable for addition to the barbed end (sequestering), binding to existing filaments to prevent further growth (capping),[54] stimulating polymerisation (nucleation),[55] stabilising existing filaments[56] and active breakdown of the filaments (severing).[57,58] It is not surprising that many naturally occurring toxins interfere with these processes considering the key role of the actin equilibrium in healthy cell function.[59]

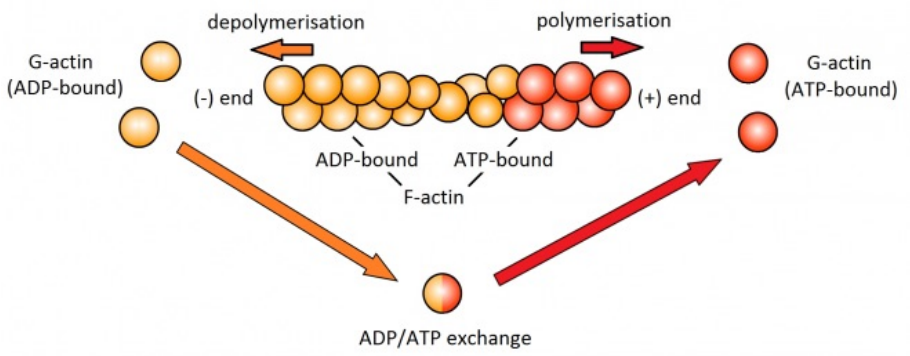

Figure 10 An illustration of the actin treadmilling process*

Based on the effects exerted on the actin equilibrium, actin-binding natural products fall into either of the two main groups: compounds which prevent actin polymerisation and/or destabilise existing filaments, and those that stabilise them. Aplyronine A belongs to the former category by sequestering G-actin through formation of a 1:1 complex which reduces the free monomer presence below the critical concentration for treadmilling.[49] Additionally, it can cap existing filaments at the barbed end, sever F-actin and bind to proteins involved in forming branched actin polymer networks (Arp 2/3).[45] There are at least six different natural product binding sites on actin, however, the majority of compounds appear to bind at the barbed end.[60]

More than 80 known actin-binding natural products can be arranged into just eight major skeletal types.[61] Aplyronines belong to a specific class of structurally related compounds, which posess a hydrophobic macrocycle and an 11-carbon aliphatic chain.[62] Several illustrative examples are shown in **Figure 11**.

Studies by Rayment first confirmed the correlation between the actin-binding ability and the highly conserved groups along the tail of these macrolides.[63] Ring architectures range from polyketide-type backbones of reidispongiolide A (**19**),[64] tolytoxin (**20**)[65] and the aplyronines to tris-oxazoles such as kabiramide C (**21**) and halichondramide (**22**)[66,67] or even macrodiolides rhizopodin A (**23**)[68,69] and luminaolide (**24**).[61,70]

* Image by Dr James Sleigh, Scientific Research Correspondent for Spinal Muscular Atrophy Support UK. Reproduced with permission of the author.

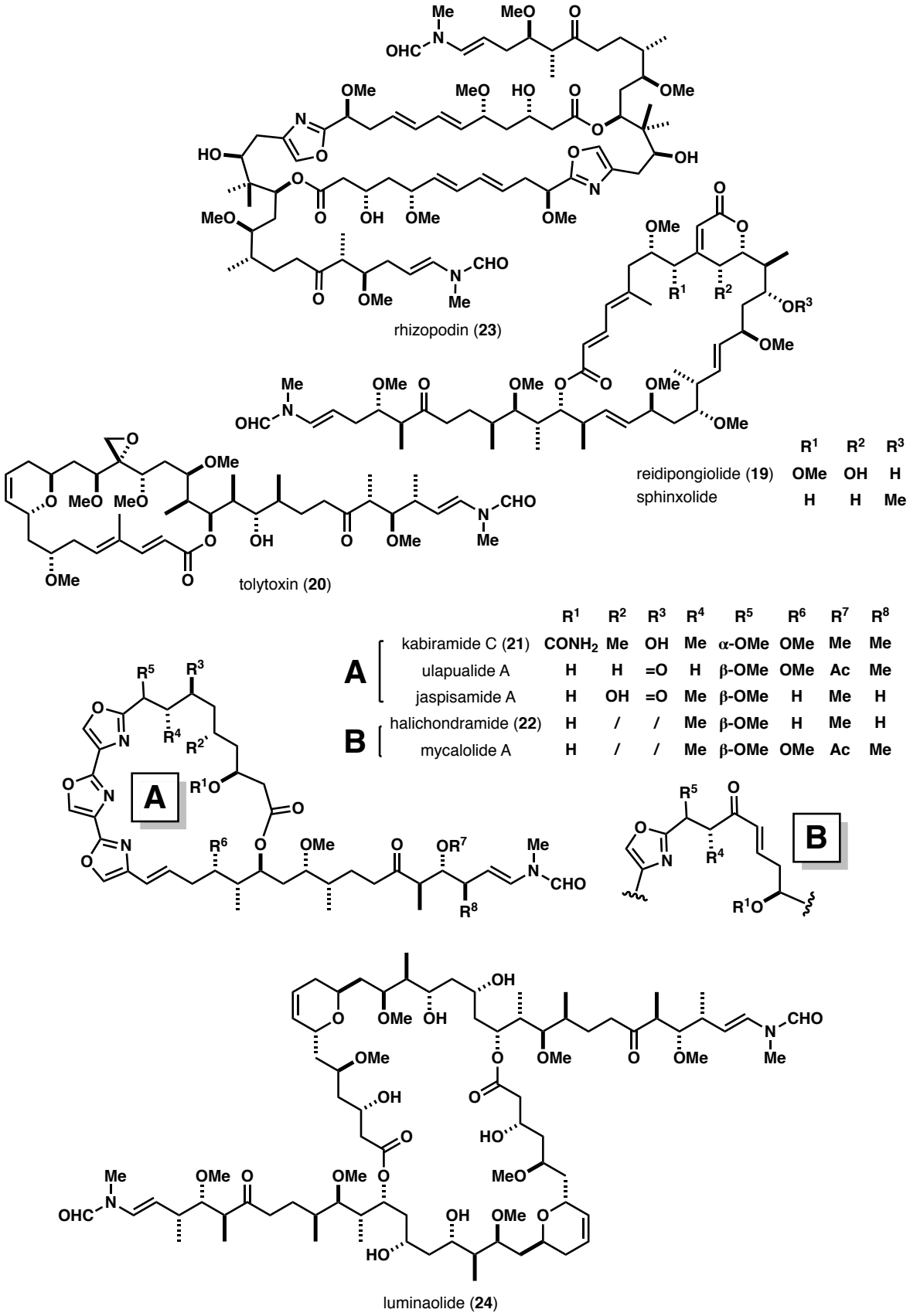

Figure 11 Selected structurally related actin-binding natural products with a conserved side chain

A more detailed understanding of the underlying affinity for actin came from the synthesis and biological evaluation of a wide range of analogues based on the aplyronines or the structurally related reidispongiolide A (**19**) by the Yamada[46,71,72] (**Figure 12**) and Paterson[73,74] groups, respectively. Yamada found that the side chain is essential for actin binding as more than a 100-fold decrease in actin-binding activity is observed when the tail is heavily truncated (**27**) and when completely removed it renders macrocycle **28** inactive. Modifications to the ring are generally well tolerated, as exemplified by the mostly retained potency of a tetrahydro macrocycle lacking either the C_2–C_5 diene or the C_{13} methyl, aplyronine A without one or both amino acids (**30** and **31**) or an acyclic analogue with the full length of the carbon backbone. Replacing the *N*-vinylfomamide with another hydrophilic group such as an alcohol was reasonably well tolerated (**29**) and interestingly even small fragments such as **25** and **26** exhibited relatively strong activity considering their size and reduced complexicity compared to the parent compound.

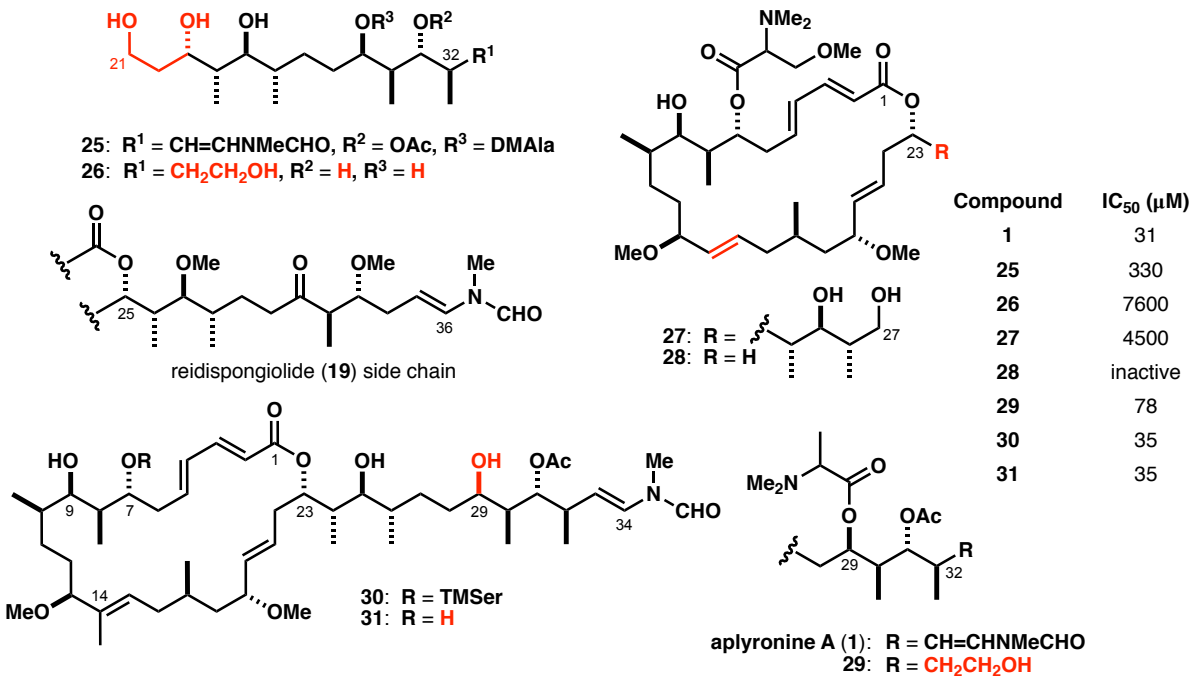

Figure 12 Representative aplyronine analogues from Yamada's SAR studies their actin depolymerising activity values. IC_{50} indicates the concentration required to depolymerize F-actin (3.7 mM) to 50% of its control amplitude.

The Paterson group prepared a library of reidispongiolide tail analogues to probe the role of various moieties on the backbone.[74] The markedly different activities were attributed to the variation in the hydrogen bonding ability and flexibility of the chain, thus Paterson and Marriott postulated that the tail may be forced into a twisted conformation to fit the tight binding space.[73]

The overall results of these studies are in agreement with the crystal structure for the actin-bound aplyronine A, obtained by Takata in 2006 (**Figure 13**)[75] as well those of related natural products.[63,76,77] The side chain intercalates into a narrow hydrophobic cleft of actin between subdomains 1 and 3 with the macrolide only making contacts at the small surface patch at the hydrophobic entrance. Depending on the stereochemistry at the junction of the ring and tail regions, the macrocycle is directed to either subdomain 1 or subdomain 3 (as observed with aplyronine A) with the distal portion of the ring structure protruding into space. The *N*-vinylformamide terminus maintains critical interactions with two backbone amide residues on actin through bridging water molecules, which stabilise the complex.

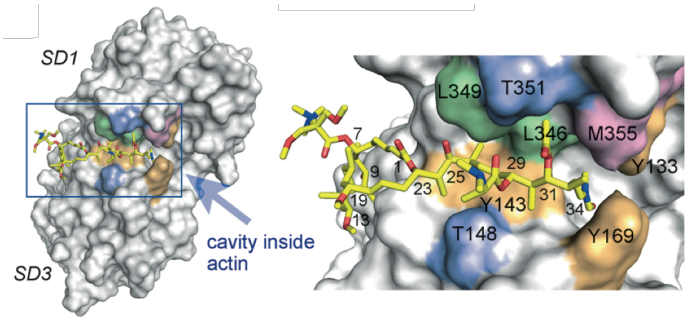

Figure 13 Crystal structure of actin–aplyronine A complex with the side chain inserted into the cleft between subdomains 1 and 3 and the macrolide making surface contacts at the entrance.[45]

The mechanistic proposal for F-actin severing by barbed-end actin binders is based upon intercalation of the small molecule between two longitudinal monomers within the actin filament (**Figure 14**). Binding into the region of the DNAse-binding loop on one actin protomer and the aforementioned hydrophobic cleft on the adjacent subdomain outcompetes the protomer–protomer contacts in place and causes filament breakage at the point of intercalation.[78] If binding occurs at the barbed end of a growing filament, the toxin prevents monomer addition by remaining attached, thereby capping the structure.

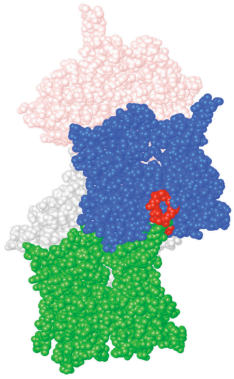

Figure 14 Kabiramide C (**21**) in G-actin-bound conformation (red), superimposed onto the model for F-actin, showing steric clash between the natural product and the DNAse I-binding loop of the lower monomer (green).[77] The filament axis is vertical with the barbed end at the bottom.

1.2.4. Structure-Activity Relationship Studies and Cytotoxicity

The exact origin of cytotoxicity to date remains unsolved, though there is an obvious disconnect between the observed IC_{50} values for actin depolymerising activity and cytotoxicity. Aplyronines A–C bind actin with equal affinity yet cytotoxicity data on HeLa-S_3 cells acquired by Yamada reveals that aplyronine A is six times more potent than aplyronine B, which is in turn tenfold more active than aplyronine C. Minor congeners D–H are comparably cytotoxic with two notable exceptions: aplyronine H, in which the amino acid is appended at C_9, and aplyronine D with a dimethylglycine (DMGly) residue in place of dimethylalanine (DMAla) at C_{29}.

Linking biological data to the structural discrepancies between the congeners reveals the paramount importance of the C_7 trimethylserine (TMSer) residue in displaying strong cytotoxicity. More minor increases in activity are caused by *N*-demethylation of either the DMAla or TMSer, or presence of an additional methyl group at C_{22}. However, Yamada did not specify whether the assays were repeated for the entire panel of aplyronines (A–H) or simply the newly isolated congeners (aplyronines D–H) two decades after the first isolation paper was published.[2] Therefore, the exact IC_{50} values may have a degree of procedural error embedded in them and should notionally only be considered in the context of a general trend.

Yamada also carried out extensive structure-activity relationship (SAR) studies on synthetic analogues to identify further features with an impact on cytotoxicity. The alterations within the side chain region were generally tolerated whereas changes to the macrocycle were more deleterious. The analogue **32** (**Figure 15**) containing a primary alcohol in place of the *N*-vinylformamide and lacked the C_{14} methyl retained 28% of the activity compared to aplyronine A (**1**). The further simplified analogue **33** where the dimethylalanine at C_{29} has also been removed resulted in a further drop in potency to less than 1% of the parent natural product. However, the greatest impact was observed upon altering the trimethylserine at C_7. While aplyronine D with the C_{29} dimethylglycine is extremely active as mentioned above, the same cannot be said if this amino acid is attached in the C_7 position as well in place of the trimethylserine (**34**). A highly relevant feature also appears to be the C_2–C_5 dienoate moiety, which is likely to influence the conformational rigidity of the ring in analogue **35**.

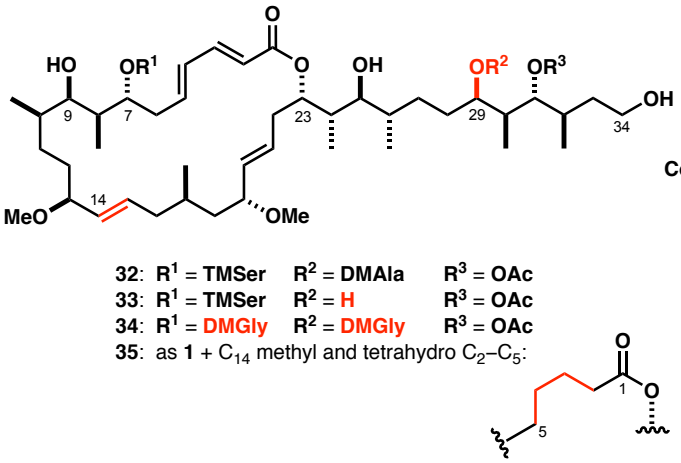

Compound	IC_{50} (ng/mL)
1	0.48
32	2.6
33	37
34	> 2000
35	57

Figure 15 Further analogues prepared by the Yamada group for SAR studies on cytotoxicity

The influence of the structural elements near C_{23} can be observed from the bioactivity of a mycalolide B–aplyronine A hybrid **36** (**Figure 16**), synthesised by Kigoshi.[79] The structure borrows from the side chain of the superior actin binder, mycalolide B, and the C_1–C_{23} macrocyclic core of aplyronine A. Loss of the C_{24} methyl, inversion and methylation of C_{25} and alteration of the C_{29} ester result in a moderate increase in actin depolymerisation. On the other hand, cell growth inhibition is reduced by 1000-fold compared to aplyronine A, supporting the conclusion than the two activities are not directly correlated (**Figure 17**).

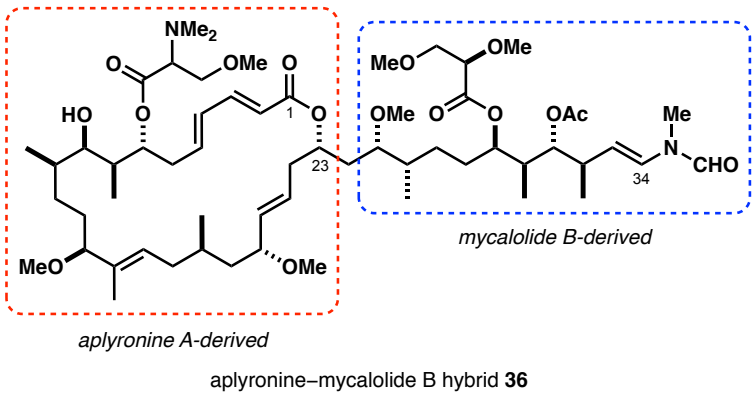

Figure 16 Kigoshi's aplyronine A–mycacolide B hybrid **36**

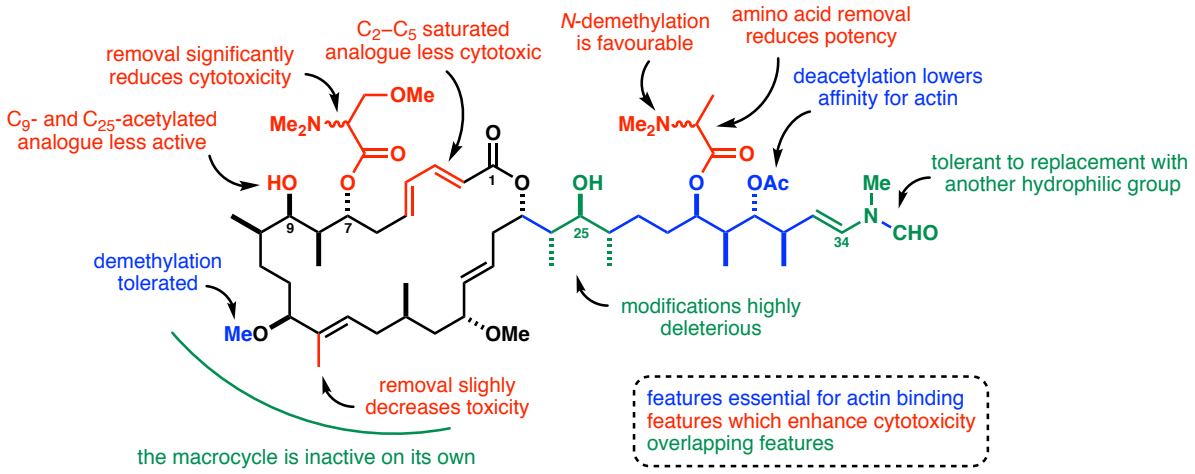

Figure 17 Summary of structure-activity relationship studies for the aplyronines

More recently, the idea of a secondary biomolecule target for the aplyronines has emerged as a possible explanation for the observed phenomenon. To initiate investigations of this hypothesis, Kigoshi prepared a series of C_{34}-modified aplyronine derivatives incorporating an aryl diaziridine tag (**37**),[80] a polyethyleneglycol (PEG)-tethered biotin moiety (**38**)[45] or a tetramethylrhodamine (TAMRA) conjugates (**39–40**) (**Figure 18**).[81] Fluorescence experiments with these probes confirmed the specific interaction of aplyronines A and C with β-actin.

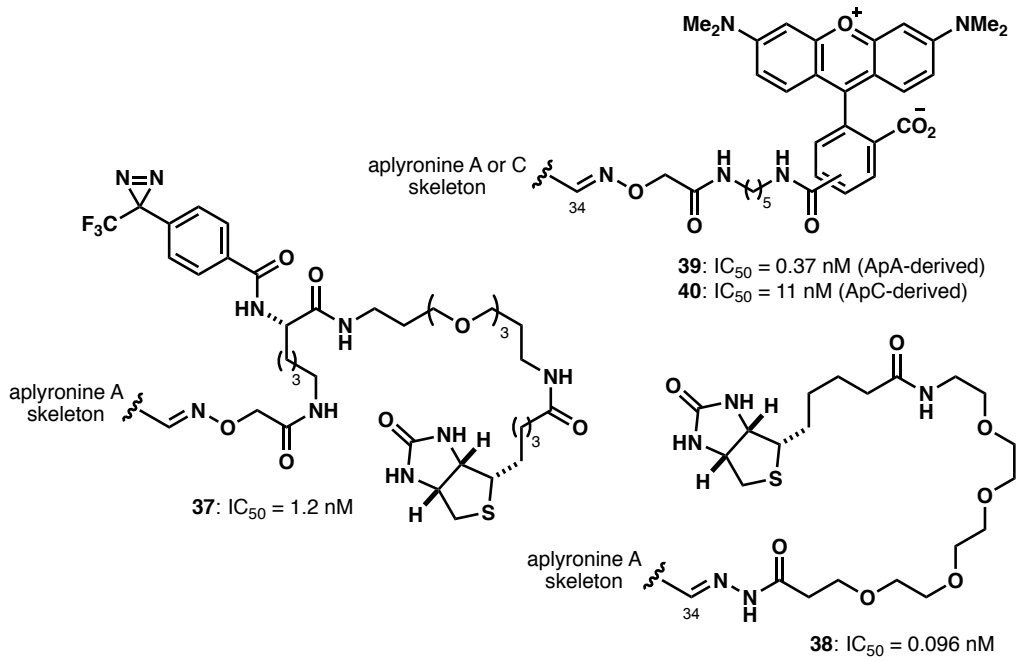

Figure 18 Kigoshi's aplyronine-derived probes for studies of binding to actin and their cytotoxicity IC_{50} values against the HeLa-S_3 cells

A significant breakthrough in elucidating the mechanism of action of aplyronines was communicated in 2013 when tubulin was identified as the second biomacromolecule target of aplyronine A.[82] Kigoshi observed the formation of a 1:1:1 heterotrimeric structure which formed upon tubulin binding to a pre-formed 1:1 complex of actin and aplyronine A (**Figure 19**). Considering the size and spatial proximity of both biomacromolecules the contacts formed must be carefully optimised when facilitated by a comparatively small molecule. This suggests that actin undergoes a conformational change upon binding to aplyronine A to create a tubulin binding site. Kigoshi later studied the kinetics of the proposed interactions with surface plasmon resonance (SPR), measuring K_d for each binding event.[83] The ternary complex assembly was also found to be accelerated by a non-competitive actin depolymerising agent lantriculin A, presumably through increased effective actin monomer concentration.

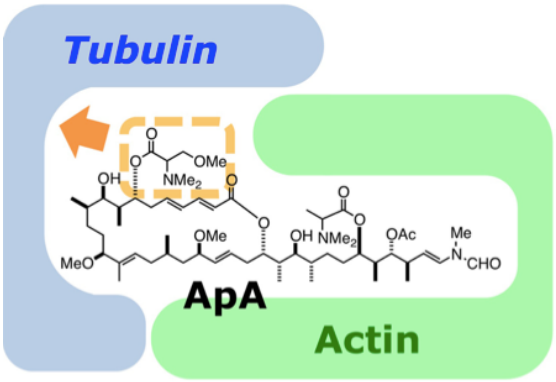

Figure 19 Kigoshi's proposed 1:1:1 ternary complex of actin and tubulin[82]

Cell permeability and accumulation levels for aplyronines A and C based on observed fluorescence were comparable,[81] hence the discrepancy in cytotoxicity cannot stem simply from varying exposure levels of each toxin. Concentrations of the toxin required to inhibit microtubule assembly in living cells are much lower than those necessary for actin disassembly (0.1 nM compared to 100 nM, respectively). A possible explanation, consistent with the SPR studies, could be that high intracellular quantities of actin facilitate rapid formation of a 1:1 complex with aplyronine A which remains trapped within the cell. Binding to tubulin then exerts an enhanced cytotoxic effect due to localisation of the ternary complex in the tumour.

However, exactly how the heterotrimeric complex induces cytotoxicity is still unknown. One likely mode of action might be disruption of spindle microtubule dynamics during mitosis. Similar antimitotic agents such as vinblastine or paclitaxel act by being embedded into the microtubule lattice or kinetically stabilising spindles, both of which lead to blocking mitosis and eventual cell death.[84,85] The aplyronines may also be able to mimic proteins which mediate actin-tubulin interactions associated with the cytoskeleton dynamics like the mammalian diaphanous-related (mDia) formin proteins which regulates microtubule stabilisation.[86]

The challenge remains to identify the relevant binding site on tubulin and the residues involved. Tubulin-targeting drugs are namely a successful area of anticancer therapy which heavily relies on highly potent natural products with known mode of action in certain types of tumours.[87,88] While the aplyronines fit this category and are immensely potent, their true potential lies in the unique dual-targeting mechanism of action which holds tremendous promise in overcoming resistance in multi-drug resistant cancers as it is extremely rare.

1.3. Antibody–Drug Conjugates

Use of highly potent cytotoxic agents from nature in systemic cancer treatment relies on higher proliferation rates of tumour cells, targeting the mitosis cycle. For many seemingly promising candidates the maximum tolerated clinical dosage does not reach the therapeutic threshold or displays only a very narrow safety margin, leading to a high chance of failure in clinical trials. Actin-binding agents suffer from a similarly crippling limitation related to the abundance of actin and its importance in non-neoplastic cells, making toxicity-related side effects unacceptable for direct clinical use.

Cancer therapy has seen tremendous breakthroughs in the last few decades through the advent of monoclonal antibody (mAb) technology in the 1970s. Antibodies are large proteins produced by plasma cells with the task of eliciting an immune response upon binding to a pathogen. They exhibit exquisite specificity for the cognate target proteins (antigens) on the surface of a foreign body through non-covalent interactions. mAbs embody ideal vehicles to deliver toxins directly to the sourse of the disease with specific genetic abnormalities. Attachment of cytotoxic warheads to amino acid functional handles on the antibody as the delivery vehicle has given rise to a new drug modality known as antibody–drug conjugates (ADCs).

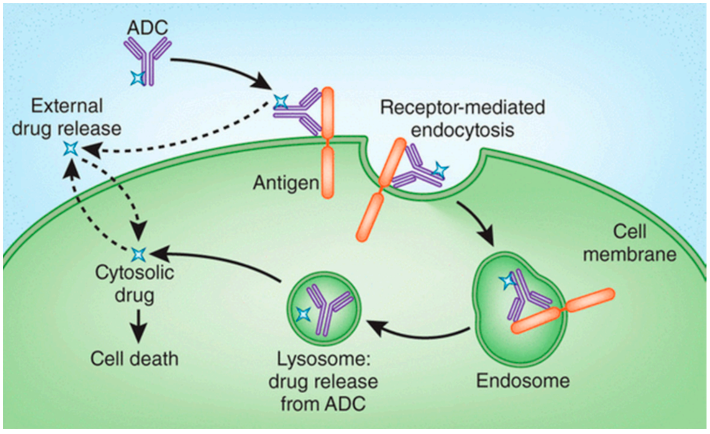

Figure 20 Schematic representation of the mechanism of ADC drug delivery. Dash line arrows represent antimitotic activity through extracellular payload release.[89]

The principal advantage of ADCs lies in the efficient shuttling of the payload to the intended target, binding to the surface antigen and subsequent internalisation through endocytosis (**Figure 20**). Intracellular trigger mechanisms within the lysosome facilitate the release of the drug of which maximises accumulation directly at the tumour site or in the nearby cells through trafficking.[90] The balance between prolonged half-life of ADCs within the bloodstream yet sufficient lability near the malignant tissue reduces clearance rates and ensures that healthy tissue is bypassed during treatment. The crucial parameters regarding the complex process of design and production of ADCs have been extensively reviewed and selected publications on these topics form the basis of the discussion below.[91–102]

1.3.1. The Antibody and Targets

The highest degree of targeted delivery can be achieved if the mAb is able to select for an antigen which is known to be expressed exclusively at the surface of neoplastic cells but such discoveries are rare. ADC technology thus capitalises on accessible tumour-associated markers and proteins which are abundantly expressed at the site of the disease in a homogeneous manner and little expression in normal cells, often also limited to a given tissue type allowing for high levels of selectivity for cancer cells. The mAbs currently in use are three types of human immunoglobulin G (IgG) which display a prolonged half-life in blood and reduced immunogenicity issues compared to the murine and chimeric antibody sequences utilised previously.

1.3.2. The Linker

The linker represents a connecting piece between the antibody and the pendant warhead, fulfilling two key requirements: chemical stability in the bloodstream and efficient payload release at the intended site of action.[94,99] The mode of drug liberation affects whether the payload can be freed and act in the vicinity of the tumour cell prior to endocytosis, exerting what is known as the bystander killing effect.[103]

Examples of cleavable linkers with labile functional groups are hydrazones (e.g. **41**, **Figure 21**), sensitive to hydrolysis at low pH following internalisation, or disulfides (e.g. **42**), which are reductively cleaved by glutathione, present in a higher concentrations inside the cells. The third common type of linkage are peptide bonds (e.g. **43** or **44**), often used in combination with a spacer unit such maleimide or as *para*-aminobenzylcarbamate (PABC), which separates the drug from the site of enzymatic cleavage. Upon the action of lysosomal proteases (e.g. cathepsin B), the spacer undergoes self-immolation, releasing the toxin in a chemically unmodified, fully active form.

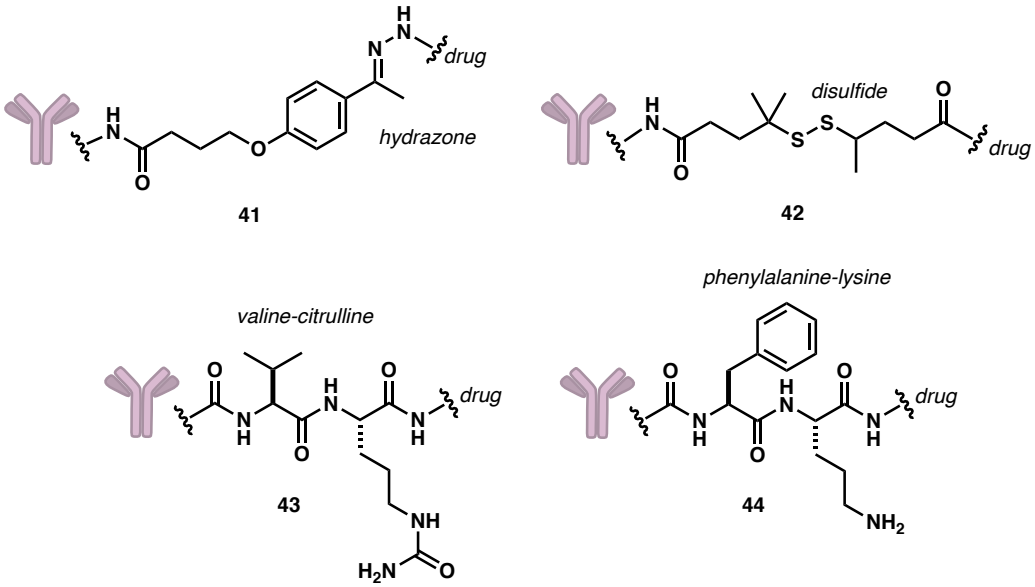

Figure 21 A representative selection of commonly utilised cleavable linkers in ADCs

Non-cleavable linkers rely on proteolytic degradation of the whole antibody into amino acids in the lysosome, which liberates a modified version of the cytotoxin with attached remnants of the linker or the antibody. Structurally, they are typically alkyl, sulfonyl or polyethyleneglycol (PEG) chains with suitable functionality at the terminus to facilitate conjugation.

1.3.3. The Payload

Due to drug decomposition and metabolic processes in the body, only 0.01–0.1% of the injected dose of ADCs comes into action per gram of tumour mass, then further reduced by inefficient payload release, extracellular trafficking or poor permeability into the tumour.[96] The number of drug molecules required for antimitotic activity should thus be substantially below the delivery threshold of an ADC and the required IC_{50} value of the unconjugated toxin in the subnanomolar range (100–1000 times more potent than regular chemotherapeutics). The therapeutic dose *via* this delivery route is merely a fraction of the quantity administered by traditional chemotherapy in comparison, which is favourable from the point of view of large-scale ADC manufacturing.

At present, the majority of marketed ADCs or those in clinical research fall into two categories based on their mechanism:[93] microtubule inhibitors (e.g. maytansines, tubulysins, auristatins) or DNA-damaging agents (e.g. duocarmycins). Further advances towards optimising the payload need not to be geared strictly towards increasing potency but also finding alternative mechanisms of action which set them apart from the ones currently dominating the field. One such successful example recently emerged are

benzodiazepines, natively potent DNA crosslinkers which were developed into DNA alkylating agents through purely chemical design.[95]

1.3.4. Conjugation Methods

To achieve predictable properties, the ADCs must be produced with a highly controlled drug to antibody ratio (DAR), which affects the drug's efficacy and rate of aggregation.[104] The ideal DAR is typically 2–4, though highly dependent on the nature of each ADC component and must be empirically determined. The majority of ADCs in development are prepared using the non-specific conjugation techniques *via* either the highly reactive, solvent-accessible lysines or the cysteine residues on the antibody. Lysine ligation almost always involves acylation chemistry and due to the uneven distribution of approximately 30 available lysines on the mAb, non- specific linkage causes substantial heterogeneity in the ADC.[105] Conjugation through cysteine on the other hand is executed through thiol groups on the mAb which are tethered as four inter-chain disulfide bridges and liberated prior to conjugation by mild S –S bond reduction. Michael addition of the liberated thiol handles onto a maleimide group then produces non-cleavable succinimide thioether linkages, which are featured in both currently marketed ADCs (*vide infra*). Additional control of the ligation can be achieved by engineering non-native cysteines on the mAb surface or linking both bridge thiols to a single moiety (e.g. PolyTherics' ThioBridge™ technology, **Scheme 3**).[99] Importantly, these alterations must not perturb the three-dimensional structure of the mAb.

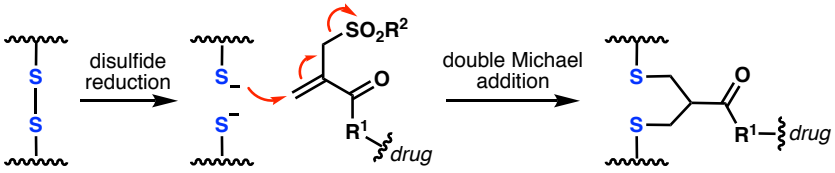

Scheme 3 Schematic of the ThioBridge™ disulfide conjugation technology[99]

Other methods of site-specific linkage *via* sequence editing include introduction of serines for oxime ligation (pioneered by MedImmune and Immunogen),[106] glycoconjugation with unnatural fucose derivatives or biorthogonal reactions of engineered unnatural amino acids (e.g. azide click chemistry).

1.3.5. Challenges for Next-Generation ADC Development

The expensive development process, combined with the low success rate in clinical trials makes ADCs not only a high-investement, but also a high-risk venture for pharmaceutical companies. Despite these drawbacks, the field has reached defined milestones following the FDA approval and launch of trastuzumab emtansine **45** (Kadcyla®) and brentuximab vedotin **46** (Adcetris®, **Figure 22**). Each subsequent generation of ADCs has a greater chance of success in clinical trials due to increased control

of factors in the manufacture process, widening the therapeutic window.[91,92,107] In particular, this pertains to the diversification of linker strategies and recognition of new tumour-specific antigens.

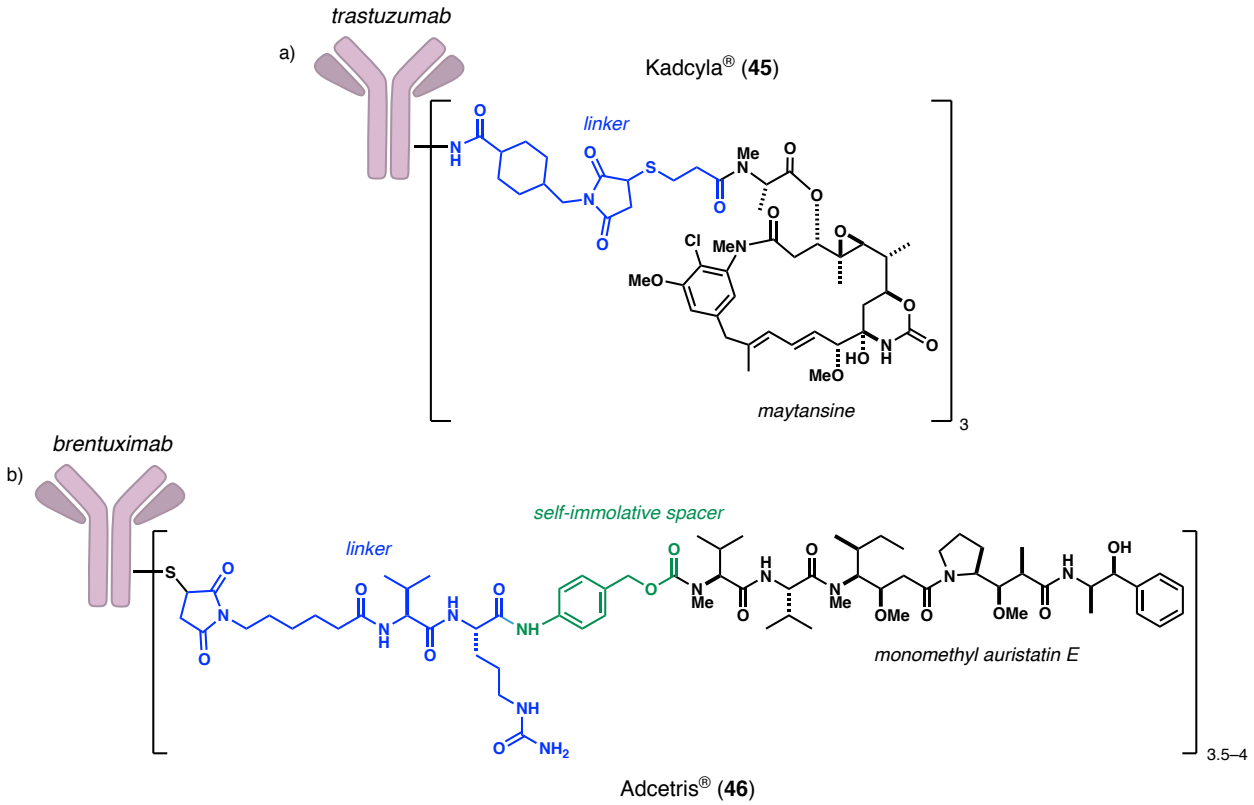

Figure 22 ADCs currently in clinical use. a) Trastuzumab emtansine contains a non-cleavable peptide linker conjugated *via* the pre-functionalised maleimide on the mAb. b) Brentiximab vedotin features a cleavable valine-citrulline linker with maleimide conjugation to the mAb and a self-immolative spacer unit.

ADCs are not immnue to resistance mechanisms, which are already beginning to emerge in the clinic.[95] Treatment with ADCs may induce downregulation of either tumour-associated antigen expression or slowing down of antigen–ADC internalisation as a mode of escape.[91] Resistance to the payload itself may be overcome with the search for therapeutics with novel mechanisms of actions, though they are extremely rare. In the meantime, the ADC technology offers an ideal opportunity to examine the warhead potential of potent cytotoxins, which previously failed in clinical trials as standalone treatments.[29,97]

1.3.6. The Aplyronines as Payload Candidates

Despite the seemingly unattainable requirements for an ideal ADC payload, the aplyronines meet nearly all the fundamental ones. Their *in vitro* activity has been assessed against a vast range of cancer cell lines and even *in vivo* which ascertained an excellent potency across the board. Extensive SAR studies by Yamada have revealed the key binding regions within the molecule, leaving several possible functional

handles for linker attachment as well as chemical modifications through analogues to further boost the potency. The most promising feature of all is undisputedly the exciting, unprecedented mechanism of action, which while still not yet fully elucidated, holds tremendous promise with regards to battling resistance pathways. Conjugation to an antibody would both reduce the high likelihood of toxicity given the aplyronines' biological targets but also bring down the amounts of these scarce compounds for therapeutic use. The currently supply, however, is minute and thus the potential advances towards the aplyronine ADCs are entirely reliant upon devising an efficient and scalable synthetic route.

1.4. Previous Synthetic Efforts

The aplyronines are evidently a formidable synthetic target with some truly impressive efforts published by a number of research groups. To date, three total syntheses have been disclosed beginning with the pioneering work by Yamada in 1994 which confirmed the structure and absolute configuration of aplyronines A[38,42] and later congeners B and C.[41] The Paterson group completed the synthesis of aplyronine C in 2013,[108–110] and additionally aplyronines A and D in 2015.[111] In early 2017, Kigoshi reported a second-generation route towards aplyronine A,[112] building upon the strategy of an aplyronine A–mycalolide B hybrid previously targeted by the same group.[79,113]

Marshall,[114] Calter[115,116] and Fuchs[117–119] have also prepared several fragments, implementing the groups' own methodologies for the construction of stereotetrads. On the whole, there is very little divergence from the major disconnections and fragment assembly strategies utilised in the Yamada and Paterson routes apart from Kigoshi's unique approach to the macrocycle assembly. A brief comparison of the similarities in the overall retrosynthetic analysis is shown in **Figure 23**. The Paterson route is discussed in greater detail in Chapter 2.

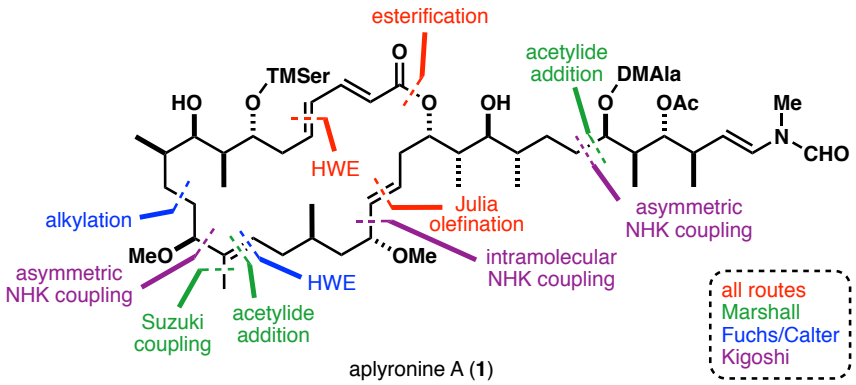

Figure 23 Common disconnections in the Marshall, Calter, Fuchs and Kigoshi approaches to the aplyronines

1.4.1. Yamada Synthesis of Aplyronines A, B and C

A year after their first publication on the discovery of the aplyronines,[2] Yamada and co-workers completed the total synthesis of aplyronine A.[42] This work provided conclusive evidence of the absolute configuration of stereocentres through enantioselective synthesis following the initial elucidation of the gross structure.[38–40] Retrosynthetic analysis of Yamada's route is illustrated in **Scheme 4**. The pivotal disconnections break the molecule into the C_5–C_{20} aldehyde **47** and the C_{21}–C_{34} sulfone **48**. Both can be further fragmented into five appropriately functionalised subunits (**49**–**53**), which largely mirror the segments obtained in the degradation studies.[39] These segments were linked together by utilising sulfone chemistry, namely Julia olefinations and alkylations. Other key steps are the Horner–Wadsworth–Emmons (HWE) reaction to install the C_1–C_5 (*E*,*E*)-dienoate, regioselective Yamaguchi macrolactonisation with the complete C_1–C_{34} carbon framework in place and a late-stage condensation to introduce the sensitive *N*-methyl-*N*-vinylformamide moiety.

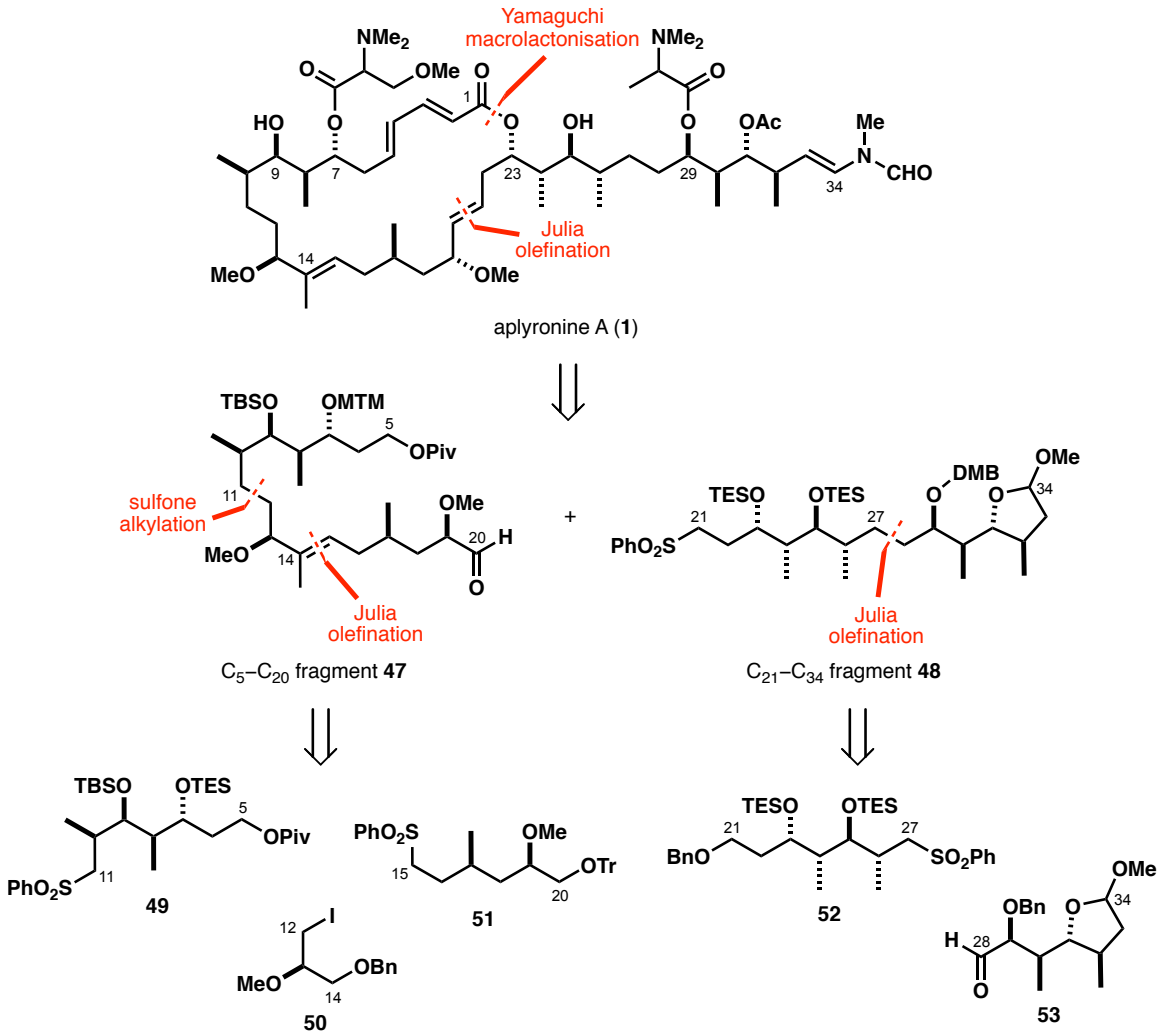

Scheme 4 Yamada's synthetic approach to aplyronine A (**1**)

The contiguous stereoclusters at C_7–C_{10}, C_{23}–C_{26} and C_{29}–C_{32} were conveniently segregated into three small subfragments. Each stereotetrad was introduced using a common eight-step protocol (**Scheme 5**) starting with a *syn* Evans aldol reaction[120,121] between the required enantiomer of the chiral imide (**54** or **55**) to induce stereocontrol and a suitable aldehyde electrophile. Protected aldol adducts underwent HWE[122] olefination to introduce an allylic alcohol moiety for epoxidation under Sharpless conditions[123] and regioselective opening of the ensuing epoxide to afford 1,3-diols **56**–**58**. All three fragments were further manipulated at the termini to provide the necessary functional handles for elongation of the carbon chain.

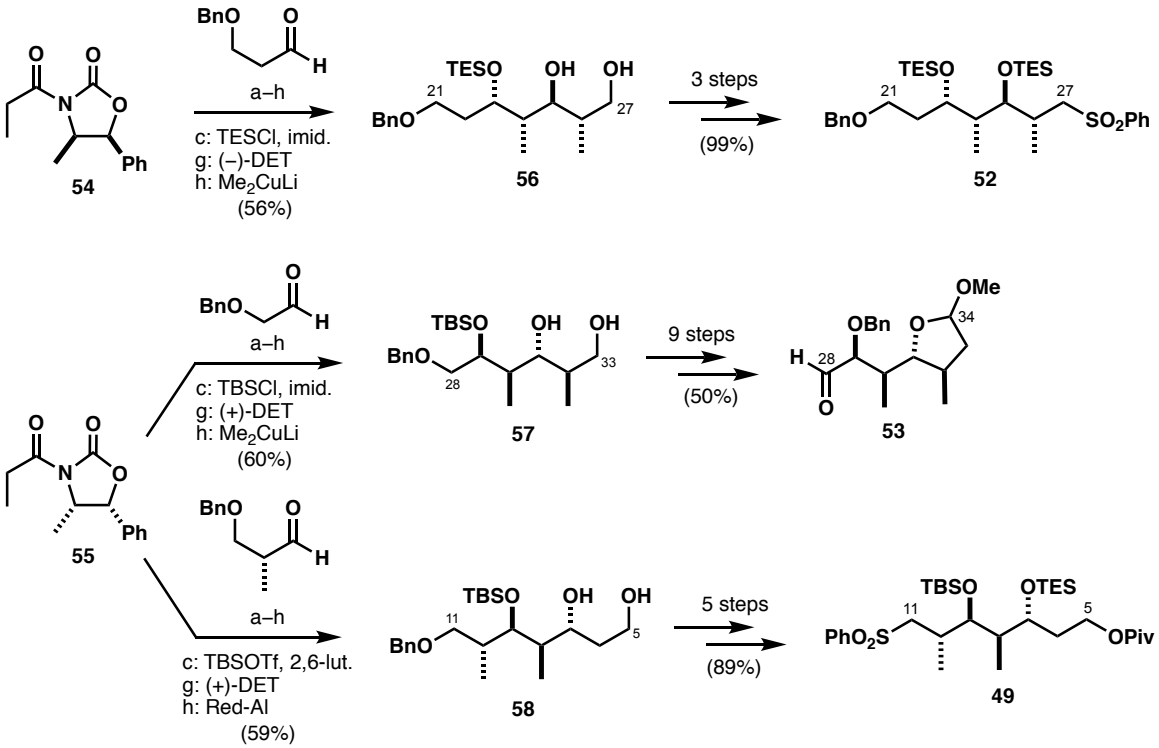

(a) Bu_2BOTf, Et_3N; (b) $Me_2AlN(Me)OMe$; (c) silyl protection; (d) DIBALH; (e) $(^iPrO)_2P(O)CH_2CO_2Et$, ^{t}BuOK; (f) DIBALH; (g) $Ti(^iPrO)_4$, diethyl tartrate, ^{t}BuOOH, 4 Å MS; (h) epoxide opening

Scheme 5 Enantioselective synthesis of the stereotetrads *via* the Evans aldol/Sharpless asymmetric epoxidation sequence by Yamada

Iodide **50** was prepared in seven steps from acetonide **59**, making C_{13} one of only two stereocentres sourced from the chiral pool (**Scheme 6**). Similarly, Yamada utilised the known furanone **60**, which enabled the configuration of the remote C_{17} methyl by facially selective alkylation, reductive ring opening and functionalisation of the terminal carbon atoms.

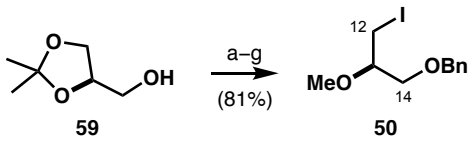

(a) NaH, BnBr; (b) HCl, aq. acetone; (c) TBSCl, Et_3N, DMAP; (d) NaH, MeI; (e) TBAF; (f) TsCl, pyr; (g) NaI

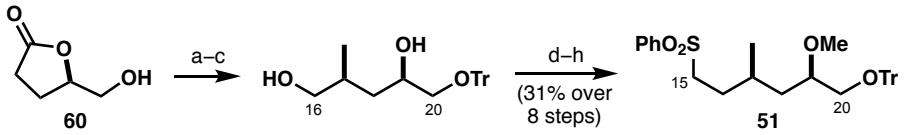

(a) TrCl, pyr; (b) LDA, MeI; (c) $LiAlH_4$; (d) TBDPSCl; (e) NaH, MeI; (f) TBAF; (g) TsCl, pyr; (h) ^{n}BuLi, $PhSO_2Me$

Scheme 6 Yamada's synthesis of the C_{12}–C_{14} iodide **50** and C_{15}–C_{20} sulfone **51**

Julia olefination[124] forged the C_{20}–C_{21} bond between sulfone **52** and aldehyde **53** (9:1 *E*/*Z*), which was subsequently subjected to hydrogenation. Concomitant double debenzylation enabled a protecting group change at C_{29} and sulfone installation at C_{21} to furnish C_{21}–C_{34} fragment **48** in 24 steps longest linear sequence (LLS) and 22% yield (**Scheme 7**).

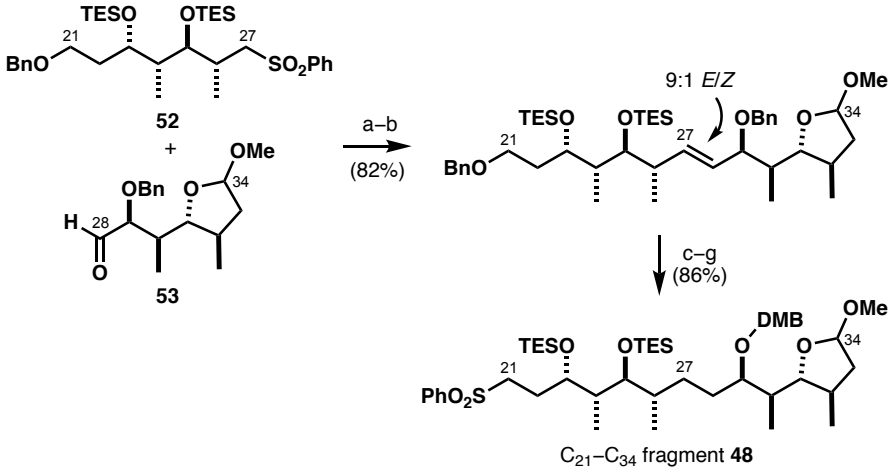

(a) ^{n}BuLi; (b) 5% Na-Hg, Na_2HPO_4; (c) Ca, ^{i}PrOH, liquid NH_3; (d) H_2, 5% Rh/Al_2O_3; (e) $(PhS)_2$, PBu_3; (f) *m*-CPBA; (g) DMBCl, ^{i}PrNEt$_2$

Scheme 7 Union of **52** and **53** and elaboration to the C_{21}–C_{34} sulfone **48** in the Yamada route

The remaining three segments were coupled by alkylation of sulfone **49** with iodide **50** and derivatisation of the C_{14} terminus into a methyl ketone (**54**) set the scene for a Julia reaction with the C_{15}–C_{20} sulfone **51**. Construction of the trisubstituted olefin transpired to be problematic as the product was isolated as a mixture of (*E*)-isomer **55** in 44% yield, along with 19% of the undesired (*Z*)-olefin **56** and 25% tertiary alcohol **57** as the two major side products. Next, the C_{20} terminus was engaged in another Julia coupling reaction with the C_{21}–C_{34} fragment **48** with reasonable *E*/*Z* selectivity and good yield (9:1 *E*/*Z*, 88%).

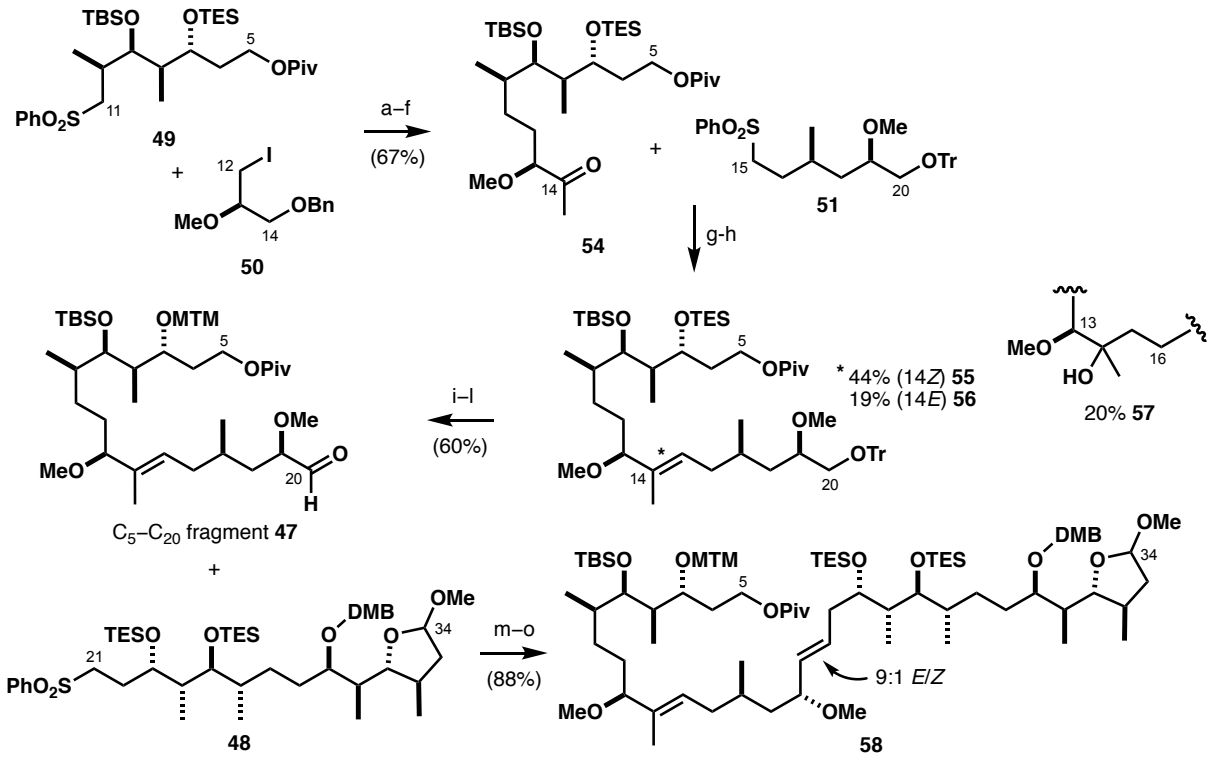

(a) LDA, HMPA; (b) 5% Na-Hg, Na_2HPO_4; (c) H_2, 10% Pd/C, $NaHCO_3$, EtOH; (d) Dess–Martin periodinane, pyr; (e) Me_2CuLi; (f) Dess–Martin periodinane, pyr; (g) ^{n}BuLi; (h) 6% Na-Hg, Na_2HPO_4; (i) AcOH, H_2O, THF; (j) DMSO, Ac_2O, AcOH; (k) HCO_2H; (l) Dess–Martin periodinane, pyr; (m) ^{n}BuLi; (n) Ac_2O, DMAP, pyr; (o) 5% Na-Hg, Na_2HPO_4

Scheme 8 Coupling of the C_5–C_{20} aldehyde **47** and C_{21}–C_{34} sulfone **48** by Yamada

The C_5 position was unmasked prior to HWE attachment of the C_1–C_5 (*E*,*E*)-dienoate (15:1 *E*/*Z*), which was followed by hydrolysis of the methyl ether and the silyl ethers at C_{23} and C_{25} to reveal the macrolactonisation sites (**Scheme 9**). Under the modified Yamaguchi protocol,[125] ring closure afforded a 4:3 mixture of regioisomers with the preference for the smaller, 24-membered macrocycle **61** in 68% combined yield. The undesired 26-membered macrocyclic byproduct **60** was subjected to a Lewis acid-mediated transesterification to further increase the yield of the desired macrolactone **61**. This intermediate represents a common precursor to multiple aplyronine congeners by attaching the appropriate amino acids in the final steps, relying on an orthogonal protecting group strategy.

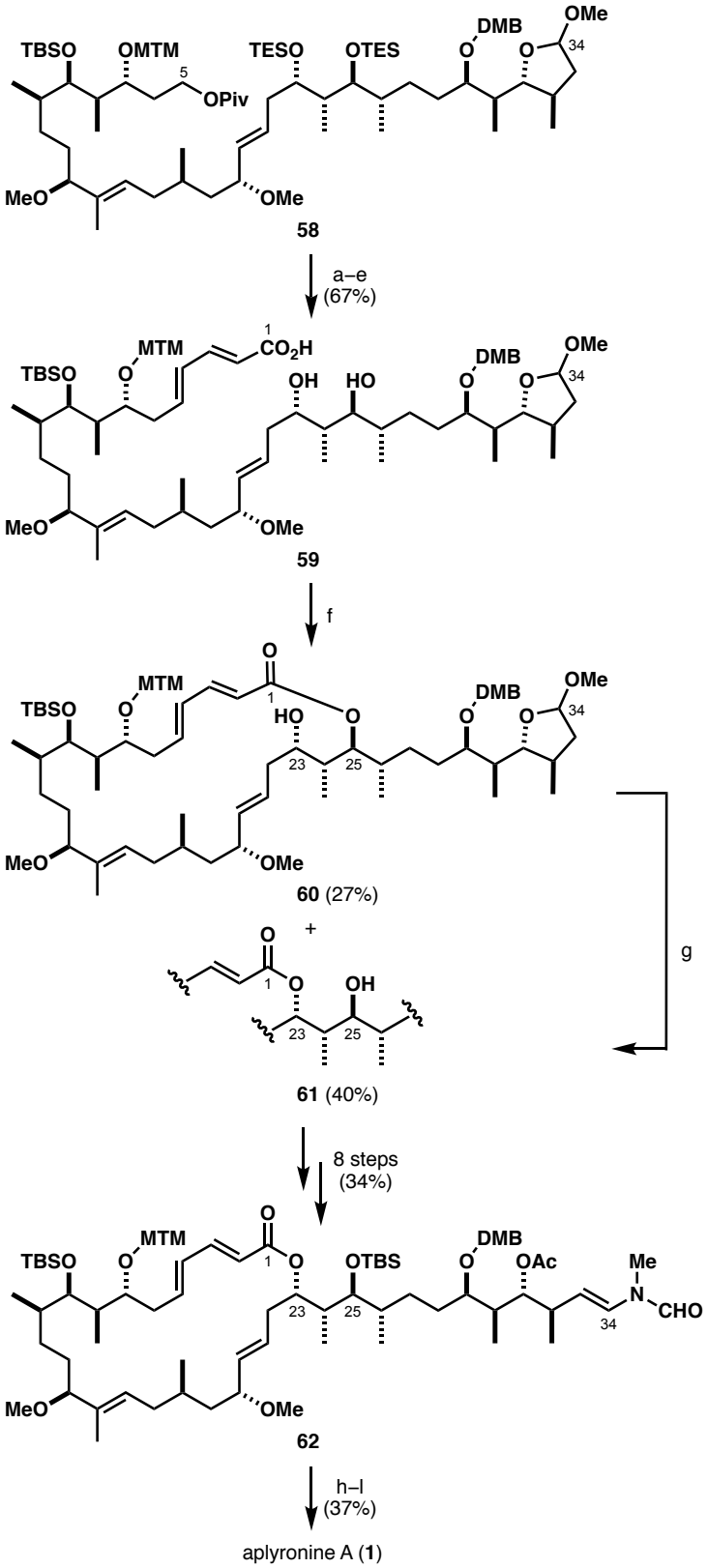

(a) DIBALH; (b) Dess–Martin periodinane, pyr; (c) $(EtO)_2P(O)CH_2CH{=}CHCO_2Et$; (d) HF·pyr, pyr; (e) LiOH, MeOH; (f) TCBC, DMAP, Et_3N; (g) $Ti(^iPrO)_4$; (h) DDQ; (i) *N*,*N*-dimethylalanine (3:2 *S*/*R*), DCC, DMAP, CSA; (j) $AgNO_3$, 2,6-lut.; (k) *N*,*N*-trimethylserine (5:2 *S*/*R*), DCC, DMAP, CSA; (l) HF·pyr, pyr

Scheme 9 Yamada's endgame and total synthesis of aplyronine A (**1**)

After silyl protection of the C_{25} hydroxyl, the terminal acetal was hydrolysed and condensed with *N*-methylformamide under the Pattenden conditions[126] (PPTS, hydroquinone) to install the *N*-vinylformamide in a modest yield (48%). The C_{29} and C_7 amino acids were appended by sequential removal of the 3,4-dimethoxybenzyl (DMB) and methylthiomethyl (MTM) ethers, then esterification with the DMAla or TMSer under the Keck variant of the Steglich conditions (DCC, DMAP, CSA).[127] Yamada observed that the amino acids partially epimerised in the activated form and thus a carefully chosen scalemic mixture of *R*/*S* enantiomers had to be added to the substrate for the ratio in the product to match that found in natural aplyronine. After a global deprotection, aplyronine A (**1**) was obtained in 0.4% yield from the (*S*)-Evans imide **55** in 47 steps LLS and 98 steps in total. As noted above, Yamada was also able to use the late-stage intermediate **62** to complete the first total syntheses of aplyronines B (**12**) and C (**13**).

Despite an impressive effort towards the total synthesis of the aplyronines the route does suffer from several drawbacks. At the time it was imperative to construct the stereocentres in a way that enabled a divergent route to all possible permutations of the 15 chiral centres present. Yamada's approach was therefore designed with a high degree of flexibility in mind, which inevitably sacrificed conciseness on the account of numerous functional group manipulations and resulted in a synthesis consisting of nearly 100 steps in total. The number may seem daunting but the average yield per step is impressively high when excluding several obvious weak points, e.g. the C_{14}–C_{15} Julia coupling and formation of the terminal *N*-vinylformamide.

Yamada was able to apply the strategy to carry out extensive structure-activity relationship studies, which provided a large body of knowledge on the activity of the aplyronines.[71,72] However, in order to supply material for further biological studies, an entirely new synthesis would have to be devised to improve the overall process.

1.4.2. Marshall, Calter and Fuchs' Approach

In 2000, Marshall reported the synthesis advanced fragments, C_5–C_{20} (**63**) and C_{21}–C_{34} (**64**) which contained all 15 stereocentres of the core aplyronine structure (**Scheme 11**). The retrosynthetic plan showcases Marshall's diastereoselective propargylation,[128] which can set up six new stereocentres in three separate stereotriads (C_8–C_{10}, C_{24}–C_{26} and C_{30}–C_{32}). A highly distinct feature of Marshall's synthetic plan is the construction of the trisubstituted C_{14}–C_{15} double bond through acetylide addition and Suzuki coupling,[129] starting from the (*Z*)-vinyl triflate.[130]

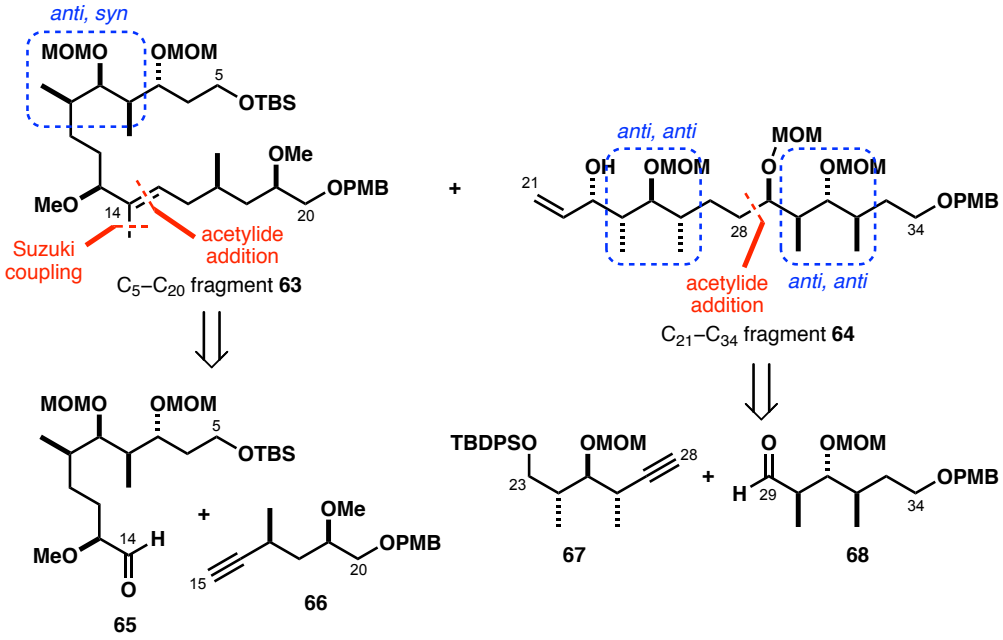

Scheme 11 Marshall's retrosynthetic strategy for the key fragments **63** and **64**

The foundation of Marshall's approach lies in the *in situ* formation of allenylindium species from chiral secondary propargyl mesylates in the presence of an indium(I) salt, followed by reagent-controlled addition into an α-chiral aldehyde (**Scheme 12**). The resulting stereotriads are formed in comparable selectivity for both the Felkin and *anti*-Felkin attack.[131]

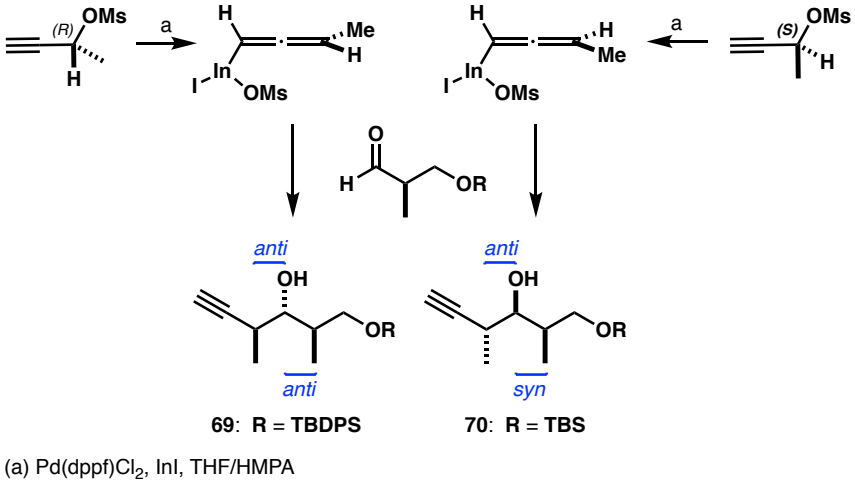

Scheme 12 Marshall's allenylindium methodology for constructing stereotriads[128]

The C_5–C_{14} fragment **63** was prepared by functionalisation of the *anti*, *syn* addition product **70** at the C_7 and C_{12} termini to install the C_7 and C_{13} stereocentres, respectively (**Scheme 13**). This was achieved by a sequence involving chain homologation, Sharpless asymmetric epoxidation, iodination and epoxide opening (Scheme **13**). The C_{15}–C_{20} unit **66** was synthesised in six steps from the chiral lactone **60** *via*

facially selective alkylation and Seyferth–Gilbert homologation.[132] After coupling of fragments **65** and **66** *via* acetylide addition and construction of the trisubstituted olefin, the fully elaborated C_5–C_{20} fragment **63** was accessed in 24 steps LLS and 4% yield from TBS-protected aldehyde **71**.

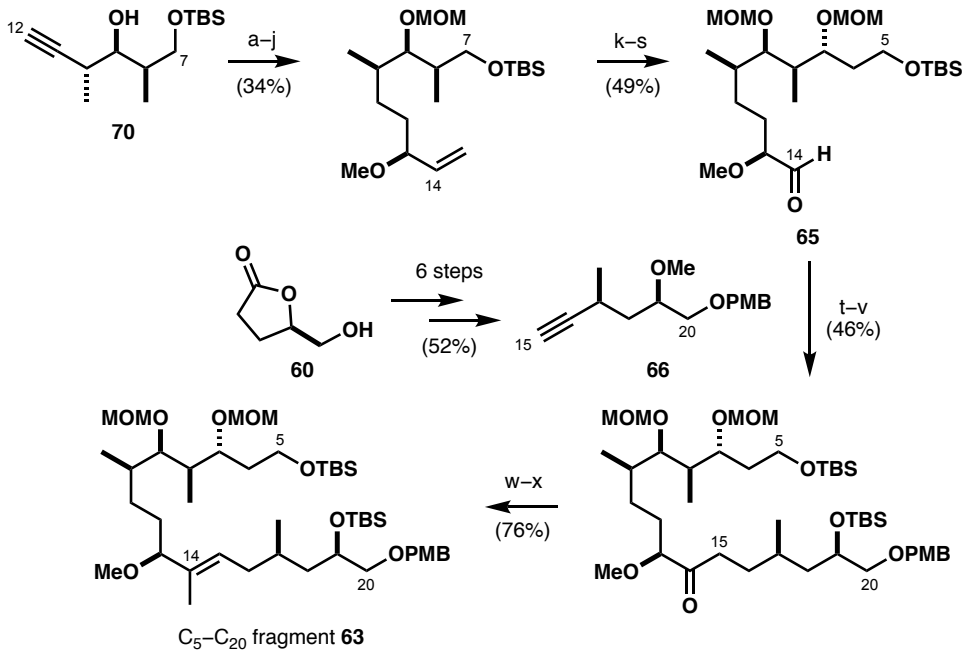

(a) MOMCl, TBAI, $^{i}Pr_2NEt$; (b) $^{n}BuLi$, $(CH_2O)_n$; (c) $TsNHNH_2$, NaOAc; (d) Dess–Martin periodinane, $NaHCO_3$; (e) $Ph_3P{=}CHCO_2Et$; (f) DIBALH; (g) $Ti(O^{i}Pr)_4$, (+)-diisopropyl tartrate, $^{t}BuOOH$; (h) I_2, PPh_3, imid.; (i) Zn, EtOH; (j) NaH, MeI, 15-crown-5; (k) TBAF; (l) Dess–Martin periodinane, $NaHCO_3$; (m) $Ph_3P{=}CHCO_2Et$; (n) DIBALH; (o) $Ti(O^{i}Pr)_4$, (+)-diisopropyl tartrate, $^{t}BuOOH$; (p) Red-Al; (q) TBSCl, imid.; (r) MOMCl, TBAI, $^{i}Pr_2NEt$; (s) O_3, *then* Me_2S; (t) $^{n}BuLi$, **66**; (u) $TsNHNH_2$, NaOAc; (v) Dess–Martin periodinane, $NaHCO_3$; (w) LiHMDS, Comins' reagent; (x) MeLi, 9-BBN-OMe, $Pd(dppf)Cl_2$, K_3PO_4

Scheme 13 Synthesis of the C_5–C_{20} fragment **63** by Marshall

The C_{21}–C_{34} fragment **64** was accessed from propargyl alcohols **69** and **72**. Coupling of the appropriately functionalised units by lithium acetylide addition was followed by installation of the final C_{22} stereocentre *via* the familiar sequence based around Sharpless epoxidation (**Scheme 14**) to produce the C_{21}–C_{34} fragment **64** in 18 steps LLS from alcohol **72**. Overall, Marshall's route heavily relies on chiral pool starting materials and is unlikely to lead to the aplyronines without a revision of the protecting group strategy given the current lack of differentiation between the key hydroxyls.

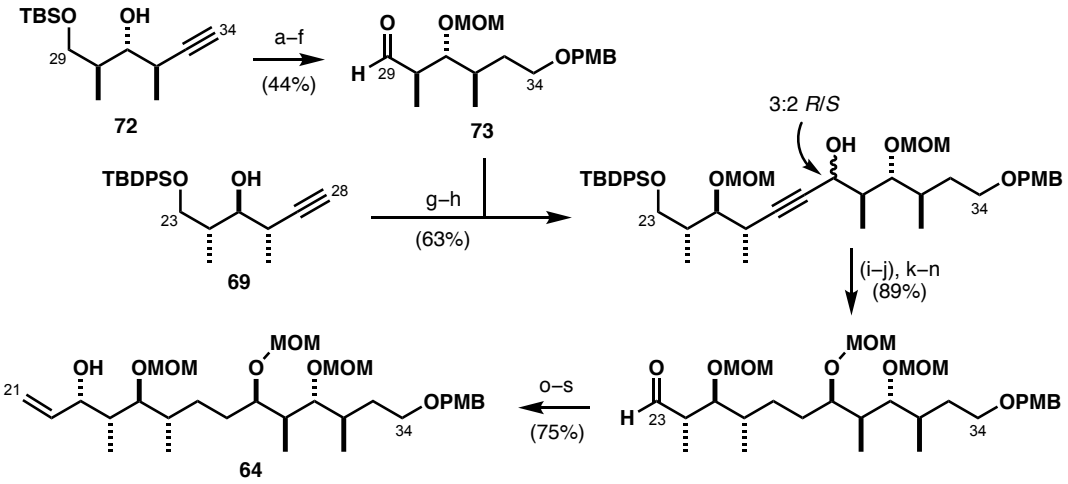

(a) MOMCl, TBAI, $^{i}Pr_2NEt$; (b) Cy_2BH, *then* H_2O_2, NaOH; (c) DIBALH; (d) NaH, PMBCl, TBAI, 15-crown-5; (e) TBAF; (f) Dess–Martin periodinane, $NaHCO_3$; (g) MOMCl, TBAI, $^{i}Pr_2NEt$; (h) $^{n}BuLi$, ; (i) DIAD, *p*-$NO_2C_6H_4CO_2H$, PPh_3; (j) DIBALH; (k) $TsNHNH_2$, NaOAc; (l) MOMCl, TBAI, $^{i}Pr_2NEt$; (m) TBAF; (n) Dess–Martin periodinane, $NaHCO_3$; (o) $Ph_3P{=}CHCO_2Et$; (p) DIBALH; (q) $Ti(O^{i}Pr)_4$, (+)-diisopropyl tartrate, $^{t}BuOOH$; (r) I_2, PPh_3, imid.; (s) Zn, MeOH

Scheme 14 Marshall's route towards the C_{21}–C_{34} fragment **64** from propargyl alcohol **72**

Calter's efforts towards the aplyronines culminated in the synthesis of the C_{21}–C_{34} sulfone **74**[115] and an advanced C_1–C_{27} intermediate **76** (**Scheme 15**).[116] The skeleton assembly follows the disconnections of Yamada and Paterson whereas the stereocentres are introduced by Calter's asymmetric dimerisation reactions[133,134] and diastereoselective aldol reactions.[135]

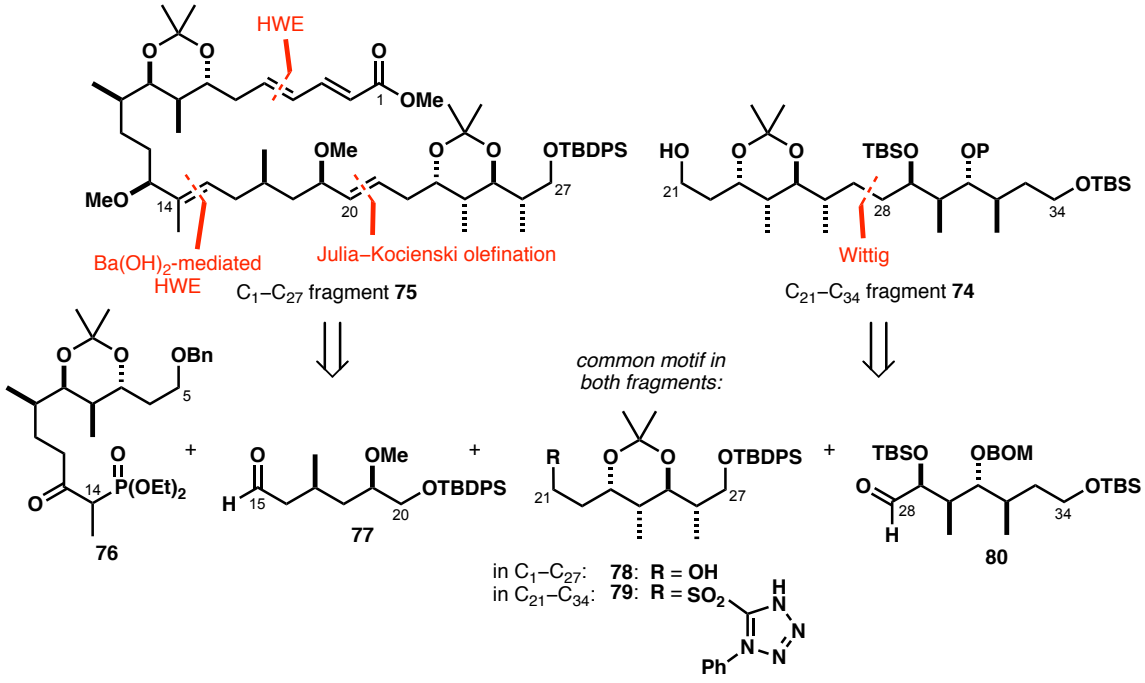

Scheme 15 Retrosynthetic analysis of fragments C_1–C_{27} (**75**) and C_{21}–C_{34} (**74**) by Calter

Calter's methodology employs cinchona alkaloid catalysts (TMSQ or TMSQD) to induce enantioselectivity in dimerisation of *in situ* formed methylketene *via* formation of an ammonium enolate, followed by a formal Claisen condensation of the second ketene unit (**Scheme 16**).[133,134] The resulting chiral β-lactones are then transformed into suitable enolate derivatives and used as aldol substrates to produce β-hydroxy ketone adducts **81** and **82** contain the required 1,4-*syn*-3,4-*syn* motifs.

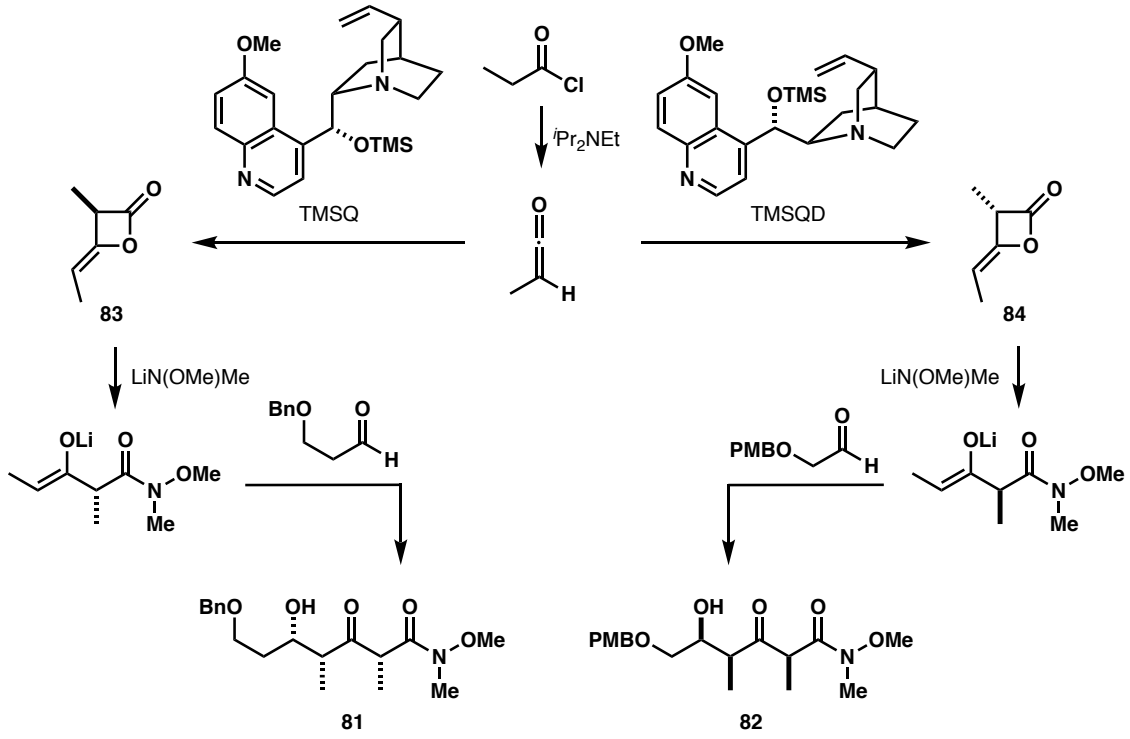

Scheme 16 Calter's organocatalytic asymmetric ketene dimerisation and stereoselective aldol reactions[133,135]

The C_{21}–C_{27} subunits **78** and **79**, derived from the common intermediate **85**, were elaborated to provide the suitably functionalised to furnish sulfone **79** and ylid **86** (Scheme **17**).[115]

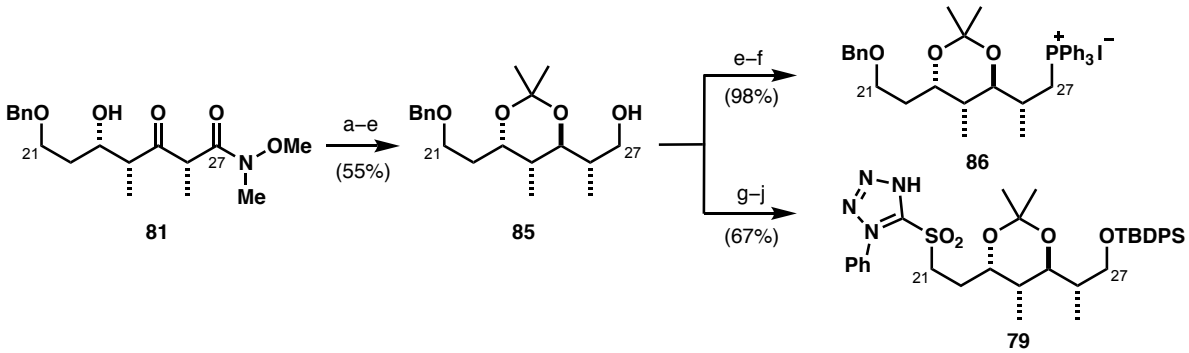

(a) $NaBH(OAc)_3$, AcOH; (b) 2,2-dimethoxypropane, TsOH; (c) DIBALH; (d) $NaBH_4$; (e) I_2, PPh_3, imid.; (f) PPh_3, $^iPrNEt_2$; (g) TBDPS-Cl, Et_3N; (h) LiDBB; (i) 1-phenyl-1H-tetrazole-5-thiol, DIAD, PPh_3; (j) H_2O_2, $(NH_4)_2MoO_4$

Scheme 17 Calter's synthesis of the C_{21}–C_{27} fragments **79** and **86** from β-hydroxy ketone **81**

β-Hydroxy ketone **82** was homologated at C_{33} in preparation for Wittig olefination with ylid **86**, which led to the C_{21}–C_{34} alcohol **74** in three further steps and an overall 13% yield from lactone **83** (**Scheme 18**).

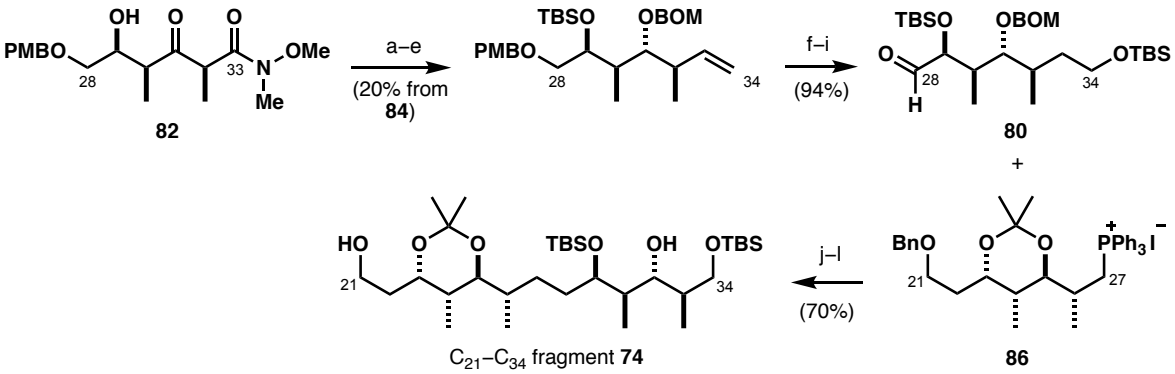

(a) TBSOTf, 2,6-lut.; (b) $KBEt_3H$; (c) BOMCl, $^iPrNEt_2$; (d) DIBALH; (e) NaHMDS, $MePPh_3^+Br^-$ (f) 9-BBN-H, *then* H_2O_2, NaOH; (g) TBSOTf, 2,6-lut.; (h) DDQ; (i) Dess–Martin periodinane, pyr; (j) LiHMDS; (k) H_2 (1 atm), 20% $Pd(OH)_2$/C, EtOH; (l) H_2 (55 psi), 5% Rh/Al_2O_3, EtOAc

Scheme 18 Preparation of the C_{28}–C_{34} aldehyde **80** from aldol adduct **82** and fragment coupling to the C_{21}–C_{34} alcohol **74** by Calter

The C_7–C_{10} cluster required an alternative approach *via* a boron aldol with the α-chiral ethyl ketone **87**. With the exception of the delayed C_1–C_5 dienoate installation, the sequence of steps to functionalise the fragment at the C_{11} terminus mirrors the Paterson strategy for that region of the macrocycle (**Scheme 19**), ending with the β-ketophosphonate moiety appendage.[110] The C_{15}–C_{20} aldehyde partner **77** for the HWE coupling was prepared in five steps from the furanone **88**.

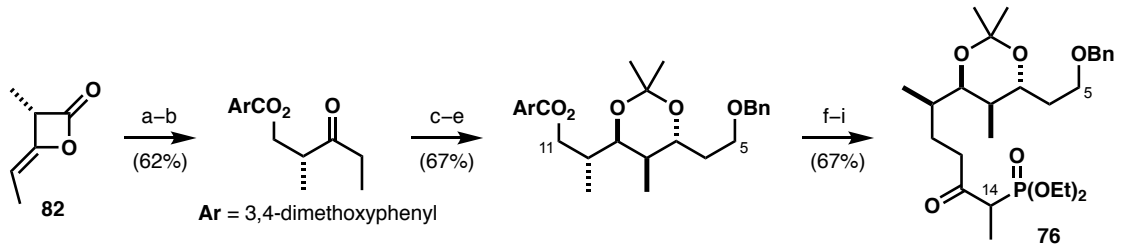

(a) $LiAlH_4$; (b) $[C(O)Ar]_2$, DMAP, pyr; (c) Cy_2BCl, Et_3N, *then* 3-(benzyloxy)propanal; (d) $NaBH(OAc)_3$, MeCN, AcOH; (e) 2,2-dimethoxypropane, PPTS; (f) K_2CO_3, MeOH; (g) I_2, PPh_3, imid.; (h) diethyl (3-oxobutan-2-yl)phosphonate, NaH, ^{n}BuLi

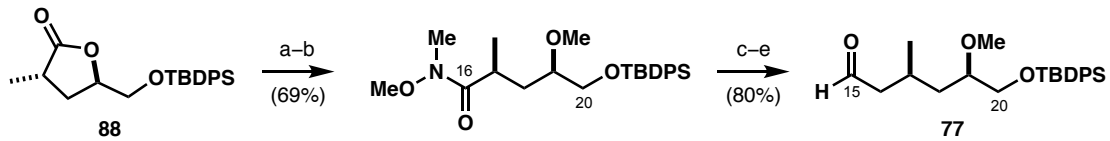

(a) Me(OMe)NH·HCl, $AlMe_3$; (b) MeOTf, di-^{t}Bu-pyr; (c) DIBALH; (d) Ph_3P=CH(OMe); (e) HCl

Scheme 19 Construction of the C_5–C_{14} phosphonate **76** from lactone **84** and aldehyde **77** from chiral furanone **88**

The HWE olefination-CBS reduction-methylation sequence was followed by appendage of the dienoate (6:1 *E*/*Z*) at C_5 and a Julia–Kocienski reaction (7:1 *E*/*Z*) to construct the C_{20}–C_{21} double bond. The C_1–C_{27} fragment **75** was accessed in 5% yield and 17 steps LLS from methylketene dimer **84**. Strengths of Calter's strategy are convergence and formation of chiral centres with a high degree of control.

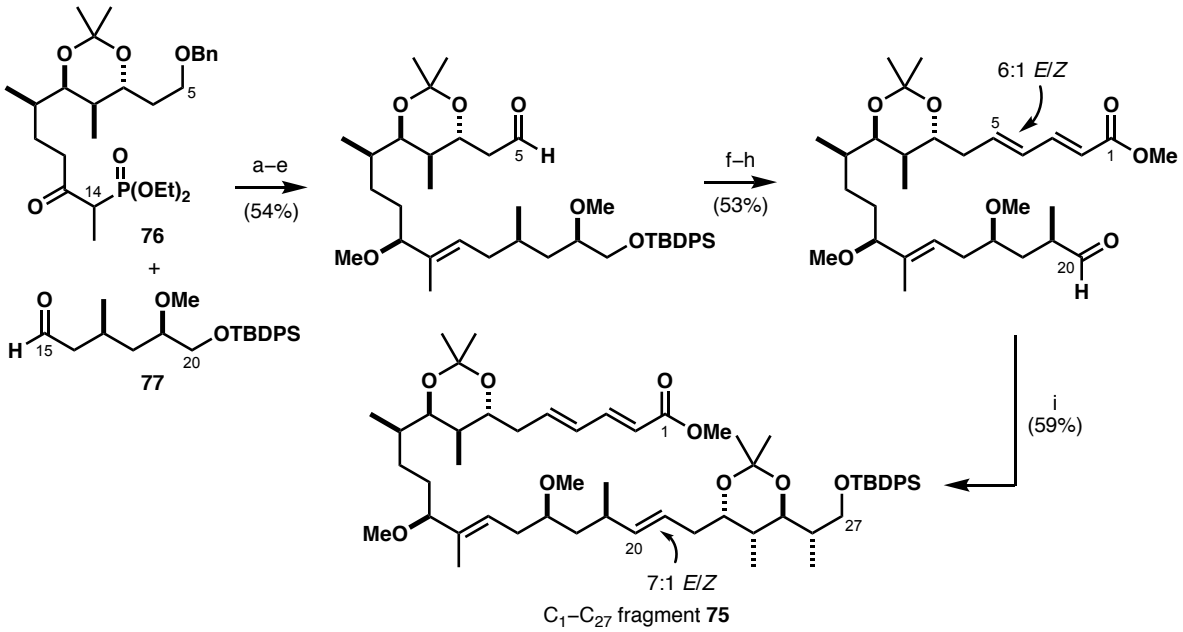

C_1–C_{27} fragment **75**

(a) $Ba(OH)_2$; (b) (*R*)-Me-CBS catalyst, $BH_3 \cdot SMe_2$; (c) NaH, MeI; (d) LiDBB; (e) $(COCl)_2$, DMSO, Et_3N; (f) LiOH, 4 Å MS; (g) TBAF, AcOH; (h) $SO_3 \cdot pyr$, Et_3N, DMSO; (i) KHMDS, **79**

Scheme 20 HWE coupling of **76** and **77** and elaboration to the C_1–C_{27} fragment **75** by Calter

Fuchs achieved an enantioselective syntheses of the C_1–C_{20} and C_{15}–C_{27} segments **89** and **90**[119] and a C_{32}-desmethyl analogue of the C_{28}–C_{34} fragment **91**.[136] Chirality was introduced by Fuchs' oxidative cleavage of cyclic vinyl sulfones, each containing one of the polypropionate clusters highlighted in **Scheme 21** below.[117] The envisaged major disconnections in the Fuchs route towards the aplyronines match those of Calter.

Fuchs' methodology is based on preparing termini-differentiated acyclic arrays of contiguous stereocentres starting by regioselective Jacobsen epoxidation[137] of achiral, cross-conjugated dienyl sulfones.[138] Further derivatisation exploits the reactivity of allylic or vinylic positions, diene transposition and facial bias of the 6- or 7-membered rings. In particular, Fuchs makes use of the double Lawton S_N2' addition[139] to an allylic epoxide with 3,5-dimethylpyrazole nucleophile or direct opening of the epoxide with a methyl source, depending on the exact substitution pattern on the carbon chain.

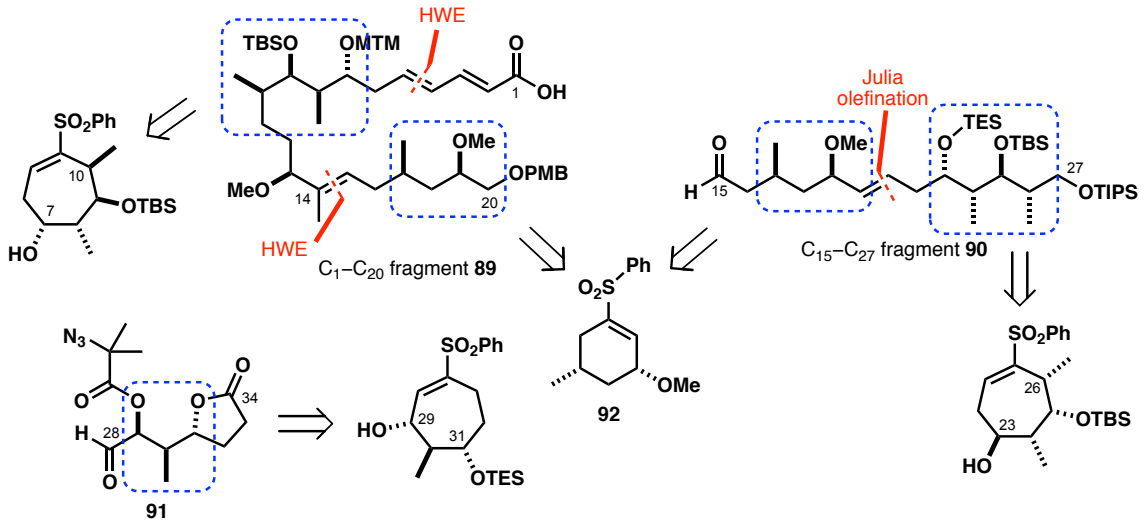

Scheme 21 Retrosynthetic analysis of the aplyronine fragments **89** and **90** prepared by Fuchs

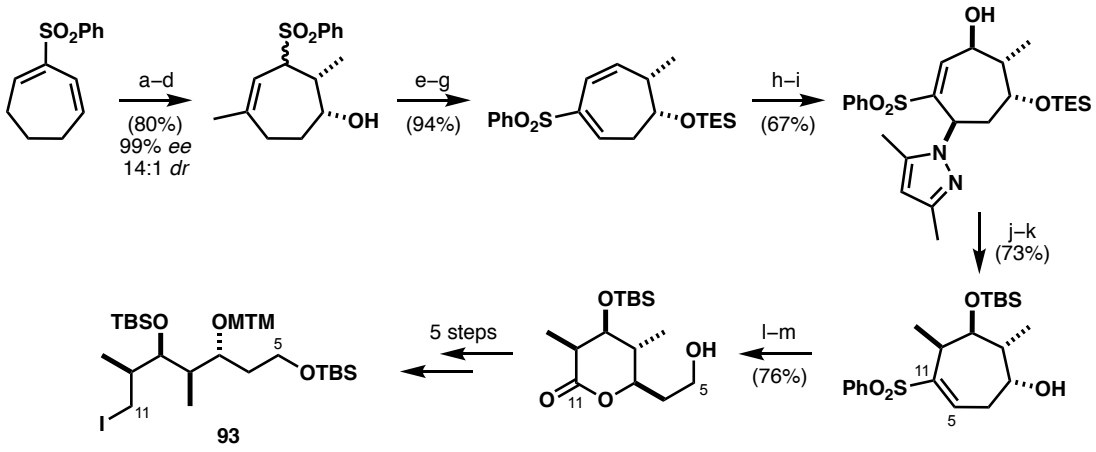

(a) [(*R*,*R*)-Mn(salen)Cl] **95** (1 mol%), NH_4OAc, H_2O_2, MeOH; (b) K_2CO_3, MeOH; (c) MeMgBr, *then* PhSSPh; (d) DBU; (e) TESCl, imid.; (f) $AlMe_3$, $^{i}PrNEt_2$; (g) 30% aq. H_2O_2, Na_2WO_4, $PhP(OH)_2$, $oct_3MeNHSO_4$; (h) Oxone®, $NaHCO_3$; (i) 3,5-dimethylpyrazole; (j) MeMgBr; (k) TBSOTf, 2,6-lut., *then* CSA; (l) O_3, $NaHCO_3$; (m) $BH_3 \cdot {}^{t}BuNH_2$

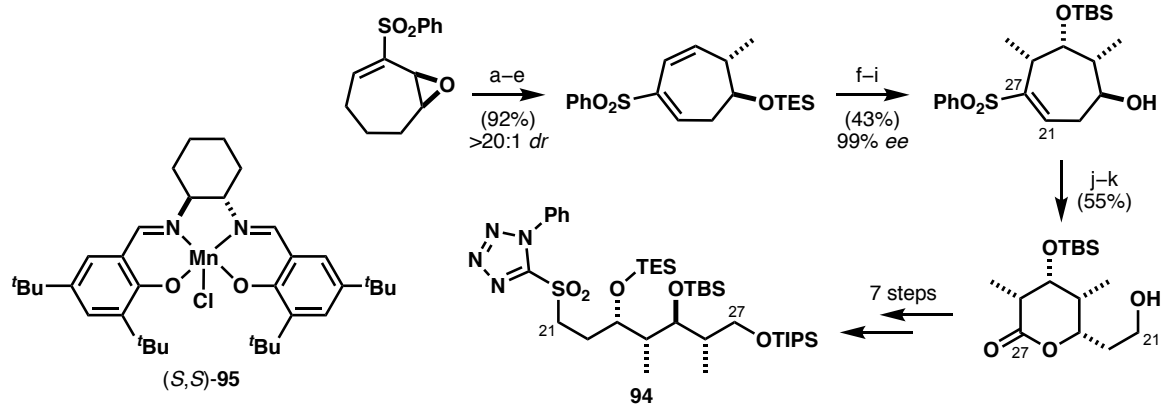

(a) $AlMe_3$; (b) NaHMDS, *then* PhSSPh; (c) TESCl, imid.; (d) $AlMe_3$, $^{i}PrNEt_2$; (e) 30% aq. H_2O_2, Na_2WO_4, $PhP(OH)_2$, $oct_3MeNHSO_4$; (f) [(*S*,*S*)-Mn(salen)Cl] **95** (1 mol%), NaOCl, NaH_2PO_4, pH 9.5; (g) 3,5-dimethylpyrazole; (h) MeMgBr; (i) TBSOTf, 2,6-lut., *then* CSA; (j) O_3, $NaHCO_3$; (k) $BH_3 \cdot {}^{t}BuNH_2$

Scheme 22 Fuchs' synthesis of the C_5–C_{11} iodide **93** and C_{21}–C_{27} sulfone **94**

Scheme 22 shows how such a sequence of transformations led to the C_5–C_{11} iodide **93** or the C_{21}–C_{27} sulfone **94** with the absolute stereochemistry dictated by the choice of the Mn *N*,*N*'-ethylenebis(salicylideneiminato) (salen) ligand in the asymmetric epoxidation step. Fragment **94** was coupled to the C_{15}–C_{20} aldehyde **96**, derived from sulfone **92** (**Scheme 23**) and reduced to give the complete C_{15}–C_{27} aldehyde **90**.[118]

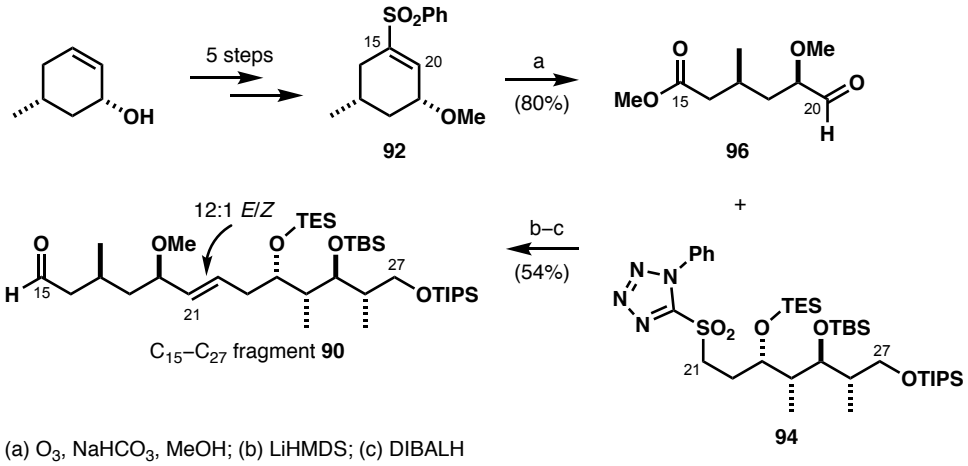

Scheme 23 Preparation of the C_{15}–C_{20} unit **96** and route to the C_{15}–C_{27} aldehyde **90** by Fuchs

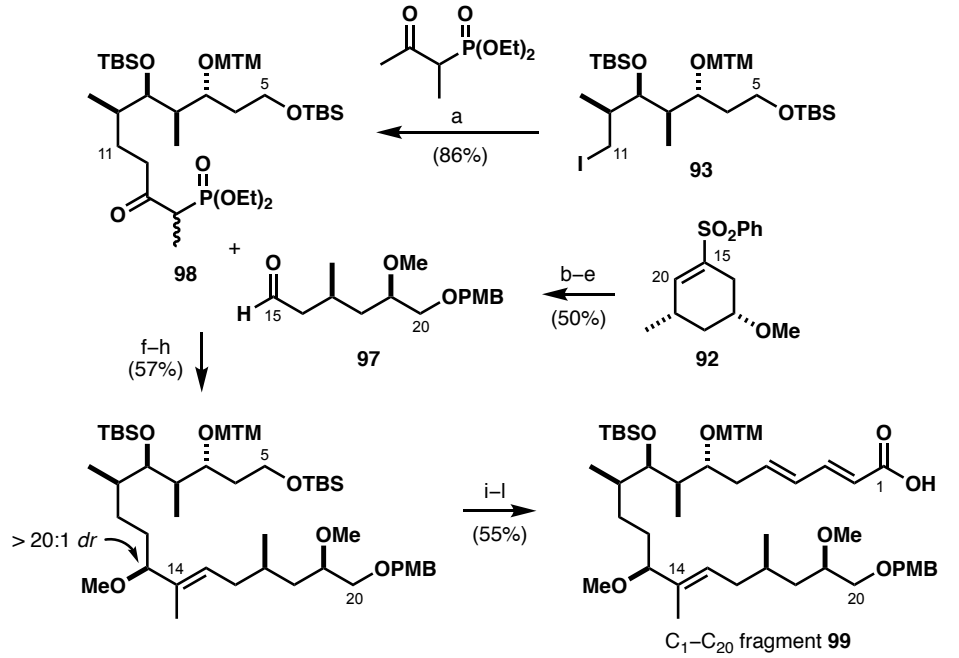

Scheme 24 Fuchs' synthesis of an alternative C_{15}–C_{20} aldehyde **97** and fragment linkage *via* HWE coupling to afford the C_1–C_{20} carboxylic acid **99**

The alternative C_{15}–C_{20} subfragment **97** was obtained from sulfone **92** (**Scheme 24**) and linked to the C_{12}–C_{14} β-ketophosphonate **98** to furnish the C_1–C_{20} carboxylic acid **99** in a similar sequence as previously detailed in **Scheme 20**.

The C_{32}-desmethyl analogue **91** was prepared as part of the studies towards the C_{28}–C_{34} side chain *via* cleavage of the vinyl sulfone **100**,[136] followed by modified Upjohn dihydroxylation and Crigee oxidation (**Scheme 25**).

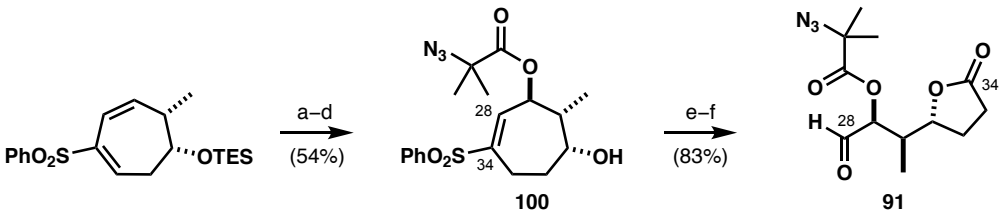

(a) Oxone®, $NaHCO_3$; (b) $NaBH_4$; (c) 2-azido-2-methylpropanoic acid, $(COCl)_2$, Et_3N, DMAP; (d) $CeCl_3$, MeOH; (e) $K_2OsO_4 \cdot 2H_2O$, NMO, citric acid; (f) $Pb(OAc)_4$

Scheme 25 Fuchs' synthesis of a C_{32}-desmethyl unit **91**

1.4.3. Kigoshi's Synthesis of Apyronine A

Kigoshi was involved in the first total synthesis of the aplyronine A as part of the Yamada group in 1994[38,42] and later developed an entirely novel approach with the aim to address the drawbacks of the original route (**Scheme 26**).[113] Poorly selective and low yielding olefination steps were to be superseded by the Nozaki–Hiyama–Kishi (NHK) fragment coupling[25,26,140] on three occasions. Furthermore, the esterification at C_1 was envisaged as an intermolecular step prior to macrocycle closure to prevent regioselectivity issues which had been observed in the previous synthesis. Using ths strategy, Kigoshi first prepared an aplyronine A–mycalolide B hybrid **36** (**Section 1.2.4.**)[79] before completing second-generation synthesis of aplyronine A itself.[112] The endgame intersects a known common intermediate **62** from Yamada's route.

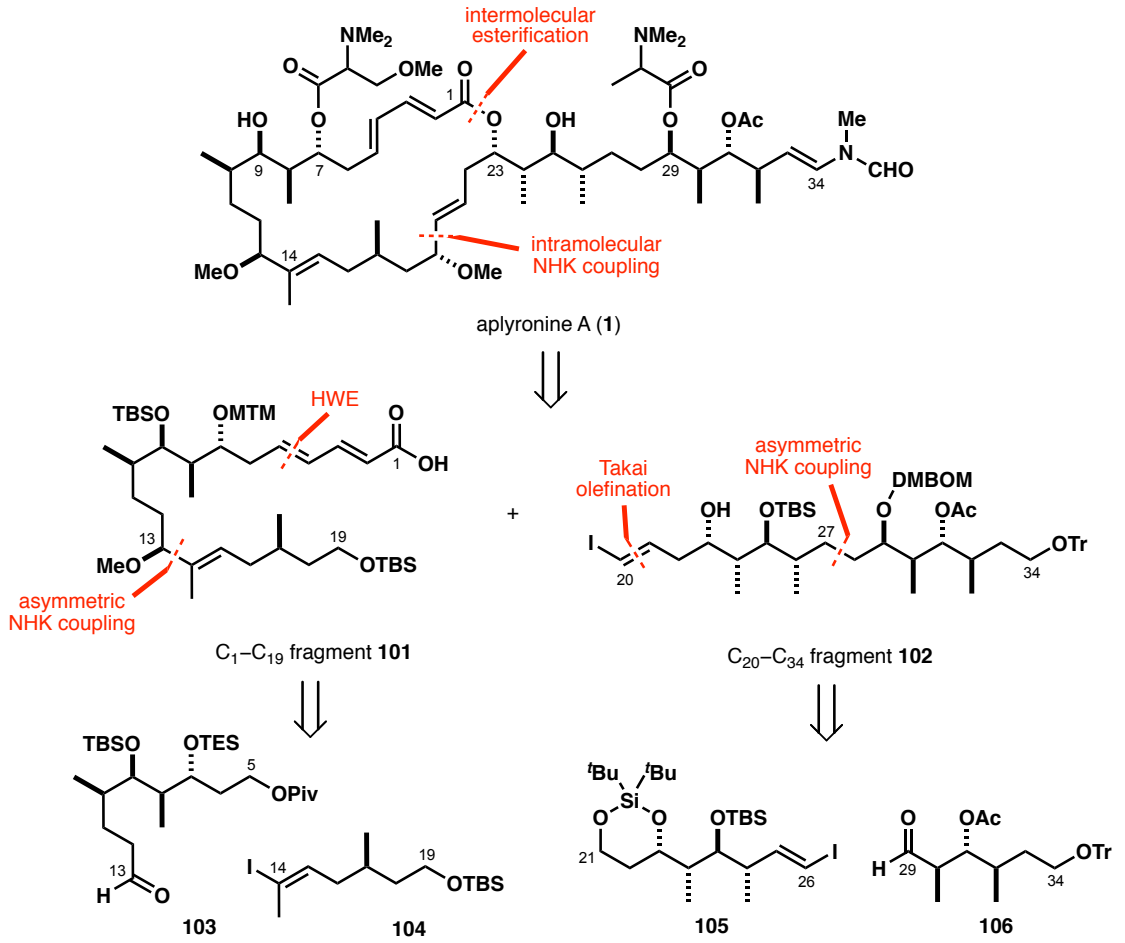

Scheme 26 Kigoshi's synthetic plan for aplyronine A (**1**)

The C_{14}–C_{19} vinyl iodide **104** was obtained from chiral alcohol **107** by homologation at C_{15} with the Ohira–Bestmann reagent **108**,[141] methylation of the alkyne and a silylcupration-iododesilylation. Fragment **104** was formed as a single geometric isomer (**Scheme 27**).

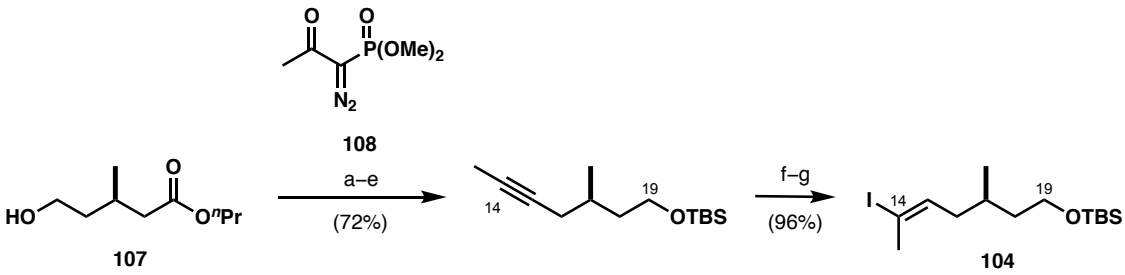

(a) TPAP, NMO; (b) **108**, K_2CO_3, MeOH; (c) DIBALH; (d) TBSCl, imid.; (e) ^{n}BuLi, MeI; (f) $Me_2PhSiLi$, CuCN; (g) NIS

Scheme 27 Kigoshi's preparation of vinyl iodide **104** from alcohol **107**

The C_5–C_{13} aldehyde **103** was prepared *via* an intermediate **52** in the Yamada route (**Scheme 5**) from Evans imide **55** by carbon chain elongation at C_{11}, dihydroxylation and oxidative cleavage of the ensuing

terminal diol to construct the aldehyde in preparation for the Ni/Cr coupling. Fragments **103** and **104** were joined in an asymmetric variant of the NHK reaction[140] with the bespoke sulfonamide ligand **109** to yield methyl ether **110** after methylation of the C_{13} hydroxyl in a much improved 7.3:1 *dr* compared to the result from the Yamada synthesis.

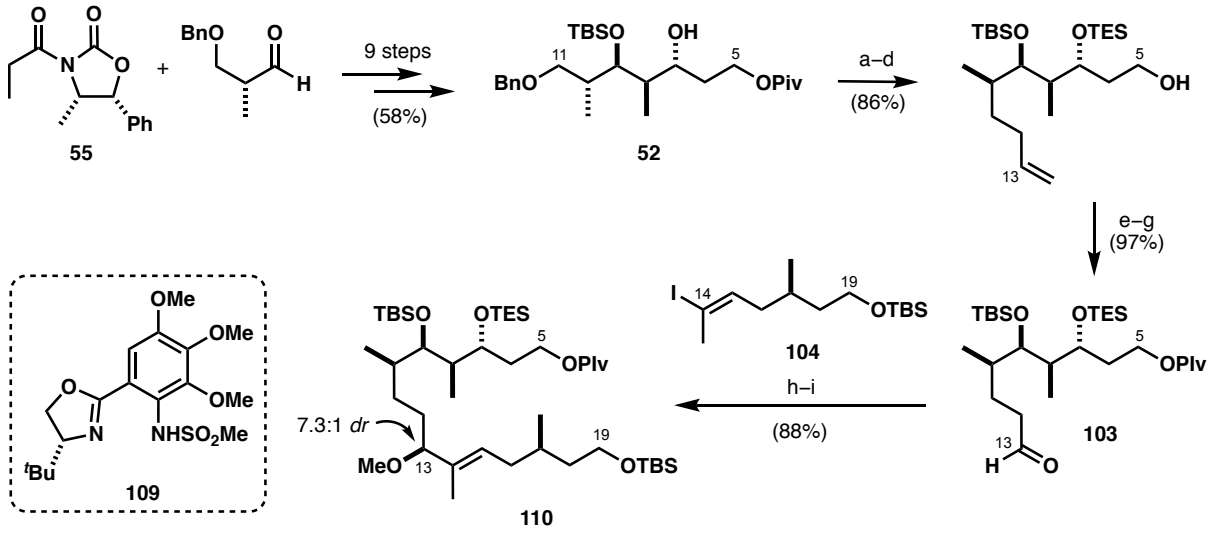

(a) TESCl, imid.; (b) H_2, Pd/C, EtOH; (c) TsCl, pyr; (d) allylMgBr; (e) PivCl, DMAP, pyr; (f) OsO_4, NMO; (g) $NaIO_4$; (h) $NiCl_2$(dppp), $CrCl_2$, ligand **109**, Proton-sponge®; (i) NaH, MeI

Scheme 28 Preparation of the C_5–C_{13} aldehyde **103** *via* the Evans aldol reaction and subsequent NHK coupling with the vinyl iodide **104** by Kigoshi

The smaller subunit **106** was accessed in 10 steps from methyl (*R*)-3-carboxybutanoate **111**[142] where the *anti*, *anti*-stereotriad was forged in a Roush crotylation[143] of the α-chiral aldehyde **112** (**Scheme 29**). The secondary alcohol **113** was obtained in 14:1 *dr via* the anti-Felkin transition state and three further transformations led to fragment **106**.[131] Vinyl iodide **105** was accessed from ethyl ketone **114** *via* a 1,3-*syn*-3,4-*syn* tin-mediated aldol reaction,[144] followed by Evans–Saksena 1,3-*anti* reduction[145,146] to complete the stereotetrad and Takai olefination[147] at C_{27} with excellent *E*/*Z* selectivity.

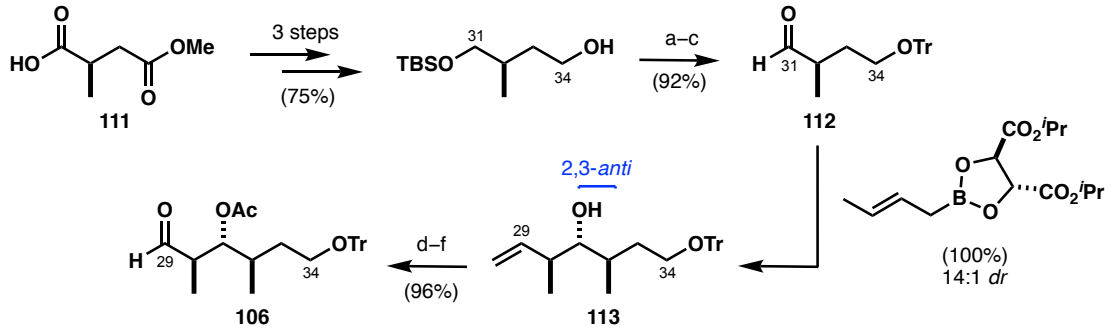

(a) TrCl, Et_3N, DMAP; (b) TBAF; (c) Dess–Martin periodinane; (d) Ac_2O, DMAP, pyr; (e) OsO_4, NMO; (f) $NaIO_4$

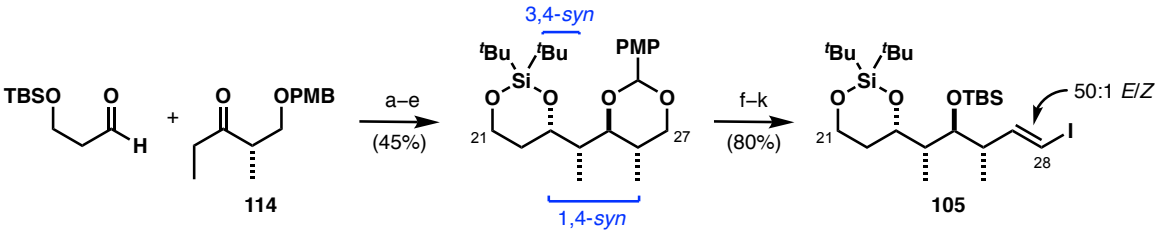

(a) $Sn(OTf)_2$, Et_3N; (b) $Me_4BH(OAc)_3$, MeCN, AcOH; (c) DDQ; (d) TBAF; (e) $^tBuSi(OTf)_2$, 2,6-lut.; (f) H_2, $Pd(OH)_2/C$; (g) PivCl, pyr; (h) TBSCl, imid.; (i) DIBALH; (j) Dess–Martin periodinane; (k) $CrCl_2$, CHI_3

Scheme 29 Kigoshi's synthesis of the C_{21}–C_{28} and C_{29}–C_{34} fragments **105** and **106**

The second asymmetric Ni/Cr coupling between fragments **105** and **106** with the aforementioned chiral ligand **109** proceeded with complete control of stereochemistry at C_{29} (**Scheme 30**). After the necessary protecting group manipulations, Takai olefination at the C_{21} terminus gave a modest a 4.5:1 mixture of *E*/*Z* olefin isomers and selective cleavage of the C_{23} TES group exposed a single site for esterification. The synthesis of fragment **102** was completed in 20 steps LLS and 16% yield from ketone **114**.

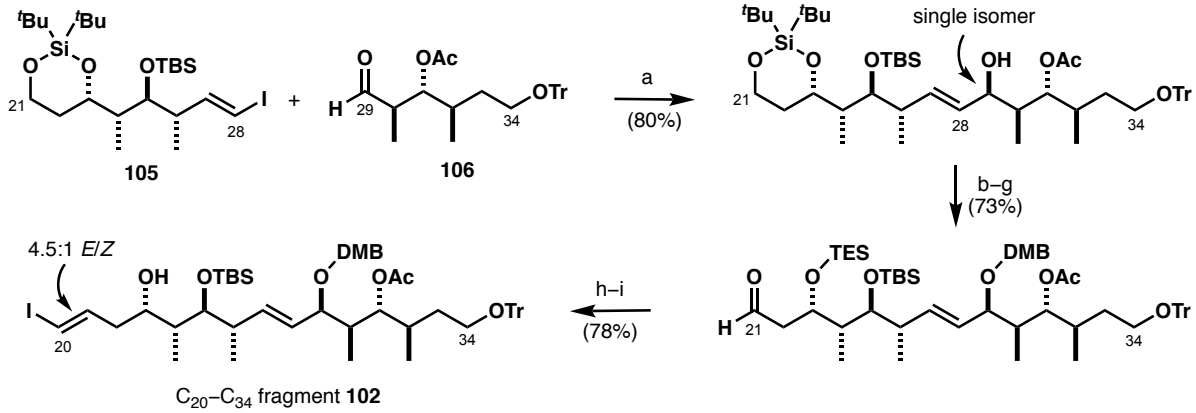

(a) $NiCl_2$(dppp), $CrCl_2$, ligand **109**, Proton-sponge®; (b) H_2, $Pd(OH)_2/C$, $NaHCO_3$, EtOH; (c) DMBCl, $^iPrNEt_2$; (d) TBAF, AcOH; (e) TESCl, imid.; (f) NH_4F, MeOH; (g) Dess–Martin periodinane, pyr; (h) $CrCl_2$, CHI_3; (i) AcOH, H_2O, THF

Scheme 30 Fragment assembly and functionalisation to the C_{20}–C_{34} vinyl iodide **102** by Kigoshi

The C_5–C_{19} intermediate **110** was elaborated in preparation for the HWE olefination to append the key C_1–C_5 dienoate, followed by ester hydrolysis. Site-specific intermolecular esterification between carboxylic acid **115** and vinyl iodide **102** under modified Yamaguchi conditions[125] and conversion of the C_{19} silyl ether into the aldehyde provided the appropriate precursor for the anticipated NHK macrocyclisation (**Scheme 31**). Ring closure could be achieved either in presence or absence of the chiral ligand **109** with the best result being 89% yield of the allylic alcohol as a 1.5:1 ratio of the (19*R*) and (19*S*) isomers. Methylation of the secondary hydroxyl generated the known intermediate **62** from which aplyronine A can be provided in eight further steps.[42]

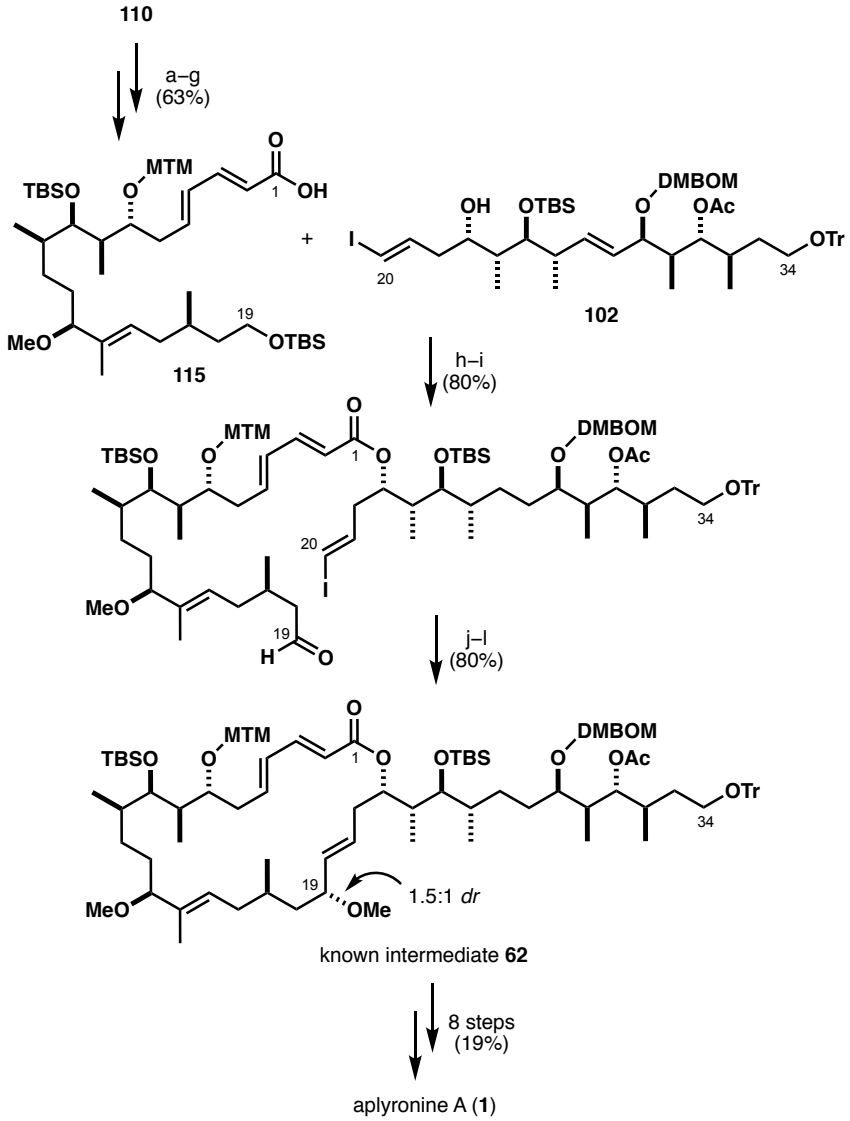

(a) AcOH, H_2O, THF; (b) TBSCl, Et_3N, DMAP; (c) DMSO, Ac_2O, AcOH; (d) DIBALH; (e) Dess–Martin periodinane; (f) $(EtO)_2P(O)CH_2CH{=}CHCO_2Et$, LDA; (g) 4 M LiOH, MeOH; (h) TCBC, Et_3N, DMAP; (i) AcOH, H_2O, THF; (j) Dess–Martin periodinane; (k) $NiCl_2$, $CrCl_2$; (l) NaH, MeI

Scheme 31 Kigoshi's synthesis of aplyronine A (**1**) by intermolecular esterification and ring closure by Ni/Cr NHK coupling

Kigoshi's synthesis consists of a total of 80 steps from commercially available materials, 38 steps LLS and 1.4% yield. The thoughtful application of the asymmetric NHK coupling bolstered the efficiency of the trisubstituted olefin construction and installation of the isolated C_{13} stereocentre, though the use of superstoichiometric chromium salts and poorly selective macrocyclisations left room for improvement.

1.5. Summary

The aplyronines are a highly attractive family of marine natural products and have garnered interest due to their complex structure as well as potent bioactivity. To date, the total syntheses of several congeners have been accomplished by Yamada, Paterson and Kigoshi. Other groups have reported the syntheses of smaller fragments, demonstrating that the stereotetrads on the carbon skeleton present an inspiration for development of new methodologies for their construction. Chemical synthesis has provided the tools to ascertain the aplyronines' structure and to gain major insight into biological activity through extensive SAR studies and probe attachment for *in vitro* imaging. The latter established a strong the case for the aplyronines as ADC payloads due to their highly unique binding to actin and tubulin.

However, limited supply from natural sources has precluded the development of aplyronine ADCs and thus any future efforts rely entirely upon synthesis to provide sufficient stocks of material. The next chapter details the story of the Paterson first-generation route to aplyronines A, C and D, which aimed to address this matter and strongly influenced other group's work.

.

Chapter 2

Introduction – Part II

The Paterson Strategy Towards the Aplyronines

2.1. Retrosynthetic Analysis and the Overall Strategy

Shortly following Yamada's first publication on the isolation of aplyronines A–C (**1**, **12**–**13**)[2] synthetic studies towards this family of natural products were also initiated in the Paterson group. The task of designing a retrosynthetic strategy was somewhat simplified as the stereochemistry had already been fully assigned by Yamada which allowed for a direct approach to the natural product.[38,43] The primary focus of forward planning therefore revolved around shortening Yamada's route, which is comprised of nearly 100 individual transformation in total (47 steps LLS for aplyronine A and 0.4% overall yield). As an aside, it was hoped that the project would also provide opportunities to tackle the challenging steps by developing new synthetic methodologies.

The means of achieving this goal relied on a highly stereocontrolled construction of the fragments, carefully designed to maximise convergency. A second consideration focused on a judicious selection of orthogonal protecting groups which could facilitate installation of highly diverse functionality of the carbon backbone. In addition, the presence of the three stereotetrads at C_7–C_{10}, C_{23}–C_{26} and C_{29}–C_{32} offered the ideal opportunity to apply stereoselective aldol methodology developed by Paterson which would improve upon Yamada's divergent but steppy protocol of Evans aldol reactions and Sharpless epoxidations. The exact choice of conditions for each aldol reaction dictates the pattern of the four stereocentres within the moiety and will be discussed in more detail in **Section 2.2.**

Synthetic endeavours commenced with these directions in mind and in 1998, Paterson, Woodrow and Cowden reported a completed synthesis of the C_1–C_{27} macrocycle **121**,[109,110] followed by a publication on the first-generation side chain studies with Blakey in 2002.[148] After further revisions of the strategy for *N*-

vinylformamide installation, as well as a more substantial macrocycle scale-up campaign, the total synthesis of aplyronine C (**1**) was accomplished in 2012.[108]

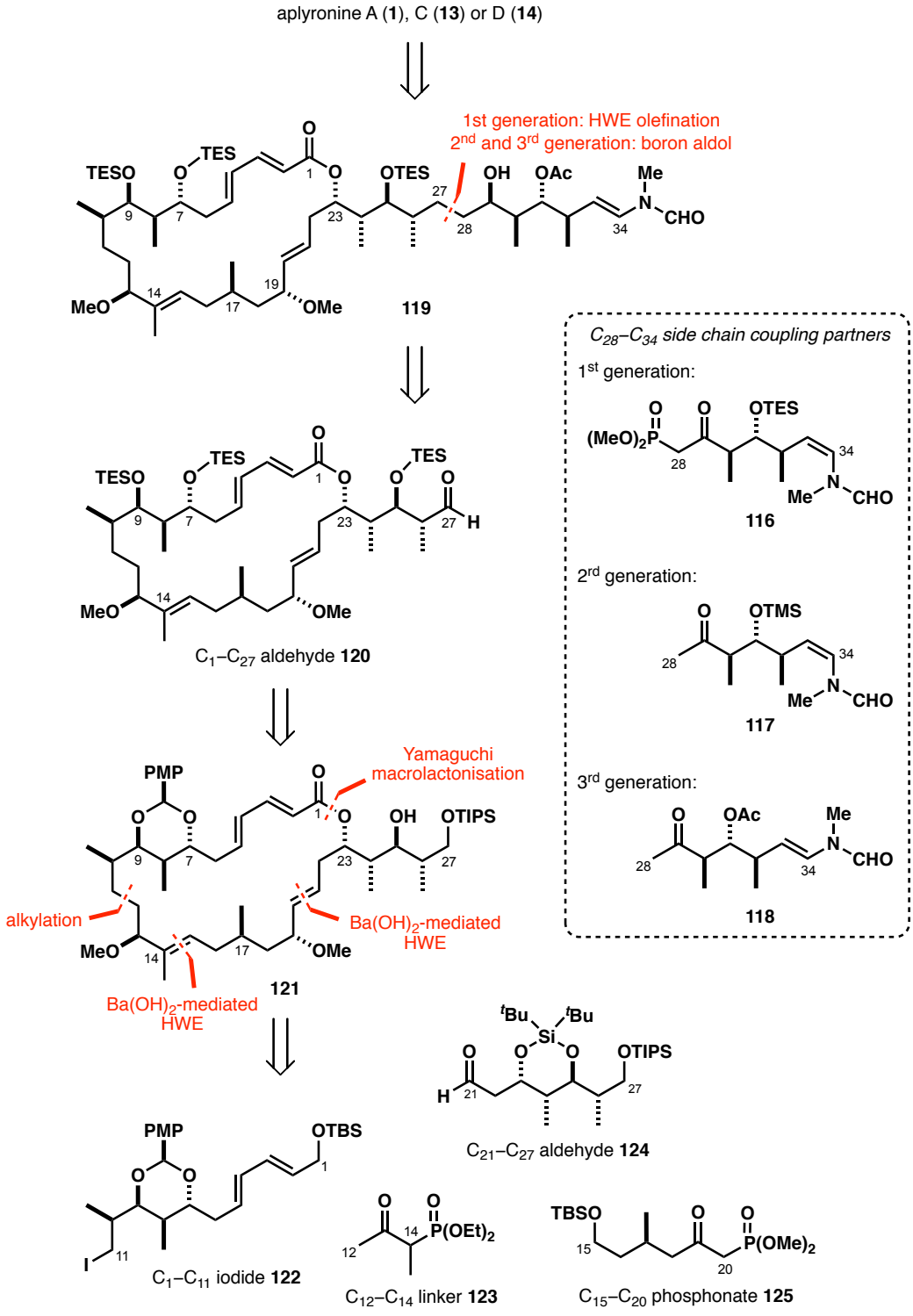

Scheme 32 Paterson first-generation total synthesis of aplyronines A (**1**), C (**13**) and D (**14**)

A unique feature of the strategy was the disconnection across the C_{27}–C_{28} bond which splits the molecule into an appropriately functionalised macrolide core and side chain, containing the sensitive *N*-methyl-*N*-vinylformamide (**116**–**118** as the strategy evolved) as shown in **Scheme 32**. Its delicate nature raised the concern of not just how but also when to install it. Yamada introduced this moiety by condensation of a C_{34} aldehyde with *N*-methylformamide but the reaction was low-yielding. The decision was thus made to opt for a more adventurous approach and to implement it as part of the side chain fragment before linkage to the macrocycle.

Another important consideration was attachment of the pendant amino acids which was vital for the purposes of accessing multiple congners. With the exception of aplyronines B, E and H, the variation in the number and identity of the amino acids occurs at the C_7 and C_{29} hydroxyl groups. As they greatly increase the polarity of the ensuing compounds and affect the ease of compound handling, the synthetic plan must allow for esterification at a very late-stage, ideally *via* a common precursor which can readily be diversified. In principle, differentiation can be achieved by introducing orthogonal protecting groups and selectively unmasking each site as and when needed. However, at the onset of the studies, this option was to a certain extent sacrificed to instead exploit the stereoelectronic and conformational effects of carefully selected protecting groups to bias the outcome of key steps such as the macrolactonisation.

The macrocycle was disconnected to the preceding *seco*-acid, which was anticipated to selectively cyclise onto the C_{23} hydroxyl of a free 1,3-diol at C_{23}/C_{25}. A very similar ring closure is featured in Yamada's route, albeit the regioisomeric ratio is in favour of the undesired, 26-membered ring (as seen in **Section 1.4.1.).** Woodrow's supporting argument for proposing this step is hinged upon the idea that a utilising cyclic *para*-methoxyphenyl (PMP) protecting group would favour the formation of the smaller, 24-membered ring owing to the rigidity imposed on the carbons in the immediate the proximity of the acetal.[149] This effect would be reinforced by placing a bulky triisopropylsilyl (TIPS) protecting group at the C_{27} position, further discouraging side reactions through the C_{25} alcohol based on steric grounds.

The assembly of the C_1–C_{27} linear precursor would proceed *via* an expedient construction of the (14*E*)-trisubstituted olefin using the $Ba(OH)_2$-promoted HWE reaction.[150] This step brings together four designated constituents of the macrocyclic backbone: the C_1–C_{11} iodide **122**, the C_{15}–C_{20} phosphonate **125**, the C_{21}–C_{27} aldehyde **124** and the C_{12}–C_{14} linker unit **123** which is appended by regioselective alkylation[151] at C_{11} ahead of the HWE coupling. The (*E*,*E*)-dienoate is formed by PPh_3/PhOH-catalysed isomerisation of the C_1–C_3 ynoate ester,[152] which is another efficient transformation, utilised exclusively in the Paterson strategy. The C_{13} and C_{19} stereocentres, which are not a part of the key stereotetrads, can be introduced by reagent-controlled Corey–Bakshi–Shibata (CBS) reduction of α,ß-unsaturated carbonyls[153] resulting from HWE olefinations. In contrast, the remote C_{17} stereocentre was sourced from the chiral pool materials as proposed by Woodrow (noted in **Section 3.4.1.**).

2.2. Aldol Methodology

The stereotetrads present in the aplyronines are common motifs in polyketide natural products which stem from iterative addition of malonyl CoA or methylmalonyl CoA to the growing carbon chain, orchestrated by the polyketide synthase enzymes. Each cycle can introduce up to two new stereocentres, depending on whether the condensations are of polyacetate or polypropionate type, producing a typical β-hydroxy ketone unit (**Figure 24**). This process is the origin of the ubiquitous 1,3-oxygenation patterns in polyketides, which can also be further derivatised to give 1,3-polyols through reduction or dehydration to produce α,β-unsaturated carbonyls.[154]

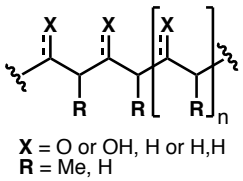

Figure 24 Typical polyketide structural motif

Such construction of stereogenic centres by means of chemical synthesis has been emulated using methyl or ethyl ketones in aldol reactions (**Figure 25**). Tremendous efforts in this field in the past decades have yielded arguably some of the most pivotal methodology for constructing C–C bonds from carbonyl compounds in a regio-, stereo- and enantioselective manner. Comprehensive understanding of how to generate aldol coupling partners with tuneable properties in combination with *syn*- or *anti*-selective reductions has provided access to every possible permutation of the stereotetrad pattern. The applicability of this approach spans from generating very small building blocks to stereoselective union of highly complex fragments in the assembly of polyoxygenated natural products.[154]

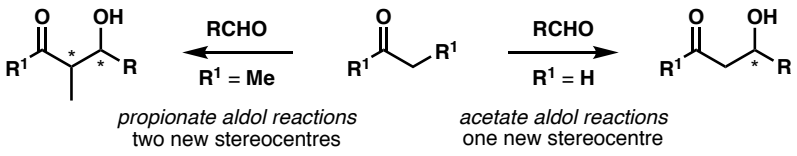

Figure 25 Aldol reactions using methyl or ethyl ketones

The relative topicity of aldol reactions with metal enolates can be predicted from the general mechanistic pathways. The reactions proceeds *via* a Zimmerman–Traxler transition state (TS)[155] where the aldehyde carbonyl is coordinated to the enolate metal and the positioning of substituents in a chair-like conformation is governed by the minimisation of 1,3-diaxial interactions (**Scheme 33**).[156] For this reason, (*Z*)-enolates generally proceed to give 1,2-*syn* aldol adducts whereas (*E*)-enolates produce a 1,2-*anti* relationship, thus it is vital to form the enolate with high stereochemical fidelity.

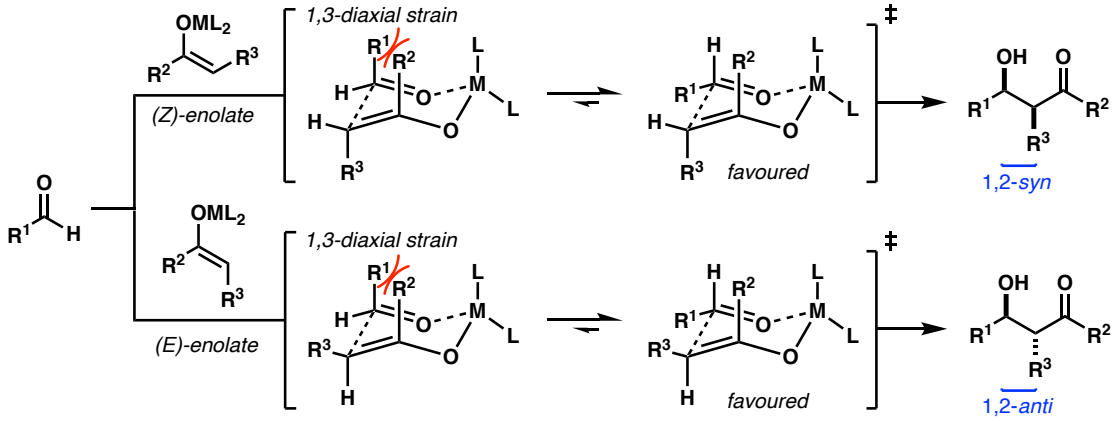

Scheme 33 Relative stereochemical outcome of aldol reactions with (*Z*)- or (*E*)- metal enolates

While the enolate can impart relative configuration on the alpha methyl and beta hydroxyl groups in the the aldol adduct, the enantioselectivity must be conferred by one or more additional stereocontrolling elements. In particular, chiral ketones frequently furnish products with very high levels of induction and offer an attractive alternative to auxiliary-based methods. One of the most simple and efficient substrates for this purpose is methyl-3-hydoxy-2-methyl propionate ((*S*)- or (*R*)-Roche ester **126** and **127**, *vide infra*), a dipropionate equivalent, which has been used in the syntheses of numerous polyketide natural products such as spirangien A[157] and callipeltoside.[158] The configurations of the three aplyronine stereotetrads lend themselves well to the aldol reactions of boron- and tin enolates of ketones **128** and **129**, developed by Paterson (**Scheme 34**). The basis for the selectivity in these key aldol reactions will be discussed in the following sections where appropriate.

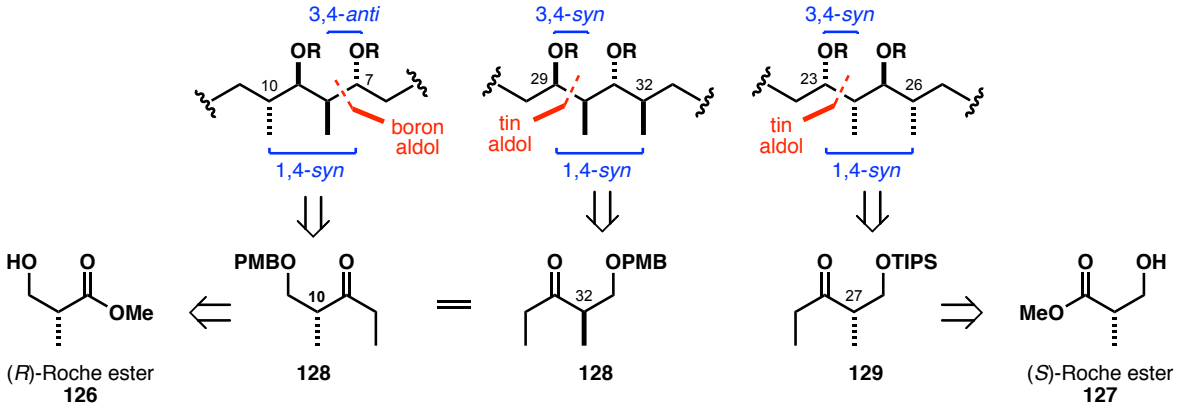

Scheme 34 Retrosynthetic analysis of the stereotetrads in aplyronines

2.3. First-Generation Total Synthesis of Aplyronines A, C and D

2.3.1. Synthesis of C_1–C_{11} Iodide 122

Synthesis of the C_1–C_{11} fragment **122**, began with the 1,4-*syn*-3,4-*anti*-selective boron-mediated aldol reaction with ethyl ketone **128** and aldehyde **130** (**Scheme 35**), prepared in four steps from 5-hexyn-1-ol.

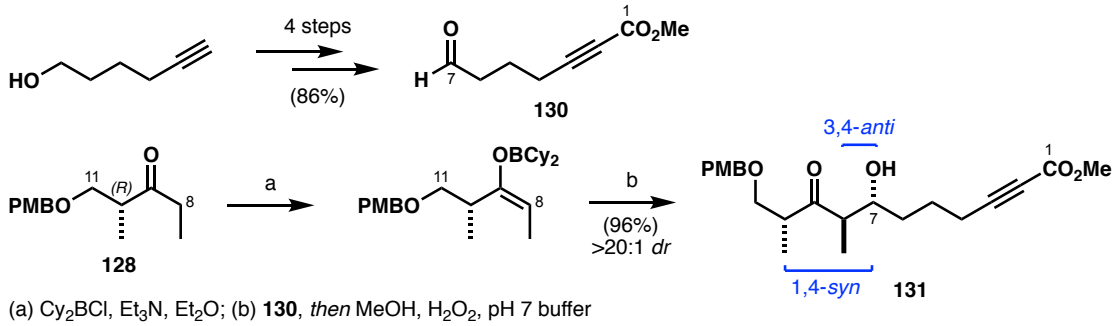

Scheme 35 Boron-mediated aldol reaction in the Paterson synthesis of C_1–C_{11} iodide **122**

Enolisation with dicyclohexylboron chloride (Cy_2BCl) and triethylamine (Et_3N) produced the (*E*)-boron enolate, which proceeded to react with aldehyde **130** to form aldol adduct **131** in 96% yield and >20:1 *dr*. High levels of stereoinduction in aldol reactions of β-alkoxy (*E*)-enol borinates have been rationalised by Paton and Goodman using density functional theory (DFT) studies. It was found that the transition state structure is boat-shaped, which is in agreement with a postulated stabilising interaction between the aldehyde proton and the lone pair electrons on the *para*-methoxybenzyl (PMB) group (**Scheme 36**).[159,160] The facial preference of enolate attack is thus dictated by the minimisation of 1,3-allylic strain ($A_{1,3}$) around its double bond in **TS 1** which is able to facilitate the formyl hydrogen bond.

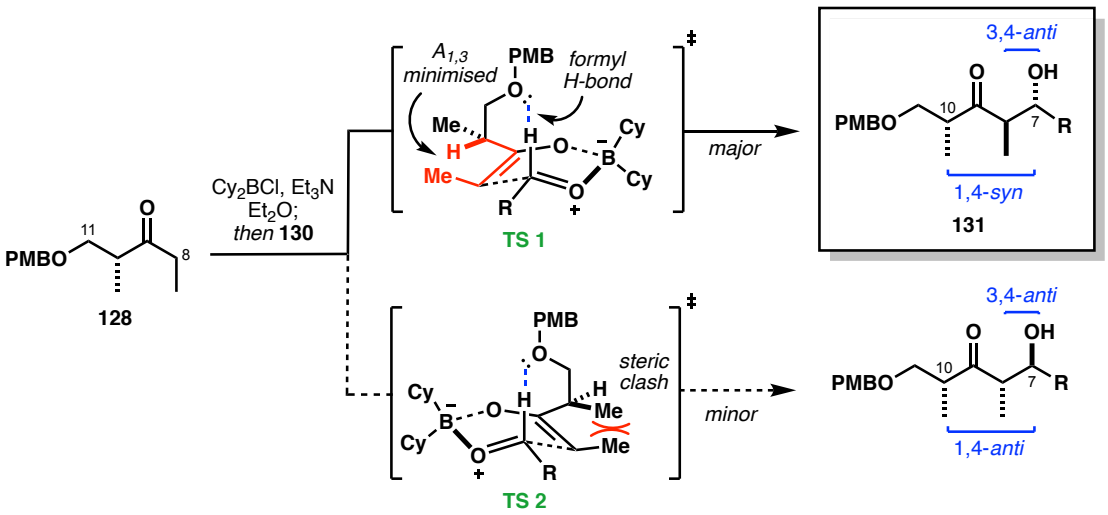

Scheme 36 Competing transition states **TS 1** and **TS 2** for the aldol reaction of ethyl ketone **128** with aldehyde **130**

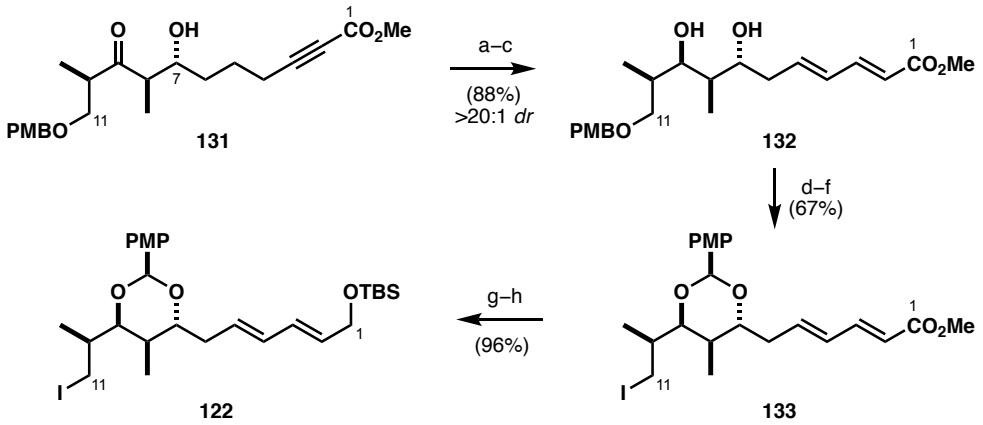

(a) SmI_2, EtCHO, THF; (b) PPh_3, PhOH, PhH; (c) K_2CO_3, MeOH; (d) anisaldehyde dimethyl acetal, PPTS, CH_2Cl_2; (e) DDQ, CH_2Cl_2/pH 9.2 buffer (4:1); (f) I_2, PPh_3, imid., Et_2O/MeCN (1:1); (g) DIBALH, CH_2Cl_2; (h) TBSOTf, 2,6-lut., CH_2Cl_2; (i) $Me_4NBH(OAc)_3$, MeCN/AcOH (1:1); (j) Ac_2O, pyr, Et_3N, DMAP, CH_2Cl_2

Scheme 37 Elaboration of aldol adduct **131** to iodide **122**

The directed 1,3-*anti* reduction was carried out under the Evans–Tishchenko protocol (SmI_2, EtCHO),[161] which installed the final chiral centre in the C_7–C_{10} tetrad (**Scheme 37**). Next, the conjugated alkyne was isomerised to the dienoate under Rychnovsky's protocol (PPh_3, PhOH),[152] which afforded the product with complete selectivity for the thermodynamically favoured (*E*,*E*)-configuration. As discussed in **Section 1.4.**, other group's routes towards the aplyronine fragments feature an HWE reaction to construct the dienoate which results in mixtures of double bond isomers containing the undesired (*Z*)-olefins.

The pendant propionate at C_7 provided an opportunity for differentiation of the C_7 and C_9 hydroxyls which would simplify the diversification of late-stage intermediates towards multiple aplyronine congeners. Woodrow instead opted to cleave the ester with K_2CO_3 in MeOH to the corresponding 1,3-diol **132** and inserted a rigid PMP acetal moiety. The resuting intermediate was further elaborated to the iodide at the C_{11} terminus to obtain a suitable leaving group for the envisaged alkylation. The PMB group was best cleaved with 2,3-dichloro-5,6-dicyano-1,4-benzoquinone (DDQ) in a mildly basic aqueous buffer (pH 9.2) to suppress the problematic migration of the PMP acetal or its overoxidation to the orthoester.[162] The C_{11} alcohol was then subjected to Appel conditions (I_2, PPh_3, imidazole)[163] to produce the primary iodide **133**.

To prevent the C_1 ester interfering in the subsequent alkylation step, the carbonyl was reduced with diisobutylaluminium hydride (DIBALH) and protected with TBSOTf to give an allylic TBS ether. A fortuitous discovery made during this project was that this functionality can be directly transformed to an aldehyde[149,164] which was subsequently incorporated as one of the cornerstones of the macrocycle synthesis and will be discussed in **Section 3.2**. Overall, the C_1–C_{11} iodide **133** was synthesised in nine steps and 54% yield from ketone **128**.

2.3.2. Synthesis of C_{15}–C_{27} Aldehyde 134

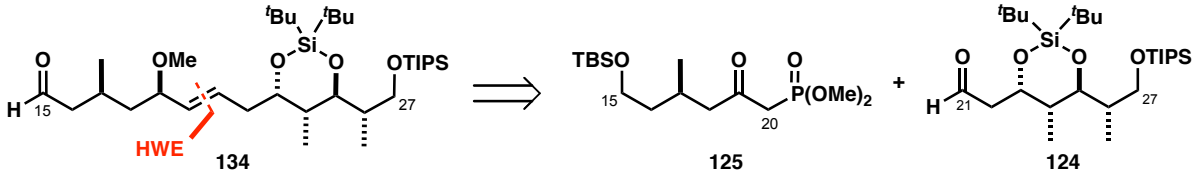

Scheme 38 Retrosynthesis of the C_{15}–C_{27} aldehyde **134**

Lydia Lee assembled the C_{15}–C_{27} aldehyde **134** from two smaller subfragments (**Scheme 38**). The C_{21}–C_{27} segment **124** bears the C_{23}–C_{26} stereotetrad and was installed using the Paterson tin(II)-mediated aldol methodology,[144] which resulted in the required 1,4-*syn*-3,4-*syn* motif. The (*S*)-Roche ester-derived ketone **129** formed the (*Z*)-enolate upon treatment with tin(II) triflate and Et_3N, then reacted with aldehyde **135** to produce aldol adduct **136** in 88% yield and 9:1 *dr*. The origin of stereoselectivity imparted by the chiral ketone can be deduced from either Zimmerman–Traxler transition states[155] **TS 3** and **TS 4**.

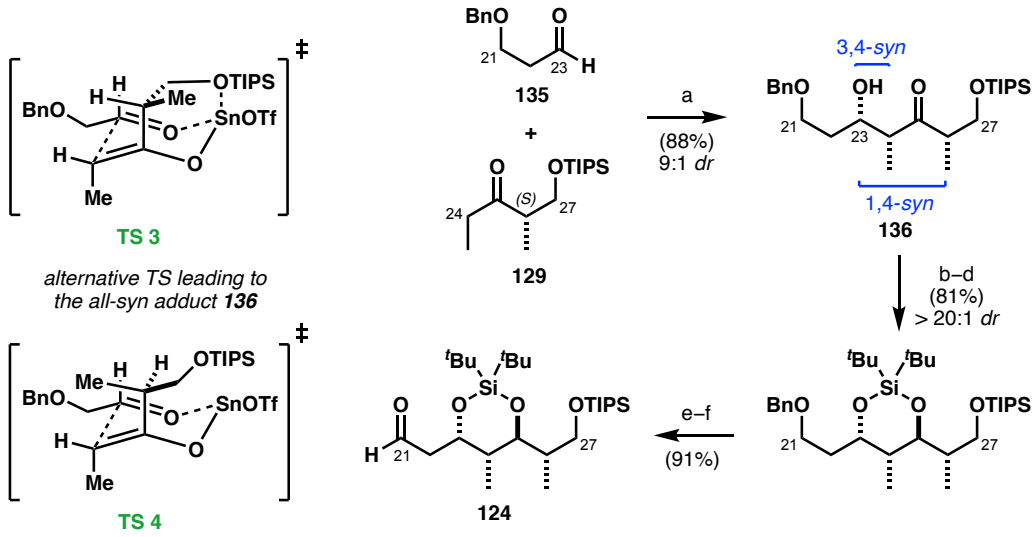

(a) $Sn(OTf)_2$, Et_3N, CH_2Cl_2; (b) SmI_2, EtCHO, THF; (c) K_2CO_3, MeOH; (d) $^tBu_2Si(OTf)_2$, 2,6-lut., CH_2Cl_2; (e) Pd/C, H_2, EtOAc; (f) $(COCl)_2$, DMSO, Et_3N, CH_2Cl_2; (g) $Me_4NBH(OAc)_3$, MeCN/AcOH (2:1)

Scheme 39 The synthesis of C_{21}–C_{27} aldehyde **124**

136 was subjected to an Evans–Tishchenko reaction, followed by methanolysis of the residual ester to furnish a 1,3-*anti* diol (94%, >20:1 *dr*). As before, the C_{23} and C_{25} hydroxyls could have been differentially protected at this stage. However, after careful deliberation the decision was made to protect the diol as a di-*tert*-butyl silylene protecting group with the aim of inducing a conformational bias to achieve the desired regioselectivity in the macrocyclisation step. The C_{21} aldehyde functionality for the planned HWE coupling was revealed by facile hydrogenation of the benzyl ether with Pd/C, followed by

Dess–Martin oxidation.[165] The C_{21}–C_{27} fragment was thus prepared in six steps and 65% yield from ketone **129**.

The C_{15}–C_{20} phosphonate **125** bearing an isolated (17*R*) methyl stereocentre was obtained by functionalisation of commercially accessible methyl-(*R*)-3-methyl glutarate **137** (**Scheme 40**). The C_{15} silyl ether was formed by chemoselective reduction of the carboxylic acid with $BH_3{\cdot}SMe_2$.[166] and the resulting primary alcohol was immediately protected with TBSCl to avoid spontaneous lactonisation onto the C_{19} carbonyl. The required β-ketophosphonate moiety was attached by homologation with lithiated dimethyl methylphosphonate,[167] which concluded the synthesis of the C_{15}–C_{20} fragment **125** in three steps and 85% yield from the chiral acid **137**.

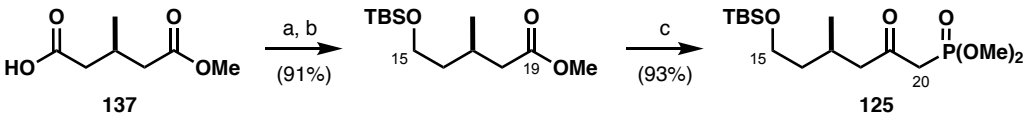

(a) $BH_3{\cdot}SMe_2$, THF; (b) TBSCl, imid., CH_2Cl_2; (c) ^{n}BuLi, $MeP(O)(OMe)_2$, THF

Scheme 40 Synthesis of the C_{15}–C_{20} phosphonate **125** from the chiral acid **137**

The $Ba(OH)_2$-mediated HWE reaction[150] of fragments **124** and **125** to forge the C_{20}–C_{21} olefin proceeded in 91% yield and a 14:1 ratio of *E*/*Z* isomers (**Scheme 41**). The C_{19} stereocentre was installed in a catalyst-controlled enantioselective carbonyl reduction step by employing (*S*)-Me-CBS **138** and $BH_3{\cdot}SMe_2$ as the source of hydride (91%, 15:1 *dr*).[153,168] The ensuing secondary alcohol was methylated with NaH and MeI, followed by acidic hydrolysis of the TBS ether and Dess–Martin oxidation[165] of the C_{15} terminus to produce the C_{15}–C_{27} southern fragment **134** in 11 steps LLS and 49% yield from the (*S*)-ethyl ketone **129**.

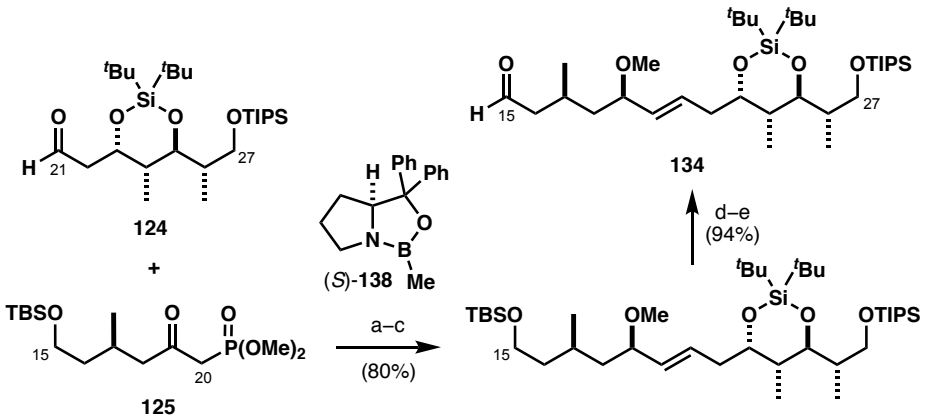

(a) $Ba(OH)_2$, THF/H_2O (40:1); (b) (*S*)-Me-CBS catalyst **138**, $BH_3{\cdot}SMe_2$, THF; (c) NaH, MeI, THF; (d) CSA, CH_2Cl_2/MeOH (2:1); (e) Dess–Martin periodinane, $NaHCO_3$, CH_2Cl_2

Scheme 41 Lee's synthetic efforts towards the C_{15}–C_{27} aldehyde **134**

2.3.3. Synthesis of C_1–C_{27} Macrocycle 120

The Paterson strategy for macrocycle assembly was centred around the HWE reaction to forge the trisubstituted (14*E*) olefin in presence of a mild base as shown in **Scheme 42**. The phosphonate component for this step was appended to the C_1–C_{11} iodide **122** by alkylation with the dianion of β-ketophosphonate **123**.[151] The reaction is carried out under kinetic conditions to encourage the attack through the less hindered γ-carbon. However, Lee identified a regioisomeric α-alkylation product in the mixture and efforts to suppress its formation only resulted in a modest improvement.[162] The phosphonate product **139** was then subjected to deprotonation with $Ba(OH)_2$ and reacted with aldehyde **134** to forge the enone in 91% yield and 14:1 mixture of *E*/*Z* double bond isomers. This impressive result greatly surpassed the 44% yield and 2.3:1 *E*/*Z* product ratio from Yamada's Julia coupling and even to date remains the most efficient method of constructing the C_{14}–C_{15} bond. Moreover, both components were prepared from the Roche ester-derived ethyl ketones **128** and **129** in ten and eleven steps, respectively, maximising the convergency of this synthetic plan.

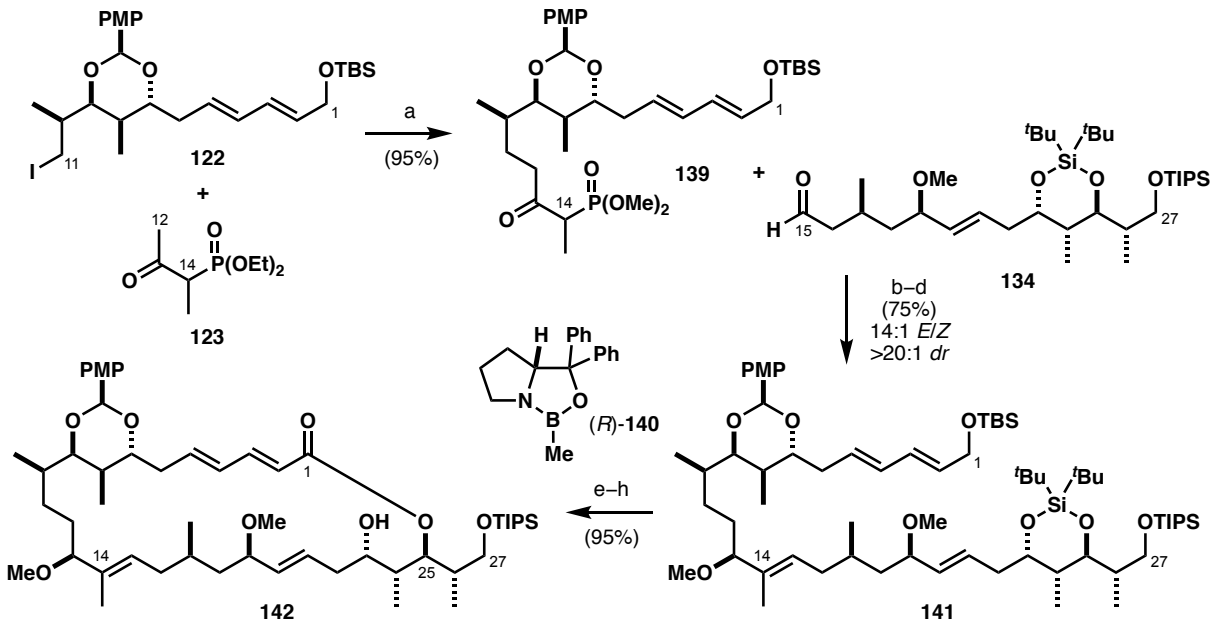

(a) NaH, ^{n}BuLi, THF; (b) $Ba(OH)_2$, THF/H_2O (40:1); (c) (*R*)-Me-CBS catalyst **140**, $BH_3 \cdot SMe_2$, THF; (d) NaH, MeI, THF; (e) DDQ, CH_2Cl_2/pH 7 buffer (4:1); (f) HF·pyr, pyr, THF; (g) $NaClO_2$, $NaH_2PO_4 \cdot 2H_2O$, ^{t}BuOH, H_2O, 2-Me-2-butene; (h) TCBC, Et_3N, DMAP, THF, PhMe

Scheme 42 Fragment coupling and macrolactonisation to the undesired regioisomer **142** by Woodrow and Cowden

The remote C_{13} chiral centre was installed in a similar fashion to C_{19}. Reduction with the enantiomeric (*R*)-Me-CBS **140** (82%, >20:1 *dr*) and methylation afforded the allylic TBS ether **141**, which was rapidly oxidised to the corresponding dienal when subjected DDQ.[164] At this stage two additional transformations were necessary prior to macrocycle formation; oxidation of the aldehyde to the *seco*-acid and cleavage of

the di-*tert*-butyl silylene to expose the 1,3-diol for cyclisation. Due to high polarity of several late-stage intermediates, the best mass recovery was obtained when the silylene was first removed with HF·pyr, followed by chemoselective oxidation at C_1 under Pinnick conditions.[169]

Despite attempting to leverage the steric bulk of the TIPS group at C_{27} to favour the esterification of the C_{25} hydroxyl over C_{27}, the approach failed and gave exclusively the undesired 26-membered lactone **142** under the Yamaguchi–Yonemitsu protocol,[125] albeit in good yield (79%). Lee and Atkinson trialled other conditions which resulted in little success with regards to regioselectivity but the Shiina protocol was found to be comparable in yield.[162]

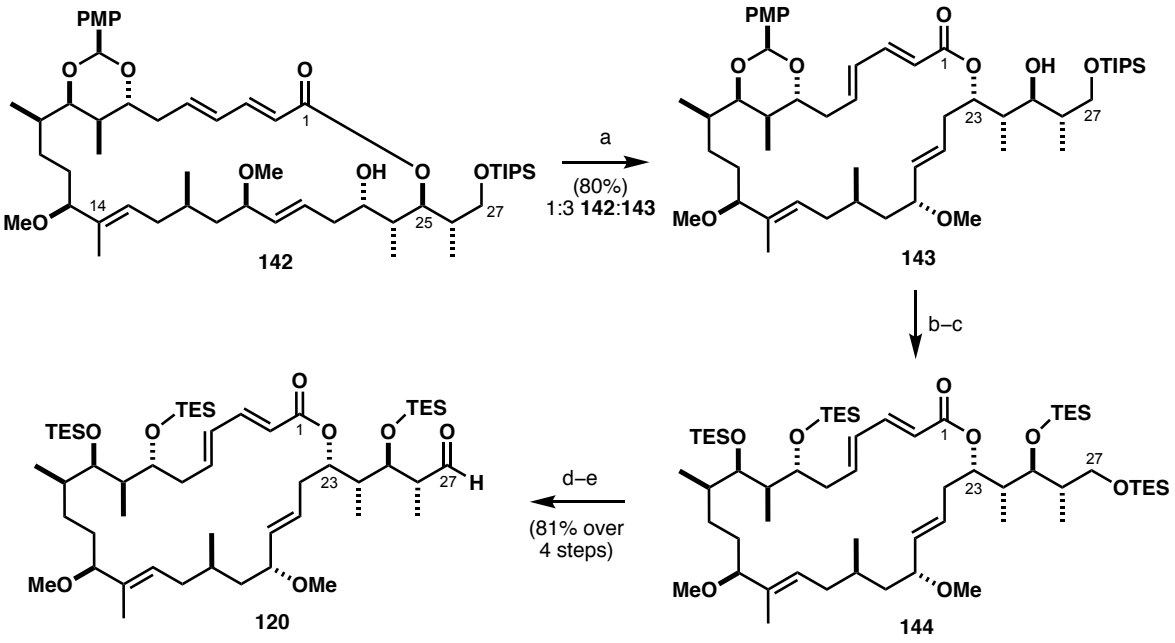

(a) Ti(^{i}PrO)$_4$, CH_2Cl_2; (b) HF (40% aq.), MeCN; (c) TESOTf, 2,6-lut. CH_2Cl_2; (d) THF/AcOH/H_2O (4:1:1); (e) $(COCl)_2$, DMSO, Et_3N, CH_2Cl_2

Scheme 43 Ti(^{i}PrO)$_4$-mediated transesterification and elaboration to the aldehyde at C_{27} by Blakey and Fink[108]

Fortunately, translactonisation upon treatment with Ti(^{i}PrO)$_4$ returned a mixture of regioisomers in the varying range of 1:1 to 3:1 in favour of the thermodynamically preferred 24-membered ring **143**. As the isomers were separable by column chromatography, resubmission of the undesired isomer **142** to isomerisation facilitated acceptable material throughput to the subsequent steps. Global deprotection with aqueous HF, followed by persilylation of the tetraol with TESOTf led to the key *tetra*-TES intermediate **144**. Over the course of the project, nearly 1 g of this precursor was prepared which enabled the pivotal studies of side chain attachment on advanced material. The delicate α-chiral aldehyde at C_{27} was accessed by hydrolysis of the most labile primary TES ether under mildly acidic conditions and careful Swern oxidation[170] to avoid the risk of epimerisation. This concluded the synthesis of the C_1–C_{27} macrocycle **120** in 21 steps LLS and 14% yield.

2.3.4. Side Chain Attachment Studies

The initial retrosynthetic plan envisaged a Masamune–Roush[171] olefination to forge the C_{27}–C_{28} bond between the macrocyclic aldehyde **120** and a suitable phosphonate **116**. This fragment, which features the delicate *N*-vinylformamide, was prepared by Blakey and subsequently used in a model olefination with truncate aldehyde **145** to probe the feasibility of this approach. The initial studies were promising (**146**), though unfortunately this could not be replicated on the real system (**Scheme 44**). Despite the mild nature of the Masamune–Roush protocol,[171] the reaction with aldehyde **120** returned solely the C_{25} TES elimination product **147**.

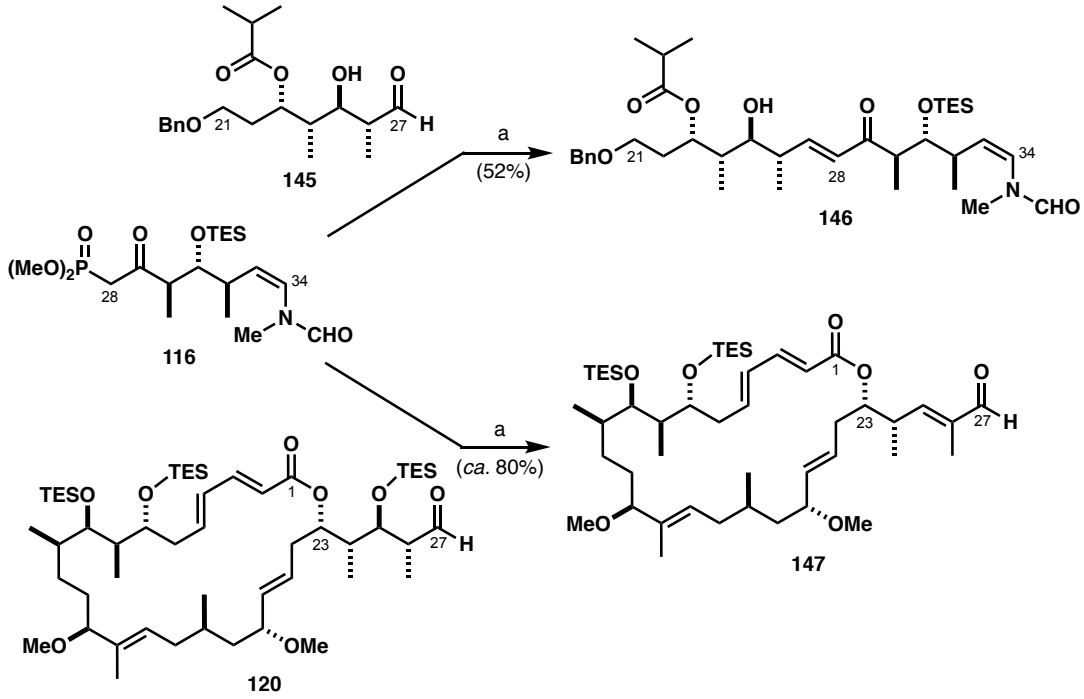

Scheme 44 Blakey's model study and failed side chain attachment of the first-generation C_{28}–C_{34} phosphonate **116** to macrocycle **120**[172]

In light of this disappointing outcome, Blakey revised the strategy to retain macrocycle **120** and instead achieve the side chain union *via* a boron aldol/mesylation/elimination sequence with a new C_{28}–C_{34} methyl ketone fragment **117** as illustrated in **Scheme 45**. Early studies of subsequent steps showed promise, though an unsurmountable issue was faced upon installing the final stereocentre at C_{29} with the Evans–Tishchenko protocol. Even with increased loading of SmI_2, high excesses of acetaldehyde were necessary to achieve good conversion, which often resulted in substantial amounts of the *bis*-acetylated byproduct **148** being formed.

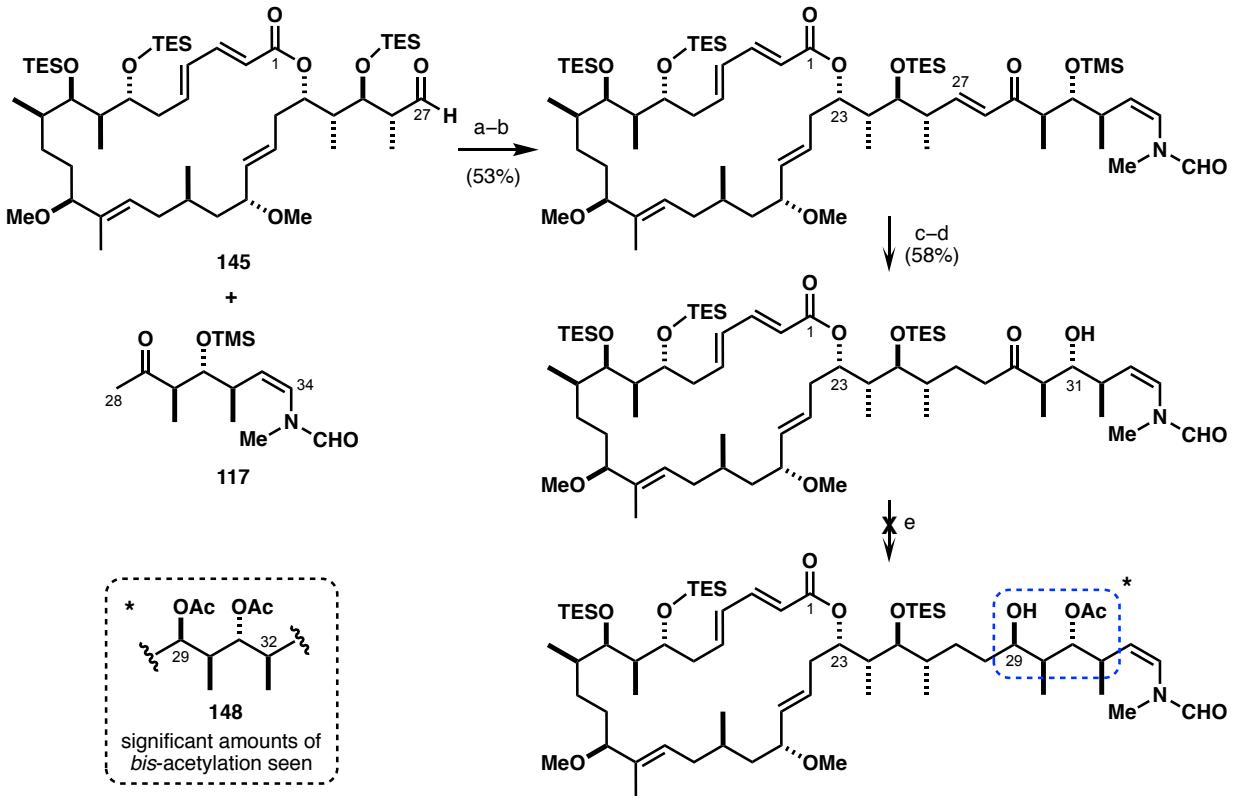

(a) Cy_2BCl, Et_3N, Et_2O; (b) MsCl, Et_3N, DBU, CH_2Cl_2; (c) TBAF, AcOH, THF; (d) $[CuH{\cdot}PPh_3]_6$, PhH; (d) SmI_2, MeCHO, THF

Scheme 45 Attachment of the second-generation side chain fragment **117** and failed Evans–Tishchenko reaction by Blakey

2.3.5. Endgame

The strategy was refined once again to modify the precise structure of the ketone coupling partner after the boron aldol route had been successfully applied in the reaction with the macrocycle **120**. The major changes were firstly the isomerisation of the (*Z*)- to (*E*)-vinylformamide prior to the coupling step and in the later iteration, earlier installation of the potentially sensitive C_{31} acetate. The new target was methyl ketone **118**.

Fink devised a 10-step synthesis of this fragment, mirroring the tin(II)aldol/ Evans–Tishchenko sequence as applied to the C_{23}–C_{26} stereotetrad. Starting with the ethyl ketone **128** in the enantiomeric series of Roche ester, the (*Z*)-enolate was condensed with acetaldehyde to form the all-*syn* adduct **149** in 97% yield and 15:1 *dr*. This result may be attributed to the superior chelating ability of the PMB ether and the reaction proceeding through **TS 5** (**Scheme 46**).

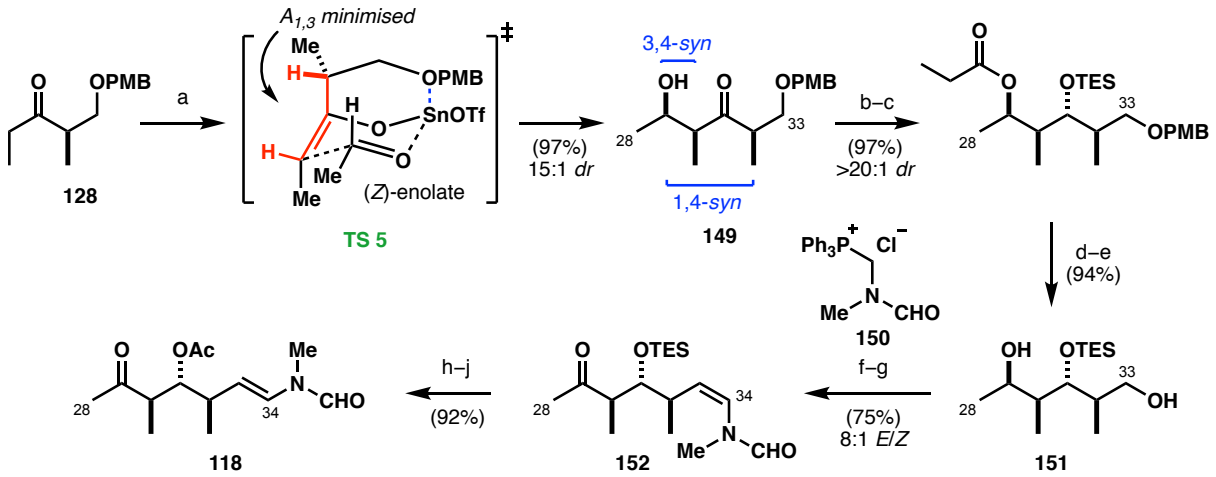

(a) $Sn(OTf)_2$, $^iPrNEt_2$, MeCHO, CH_2Cl_2; (b) SmI_2, EtCHO, THF; (c) TESOTf, 2,6-lut., CH_2Cl_2; (d) DDQ, CH_2Cl_2/pH 9.2 buffer (4:1); (e) DIBALH, CH_2Cl_2; (f) $(COCl)_2$, DMSO, Et_3N, CH_2Cl_2; (g) LiHMDS, **150**, THF; (h) TBAF, AcOH, THF; (i) Ac_2O, Et_3N, DMAP (cat.), CH_2Cl_2; (j) I_2, CH_2Cl_2, dark

Scheme 46 Fink's synthesis of the third-generation side chain fragment **118**

After a directed 1,3-*anti* reduction of the C_{31} carbonyl (97%, >20:1 *dr*), the β-hydroxyl was masked as a TES ether. Protecting group removal and double Swern oxidation of diol **151** concomitantly formed the methyl ketone at C_{29} and aldehyde at C_{33}. The latter then participated in a modified Wittig reaction to install the *N*-vinylformamide moiety with the ylid derived from the phosphonium salt **150**.[173] The C_{33}–C_{34} olefin was forged in an inconsequential 8:1 *Z*/*E* ratio. Fink found that the isomerisation to the thermodynamically favoured (*E*)-geometry failed with silyl ethers at the C_{31} hydroxyl and thus the protecting group was first replaced with the electron-withdrawing acetyl. Treatment of **152** with tetrabutylammonium fluoride (TBAF)/AcOH and esterification of the free hydroxyl with acetic anhydride yielded the suitable substrate for iodine-mediated isomerisation, which converted the olefin to the exclusively (*E*)-isomer. The C_{28}–C_{34} fragment **118** was synthesised in 10 steps and 43% yield from ethyl ketone **128**.

With the two key fragments in hand the stage was set for the boron aldol coupling, followed by dehydration using Burgess' reagent[174] which reliably proceeded in 65% over two steps from the macrocyclic aldehyde **120** to return the corresponding enone (**Scheme 47**) with minimal elimination of the C_{31} acetate. A chemoselective reduction of the enone was cleanly achieved with Stryker's reagent[175] with the yields consistently exceeding 80%. Williams implented Yun's simplified procedure for the preparation of the reagent solution[176] and hence ketone **153** was reliably accessible in an operationally undemanding manner. The final stereocentre was configured in a substrate-controlled reduction with freshly prepared $Zn(BH_4)_2$ which formed a 10:1 mixture in favour of the desired (29*R*) isomer **154**, though the outcome was highly dependent on the quality of the reagent.

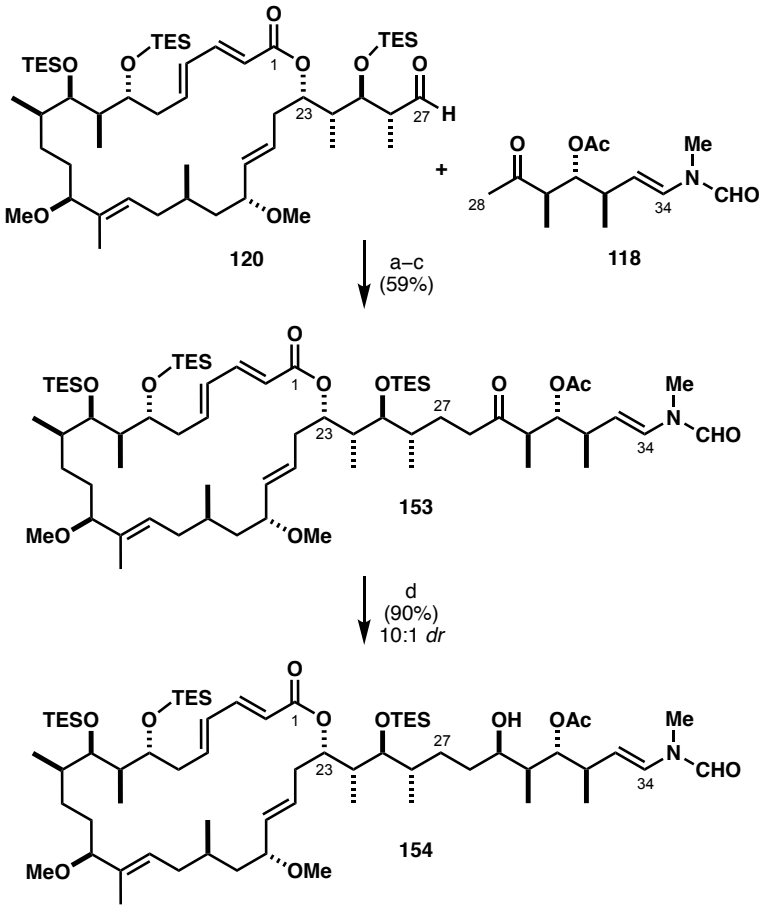

(a) Cy_2BCl, Et_3N, Et_2O; (b) Burgess' reagent, THF; (c) $[CuH{\cdot}PPh_3]_6$, PhMe; (d) $Zn(BH_4)_2$, Et_2O

Scheme 47 Boron aldol side chain attachment and reduction of the C_{29} ketone by Fink[177]

Fink completed the total synthesis of aplyronine C (**13**) by forming the ester on the C_{29} position using the Keck protocol[127] with DMAla **156** then global deprotection of the three remaining silyl ethers. The overall yield of the sequence was 5% over 29 steps LLS from the Roche ester-derived ketone **129**. Williams later demonstrated that that aplyronine C (**13**) is in fact a direct precursor to aplyronine A (**1**) without the need for differential protection of the hydroxyls at C_7/C_9. The free 1,3-diol undergoes regioselective esterification under Yamaguchi–Yonemitsu conditions[125] with TMSer **158** when carefully monitored to prevent byproduct formation and pushed to 50–80% conversion before *bis*-acetylaton occurs. Aplyronine A (**1**) was obtained in 55% yield and 46% recovery of the precursor with a 2.2% overall yield over 30 steps LLS. By appending the DMGly **155** at C_{29} onto the *tris*-TES intermediate **154**, the same route was able to provide aplyronine D (**14**, 61% yield with 25% recovered aplyronine C) in 2.6% overall yield over the same number of steps in the LLS, which constituted the first completed total synthesis of this congener.

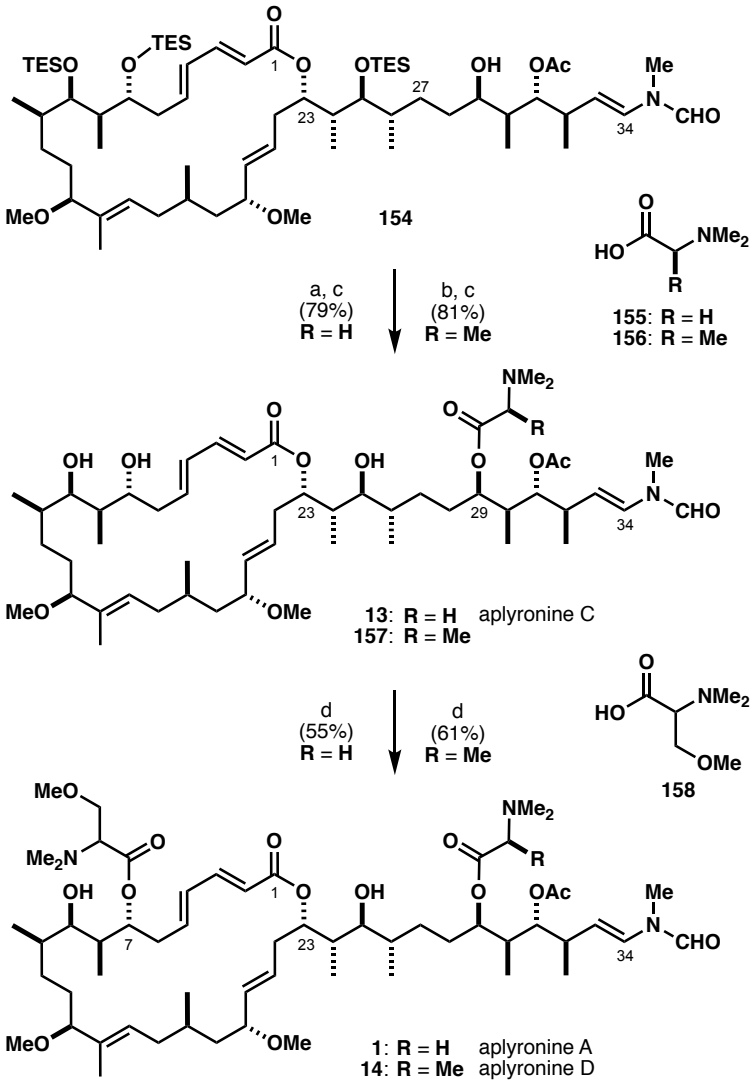

(a) **156**, TCBC, Et_3N, DMAP, THF, PhMe; (b) **155**, DCC, DMAP·HCl, DMAP, CH_2Cl_2; (c) HF·pyr, pyr, THF; (d) **158**, TCBC, Et_3N, DMAP, PhH, CH_2Cl_2

Scheme 48 Divergent endgame strategy and synthesis of aplyronines A, C and D by Williams[111]

2.4. Summary

At the onset of the work within the Paterson group, the main objective was to devise a shorter and more efficient route to the aplyronines as compared to the first reported synthesis by Yamada. A side-by-side overview of yields and step counts confirms that this goal had indeed been met (**Table 3**). A critical analysis of the existing total synthesis reveals several major advantages over other group's strategies. For example, all three stereotetrads are set up using the Paterson aldol methodology/1,3-*anti* reduction sequence in high *dr* and 85% yield or better. Next, the (*E*,*E*)-dienoate is introduced with complete selectivity at an early stage in the C_1–C_{11} iodide synthesis. Perhaps the most crucial advancement first seen in the Paterson approach is the convergent HWE olefination to assemble the C_1–C_{27} carbon skeleton,

which brings together two fragments of similar size and complexity in a superb 91% yield and 14:1 ratio of *E*/*Z* isomers. Finally, the delicate *N*-vinylformamide is present in the side chain fragment **118** and is remarkably unaffected by any transformations following its appendage in the boron aldol reaction with the macrocycle **120**.

Table 3 Overview of the total synthesis routes to aplyronines A (**1**), C (**13**) and D (**14**)

	Yamada		Kigoshi	**Paterson**		
Congener	*ApA*	*ApC*	*ApA*	*ApA*	*ApC*	*ApD*
Steps LLS	47	46	38	30	29	30
Steps total	98	97	80	48	47	48
Yield (%)	0.39	0.14	1.4	2.6	3.6	2.2

However, despite several advantages there remain a number of issues which must be addressed if this route is to be implemented on a large enough scale to deliver material for further biological studies. In particular, several steps remain capricious and appear to be greatly influenced by quality of starting materials or reagents in key stereoselective reactions. The majority of these pertain to the macrocyclic portion of the natural product and are undoubtedly the main areas to which attention should be turned in future refinements of the synthesis.

Starting with the overall retrosynthetic analysis, the site-selective macrolactonisation plan had unfortunately failed and introduced an inefficient series of protecting group manipulations after the HWE coupling of the northern and sourthern fragments **139** and **134** (shown previously in **Scheme 42**). Furthermore, the translactonisation of macrolide **142** to the desired ring size (**143**) was found to be unreliable, giving mixtures of the two macrolactones which severely limits the throughput of these relatively late-stage intermediates.

In the early fragment synthesis, yields for the tin aldol step on the C_{21}–C_{27} aldehyde **124** were not be reproducible and the use of capricious $Sn(OTf)_2$ was be cumbersome on large scale. Despite the studies on the side chain fragment **118** being more encouraging, the decision was made to investigate other suitable substitute for this methodology towards this fragment. With regards to the northern C_1–C_{14} phosphonate **139**, the choice of the C_7/C_9 PMP acetal proved counterproductive and the appendage of the β-ketophosphonate was only recently identified as less regioselective than deemed by Woodrow and Blakey.

In summary, the Paterson route to aplyronine A reduced the number of linear steps by more than 15 compared to the first total synthesis by Yamada, accompanied by a dramatic increase in yield.

Nevertheless, there is plenty of scope for improvement. It is conceivable that this may be achieved by implementing more modern synthetic methodology developed after the early investigations in the late 1990s and a more informed protecting group strategy.

Chapter 3

Results and Discussion – Part I

Synthesis of C_1–C_{11} Iodide 160 and C_{15}–C_{27} Aldehyde 161

3.1. Project Aims

Chapter 2 discussed the accomplishment of a divergent synthesis of multiple aplyronine congeners within the Paterson group. However, more recent findings on the mode of action of the aplyronines by Kigoshi[75,81–83,178] gave the existing body of work an entirely new direction. Owing to the rare combination of picomolar potency and a novel mechanism of action the aplyronines have been identified as ideal candidates for ADC payloads.

Detailed investigations into this potential application are currently limited by the prohibitively low isolation yields of aplyronines from natural sources. A successful campaign to develop them into serious ADC candidates will require a sustainable supply of stable late-stage precursors, which can only be achieved through chemical synthesis. This is an adventurous but realistic prospect for the future of this project based on the current concise endgame sequence following the assembly of the complete carbon skeleton. Williams also proved that the final steps of the strategy yield appropriate intermediates for diversification without the need for a strategy revision to include differential protection of amino acid-bearing hydroxyls.

To ultimately initiate investigations into the aplyronines as ADC payloads, multigram stocks of both the macrocycle **120** and the side chain **118** have to be replenished as the first priority to meet the demands. This goal calls for a large-scale synthesis of the C_1–C_{27} alcohol **159** (*vide supra*), and offers the opportunity to develop an improved route drawing on the lessons learned *en route* to the first-generation

Paterson approach. Addressing the most pressing issues highlighted in **Section 2.4** is expected to yield a more robust synthesis of individual fragments as well as a more convergent protecting group strategy in the ideal scenario.

3.2. Second-Generation Protecting Group Strategy

The major skeletal disconnections from the first-generation route had generally proved successful and so it was decided that these would be retained in developing a revised synthesis (**Scheme 49**). The challenge then became designing a streamlined protecting group strategy and improving upon the synthesis of the individual fragments.

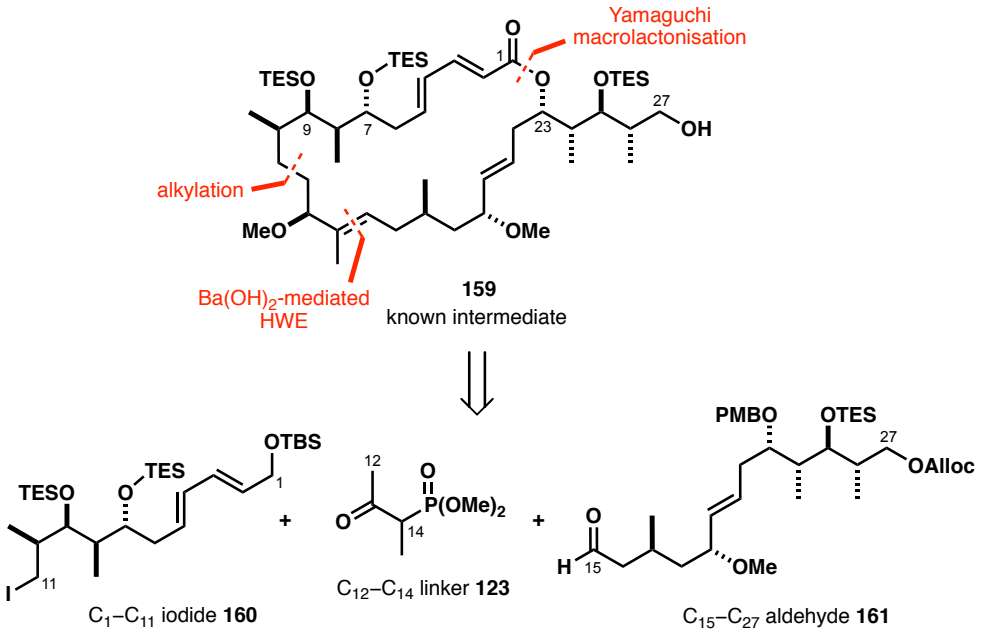

Scheme 49 Retrosynthetic analysis of macrocycle **159** and second-generation protecting group strategy

The main goal of altering the protecting groups was to reduce the number of manipulations in the later stages of the synthesis of alcohol **159** and to provide a suitable substrate for site-specific macrolactonisation. The selection was largely inferred from the conclusions of the first-generation route combined with previous experience with the stability of individual moieties with regards to planned transformations. Firstly, alcohol **159** possesses TES ethers at the C_7, C_9 and C_{25} hydroxyls and it is favourable to introduce them at the earliest opportunity. C_7 and C_9 are differentiated by a pendant amino acid at C_7 in the several aplyronine congeners. However, Williams has demonstrated that the required esterification can be achieved in a site-selective manner onto the C_7 hydroxyl in presence of the C_9 alcohol. There is hence no need for distinction in the masking step and *bis*-TES silylation is a suitable option from the onset. By also introducing the required TES ether at C_{25}, site-specific macrolactonisation

would be enabled by orthogonal protection and later unmasking of the C_{23} hydroxyl. It was proposed that a particularly attractive choice in this case would be a PMB group. It could be cleaved upon treatment with DDQ which coincides with the conditions used to convert the C_1 allylic TBS ether into the corresponding aldehyde. Both macrolactonisation sites would effectively be unmasked in an efficient single operation. (**Scheme 50**).

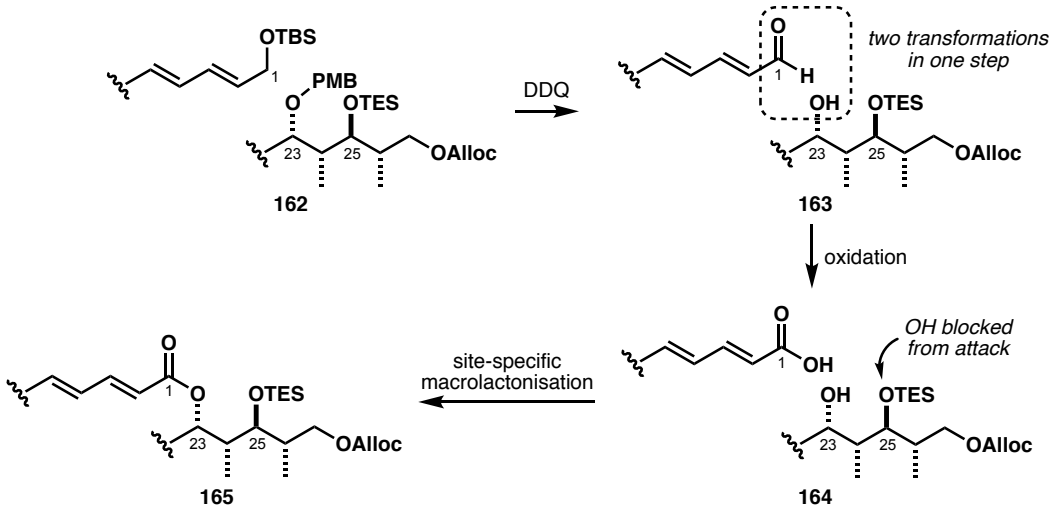

Scheme 50 One-step DDQ-mediated unmasking of C_1 and C_{23} to facilitate site-specific macrolactonisation

There is a certain risk that the steric bulk of the TES group would hinder or entirely preclude the cyclisation step. Evidence both for and against this argument can be found in syntheses of numerous other natural products with a 1,3-diol moiety as the macrolactonisaton site.[179–183] However, the conclusion drawn from inspecting the literature is that it is not straightforward to predict how the structure of substrate will affect the ring closure and hence every system must be treated on an individual basis.

The planned site-specific macrocyclisation was thus a particularly uncertain venture as its merit could only be tested at a relatively advanced stage. Williams' attempts to break the *tetra*-TES lactone **144** by saponification in order to trial such a ring closure on material already in hand had been unsuccessful (**Scheme 51**).[184] There was no surrogate path to acquiring the *seco*-acid **166** than through synthesis.

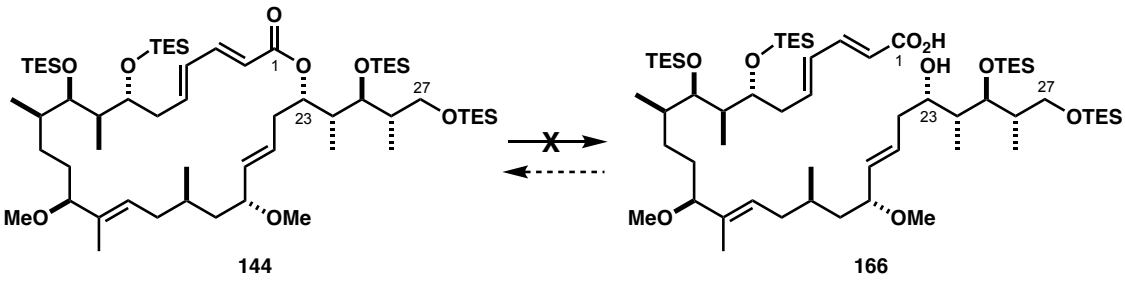

Scheme 51 Failed attempt at hydrolysing the *tetra*-TES macrolactone **144**[184]

Finally, alcohol **159** would be obtained by deprotection at C_{27} as the last step as had been demonstrated on a *tetra*-TES intermediate **144** where hydrolysis of the primary C_{27} silyl was possible, but not entirely selective.[111,162,177] In order to avoid protecting group manipulations at a later stage, this moiety at C_{27} would also have to be introduced very early on. The primary TES group was unlikely to withstand a long sequence of steps towards the macrolactone though identifying an alternative amongst conventional protecting groups was challenging. The deprotection step would need to take place in presence of silyl ethers, electron-rich and electron-poor olefins and the lactone. Eventually, the decision was made to opt for an orthogonal allyl carbonate (Alloc). Its cleavage can be affected by a source of palladium and an allyl scavenger, which was expected to leave any other functionality intact. The carbonate was anticipated to be stable to most conditions with the exception of strong nucleophiles or reducing agents[185] and the use of these reagents was not anticipated after the fragment coupling. Williams trialled the Alloc protection/deprotection sequence at C_{27} on the available macrocyclic material which showed the feasibility of this method (**Scheme 52**).[184]

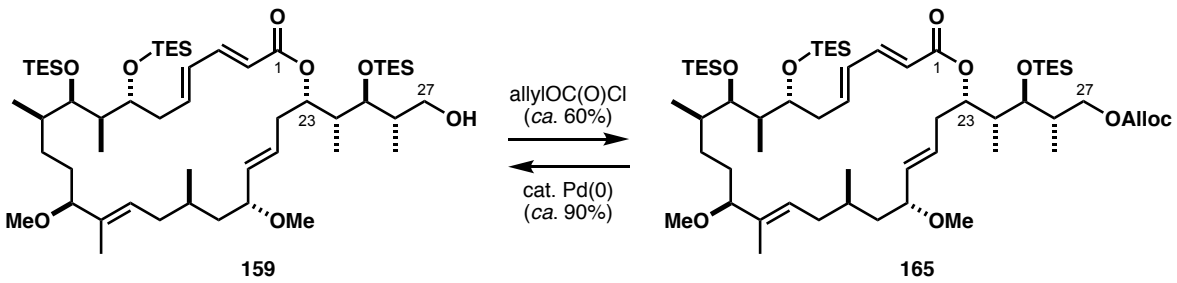

Scheme 52 Williams' small-scale trial of Alloc protection and deprotection at C_{27}

This chapter will now describe the work done by the author towards a streamlined route to the C_{15}–C_{27} aldehyde **161** and synthesis of the C_1–C_{11} iodide **160**. All modifications were implemented with a large-scale synthetic campaign in mind, carrying out as many transformations as possible on gram-quantities of substrates by devising highly scalable and robust protocols.

3.3. Synthesis of C_{15}–C_{27} Aldehyde 168

3.3.1. Retrosynthesis of the C_{15}–C_{27} Fragment 161

The key disconnections from the initial retrosynthetic analysis for the C_{15}–C_{27} fragment **134** envisioned by Woodrow and Cowden were maintained for the scale up campaign with the intention of adapting the route to the meet current needs of the project. A pivotal disconnection across the C_{14}–C_{15} bond led to two key fragments, β–ketophosphonate **167** and aldehyde **168** which would be coupled in a mild, $Ba(OH)_2$-mediated HWE reaction (**Scheme 53**). Fragment **167** contains a remote C_{17} stereocentre, which can be

incorporated by functionalising (*R*)-methyl-3-methylglutarate **137**, derived from an achiral precursor in an enzyme-mediated desymmetrisation reaction. Aldehyde **168** which carries a stereotetrad at C_{23}–C_{26}, which could be constructed through an aldol condensation.

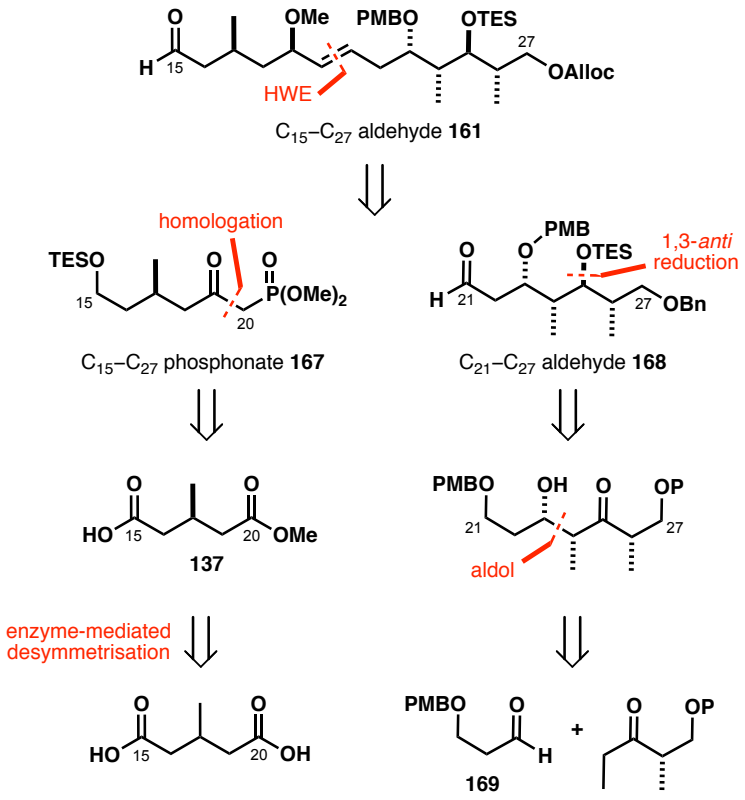

Scheme 53 Retrosynthetic analysis for the C_{15}–C_{27} aldehyde **161**

3.3.2. Tin Aldol Approach to C_{23}–C_{26} Stereotetrad

One of the key motivations to revisit the synthesis of the C_{21}–C_{27} aldehyde **168** beside adjusting the protecting groups was the requirement to produce a reliable and scalable protocol to generate the 1,3,4-*syn* configuration embedded in the C_{23}–C_{26} stereotetrad. This motif can be constructed in a $Sn(OTf)_2$-promoted aldol reaction using a chiral ketone to direct facial selectivity of the enolate. Early investigations on this methodology can be traced back to the work by Mukaiyama[186] and Evans[187] on the utility of $Sn(OTf)_2$ in asymmetric aldol reactions of α-chiral ethyl ketones or β-ketoimides as propionate equivalents. 1,3-*syn*-3,4-*syn* aldol adducts can be obtained in excellent diastereoselectivity (90–95%) without the use of chiral auxiliaries which can be attributed to substrate control and highly selective formation of (*Z*)-enolates in the presence of a tertiary amine base.

Paterson and Tillyer further expanded the substrate scope by exploring examples using Bn- and TIPS-protected Roche ester-derived ethyl ketones **129** and **170** as enolates (**Scheme 54**).[144] High levels of π-

facial selectivity observed implied that in contrast to analogous boron and titanium enolates, tin enolates are likely to be conformationally more restricted. This proposal can be rationalised by considering a chelation interaction between the hydroxyl protecting group on the enolate and the Lewis acidic tin centre. In light of this stabilising effect, the favoured Zimmerman–Traxler[155] transition state is one in which the methyl group points outwards to reduce axial steric congestion (**TS 6**). While the model is consistent for the electron-rich aryl or alkyl ethers on the ketone, it does not account for high *dr* observed with the triisopropylsilyl (TIPS) moiety as silyl groups have been shown to be poor chelating agents.[188]

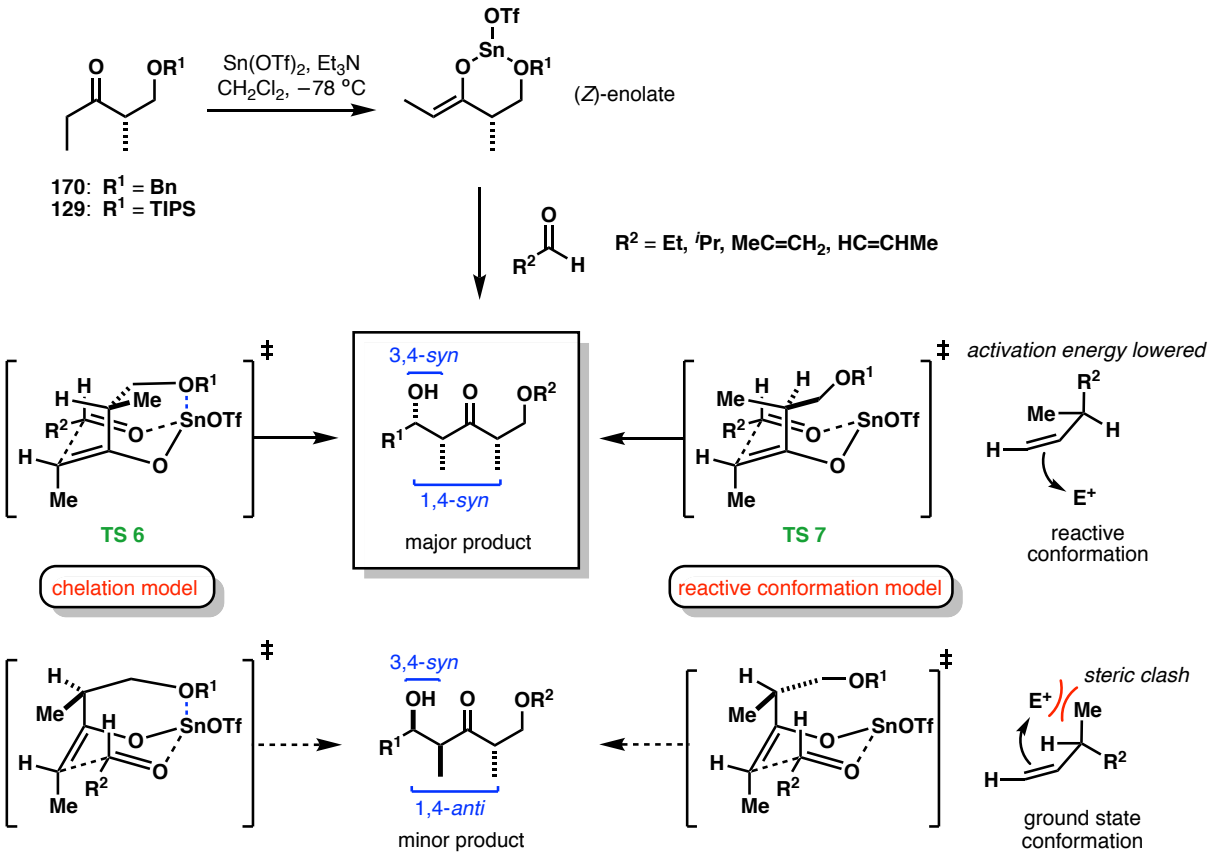

Scheme 54 Two contrasting transition state proposals for selectivity in $Sn(OTf)_2$ propionate aldol reactions

A more convincing argument may be drawn from the reactivity mode of analogous α-chiral olefins with electrophiles. In the ground state, allylic strain is preferentially minimised by having an eclipsing interaction between the hydrogen on the α-chiral stereocentre and the double bond. This forces the incoming electrophile to approach from the less sterically encumbered face (**TS 7**, **Scheme 54**). Conversely, certain have been known to react by having a methyl group eclipsing the olefin instead as the $A_{1,3}$ interaction is not large.[189] The activation energy of the system is hence lowered and the electrophile approaches past the hydrogen atom, which results in the same stereochemical outcome than the one predicted by the aforementioned chelation model (**TS 6**). In this case, greater bulk of the silyl ether is favourable and is expected to enhance the levels of selectivity.

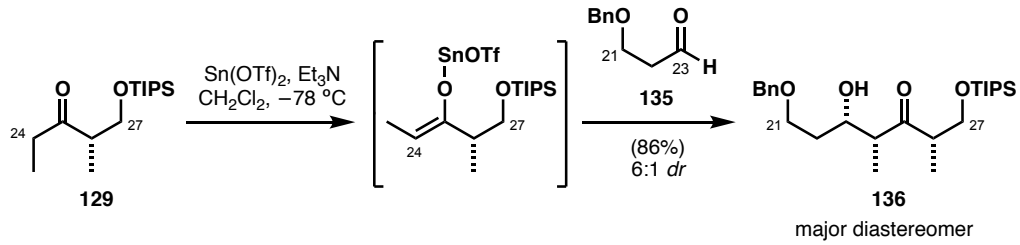

Scheme 55 Lee's synthesis of β-hydroxy ketone **136**

Woodrow initially obtained 9:1 *dr* and 88% yield for the aldol reaction between ketone **129** and aldehyde **135**, though Lee later struggled to reproduce this result (**Scheme 55**). The TIPS moiety was irreplaceable as part of the overall protecting group strategy thus efforts were focused on bolstering the yield instead. To probe the steric effect of different silyl group, the appropriate ethyl ketone bearing the *tert*-butyldimethylsilyl (TBS) group was explored as the next option.

Ketone **171** was synthesised by the controlled nucleophilic attack of ethylmagnesium bromide into Weinreb amide **172**,[†] to form chelated intermediate **173** at low temperature before collapsing upon aqueous workup (**Scheme 56**). This stable intermediate precludes undesired further addition of the Grignard reagent to the more electrophilic carbonyl product. The amide precursor had previously been made by silyl protection of commercially available (*S*)-Roche ester **127** with TBSCl, followed by treatment with *N*,*O*-dimethylhydroxylamine hydrochloride in presence of isopropylmagnesium chloride.

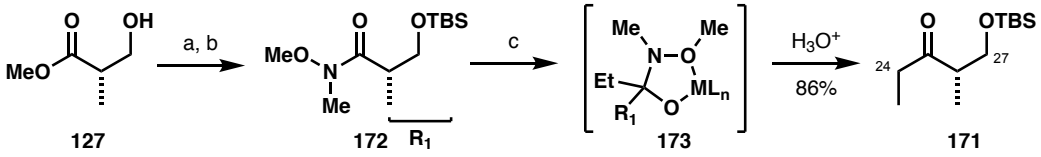

(a) TBSCl, CH_2Cl_2, imid., rt; (b) MeNH(OMe)·HCl, ^{i}PrMgCl, THF, −20 °C; (c) EtMgBr, Et_2O, 0 °C → rt, 13 h

Scheme 56 Synthesis of ethyl ketone **171**

Aldehyde **169** was produced by reacting PMBCl with excess propane-1,3-diol to achieve *mono*-protection, followed by Swern oxidation[170] of the remaining primary alcohol. Aldol coupling partner **169** was obtained in 82% yield over two steps from more than 20 mmol of PMBCl (**Scheme 57**).

[†] Stocks of Weinreb amide **172** were available in the laboratory.

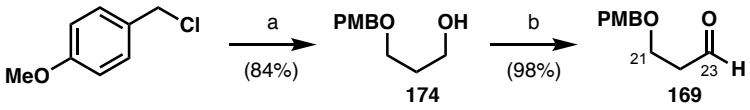

(a) 1,3-propanediol, KOH, DMSO, rt, 3.5 h; (b) $(COCl)_2$, DMSO, Et_3N, CH_2Cl_2, −78 °C, 1 h, *then* **174**, 30 min, *then* rt, 1.5 h

Scheme 57 Synthesis of aldehyde **169**

Ketone **171** was converted to the (*Z*)-enolate with $Sn(OTf)_2$ and Et_3N at −78 °C before slowly adding excess **169** to ensure complete consumption of the starting material. However, unreacted aldehyde **169** proved difficult to separate from the reaction product and so the crude mixture was subjected to Pinnick oxidation to chemoselectively convert the aldehyde functionality into the corresponding carboxylic acid **177**.[169] After purification by column chromatography, aldol adduct **175** and the minor diastereomer **176** were isolated as an 8:1 *dr* mixture in 74% yield (**Scheme 58**).

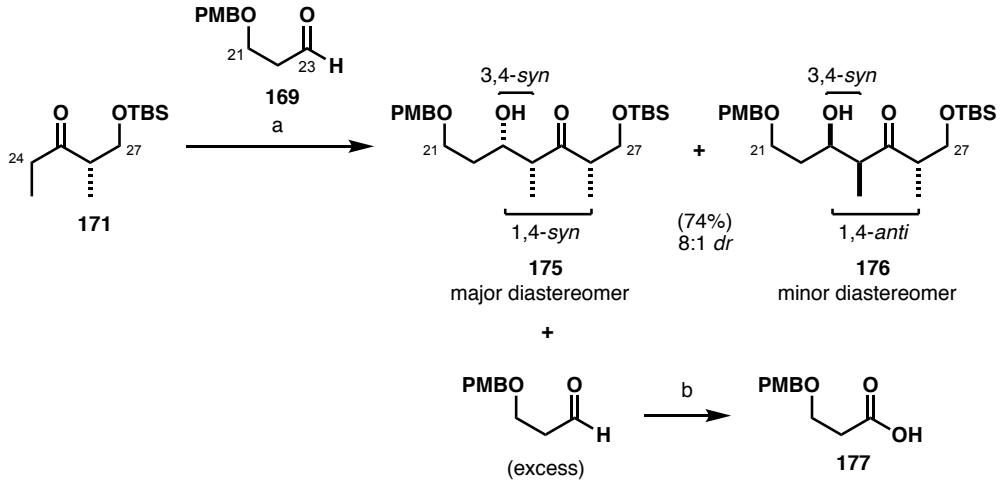

(a) $Sn(OTf)_2$, Et_3N, CH_2Cl_2, −78 °C, 2 h, *then* **169**, 15 h; (b) $NaClO_2$, $Na_2HPO_4 \cdot 2H_2O$, 2-Me-but-2-ene, ^tBuOH, H_2O, rt, 16h

Scheme 58 $Sn(OTf)_2$ aldol reaction of ketone **171** and aldehyde **169**

The changes in protecting groups at C_{21} and C_{27} were unlikely to overturn the expected all-*syn* stereochemical outcome of the aldol reaction and this could be verified by examining the characteristic coupling constants of protons at the newly formed chiral centres in the ^1H NMR spectra. Conformationally unrestricted β-hydroxy ketones preferentially adopt a 6-membered half chair conformation when intramolecular hydrogen bonding between the hydroxyl group and the ketone exerts the dominant conformational bias in a non-hydrogen-bonding solvent (**Figure 26**).[190]

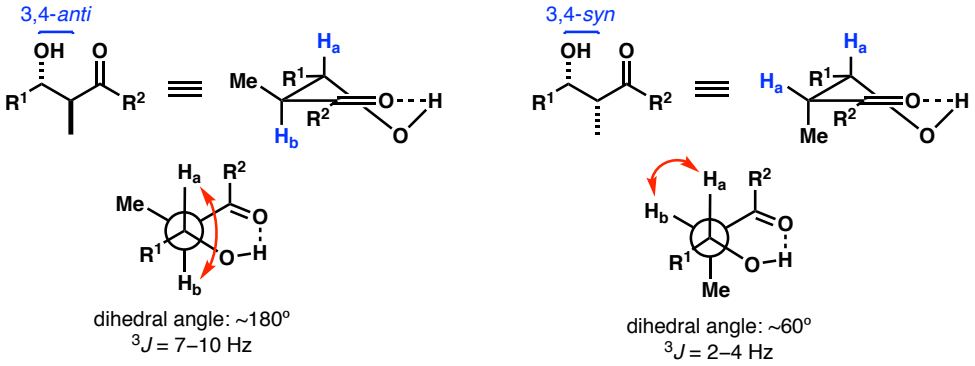

Figure 26 Favoured conformations of *anti* and *syn* aldol adducts governed by internal hydrogen bonding

If the substituents at C_{23} and C_{24} in aldol adduct **175** indeed lie *syn* to each other, the dihedral angle between H_{23} and H_{24} is expected to be close to 60°, suggesting there should be a small vicinal coupling constant (^3J = 2–4 Hz) observed between them as foreseen by the Karplus' theory[191,192] and reassured by empirical evidence. In contrast, 1,2-*anti* relationship would force a *trans*-diaxial arrangement of those protons, hence the large dihedral angle would give rise to coupling constants in the order of 7–10 Hz instead. The measured value for product **175** was 4.0 Hz, which supports the anticipated *syn* relationship between H_{23} and H_{24}.

The absolute configuration at the C_{23} carbinol centre was ascertained by Mosher ester analysis. This method is based on esterification of the chiral alcohol in question with both enantiomers of the α-methoxy-α-trifluoromethyl-phenylacetic acid (MTPA-OH), followed by ^{1}H NMR analysis of their diastereomeric derivatives.[193] The MTPA esters adopt a thermodynamically favoured conformation in solution which places the highly electronegative CF_3 group coplanar with the carbonyl and the methine proton. The phenyl ring exerts a through-space, time-weighted average shielding effect on the protons in its proximity, which causes an upfield shift in the ^{1}H NMR compared to the same set of protons in the diastereomeric ester (**Figure 27**). The configuration is then deduced from the sign of the difference ($\Delta\delta = \delta_S - \delta_R$) in chemical shifts on each side of the chiral alcohol for as many protons as possible.[194]

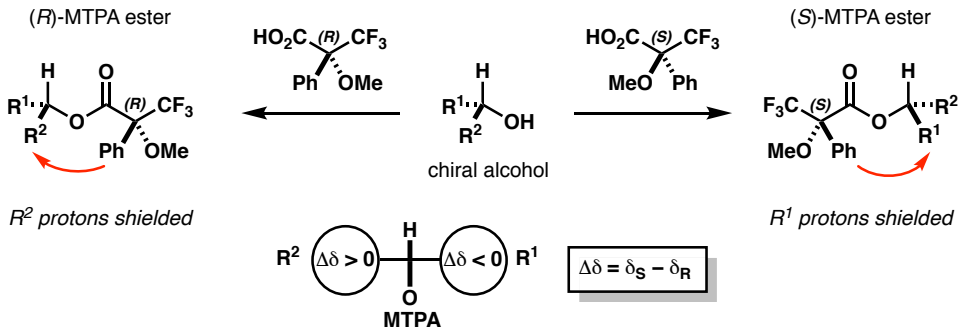

Figure 27 Mosher ester analysis model for a secondary alcohol[193,194]

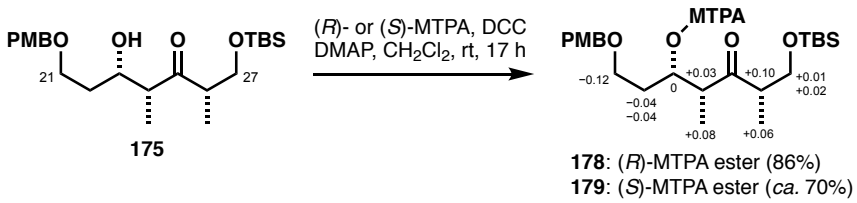

Scheme 59 Preparation of Mosher esters of alcohol **175**

β-Hydroxy ketone **175** was esterified with (*R*)- and (*S*)-MTPA-OH in presence of *N*,*N*-dicyclohexylcarbodiimide (DCC) and *N*,*N*-dimethylaminopyridine (DMAP) separately to provide the corresponding (*R*)- and (*S*)-MTPA esters **178** and **179** (**Scheme 59**). Analysis of ^{1}H NMR spectra for both compounds showed that the $\Delta\delta_{S-R}$ signs for protons in the vicinity of the carbinol centre corresponded to the pattern, in agreement with the (*S*)-configuration at C_{23}.

Unfortunately, the yield and *dr* of aldol adduct **175** were still deemed to be unsatisfactory, leading to a revision of the C_{27} protecting group. In the hope of reinforcing a chelation-controlled transition state, the C_{27} TBS was replaced by an electron-rich benzyl (Bn) ether. **Scheme 60** depicts the possible rationale for enolisation outcome of ketone **170** based on tin chelation in the deprotonation step to give the (*Z*)-enolate.

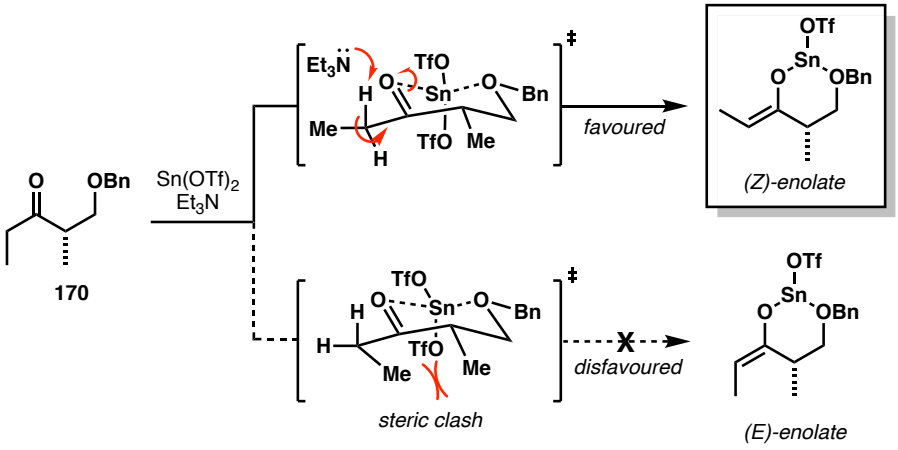

Scheme 60 Selective formation of the (*Z*)-enolate of ethyl ketone **170** with $Sn(OTf)_2$

Paterson had previously demonstrated this possibility with the enantiomeric (*R*)-ethyl ketone **180** which afforded the all-*syn* aldol adduct **181** in 92% yield and 15:1 *dr* (**Scheme 61**),[144] which was highly promising.

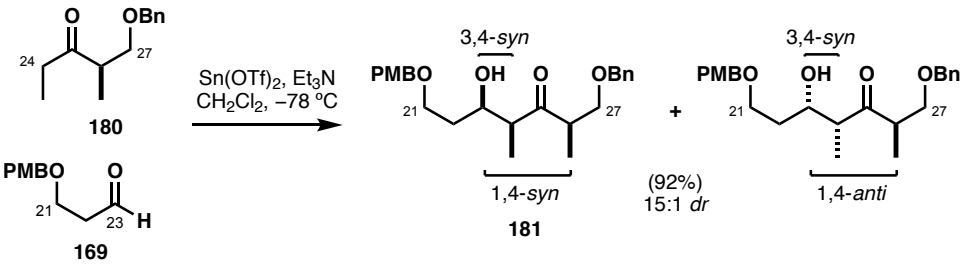

Scheme 61 Paterson's tin(II) aldol with ketone **180** and aldehyde **169**

(*S*)-Ethyl ketone **170** was prepared in the known manner from Weinreb amide **182**. Disappointingly, the aldol step failed to give the sought degree of improvement as β-hydroxyketone **183** was isolated in 10:1 *dr* and 61% yield after oxidation of the excess aldehyde (**Scheme 62**).

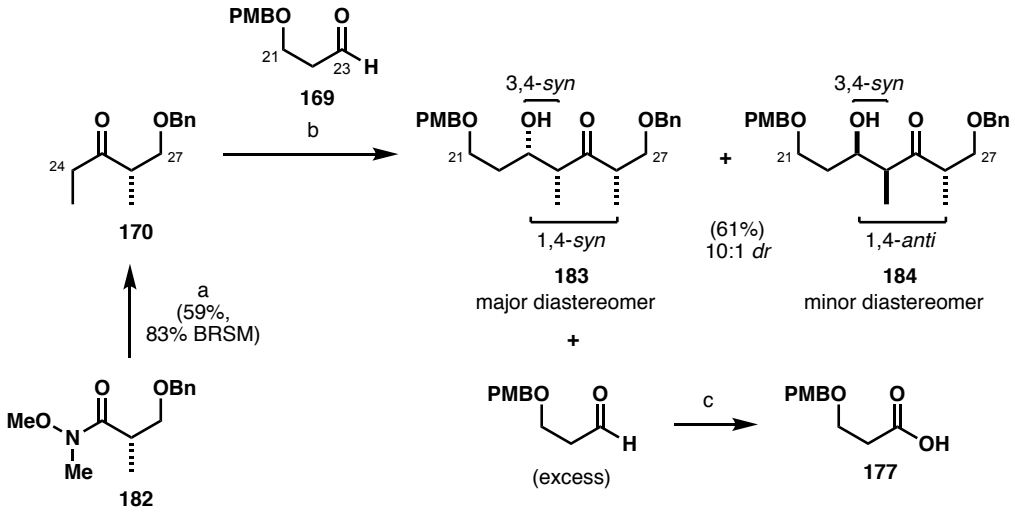

(a) EtMgBr, Et_2O, 0 °C → rt, 18 h; (b) $Sn(OTf)_2$, Et_3N, CH_2Cl_2, −78 °C, 30 min, *then* **169**, 1.5 h; (c) $NaClO_2$, $Na_2HPO_4 \cdot 2H_2O$, 2-Me-but-2-ene, ^tBuOH, H_2O, rt, 2.5 days

Scheme 62 $Sn(OTf)_2$ aldol reaction of ketone **170** and aldehyde **169**

Once again, Mosher ester analysis was carried out to reassure the (*S*)-configuration of the newly formed hydroxyl in a rigorous fashion as shown in **Scheme 63**.

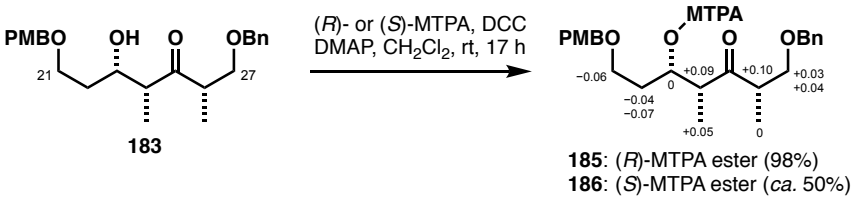

Scheme 63 Synthesis of Mosher esters of alcohol **183**

As this result compared poorly to the literature precedent, the quality of the $Sn(OTf)_2$ used in the aldol reaction appeared to be critical, leading to the variability observed. Taking into account the

drawbacks associated with the preparation and handling of $Sn(OTf)_2$ combined with ambitious scale-up goals in this project led to the decision to seek an alternative avenue to forge the C_{23}–C_{26} stereotetrad.

3.3.3. Titanium Aldol Approach to C_{21}–C_{27} Aldehyde 168

In the search for a compatible method for constructing the vital 1,3-*syn*-3,4-*syn* propionate motif a survey of the literature revealed a suitable alternative in the form of aldol reactions using titanium enolates derived from unsymmetrical carbonyls. A seminal report in this area is Evans' protocol for soft, highly (*Z*)-selective enolisation of ketones with titanium(IV) Lewis acids in combination with tertiary amine bases,[195] comparable to the analogous tin(II)-mediated process. The titanium enolates then proceed to react with aldehydes *via* a Zimmerman–Traxler transition state where the highly oxophilic titanium centre facilitates a chair-like conformation through tight Ti–O bonds. The stereoselectivity is imparted exclusively by one or more of the following elements: the stereogenic centres or chiral ligands on the enolate, chiral auxiliaries on the carbonyl, groups with chelating ability or Felkin–Anh control in reactions with α-chiral aldehydes.[196]

Urpí and Roméa have made a substantial contribution to the applications of titanium enolates derived from α- and β-hydroxy ketones for the assembly of polypropionate-like natural products.[197,198] Crucial insight into the peculiar behaviour of titanium complexes has been gathered through investigating enolisation conditions, particularly by tuning the acidity and steric demands of the metal centre. Starting from $TiCl_4$, chloride ligands were systematically replaced for one or two isopropoxides (^{i}PrO) to create softer Lewis acid species, tailored for each particular substrate for the case of α-hydroxy ketones.[197–199] The substrate scope was thus widely expanded as a greater variety of otherwise labile protecting groups on the aldol coupling partners was tolerated.

The methodology was later extended to reactions of Roche ester-derived β-hydroxy ketones **170** and **187** with the clear intention of providing alternatives to the $Sn(OTf)_2$-promoted aldol reactions to forge the 1,4-*syn*-3,4-*syn* pattern (**Scheme 64**).[200] Its relevance has since been demonstrated in several syntheses of natural product fragments.[201–203]

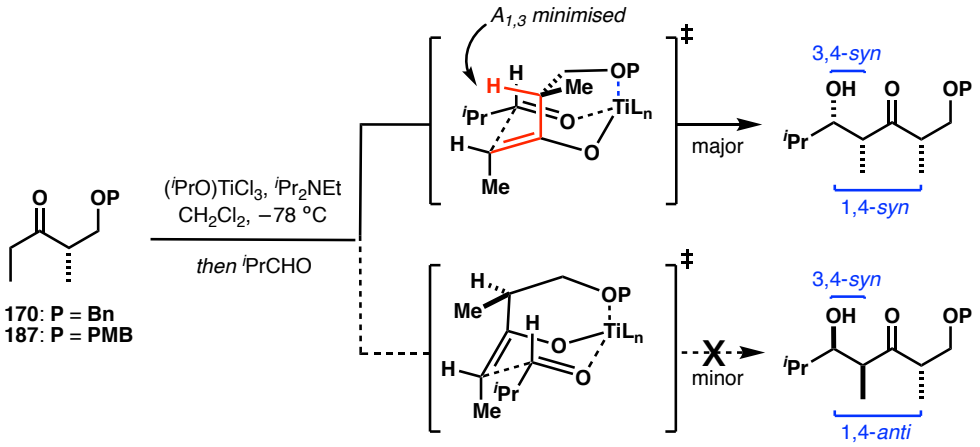

Scheme 64 Urpí and Roméa's (^{i}PrO)TiCl$_3$ aldol reations of Roche ester-derived ethyl ketones **170** and **187** with isobutyraldehyde

With the above precedent as a starting point of investigations, a screen of titanium(IV) Lewis acids was carried out to establish the optimal choice for the aldol reaction of ketone **170** and aldehyde **169**. The outcomes are summarised in **Table 4**.

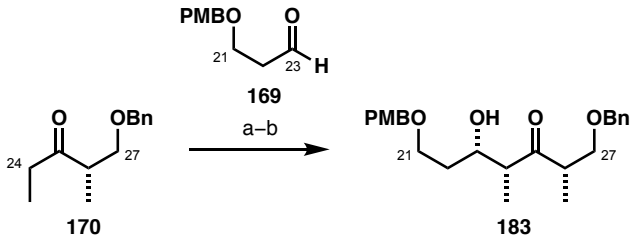

(a) (^{i}PrO)TiCl$_3$ (1.1 eq.), CH$_2$Cl$_2$, −78 °C, 10 min, *then* ^{i}Pr$_2$NEt (1.1 eq.), 45 min, *then* **169** (1.5 eq.); (b) NaClO$_2$, Na$_2$HPO$_4$·2H$_2$O, 2-Me-2-butene, ^{t}BuOH, H$_2$O, rt

Table 4 Lewis acid (LA) screen for the titanium aldol of **170**[a] and **169**

Entry	Variations from the above reaction conditions	Isolated *dr*	Yield[b] / %
1	none	8:1	75
2	1.3 eq. (^{i}PrO)TiCl$_3$ LA	7:1	77
3	–98 °C	4:1	70
4	(^{i}PrO)$_2$TiCl$_2$ LA	6:1	44
5	TiCl$_4$ (1 eq.) LA	3.5:1	62
6	TiCl$_4$ (2 eq.) LA	4.5:1	56
7	200 mg **170**	10:1	70

[a]Reactions performed on 50 mg ketone **170** [b]Overall isolated yield of the diastereomeric mixture.

The protocol developed by Urpí and Roméa[200] gave a reasonably high yield, and acceptable stereoselectivity (entries 1–2) and the excess aldehyde was cleanly removed in the subsequent Pinnick oxidation step. Monitoring the progress by thin layer chromatography (TLC) was not always reliable and variable yields may be a reflection of the reactions being terminated prematurely. In an attempt to slow down the rapid conversion (<10 min) and to increase the selectivity, the temperature was lowered to −98 °C (entry 3) though this did not boost the result due to inherent operational difficulty of maintaining that temperature constant whilst keeping strictly anhydrous conditions. Altering the Lewis acid also had a detrimental effect (entries 4–6). Unsurprisingly, the softer $(^{i}PrO)_2TiCl_2$ resulted in very limited conversion and $TiCl_4$ did not impart satisfactory selectivity. It was speculated that 2 eq. of $TiCl_4$ may favour formation of a bimetallic enolate,[204] though as Urpí and Roméa noted, any chelating groups on the aldehyde are likely to cause formation of other complexes and thus an erosion in stereocontrol. Finally, upon minor scale-up (entry 7) the selectivity and yield were comparable to the best result under the original conditions.

Scale-up was thus performed under Urpí and Roméa's original conditions as they offered the best compromise between conversion and selectivity. Gratifyingly, gram-scale experiments produced aldol adduct **183** in 85% yield and up to 15:1 *dr* and were reliably reproducible. Further scaling up to nearly 10 g of the ketone **170** resulted in 82% yield and 12:1 *dr* for the isolated product **183**, which affirmed the robustness of this methodology as well as its operational ease. Titanium Lewis acids are substantially easier to prepare than $Sn(OTf)_2$ and the reaction work up is more straightforward as titanium does not cause emulsion formation to the same extent as tin. In this regard, investigations into the titanium aldol route were indeed a great success. Crucially, by inspection of ^{1}H and ^{13}C NMRs, β-hydroxy ketone **183** was identical to the material obtained from the tin-mediated aldols.

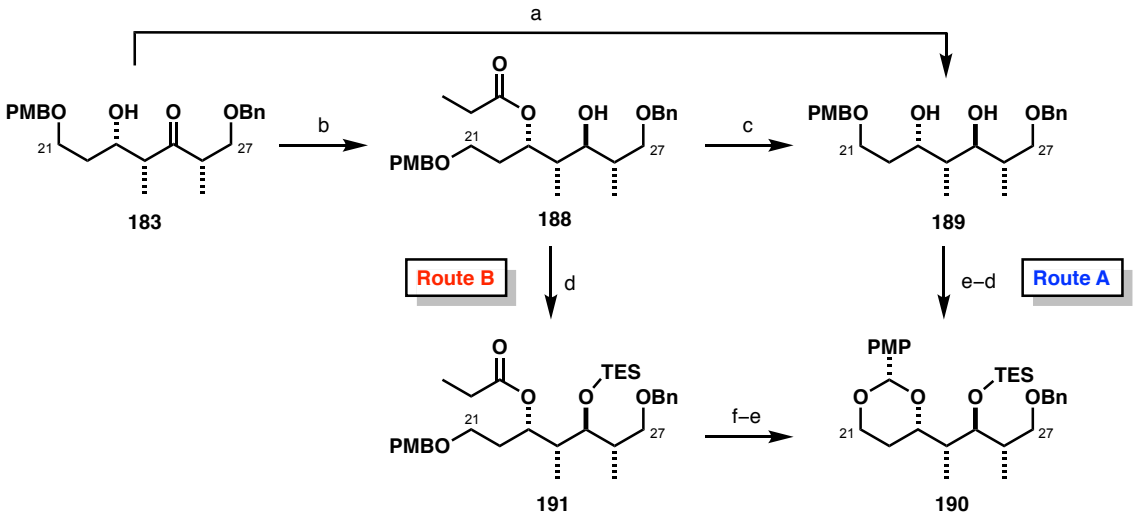

(a) $Me_4NBH(OAc)_3$; (b) SmI_2, EtCHO; (c) K_2CO_3, MeOH; (d) TESOTf, 2,6-lut.; (e) DDQ, 4 Å MS; (f) DIBALH

Scheme 65 Alternative sequences to PMP acetal **190**

The final chiral centre of the C_{21}–C_{27} fragment can be forged *via* a substrate-directed, 1,3-*anti* reduction where the stereochemical information is relayed from the existing hydroxyl. The strategy then requires transposition of the PMB group onto C_{23} which can be achieved *via* oxidative formation of a PMP acetal intermediate, followed by its regioselective opening. There are two possible methods to carry out the 1,3-*anti* carbonyl reduction (Evans–Saksena or Evans–Tishchenko) as well as a different order of steps which leads to the required compound **190** (**Scheme 65**).

Route B has one potential risk to associated with it. Due to steric hindrance around the secondary alcohol at C_{25}, TES protection would almost certainly have to be done using a silyl triflate whose Lewis acidity may be able to facilitate undesired migration of the propionate ester onto C_{25}. Therefore, route A in which the PMP acetal is formed before silyl protection was pursued as the first option.

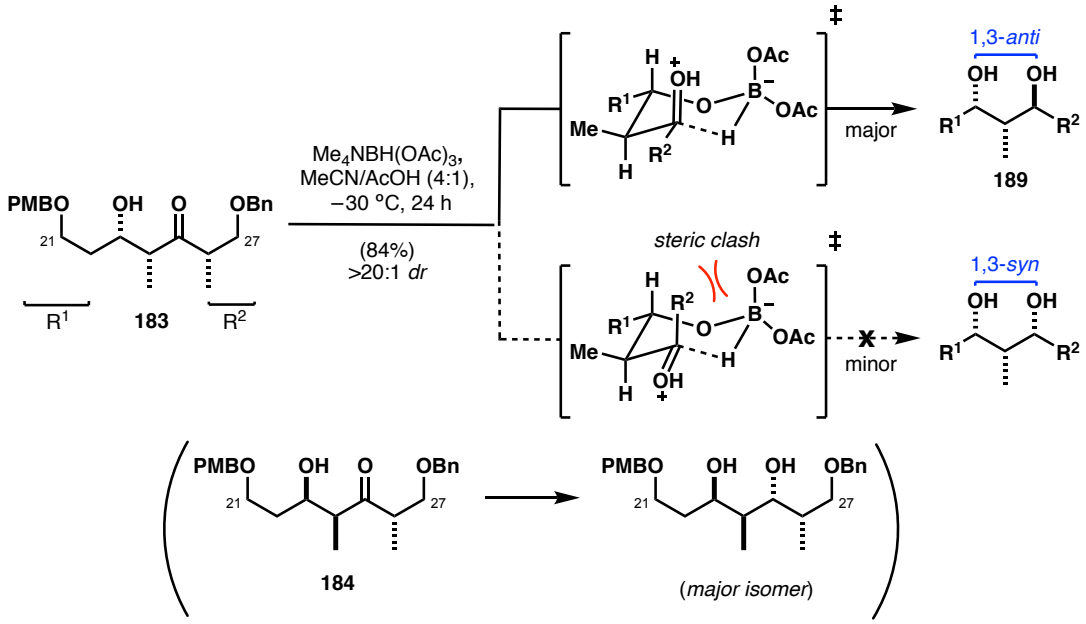

Scheme 66 Competing transition states in the Evans–Saksena reduction of ketone **183**[145,146] and observed byproduct from Evans–Saksena reduction of the 1,4-*anti* aldol adduct **184**

Diol **189** could be accessed directly by treatment of the β-hydroxy ketone **183** with $Me_4NBH(OAc)_3$ to afford the 1,3-*anti* product in 84% yield and excellent diastereoselectivity (>20:1) through intramolecular hydride delivery in a chair transition state (**Scheme 66**).[145,146] Unfortunately, the desired product was isolated as an inseparable mixture with the reduced 1,4-*anti* minor diastereomer **184** carried forward from the earlier aldol step, which could not be removed by column chromatography.

Fortunately, this was avoided by subjecting **183** to Evans–Tishchenko conditions[161] instead, then cleaving off the residual ester. The initial mechanistic step of this reaction is thought to be SmI_2-promoted reductive homocoupling of a sacrificial aldehyde. The ensuing samarium(III) pinacolate species acts as a

Lewis acid and enables the formation of a hemiacetal intermediate which undergoes hydride transfer *via* a highly organised, bicyclic, chair-like transition state (**Scheme 67**). The C_{23} hydroxy group remained masked as a propionate ester, which aided the chromatographic separation of the product derived from the minor aldol diastereomer **184** in the crude reaction mixture.

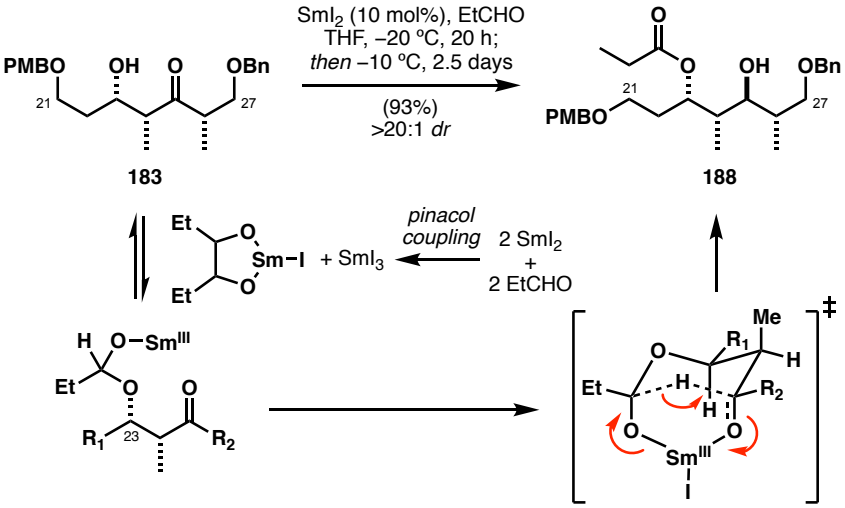

Scheme 67 Proposed mechanism for the Evans–Tishchenko reduction of ketone **183**[161]

Methanolysis of the ester under mildly basic conditions (K_2CO_3, MeOH) revealed diol **189** as a single diastereomer in 86% yield from aldol adduct **183** (**Scheme 68**). This two-step sequence was reproducible on up to 10 g of substrate **183** though the reaction was reliant on the use of high purity SmI_2. The catalytic loading could be reduced to as low as 5 mol% on larger scales which is attractive given the cost of the catalyst but required extended reaction times. The latter was found to be vital to achieve complete consumption of the starting material but it does not lead to deleterious side processes (e.g. retro-aldol).[205]

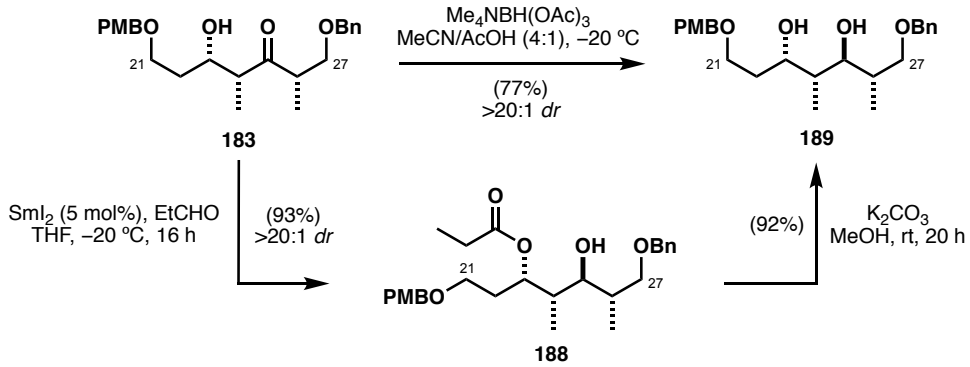

Scheme 68 Comparison of both routes to diol **189**

The newly furnished 1,3-*anti* relationship of the hydroxyls was verified by the ^{13}C NMR method of Rychnovsky.[206] Empirical observations showed that acetonides originating from 1,3-diols form two

significantly different conformations controlled by the relationship between the parent hydroxyls (*syn* or *anti*). *Anti*-acetonides predominantly adopt a twist boat shape to avoid 1,3-diaxial clashes of non-hydrogen groups whereas their *syn* counterparts exist in a more conventional chair conformation with equatorial placement of alkyl chains (**Scheme 69**). The latter puts the *gem*-dimethyl groups on the acetonide in two distinct environments, which can be identified by ^{13}C NMR.

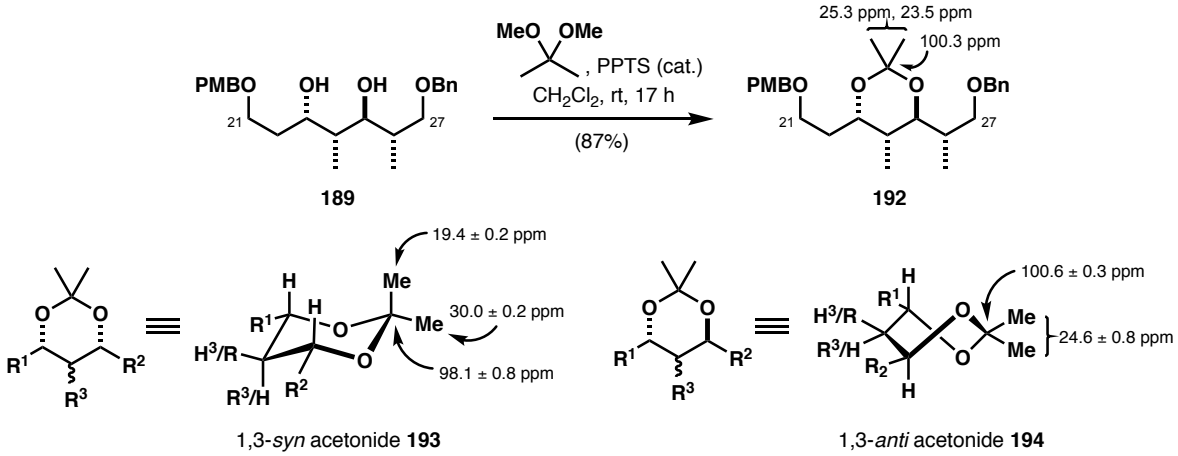

Scheme 69 Acetonide **192** formation from the 1,3-diol **189** to confirm the *anti* stereochemistry at C_{23}/C_{25}. Structures **193** and **194** show Rychnovsky's reported values for the 1,3-*anti* and 1,3-*syn* diol relationships, respectively.

Evans listed these characteristic resonances of acetonide carbons with 95% confidence limits which serve as reference values.[207] NMR data for compound **192**, prepared by treatment of diol **189** with 2,2-dimethoxypropane and catalytic pyridinium *p*-toluenesulfonate (PPTS), was in good agreement with those predicted for the 1,3-*anti* product.

As part of the planned protecting group strategy, the PMB group had to be migrated from the terminal position to the C_{23} hydroxyl. This could be accomplished by formation and later regioselective reductive opening of the ensuing PMP acetal. Subjecting diol **189** to oxidative conditions developed by Oikawa (DDQ) causes single-electron transfer (SET) oxidation of the benzylic position on the PMB ether and creates an electrophilic carbon, which is rapidly attacked by the nearby free hydroxyl in an anhydrous environment.[208] However, there is a risk of acetal **195** overoxidation if excess DDQ is used which leads to an orthoester. Fink found such undesired side process to occur on a similar 1,3-diol substrate as part of the C_{28}–C_{34} side chain synthesis.[177]

A small (0.4 eq.) excess of the oxidant proved necessary to promote complete conversion of the starting material and did indeed facilitate the formation of significant amounts of byproduct **196** (**Scheme 70**). The yields of acetal **195** varied in the range of 59–67% and the material was isolated as an inconsequential mixture of epimers at the acetal stereocentre. Nuclear Overhauser effect (nOe)

correlations supported the conclusion that the ratio is in favour of the less axially congested (*S*)-**195** in which the large groups are placed equatorially in a chair conformation. To circumvent the risk of overoxidation, DDQ was added in only substoichiometric amounts (0.9 eq.) in which case PMP acetal **195** was isolated in 77% yield and any recovered starting material could be resubmitted.

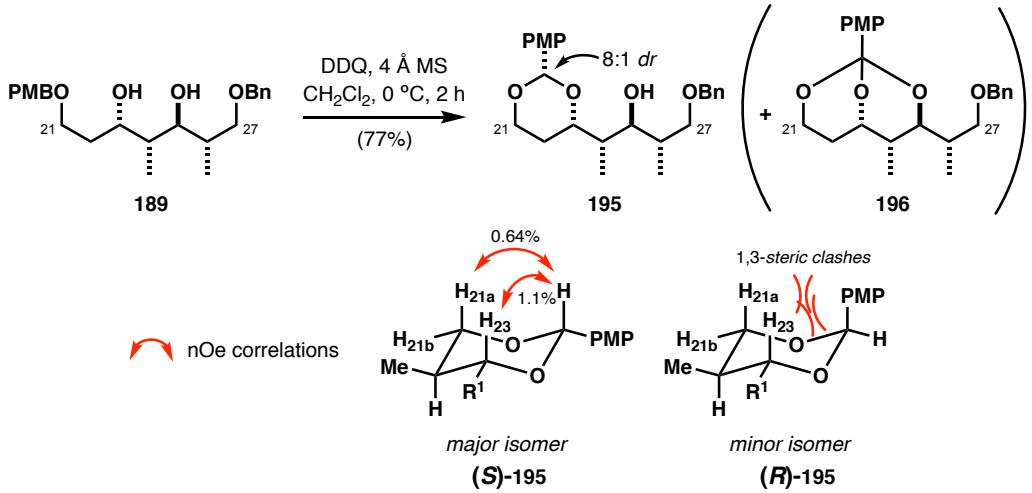

Scheme 70 Synthesis of PMP acetal **195** from diol **189** and nOe analysis

Attempts to form the C_{25} TES ether by protecting the relatively hindered free hydroxyl with TESOTf were met with disappointment. The predominant component of the isolated mixture was *bis*-TES ether **197**, which may arise from Lewis acid-promoted PMP acetal opening as proposed in **Scheme 71**. Fortunately, the alcohol could be rapidly protected with the milder TESCl to afford the desired product in 93% yield.

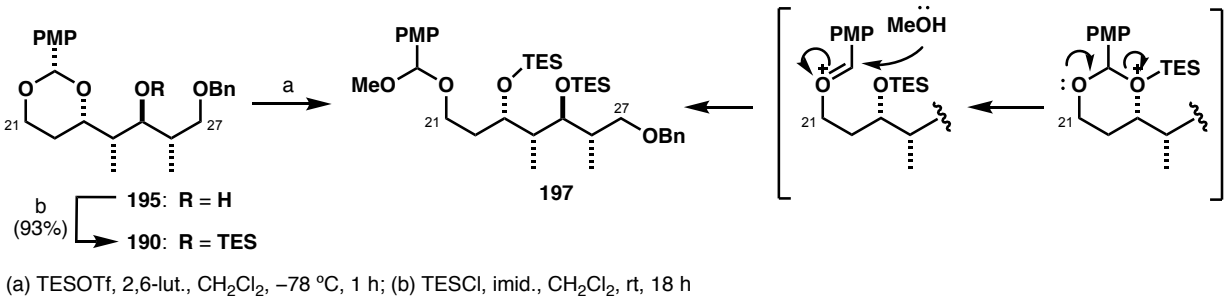

Scheme 71 TES protection of the C_{25} hydroxyl

Considering the difficulties encountered in the PMP acetal formation step, route B (**Scheme 72**) towards compound **190** was investigated as an alternative option. Despite the initial concerns regarding ester migration, TES protection of the C_{25} hydroxyl with TESOTf and reductive propionate cleavage with DIBALH proceeded smoothly (96% and 99% yield, respectively). The resulting substrate **198** was then suited to a site-specific cyclisation of the C_{23} PMB ether onto the nearby free alcohol and was thus

expected to be operationally more straightforward. Even though the yield was lower than anticipated (81%), one of the identified byproducts was PMP acetal which lacked the C_{25} TES group but this material could be easily recycled. Overall, the sequence from ester **188** to silyl ether **190** gave a 77% yield, which compares favourably to route A (66% over three steps) and was thus the preferred choice going forward.

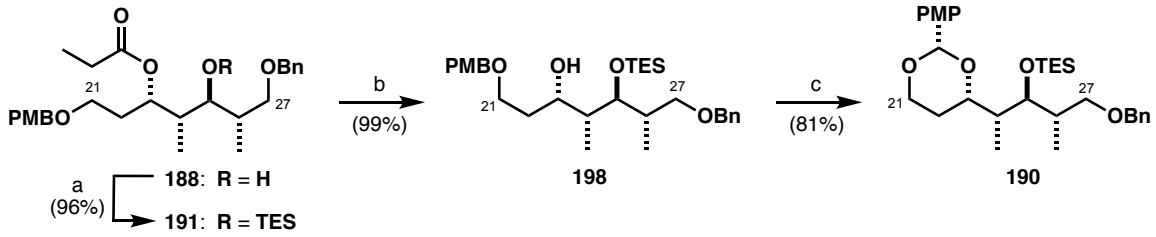

(a) TESOTf, 2,6-lut., CH_2Cl_2, –78 °C, 2 h; (b) DIBALH, CH_2Cl_2, –78 °C, 2.5 h (c) DDQ, 4 Å MS, CH_2Cl_2, 0 °C, 30 min, *then* rt, 1.5 h

Scheme 72 Synthesis of TES ether **190** *via* route B

The final step of the PMB migration was regioselective opening of the acetal **190** using DIBALH as the reducing agent. Mechanistically, steric bulk of the isobutyl groups favours coordination of the aluminium to the oxygen on the more exposed side of the acetal under kinetic control facilitating its opening to the oxocarbenium ion *via* an S_N1 process (**Scheme 73**). The primary alcohol product **199** is then formed through intramolecular hydride delivery to the proximal electrophilic carbon centre.[209] The undesired regioisomer **198** (*ca.* 10%) was also isolated but this material could be resubmitted to DDQ and the PMP acetal reformed to further increase the overall yield. Another side reaction observed in 5–10% yield was complete cleavage of the PMP acetal to reveal diol **200**. This process is believed to arise from overreduction in presence of excess DIBALH which was required to achieve full conversion. Fortunately, diol **200** was easily recycled by *bis*-TES protection with TESOTf and hydrolysis of the labile primary silyl ether under mildly acidic conditions (90% over two steps).

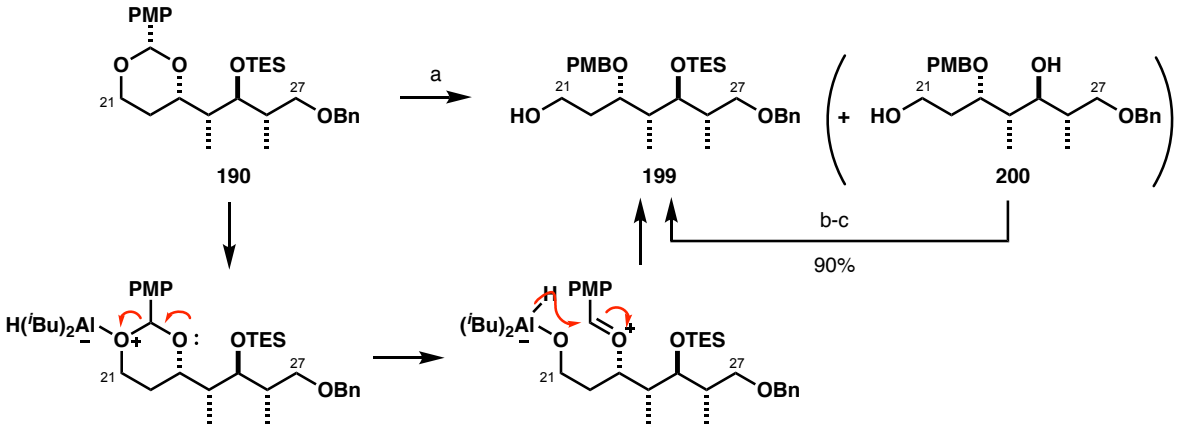

(a) DIBALH, CH_2Cl_2; (b) TESOTf, CH_2Cl_2, –78 °C, 1 h; (c) THF/AcOH/H_2O (5:2:1), rt, 5 h

Scheme 73 Proposed mechanism of PMP acetal opening with DIBALH and recycling of byproduct **200**

While all the byproducts could be identified and characterised, the crude mixture required laborious chromatographic separation of each component to retain good mass recovery. In an attempt to minimise the formation of byproducts, the reaction solvent, temperature and rate of DIBALH addition were varied to establish the optimal conditions for this step (**Table 5**).

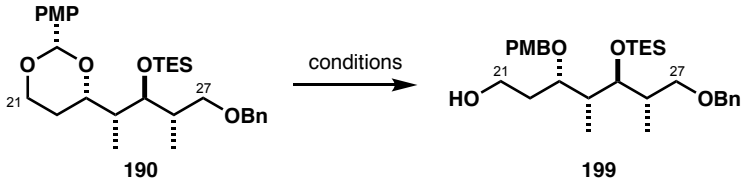

190 **199**

Table 5 Optimisation of PMP acetal **190** opening with DIBALH[a]

Entry	Reagent eq.	Solvent	Time / h	Temperature	Yield of **199**
1	3	CH_2Cl_2	1.5	0 °C	65%[b]
2	2 + 1	CH_2Cl_2	2	0 °C	65%
3	2.5 + 0.5 + 0.5	CH_2Cl_2	3	0 °C	73%
4	3	CH_2Cl_2	2	–78 °C → 0 °C	67% (75% BRSM)
5	**3**	**CH_2Cl_2**	**3**	**–78 °C → –30 °C → 0 °C**	**79%**
6	3	TBME	1.5	0 °C	65%[b]
7	2.5 + 0.5	TBME	2	0 °C	70%
8[c]	3	TBME	3	0 °C → rt	no reaction

[a] DIBALH used as a 1.0 M solution in hexanes. [b] Yield estimated by ^{1}H NMR. [c] DIBALH used as a 1.0 M solution in THF

Invariably, a minimum of 3 eq. of the reducing agent were needed to push the reaction to completion every instance. Adjusting the rate of DIBALH addition (entries 1–3) caused no major changes, though gradual addition of the final aliquots generally gave a marginally higher yield. Despite the excess reductant in the mixture, the average reaction time at 0 °C was 2–3 hours, thus it came as no surprise that any substantial decreases in temperature precluded the reactivity altogether. Upon warming, slow onset of reaction was observed around –30 °C, which then proceeded to full conversion at 0 °C (entry 4). The observed increase in yield (entry 5) was attributed to suppressed PMB deprotection, which was a welcome improvement.

Using a sterically congested ethereal solvent, e.g. *tert*-butyl methyl ether (TBME) can lead to a coordination cage being formed around aluminium. An effective increase in its size is expected to cause a stronger preference for attachment to the oxygen on the less hindered side of the acetal, increasing

regioselectivity. On the other hand, tighter coordination may also lower the reaction rate. Unexpectedly, this change made no difference to the overall outcome (entries 6–7) and using DIBALH solution in THF increased the bulk of both species to the extent that the reaction was suppressed entirely (entry 8).

Finally, acetal opening was attempted with $BH_3{\cdot}SMe_2$ as the source of hydride (**Scheme 74**). Unlike reductions with aluminium hydrides where cooling enables kinetic control, high temperatures are unavoidable to achieve good conversion rates. The reaction was slow at temperatures below 100 °C though any more substantial heating caused more rapid PMB cleavage. An initial yield of 73% on small scale (20 mg) was promising but could not be repeated on more than 100 mg of substrate **190**.

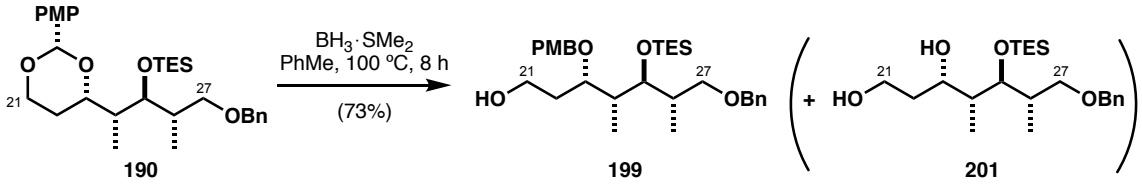

Scheme 74 Reductive acetal opening with $BH_3{\cdot}SMe_2$ Lewis acid

To this end, the transformation was best affected when DIBALH was added to the substrate at low temperature and then allowing the reaction mixture to gradually warm to 0 °C. Byproduct **201** lacking the C_{25} TES was observed very early on after warming from −78 °C and it was not possible to rationalise which factor caused its formation. Nevertheless, the protocol was easily scalable to up to 4 g of the PMP acetal **190** and enabled throughput with relatively minor losses of material.

The synthesis of aldehyde **168** was completed by oxidation of the C_{21} hydroxyl. Unexpectedly, substrate **199** was not tolerant of the standard Swern protocol[170] which resulted in complete degradation of the alcohol. However, Dess–Martin periodinane (DMP)[165] yielded the complete C_{21}–C_{27} fragment in 92% yield with no observed β-alkoxy elimination even under prolonged storage.

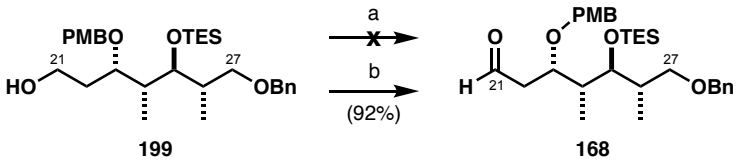

(a) $(COCl)_2$, DMSO, CH_2Cl_2, –78 ºC, 1 h, *then* **199**, 45 min, *then* Et_3N, rt, 2 h; (b) Dess–Martin periodinane, $NaHCO_3$, CH_2Cl_2, 0 ºC, 1 h, *then* rt, 1 h

Scheme 75 Oxidation at C_{21} to complete the C_{21}–C_{27} fragment **168**

One aim of the revised protecting group strategy requires an Alloc protecting group to be installed at C_{27}. This would have to be introduced by removing the existing Bn ether once the complete carbon backbone of the C_{15}–C_{27} southern fragment has been assembled. Due to the variety of functional groups present,

this may be a non-trivial step. If the debenzylation conditions were to prove too harsh for the C_{25} silyl group to be a TES, TBS is likely to be a more robust alternative. The synthesis of the TBS aldehyde **204** from the known intermediate **195** very closely resembles the route to its TES counterpart **168** and is summarised in **Scheme 76** below.

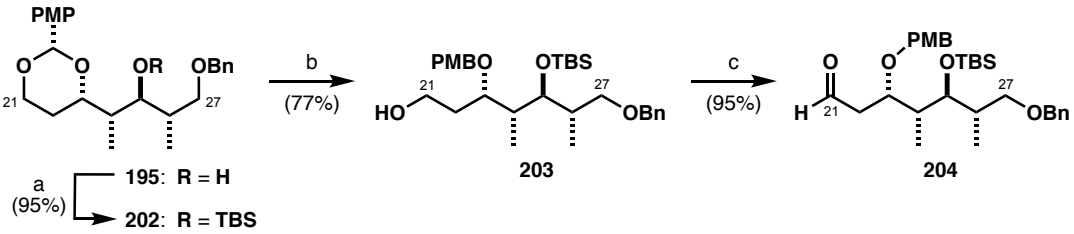

(a) TBSOTf, 2,6-lut., CH_2Cl_2, –78 °C, 2 h; (b) DIBALH, CH_2Cl_2, –78 °C → rt, 3.5 h; (c) $(COCl)_2$, DMSO, CH_2Cl_2, –78 °C, 1 h, *then* **203**, 45 min, *then* Et_3N, rt, 2 h

Scheme 76 Synthesis of aldehyde **204** from PMP acetal **195**

3.3.4. Synthesis of C_{15}–C_{20} β-Ketophosphonate 167

Via Enzyme-Mediated Diester Desymmetrisation

β-Ketophosphonate **167** can feasibly be accessed by a three-step procedure from the commercially available (*R*)-methyl-3-methylglutarate (**137**) (**Scheme 77**).

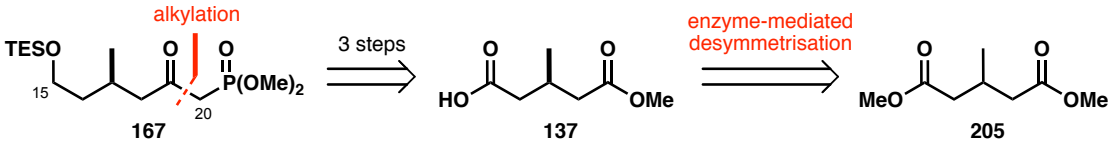

Scheme 77 Retrosynthesis of the C_{15}–C_{20} phosphonate **167**

As the C_{17} methyl stereocentre is fairly isolated, high enantiomeric excess (*ee*) of the C_{15}–C_{20} fragment is imperative to prevent impurities arising from the minor C_{17} diasteromer from being carried through the steps after the HWE coupling with the C_{21}–C_{27} aldehyde **168**. Conveniently, Tamm has reported the synthesis of monoester **137** in estimated 90% *ee* by means of a pig liver esterase (PLE)-mediated desymmetrisation reaction of dimethyl 3-methylglutarate (**205**).[210] Due to Woodrow's reservations about the reproducibility of an enzyme-catalysed reaction the ultimate decision was to source chiral acid **137** for this project from a commercial supplier in the early stages of the aplyronine project. However, benign reaction conditions and readily available racemic starting material make a compelling argument for exploring a biocatalysed transformation as an alternative.

Woodrow's concerns are to a certain extent founded. Relatively inexpensive crude porcine liver extract as a source of PLE is not only a mixture of isozymes in itself but it also consists of a multitude of other ester hydrolysing enzymes. This can induce considerable discrepancies in batches and unpredictable responses to variations in reaction parameters, which directly affects the product quality. On the other hand, the minimum guaranteed enantiomeric excess of the acid **137** from commercial sources (>80% *ee*) is also less than ideal.

Fortunately, Lam and co-workers have optimised the protocol for the PLE-mediated hydrolysis of diester **205** by observing the effects of temperature, organic co-solvent, concentration and pH.[211] Due to high substrate specificity of the enzyme binding site (**Scheme 78**), common for biocatalysed transformations, the reaction terminates itself after one ester equivalent has been consumed. Enantiomeric purity has been shown to diminish when approaching complete conversion,[212] though the excess of the desired isomer can be boosted by reacting the chiral acid with cinhonidine, recrystallisation of the resulting salt and cleavage of the amine to recover enantioenriched material.[213] Recently, Fürstner has established that this protocol is practically achievable on large scale (>20 g of substrate **205** in a single batch) in good yield and excellent *ee*, carried out in a conventional organic chemistry laboratory setting.[214] This was decided to be the most viable way to access multi-gram quantities of an otherwise expensive chiral building block.

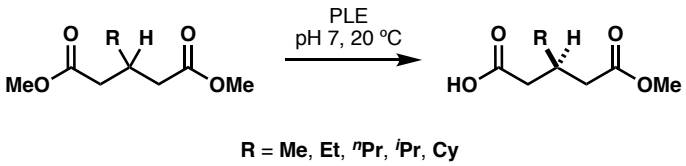

Scheme 78 Substrate scope of PLE in reactions of glutarate diesters

Preparation of the substrate for the desymmetrisation reaction commenced with esterification of 3-methylglutaric acid with acetyl chloride and methanol (89%). The following enzymatic transformation was carried out by incubating the enzyme and diester **205** in a pH 7 phosphate buffer with MeOH as the co-solvent (4:1). The reaction temperature was maintained at −10 °C and the rate of NaOH addition such that the pH was kept between 6.0 and 7.5 when monitored using a pH-stat. Gratifyingly, the reaction gave gradual, clean conversion to the enantioenriched monoester **137** in near quantitative yield (97%, 92% *ee*). The enantiomeric excess of **137** was analysed by chiral gas chromatography (GC) in comparison with the racemic sample, prepared by diester **205** hydrolysis with 1 eq. of KOH. It should be noted that due to the carboxylic acid moiety in the molecule, chromatographic separation without further derivatisation was found to be tricky and hence the *ee* value should be considered an estimate (>90%).

To enhance the optical purity by kinetic resolution, crude product **137** was crystallised with (–)-cinchonidine by heating in acetone at 40 °C, then left to precipitate overnight. The resulting co-crystals,

enriched in the (*R*)-isomer of the chiral acid, were collected by filtration and cinchonidine was cleaved using HCl to afford **137** in 96% *ee* by GC analysis. Owing to the scalability of the process, more than 25 g of the chiral acid was produced over the course of the project.

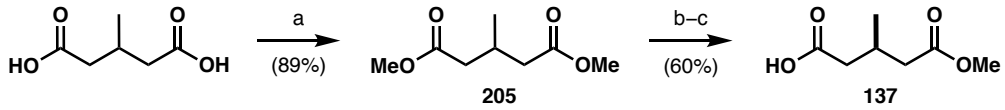

(a) AcCl, MeOH, reflux, 16 h; (b) pig liver esterase, 10% aq. NaOH, pH 7 phosphate buffer/MeOH (4:1), –10 °C, 10 h (c) cinchonidine, acetone, H_2O, 40 °C, *then* 0 °C, 16 h, *then* 2 N HCl

Scheme 79 PLE approach to the monoester **137**

The carboxylic acid was chemoselectively reduced using $BH_3 \cdot SMe_2$ (**Scheme 80**).[215] Trace acid contaminants or generation of boronic acid upon MeOH workup can facilitate rapid intramolecular cyclisation of the hydroxyl onto the C_{19} carbonyl to form the volatile lactone byproduct **207**. Switching to a mildly basic aqueous quench almost entirely suppressed this pathway and the reduction was successfully performed on up to 8 g of substrate **137**.

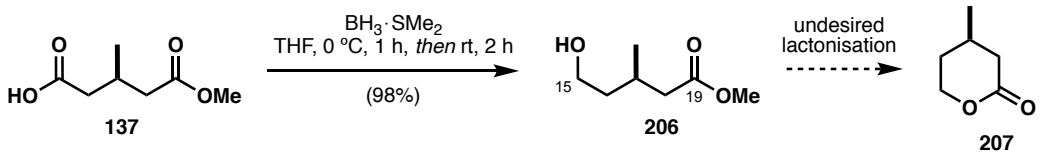

Scheme 80 Chemoselective reduction of the C_{15} carboxylic acid **137**

The C_{15}–C_{20} fragment synthesis was completed by protection of the C_{15} terminus (TESCl, imidazole) and homologation of the C_{19} ester in a Corey–Kwiatkowski condensation (**Scheme 81**).[167] Deprotonation of dimethyl methylphosphonate with ^{n}BuLi at −78 °C generated a lithium anion which underwent a single addition into the ester, attaching the phosphonate functionality for the HWE coupling to aldehyde **168**.

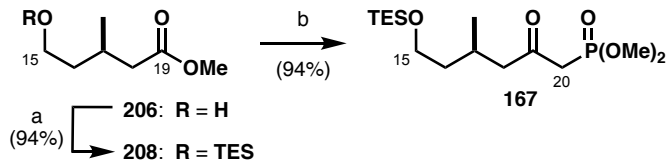

(a) TESCl, imid., CH_2Cl_2, rt, 1 h; (b) ^{n}BuLi, $MeP(O)(OMe)_2$, THF, –78 °C, 45 min, *then* **208**, 1 h

Scheme 81 TES protection of the C_{15} alcohol and homologation to the β-ketophosphonate **167**

As mentioned previously, the removal of the C_{27} benzyl group was forseen to be problematic due to the delicate protecting groups in place on the planned C_{15}–C_{27} fragment. It was envisioned that should the C_{15} TES-protected material fail to withstand the debenzylation, the more robust TBS protected intermediate

125 should provide a means to perform the deprotection without unnecessary protecting group manipulations. Its synthesis closely follows that for phosphonate **167**.

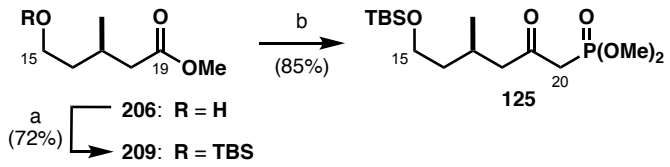

(a) TBSCl, imid., CH_2Cl_2, rt, 16 h; (b) ^{n}BuLi, MeP(O)(OMe)$_2$, THF, –78 °C, 45 min, *then* **209**, 3 h

Scheme 82 Synthesis of the TBS-protected β-ketophosphonate **125**

Via Enantioselective Hetero-Diels–Alder Reaction

While the investigations on the desymmetrisation route were underway, synthesis of the required fragment by enantioselective catalysis was explored as an alternative means to access phosphonate **167** from achiral starting material. Lactone **207** was identified as a precursor to fragment **167** and could be obtained *via* a hetero-Diels–Alder (HDA) reaction of crotonaldehyde **211** and ethyl vinyl ether (**212**) (**Scheme 83**). Enantioselectivity is induced by a chiral catalyst which activates the aldehyde and imposes a facial constraint in the transition state.

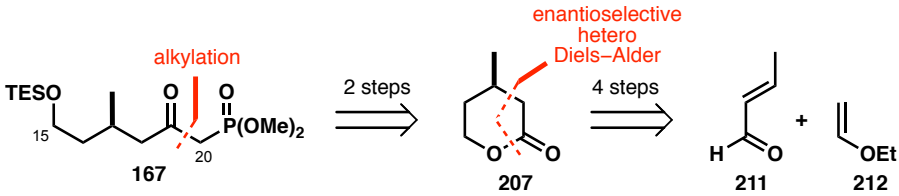

Scheme 83 Retrosynthesis of phosphonate **167** *via* the enantioselective hetero Diels–Alder reaction

The methodology in question is based upon the tridentate Schiff base chromium(III) complex **213**, introduced by Jacobsen[216] which catalyses the inverse-electron-demand HDA reaction between the aforementioned aldehyde **211** and dienophile **212** (**Scheme 84**).[217]

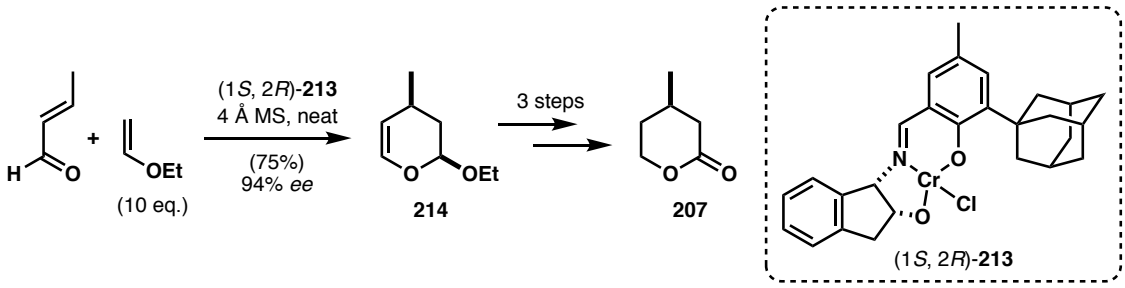

Scheme 84 Jacobsen's synthesis of lactone **207** *via* HDA using chromium(III) catalyst **213**

Despite acting solely through a single-point binding interaction to the carbonyl, impressive levels of both *endo*/*exo*- and enantioselectivity can be generated. Using a large excess (10 eq.) of the vinyl ether and addition of 4 Å molecular sieves (MS) affords dihydropyran **214** in 75% yield and 94% *ee*. Jacobsen showed that three further derivatisation steps lead can to the sought lactone **207**.

Insight into the basis for stereoinduction can be gained by inspecting the crystal structure of the catalyst,[217] whose stable form is as a water-bridged dimer **215** with one terminal water ligand on each chromium. Kinetic studies imply that this dimeric structure is maintained throughout the catalytic cycle and the crucial role of molecular sieves is likely to involve abstraction of a water molecule to open a coordination site on the metal. By linking the absolute stereochemistry of the catalyst and product, a tentative transition state structure can be postulated as illustrated in **Scheme 85**.

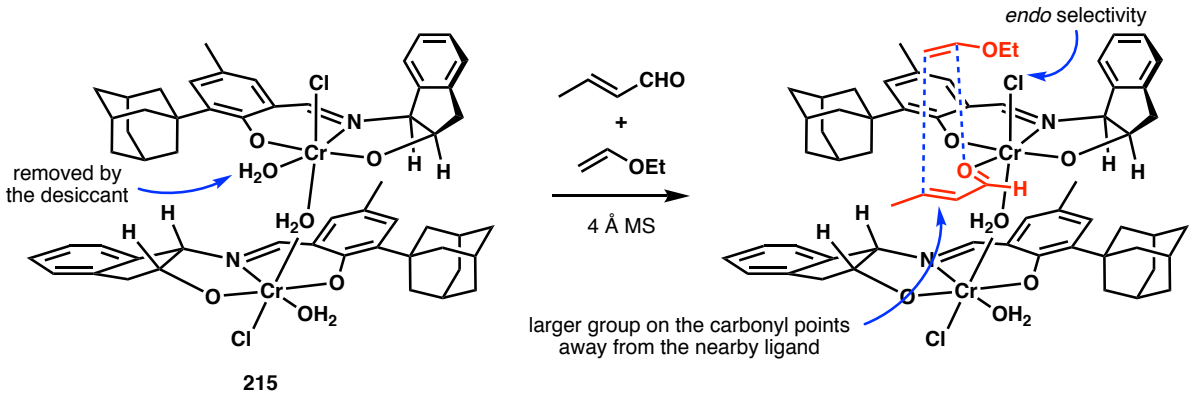

215

Scheme 85 Transition state proposal for the HDA reaction of ethyl vinyl ether and crotonaldehyde, catalysed by **213**

This seemed like an attractive way to accumulate large stocks of enantioenriched lactone **207**, ready for later homologation to attach the phosphonate at C_{19}. As has been mentioned in **Section 3.4.1**, this lactone had been previously considered an undesired byproduct of a the PLE route but was difficult to isolate after column chromatography of the crude mixture due to its volatility.

Jacobsen reported a practical synthesis of the catalyst **213** starting from *para*-cresol.[217] Friedel–Crafts alkylation of the phenol with 1-adamantanol and *conc.* H_2SO_4 to promote formation of the alkyl carbocation which attaches a single adamantanyl group in the *ortho* position (**Scheme 86**). Next, condensation of the phenol product **216** with formaldehyde and $SnCl_4$ catalyst[218] gives salicylaldehyde derivative **217** in 71% over two steps. This proceeds *via* an *ortho*-specific Friedel–Crafts step, followed by an Oppenauer-type oxidation after binding of a second equivalent of formaldehyde to the tin(IV) centre as depicted in **Scheme 86**.

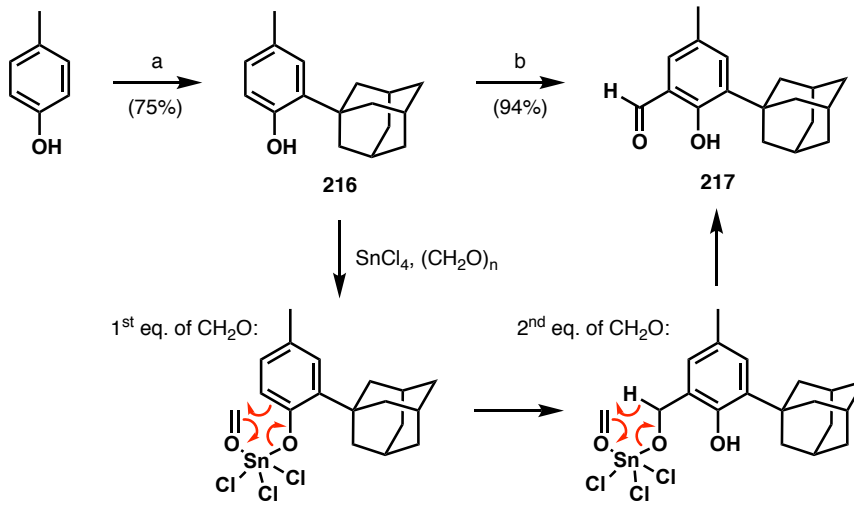

(a) adamantan-1-ol, *conc.* H_2SO_4, CH_2Cl_2, rt, 20 min; (b) $SnCl_4$, 2,6-lut., PhMe, rt, 1.5 h *then* $(CH_2O)_n$, reflux, 4 h

Scheme 86 Synthesis of aldehyde **217** *via* Friedel–Crafts alkylation/acylation and Oppenauer oxidation

The chiral portion of the ligand is incorporated in a condensation step between aldehyde **217** and (1*S*,2*R*)-aminoindanol **218** to form the crystaline imine **219** in 78% yield. Complexation of the metal ion with $CrCl_2$ forms the air-stable Cr(III) complex **213** in near-quantitative yield.[216]

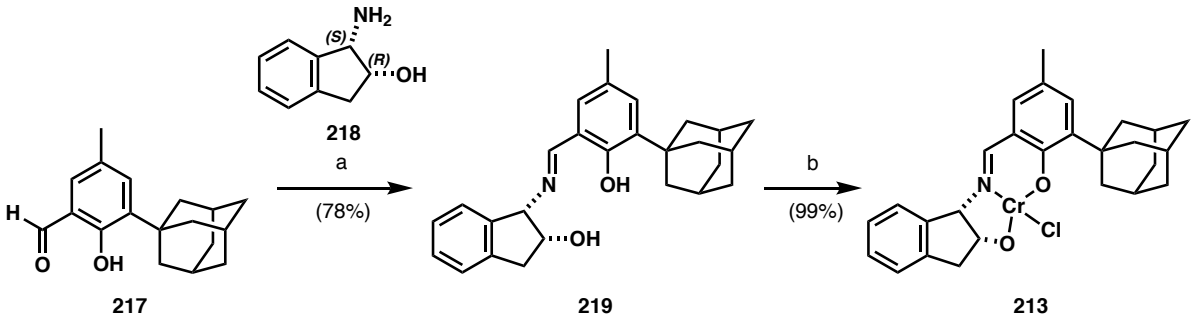

(a) EtOH, reflux, 1 h; (b) $CrCl_2$, 2,6-lut., THF, 3 h *then* air, 14 h *then* 2,6-lut., Ar, 3 h

Scheme 87 Formation of the Schiff base ligand (1*S*,2*R*)-**213** and complexation with Cr(II)

With the catalyst in hand, studies began to investigate the feasibility of the HDA. The sequence was first tested on a small scale (*ca.* 35 mmol of crotonaldehyde **211**) with 5% catalyst loading and moderate excess (5 eq.) of ethyl vinyl ether (**212**, **Scheme 88**). After 3 days the product was distilled off under reduced pressure, though the catalyst was unfortunately not recoverable. This has been been attributed to the presence of 4 Å molecular sieves as even polymer-supported chromium(III) catalysts of similar structure have degraded in the reaction of the aforementioned starting materials.[219]

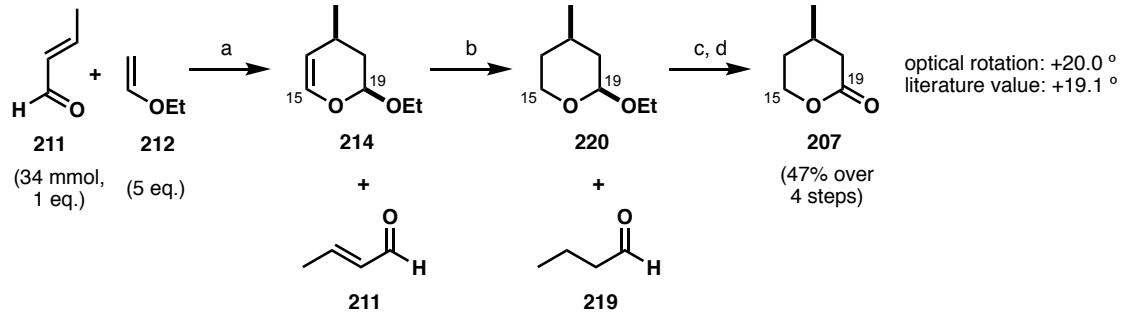

(a) (1*S*, 2*R*)-**213** (2.5 mol%), 4 Å MS, rt, 3 days; (b) H_2, Pd/C (10 wt%, cat.), Et_2O, rt, 2 days; (c) TsOH (cat.), acetone/H_2O (1:1), rt, 24 h; (d) PCC, CH_2Cl_2, rt, 20 h

Scheme 88 Small-scale test synthesis of lactone **207**

The obtained material contained some residual aldehyde **211** beside the dihydropyran **214** and was subjected to hydrogenation with catalytic Pd/C. After stirring for 2 days to ensure complete reduction the solvent was once again removed from the reaction mixture by distillation, which also separated out the butanal byproduct **219**. Next, hydrolysis of the mixed acetal was conducted in aqueous acetone and catalytic *p*-toluenesulfonic acid (TsOH) to afford a lactol which was oxidised to the corresponding lactone **207** with pyridinium chlorochromate (PCC). The overall yield of the four-step sequence was 47% and the optical rotation value was in excellent agreement with the literature,[220] which was a testament to the superior enantioselectivity of the HDA.

The remaining two steps to the C_{15}–C_{20} phosphonate **167** were homologation at C_{19} and protection of the C_{15} hydroxyl. Addition of 2 eq. of lithiated dimethyl methylphosphonate produced exclusively lactol **221** (**Scheme 89**). While it may be reasonable to expect formation of the open-chain alcohol **222** with an excess of the basic enolate in solution, stable lactol products are commonly observed in similar types of reactions.[221]

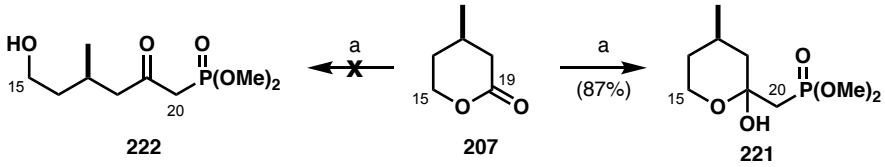

(a) ^{n}BuLi, dimethyl methylphosphonate, THF, –78 °C, 45 min; *then* **207**, 1.5 h

Scheme 89 Homologation of the C_{15}–C_{19} lactone **207**

The lactol can be opened by a strong, non-nucleophilic base (e.g. KH, K^{t}BuO) under kinetic control which enables protection of the free hydroxyl in the same step. To this end, deprotonation with NaH, followed by addition of TESCl afforded the known phosphonate **167** in 85% yield (**Scheme 90**).

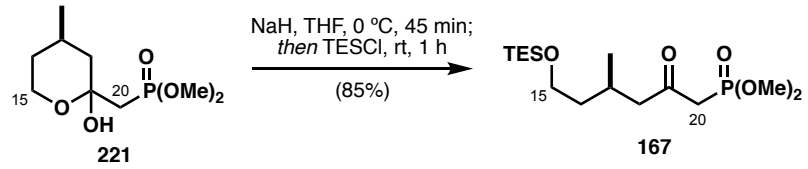

Scheme 90 Opening of the lactol **221** and silyl protection of the C_{15} hydroxyl

The route appeared highly amenable to producing large quantities of material in a single batch. After preparing a fresh supply of the catalyst, the HDA was repeated on 0.5 mol of crotonaldehyde **211**. Disappointingly, even after 14 days of reaction time, ^{1}H NMR analysis still showed about 50% residual aldehyde. It is conceivable that the catalyst decomposed during this time as Jacobsen had concluded that the uncatalysed background reaction does not take place unless the mixture is heated under pressure.[217]

Subsequent steps as per **Scheme 88** (b–d) took several days' reaction time in order for the starting materials to diminish to an acceptably low level. Even then, trace amounts made purification by distillation more cumbersome. Resubmission of unreacted substrates reduced throughput and major losses were incurred, making scale-up substantially less productive and more labour-intensive than foreseen. In hindsight, there are other downsides to this route, the most conspicuous one being the use of an expensive chromium(II) salt to form the catalyst which cannot be recovered as well as effectively six steps needed to form a single stereocentre at C_{17} although it does give the advantage of using achiral starting material (**Scheme 91**). After careful consideration and given the success of the PLE approach, the quest of building the C_{15}–C_{20} fragment *via* enantioselective catalysis was abandoned.

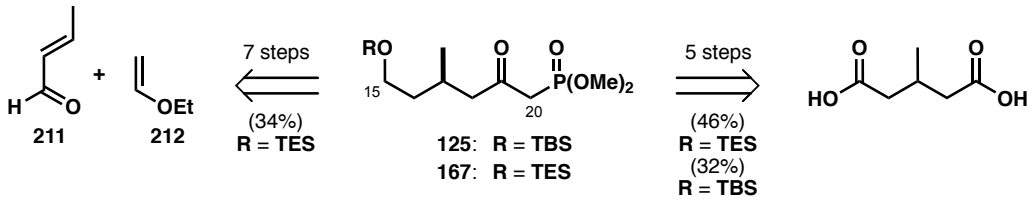

Scheme 91 Comparison of two investigated routes to phosphonates **125** and **167**

3.5. Fragment Coupling Towards the C_{15}–C_{27} Aldehyde 161

3.5.1. Synthesis of the C_{19} Methyl Ethers *via* HWE Olefination

The next important advancement towards the southern fragment **161** was the HWE olefination between aldehyde **168** and the phosphonate coupling partner **167** under very mildly basic conditions.[150] Studies previously carried out in our group provided ample precedent for use of a $Ba(OH)_2$-mediated HWE reaction to yield complex enone structures in a highly (*E*)-selective manner on delicate substrates.

Deprotonation of the β-ketophosphonate **167** with $Ba(OH)_2$ in anhydrous solvent, followed by the addition of aldehyde in 40:1 THF/H_2O forged enone **223** in 85% yield and excellent *trans*-selectivity (>20:1 *E*/*Z*, $^3J_{H20\text{-}H21}$ = 15.8 Hz), as none of the undesired (*Z*)-olefin was detected in the crude mixture by ^{1}H NMR (**Scheme 92**).

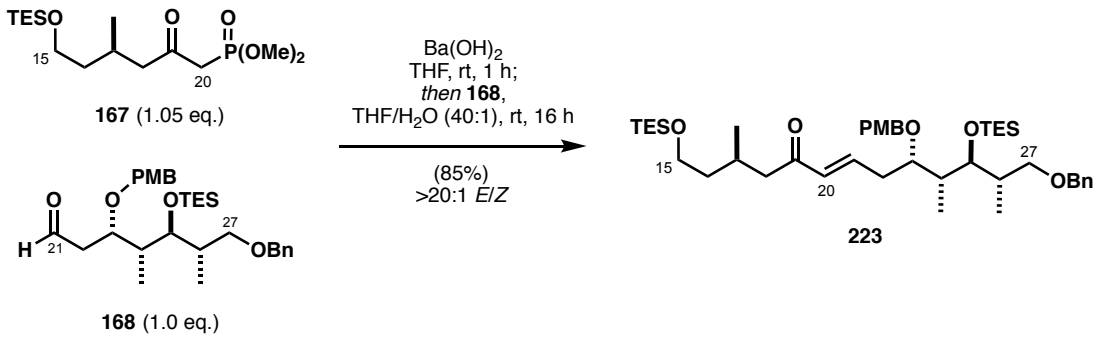

Scheme 92 HWE olefination to form enone **233**

The C_{19} stereocentre was configured in a reagent-controlled 1,2-asymmetric reduction using the (*S*)-2-Me-CBS catalyst **138** and $BH_3{\cdot}SMe_2$ as the hydride source.[168] The lack of stereochemical elements in the vicinity of the enone dictates that there should be very little inherent substrate bias towards either diastereomer in reactions with achiral reducing agents. CBS reduction can bypass this issue by employing a chiral catalyst which forms different steric interactions with the *re* and *si* faces of the carbonyl, favouring either one depending on the choice of catalyst. The mechanism[153] commences with the coordination of the $BH_3{\cdot}SMe_2$ to the nitrogen lone pair on the proline-derived oxazaborolidine to form a stable 1:1 adduct. This step activates the reducing agent and increases the Lewis acidity of the endocyclic boron. As a consequence, the catalyst coordinates to the carbonyl in a manner which minimises unfavourable steric interactions between the oxazaborolidine and the substrate (**Scheme 93**).

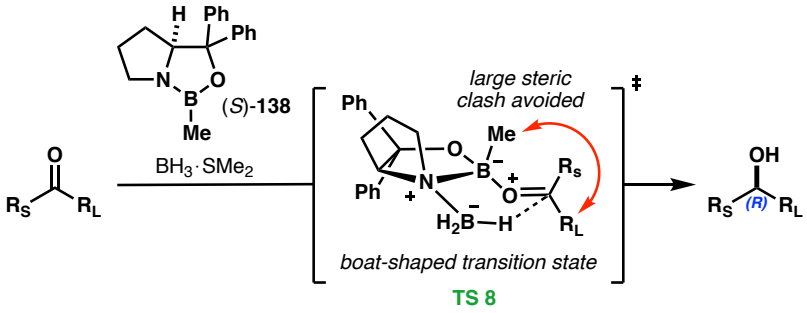

Scheme 93 Transition state model for ketone reduction with (*S*)-CBS catalyst **138**

In the case of α,β-unsaturated ketones, the olefinic portion adopts the position of the large group (R_L) in a boat-like transition state. This arrangement prevents the energetically unfavourable steric clash between the fully conjugated, coplanar C=C–C=O arrangement of the enone and the methyl group on boron

during hydride transfer. The absolute stereochemistry of the newly formed carbinol can thus be predicted from the transition state structure **TS 8**.

Enone **223** was subjected to a catalytic amount of the (*S*)-2-Me-CBS catalyst **138** (10 mol%) and $BH_3{\cdot}SMe_2$ at –20 °C before gradually increasing the temperature to –10 °C for 2 h (**Scheme 94**). Allylic alcohol **224** was isolated in 13:1 *dr* and near-quantitative yield (99%). Careful chromatography ensured that minimal quantities of the undesired (19*S*)-isomer were carried through to the next step.

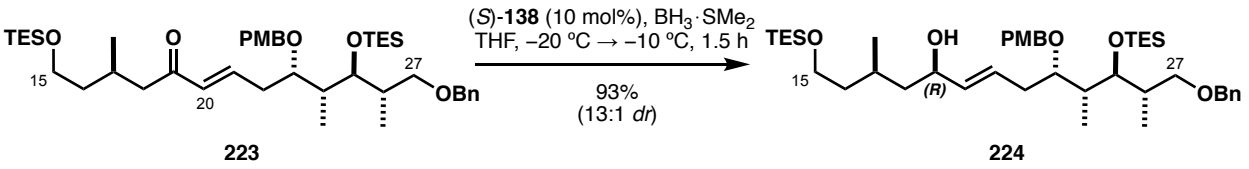

223 **224**

Scheme 94 CBS reduction of enone **223** to the allylic alcohol **224**

The fidelity of the stereochemical model was verified by the Mosher method (outlined in **Section 3.3.2.**). The corresponding (*R*)- and (*S*)-Mosher esters of alcohol **224** were synthesised by esterification with MTPA in presence of DCC and catalytic DMAP (**Scheme 95**). Finally, the C_{19} hydroxyl was methylated with NaH and MeI to yield methyl ether **227** (89%).

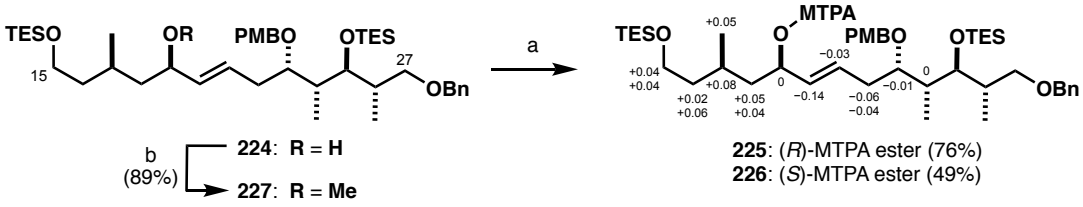

(a) (*R*)- or (*S*)-MTPA, DCC, DMAP, CH_2Cl_2, rt, 16 h; (b) NaH, THF, °C, *then* MeI, rt, 4 h

Scheme 95 Mosher ester analysis and methylation of the C_{19} alcohol **224**

The same sequence of steps (HWE/CBS reduction/methylation) was used to prepare two more permutations of the C_{15}–C_{27} fragment methyl ether. By replacing either component (or both) of the HWE reaction with their TBS analogues **125** and **204**, giving three systems of different stability which can be investigated for the subsequent deprotection steps and therefore maximising the chance of success. **Scheme 96** depicts the steps to methyl ethers **232** and **233**.

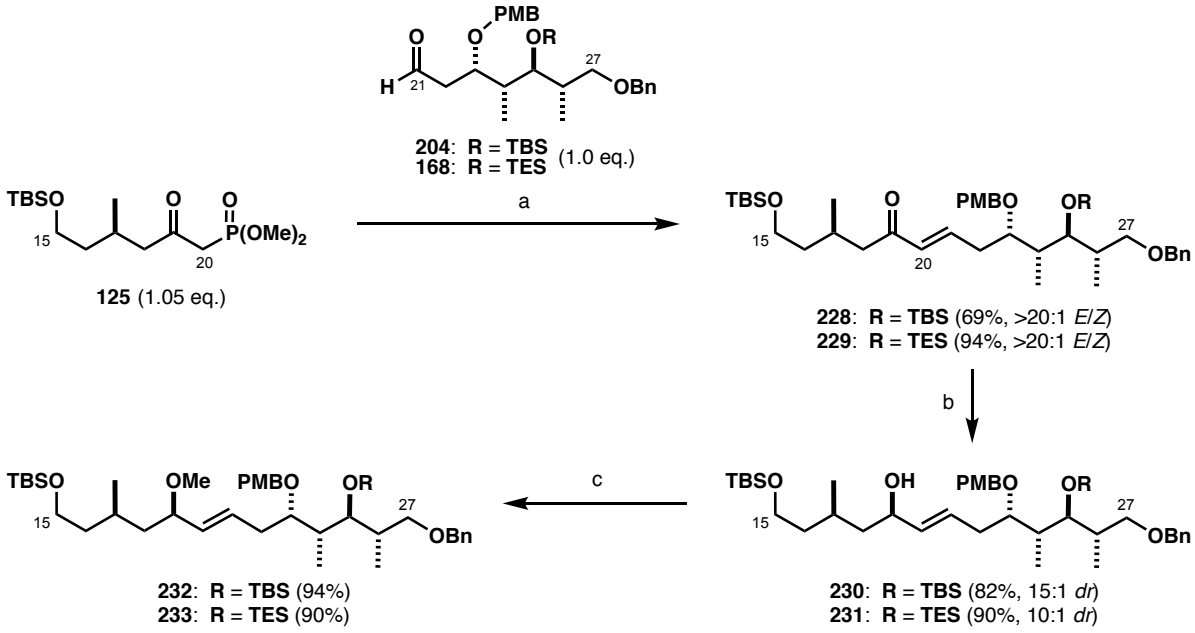

Scheme 96 Synthesis of methyl ethers **232** and **233**

3.5.2. Studies of C_{15} and C_{27} Protecting Group Removal

The success of the revised overall strategy heavily relies on selective removal of protecting groups at the C_{15} and C_{27} termini of the southern fragment in presence of potentially labile moieties, which is a non-trivial undertaking. Deprotection at each end was tested separately to determine the optimal combination of the silyl ethers to provide the needed required stability in the debenzylation step and sufficient lability to selectively expose C_{15} later on.

Arguably, Bn cleavage was the greater challenge of the two. The most commonly utilised methods for this transformation are cleavage with catalytic hydrogenation, Lewis acids, or single electron reductive methods. It is however vital to acknowledge the threat each one of them poses to one or more of the groups on the carbon backbone, highlighted in **Figure 28**.[185]

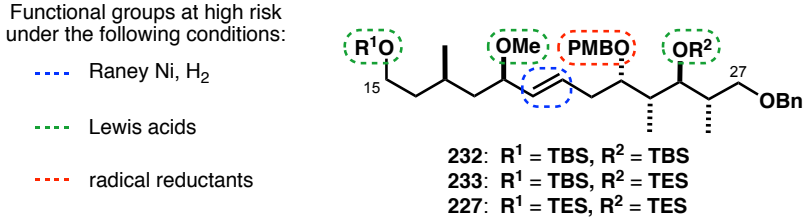

Figure 28 Lability of protecting groups in **227**, **232** and **233** under different deprotection conditions

The logical starting point for investigations was the *bis*-TBS ether **232** (**Scheme 97**) with the most robust combination of silyl groups out of the three prepared substrates shown above. Minimising the likelihood of concomitant silyl removal was expected to simplify the investigations into the selectivity for Bn over PMB ether. Raney Ni shows a degree of selectivity for Bn deprotection over olefin reduction in hydrogenation reactions compared to other common metal catalysts such as Pd/C. In addition, there is precedent for Raney Ni-catalysed Bn removal on a substrate containing a trisubstituted olefin.[222] To probe the kinetic preference for this process over the C_{20}–C_{21} double bond reduction on **232**, the reaction with Raney Ni under an atmosphere of H_2 performed and the presence of each functional group was monitored by ^{1}H NMR. Unfortunately, reduction of the double bond occurred in preference to debenzylation, thus this was not a feasible option.

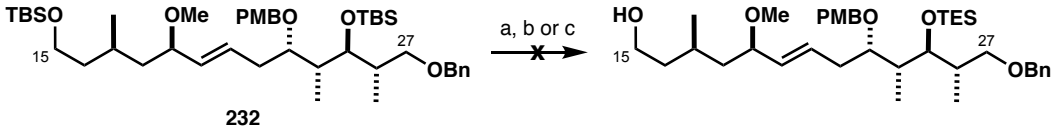

(a) Raney No, EtOH, H_2 (1 atm), rt; (b) $BBr_3 \cdot SMe_2$, CH_2Cl_2, –78 ºC; (c) $BCl_3 \cdot SMe_2$, CH_2Cl_2, –78 ºC or 0 ºC

Scheme 97 Failed attempts at C_{27} benzyl deprotection of **232**

Subjecting the substrate to trihaloborane Lewis acids at low temperatures presents another alternative method for debenzylation but poses the problem of potential side reactions arising from demethylation of the C_{19} methyl ether as well as cleavage of the silyl groups under the acidic conditions. Treatment of **232** with either $BBr_3 \cdot SMe_2$ or $BCl_3 \cdot SMe_2$ resulted in a complex mixture showing primarily the loss of the C_{25} TBS as well as the C_{19} methyl ether and even possible cyclised byproducts (**Figure 29**). This is a rather surprising result given the relative hindrance of this position compared to the seemingly more exposed primary TBS ether. The underlying argument may be the involvement of electron-rich aryl groups nearby through their coordinating ability that delivers the Lewis acid closer to the more hindered silyl ether. Therefore, substrate **233** with the C_{25} TES is likely to be even less suitable for this experiment.

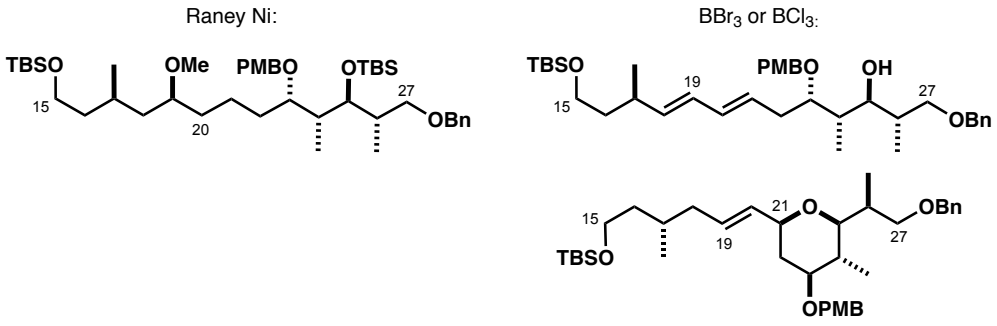

Figure 29 Observed or speculated debenzylation byproducts

Next, attention was turned to reducing methods using radicals, generated from sodium or lithium metal. One of the more common reagents for this application in even fairly complex systems is lithium 4,4'-di-*tert*-butylbiphenylide (LiDBB), which a less powerful reducing agent than lithium metal itself.[223] The moiety at risk in this case would be the electron-rich secondary PMB ether. Crimmins' synthesis of brevetoxin A showcases a step where a very similar challenge was overcome using mild excess of LiDBB which cleaved the pendant Bn group on **234** in impressive 95% yield (**Scheme 98**).[224] This example gave further evidence to support the deprotection of the benzyl group under these conditions.

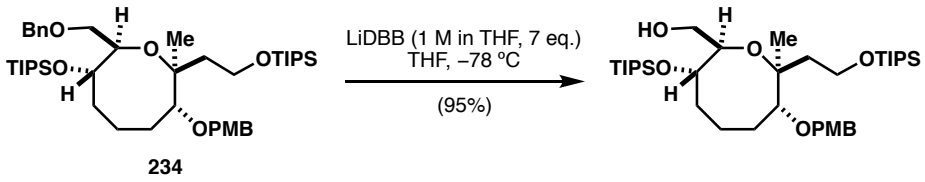

Scheme 98 LiDBB-mediated debenzylation step in the synthesis of brevetoxin A[224]

Gratifyingly, treating substrate **233** with an excess of freshly prepared LiDBB solution in THF at −78 °C preferentially deprotected the C_{27} hydroxyl without any loss of the methyl ether or silyl groups and gave an 83% yield of **235** on small scale (**Scheme 99**). Crucially, no TES migration from C_{25} to the less congested primary hydroxyl occurred in the process.

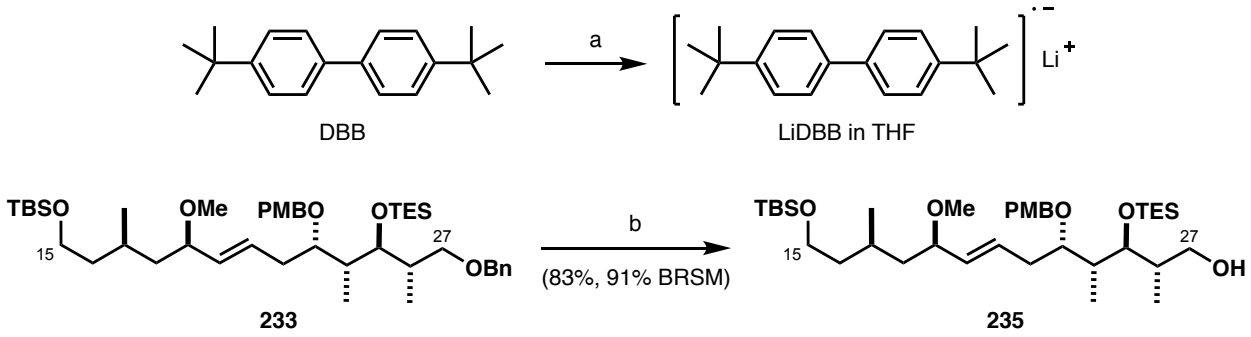

(a) Li metal, THF, 0 °C, 2 h; (b) LiDBB (0.5 M in THF, 10 eq.) THF, –78 °C, 5–10 min

Scheme 99 Formation of LiDBB radical anion and trial Bn cleavage on **233**

With conditions for the C_{27} deprotection in hand, attention now turned to ascertaining the optimal protecting group at the C_{15} position that could be cleaved selectively while leaving the C_{25} TES group intact. The reasonable methods to choose from were fluoride-based nucleophilic reagents or hydrolysis in mild acid. The reaction in buffered HF·pyr proceeded with both silyl groups being cleaved at a similar rate from the onset of the reaction, returning predominantly the diol product **237**. Catalytic *para*-toluenesulfonic acid (PPTS) in CH_2Cl_2/MeOH resulted in very slow conversion and surprisingly,

preferential removal of the C_{25} protecting group, which is identical to what had occurred with boron Lewis acids. This result is in agreement with previous bases where the C_{25} TES appeared to be more labile upon treatment with Lewis acids such as BBr_3. The use of buffered TBAF solution on the other hand removed the primary TBS first though the rate was very slow and led to appearance of other byproducts, possibly due to extended reaction time.

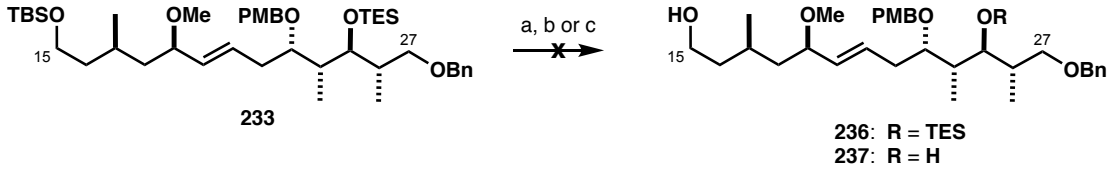

(a) HF·pyr/pyr (1:3), THF, rt; (b) PPTS (cat.), CH_2Cl_2/MeOH (10:1 or 1:1), rt; (c) TBAF/AcOH (1:1), THF, rt

Scheme 100 Unsuccessful TBS deprotection attempts on substrate **233**

As none of these options seemed feasible, let alone scalable, substrate **227** which features a more labile primary TES group became the last resort. With the silyl groups now exactly matched, it was anticipated that selective deprotection would be more facile and subject to purely the difference in sterics on each end. Using Fink's conditions for hydrolysis of a primary TES group in presence of a secondary one,[177] the C_{15} silyl ether was removed with mild acid (THF/AcOH/H_2O, 5:2:1) to generate alcohol **236** in 95% yield (**Scheme 101**).

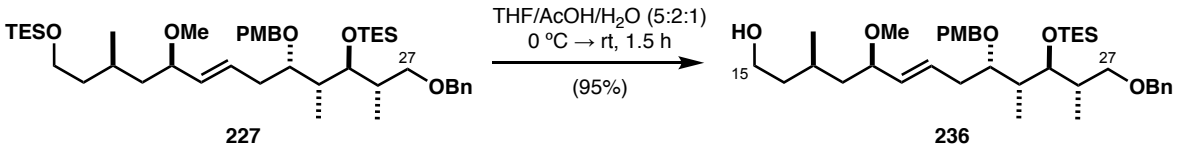

Scheme 101 Successful C_{15} deprotection of the primary silyl ether on *bis*-TES ether **227**

With alcohol **238** in hand, a viable route to the C_{15}–C_{27} aldehyde **161** was in sight. Small-scale debenzylation experiments with the *bis*-TES substrate **232** indicated no lability of either silyl group when treated with LiDBB. The insight gained in these deprotection studies was valuable and further studies focused on optimisating the process to ensure it was reproducible on scale to deliver the multi-gram of alcohol **239** required for the project (**Figure 30**).

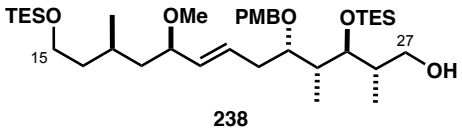

Figure 30 Desired product from LiDBB debenzylation of substrate **227**

Starting with the LiDBB debenzylation, reaction parameters were varied to obtain a reproducible protocol for a multi-gram debenzylation of **227**. The important factors given the rapid kinetics of the reaction even at low temperature were following:

1. Reaction time

This must be sufficiently long to account for the margin of error in run time due to addition of reagent at the beginning and to keep the window of preferential Bn over PMB cleavage as wide as possible. It should be noted that the reaction time is measured as the period immediately after complete addition of the reductant solution until the moment the mixture is quenched and exposed to air.

2. Quantity of reductant used

Many protocols involving LiDBB call for a gradual addition of aliquots as the substrate is consumed and the radical colour dissipates. However, the reagent is extremely air-sensitive and preparation using a literature protocol[224] immediately before use may cause discrepancies in LiDBB concentration. Addition of an excess in a single portion ensures there is a sufficient amount of the reducing agent present to complete the transformation while also trying to avoid using excess quantities unnecessarily, especially on large scale.

3. Concentration of reagent and substrate

LiDBB must be prepared at reasonably low concentration to avoid precipitation and prevent addition hot spots when adding into a significantly cooler reaction mixture (–78 °C). However, running large scale experiements at high dilution is impractical and requires efficient stirring for uniform heat transfer.

The first two factors are mutually beneficial in this process; the greater the excess of reagent, the faster the conversion rate. It is important to note that monitoring by TLC gives only a rough indication of reaction progression, thus it is not uncommon to overestimate the conversion and terminate the experiment prematurely. **Table 6** shows the results of varying the amount of LiDBB.

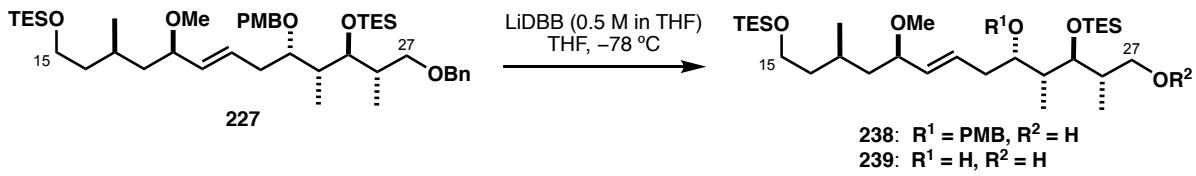

Table 6 Small-scale studies of C_{27} deprotection on benzyl ether **227**

Entry	Amount of LiDBB / eq.	Reaction time / min	Yield of **238** / %
1	5	15	80[a]
2	5	20	71[b]
3	10	5	83[b]
4[c]	20	5	71[b]
5[c]	45	10	64[b]

[a] Yield determined by ^{1}H NMR. [b] Isolated yield. [c] Run at 0.003 M concentration of **227**

(*Reactions performed on 20–50 mg of substrate **227** at standard concentration 0.03 M*)

Entries 1 and 2 represent an acceptable reaction time frame with regards to accuracy of time measurement following reagent addition. The decrease in yield was attributed to the deprotection of the PMB group to give the undesired diol **239** which cannot be easily recycled. Entries 3–5 on the other hand, with a larger excess of LiDBB, reflect an impractically fast process albeit with respectable outcomes. To follow up on promising entries 1–2, the next parameter to investigate was the reaction time (**Table 7**). To minimise the reagent addition time at the start and thereby reduce the error in time measurement, the concentration of LiDBB was increased to 1 M with no detrimental effect.

Table 7 Optimisation of reaction time

Entry	Reaction time / min	Ratio of **227** : **238** : **239** / %[a]
1	5	60 : 40 : 0
2	10	50 : 50 : 0
3	12	40 : 60 : 0
4	14	33 : 64 : 3
5	**15**	**19 : 76 : 6**
6	17	10 : 70 : 20
7	20	0 : 85 : 15
8	25	0 : 77 : 23

[a] Ratios determined by ^{1}H NMR.

There is a clear trend of gradual conversion over time, with the best results being obtained after around the 15-minutes mark (entry 5). The real test came with gram-scale experiments under the optimised

conditions. The results of the fruitful scale-up campaign, which produced more than 10 g of alcohol **238** on up to 3 g of substrate (**Scheme 102**) are summarised in **Table 8**.

Table 8 Results for gram-scale reactions

Entry	Scale / g	Reaction time / min	Yield of **238** / %
1	1.00	15	67 (99% BRSM)
2	1.00	17	69 (94% BRSM)
3	**3.00**	**18**	**77 (96% BRSM)**
4	7.13	20	69 (89% BRSM)

(*Reactions performed at substrate concentration 0.03 M with 5 eq. LiDBB (1.0 M in THF) at –78 °C)*

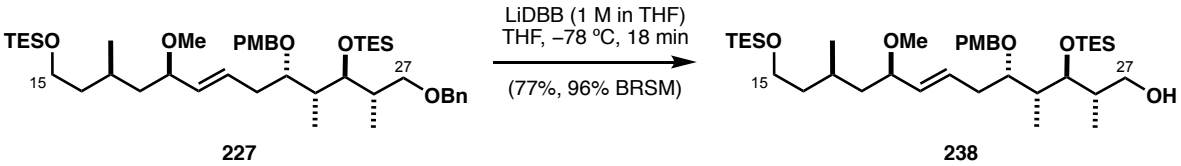

Scheme 102 LiDBB debenzylation on 3 g of benzyl ether **227**

3.5.3. Completion of the C_{15}–C_{27} Aldehyde 161

With generous stocks of alcohol **238** in hand, the C_{27} terminus was now due to be protected with an orthogonal Alloc group. As mentioned before, this moiety is not stable in presence of strong nucleophiles.[185] This is a potential concern since the union of the C_{15}–C_{27} fragment to the northern portion of the macrocycle was planned to be carried out in a $Ba(OH)_2$-mediated HWE reaction.

To gain some insight into the stability of the allyl carbonate, model substrate **240** (**Scheme 103**) was prepared with the intention of subjecting it to the above HWE conditions. Fortunately, no Alloc cleavage was seen during prolonged treatment with $Ba(OH)_2$ in aqueous THF.

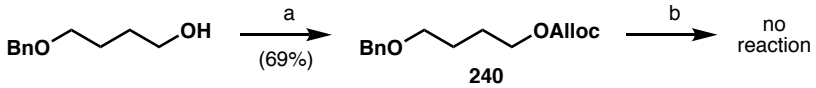

(a) allylOC(O)Cl, CH_2Cl_2/pyr (1:1), 0 °C → rt, 18 h; (b) $Ba(OH)_2$, THF/H_2O (40:1), rt, 24 h

Scheme 103 Test of Alloc stability under $Ba(OH)_2$ HWE conditions on a model substrate **240**

Allyl carbonate was then attached at the C_{15} terminus by subjecting primary alcohol **238** to excess allyl chloroformate in a mixture of CH_2Cl_2/pyr (1:1), which encourages precipitation of the formed pyr·HCl salt and precludes cleavage of the especially sensitive primary TES ether. The reaction was very rapid at

temperatures above −20 °C and despite buffered conditions produced two major undesired byproducts (**Scheme 104**), which can be rationally accounted for.

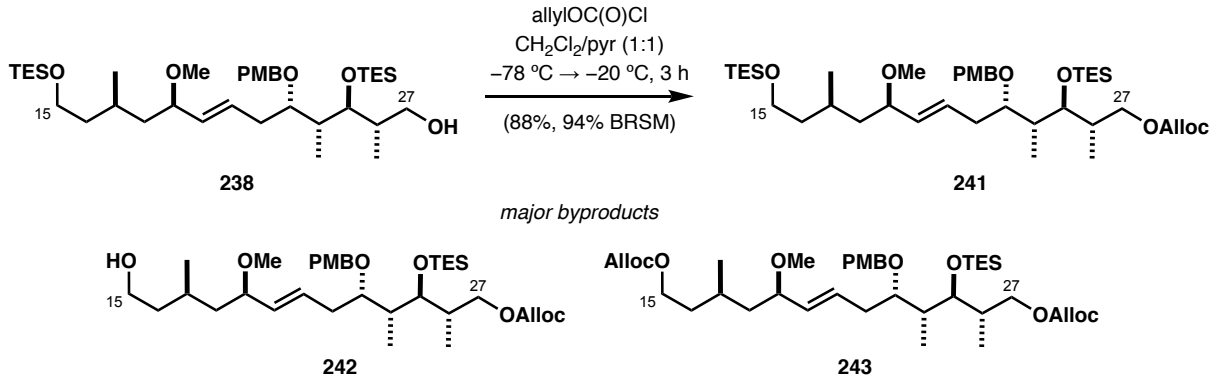

Scheme 104 Synthesis of allyl carbonate **241** and observed byproducts **242** and **243**

Primary alcohol **242** is a result of C_{15} deprotection of the desired product **241** which leaves the free hydroxyl prone to second carbonate formation. This pathway is alarming since excess allyl chloroformate can react at that terminus to yielding *bis*-Alloc material **243**, which is not synthetically useful in the current route. Fortunately, after screening a variety of conditions it was observed that performing the reaction at lower temperature (−30 °C compared to 0 °C) both undesired side reactions were largely suppressed. Product **241** was formed cleanly in high yield (88%, 94% BRSM) on multi-gram scale of starting material **238**.

The remaining transformations required to complete the fragment were TES hydrolysis at the C_{15} hydroxyl, followed by oxidation. Attempts to carry out this sequence as an efficient one-pot procedure under Swern conditions[225] were met with disappointment and resulted in material degradation (**Scheme 105**). Since the analogous experiment with Bn ether **227** directly afforded aldehyde **244** in 90% yield without difficulty it is assumed that the underlying issue is the lability of the Alloc moiety.

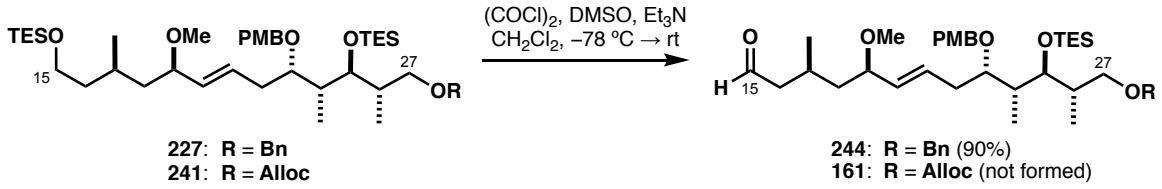

Scheme 105 Attempted one-pot oxidation of the C_{15} TES to aldehyde

Conditions for TES removal at C_{15} which had been investigated for substrate **227** (**Section 3.5.2.**) were revisited with the assumption that the Alloc group would be stable in presence of buffered TBAF or mild acid. The use of AcOH on large scale poses a practical issue as neutralising a large amount of acid with $NaHCO_3$ is a slow process during which further deprotection with residual AcOH may still occur. If

$NaHCO_3$ is added too late after the desired TES has been removed, overdeprotection can lead to the C_{15}/C_{25} diol byproduct. For this reason, TBAF was tested as the first choice to probe the stability of the C_{25} TES under buffered conditions. **Table 9** presents the outcomes of optimisation efforts, focused on controlling the rate while minimising the formation of byproduct **245**.

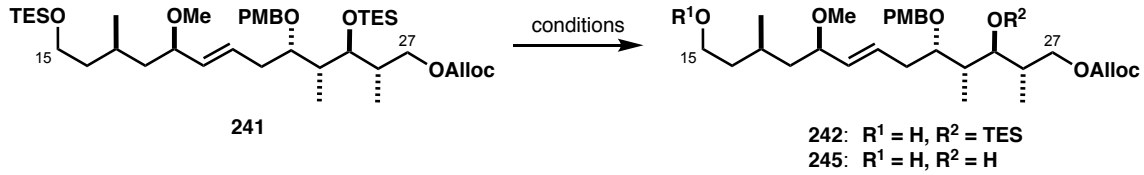

Table 9 Optimisation of C_{15} TES deprotection on substrate **241**

Entry	Conditions	Notes	Reaction time	Result
1	TBAF/AcOH (1:1), rt	1.2 eq. TBAF	3 h	55% **242** + 20% **241** + 25% **245**[a]
2	TBAF/AcOH (1:1) 0 °C → rt	1.1 + 0.5 + 0.5 eq. TBAF	5 h	64% **242**[b]
3	THF/AcOH/H_2O (5:2:1), rt	slow conversion	8 h	85% **242** [b]
4	**THF/AcOH/H_2O (2:2:1), rt**		**1 h**	**79% 242 + 11% 241**[b]
5	THF/AcOH/H_2O (2:2:1), rt	2 x more concentrated	1 h	49% **242** + 5% **241** + 24% **245**[b]
6	THF/AcOH/H_2O (2:2:1), rt	undistilled (wet) AcOH	20 min	mainly **245**[a]

[a] Yield determined by ^{1}H NMR. [b] Isolated yield.

Entries 1–2 do not support the viability of TBAF in this process. The reaction is slow at temperatures below 0 °C and before the starting material is fully consumed, diol **245** starts appearing. Returning to hydrolysis with THF/AcOH/H_2O required some tweaking of the solvent mixture before an acceptable ratio was found. Entry 3 mirrors the exact conditions from the early studies and as the proportion of THF was decreased (entry 4), the reaction time became shorter as well. Higher concentration increased the rate of *bis*-deprotection (entry 5) as did use of undistilled AcOH which in itself contains a non-negligible amount of H_2O (entry 6).

Testing the best conditions (0.1 M substrate in 2:2:1 THF/AcOH/H_2O) on 5 g of TES ether **241** gave 81% yield (89% BRSM) after 3–4 h of reaction. Although undesirable, the resulting diol **245** can be

reprotected to give the *bis*-TES **241** which can then be resubmitted to the deprotection, further increasing the yield of product **242** (**Scheme 106**).

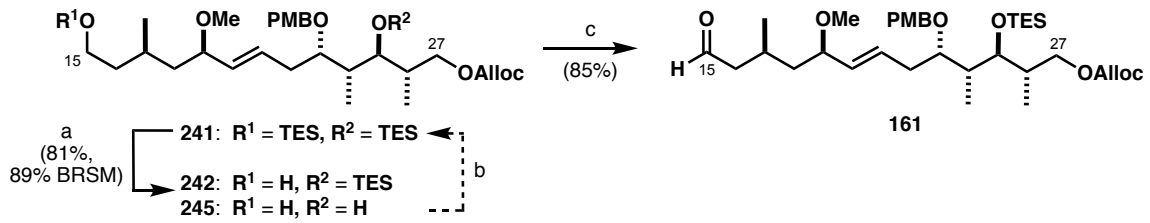

(a) THF/AcOH/H_2O (2:2:1), 0 ºC → rt; (b) TESOTf, 2,6-lut., CH_2Cl_2, –78 ºC; (c) Dess–Martin periodinane, $NaHCO_3$, CH_2Cl_2, 0 ºC → rt

Scheme 106 TES deprotection under optimised conditions and oxidation to aldehyde **161**

Finally, in light of the previous failed attempts at subjecting TES ether **241** to Swern conditions, oxidation of **242** at C_{15} was performed using Dess–Martin periodinane, which provided aldehyde **161** in 85% yield. In summary, more than 7 g of the C_{15}–C_{27} southern fragment **161** was synthesised in 14 steps and 15% yield from ethyl ketone **170** over the course of this project (**Scheme 107**).

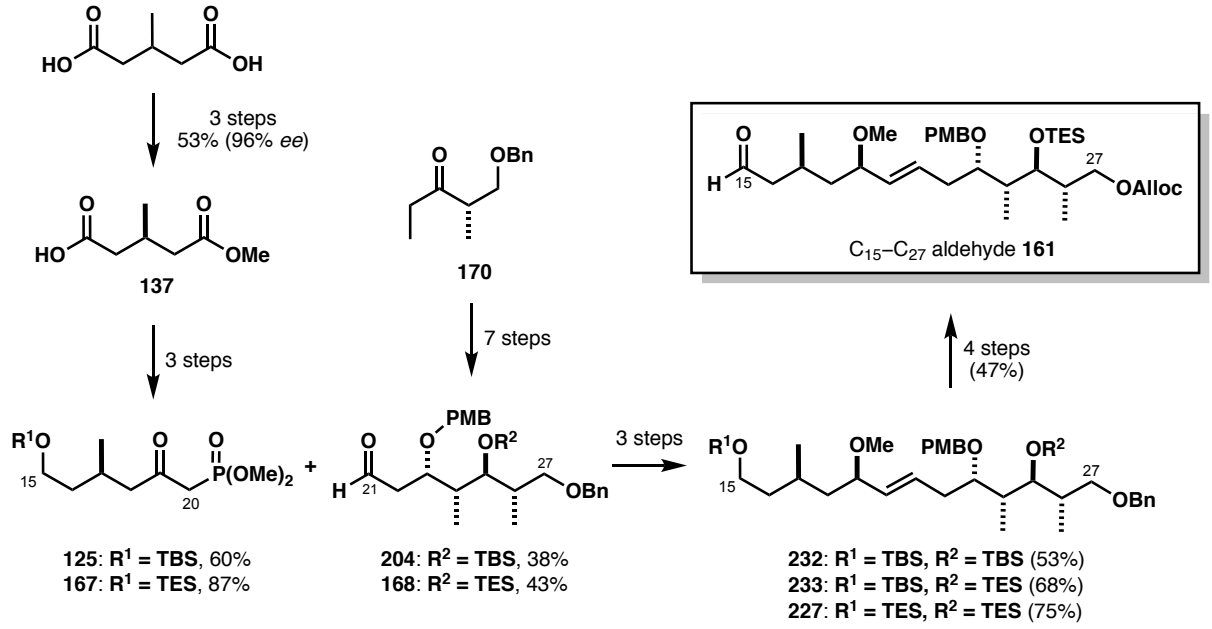

Scheme 107 Summary of the C_{15}–C_{27} aldehyde **161** synthesis

3.6. Synthesis of the C_1–C_{11} Iodide 160

3.6.1. Retrosynthesis

Synthesis of the C_1–C_{11} iodide **160** follows a well-established synthetic route by Woodrow (**Scheme 108**). The stereotetrad is constructed in a boron aldol/1,3-*anti* reduction sequence using a Roche ester-derived ethyl ketone **128** and aldehyde **130**. The diene moiety is formed in an alkyne-diene isomerisation with PPh_3/PhOH and the ester group at C_1 is masked as an allylic TBS ether.

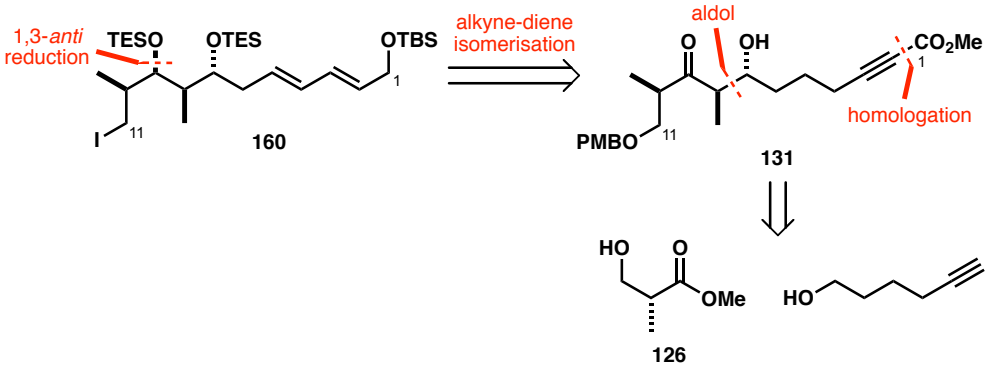

Scheme 108 Retrosynthetic analysis of the C_1–C_{11} iodide **160**

3.6.2. Synthesis of Iodide 160 from Intermediate 247

Stocks of the known diol intermediate **132** were prepared by Dr Mike Housden in 4 steps from (*R*)-Roche ester **126** (**Scheme 109**). A *bis*-TES protection was then carried out with excess TESOTf to afford **247** in 80% yield. The work detailed from this point onwards is that of the author.

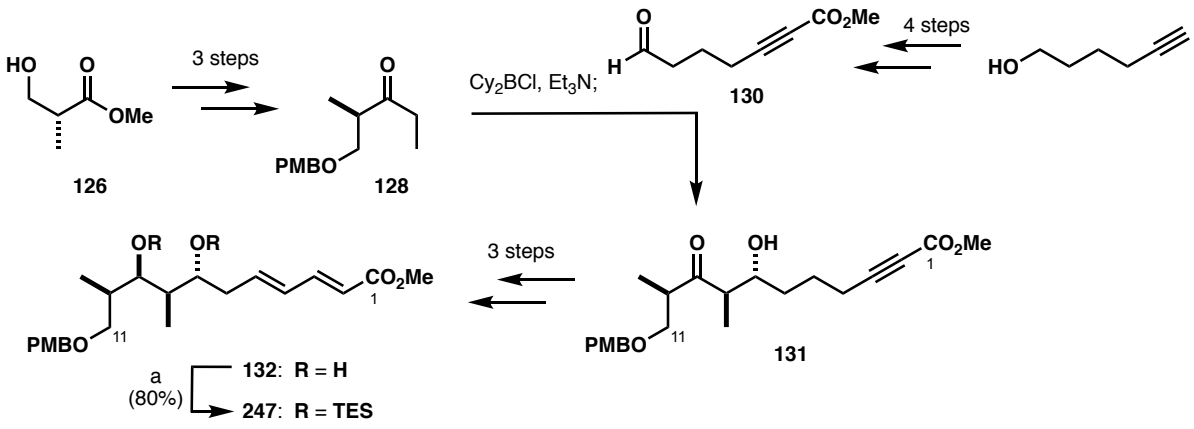

(a) TESOTf, 2,6-lut., CH_2Cl_2, –78 ºC, 45 min

Scheme 109 Summary of Housden's synthesis of *bis*-TES ether **247**

The C_{11} alcohol could be selectively revealed by oxidative cleavage of the PMB group using DDQ. Mechanistically, this step proceeds *via* a series of single electron transfer (SET) steps to form a transient charge-transfer complex between the electron-donating aromatic ring on the substrate and the electron-poor ring on the oxidant, followed by benzylic dehydrogenation (**Scheme 110**).

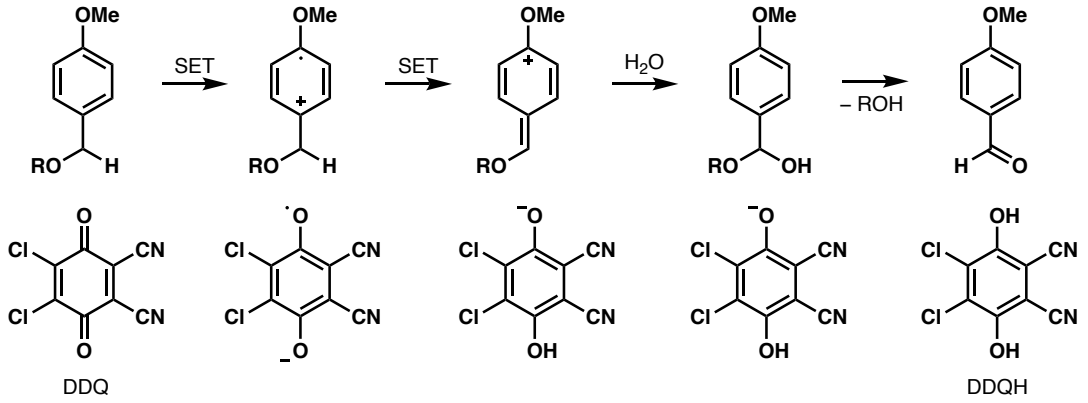

Scheme 110 Proposed mechanism of DDQ-mediated PMB cleavage[226]

Replacing the C_7/C_9 PMP acetal from the first-generation synthesis helped alleviate the issue of acetal migration or overoxidation in this step. PMB deprotection of the analogous *bis*-TES compound **247** with 1.5 eq. DDQ in neutral (pH 7) conditions formed no detectable byproducts and smoothly furnished alcohol **248** (**Scheme 111**). The silyl ethers were not expected to be labile and pleasingly, no migration to the less hindered C_{11} position was observed. Alcohol **248** was formed in 92% yield, which was an improvement in material retention in comparison to the result on the analogous PMP acetal observed by Woodrow (81%, **Section 2.3.1**).

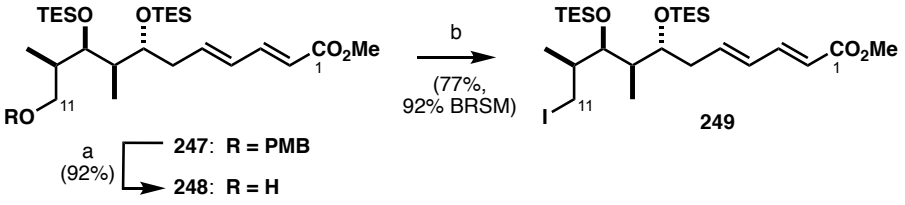

(a) DDQ, CH_2Cl_2/pH 7 buffer (2:1), rt, 1 h; (b) PPh_3, I_2, imid., Et_2O/MeCN (1:1), rt, 2 h

Scheme 111 Elaboration of the C_{11} terminus on PMB ether **247** into alkyl iodide **249**

The alkyl iodide was installed under Appel-like conditions by stirring the primary alcohol with molecular iodine, PPh_3 and imidazole.[163] Next, the ester moiety at C_1 was masked as an allylic TBS ether to prevent interference of the carbonyl in the following alkylation reaction with lithiated phosphonate **123**. Reduction of the ester with excess DIBALH, followed by protection with TBSCl and imidazole forged **160** in 95% yield over two steps (**Scheme 112**). Worryingly, iodide **160** was found to degrade upon

prolonged storage even at –20 °C, thus major stocks of material were held at the more stable preceding stage as alcohol **248**.

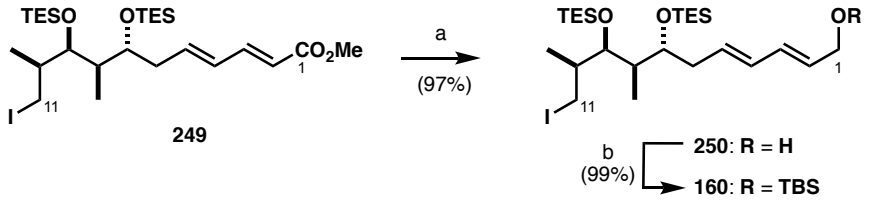

(a) DIBALH, CH_2Cl_2, –78 ºC, 1.5 h; (b) TBSCl, imid., CH_2Cl_2, 30 min, rt

Scheme 112 Reduction of the C_1 ester moiety and TBS protection of allylic alcohol **250**

3.7. Summary

This chapter details the endeavours towards an improved synthesis of the C_{15}–C_{27} southern fragment **161** with efforts focused on refining the assembly of the C_{23}–C_{26} stereotetrad and implementing the second-generation protecting group strategy for macrocyclic core of the aplyronines (**Scheme 113**). These key aims had been reached owing to the power of titanium aldol methodology and perseverance with several iterations of protecting group alterations which taught us valuable lessons regarding their stability and compatibility. Additionally, two different methods of installing the C_{17} chiral centre were explored, which culminated in a viable supply strategy for the C_{15}–C_{20} phosphonate **167**. This new approach utilises racemic starting materials and is carried out *via* enzyme catalysis. Overall, the new route ultimately provided more than 7 g of the C_{15}–C_{27} aldehyde **161** in 14 steps LLS (19 steps total) and 15% yield from ketone **170**.

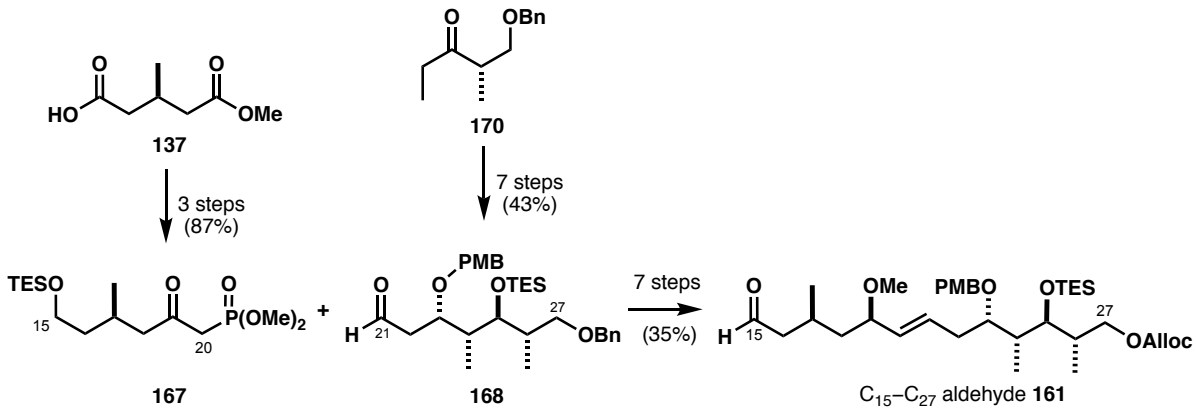

Scheme 113 Summary of steps towards the C_{15}–C_{27} sourthern fragment **161**

In addition, stocks of the C_1–C_{11} iodide **160** were synthesised from the known intermediate **247** in 4 steps and 68% yield, harnessing the efficiency and exquisite stereocontrol of the boron aldol reaction which

forges the C_7–C_{10} chiral centres (**Scheme 114**). Alignment of the protecting groups at C_7/C_9 with the newly designed macrocycle endgame ahead was predominantly straightforward, though observing degradation of iodide **160** upon prolonged storage was a crucial realisation prior to its scale-up and the following HWE reaction with aldehyde **161**. This highly anticipated event and further steps truly put to the test the merits of our ideas and are presented in the next chapter.

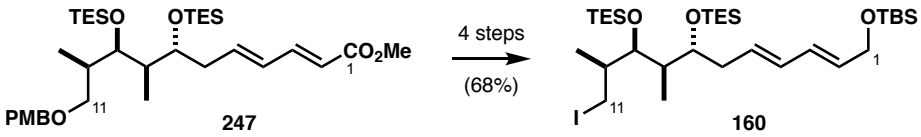

Scheme 114 Summary of steps to the C_1–C_{11} iodide **160**

Chapter 4

Results and Discussion – Part II

Synthesis of the C_1–C_{27} Macrocycle 159

4.1. Synthesis of C_1–C_{27} Allylic TBS Ether 162

4.1.1. Coupling of C_{12}–C_{14} β-Ketophosphonate 123 with C_{15}–C_{27} Aldehyde 161

The challenging task of forging the C_{14}–C_{15} trisubstituted olefin was intended to be carried out using $Ba(OH)_2$-mediated HWE methodology as this had previously served well in the first-generation aplyronine synthesis (**Scheme 115**). As the southern C_{15}–C_{27} fragment **161** was designed as the aldehyde coupling partner, the phosphonate moiety had to be appended to the C_1–C_{11} iodide **160**. This step must concomitantly homologate the carbon chain, which can be achieved in a single transformation by alkylation with the C_{12}–C_{14} β-ketophosphonate **123** under the conditions developed by Grieco and Pogonowski.[151]

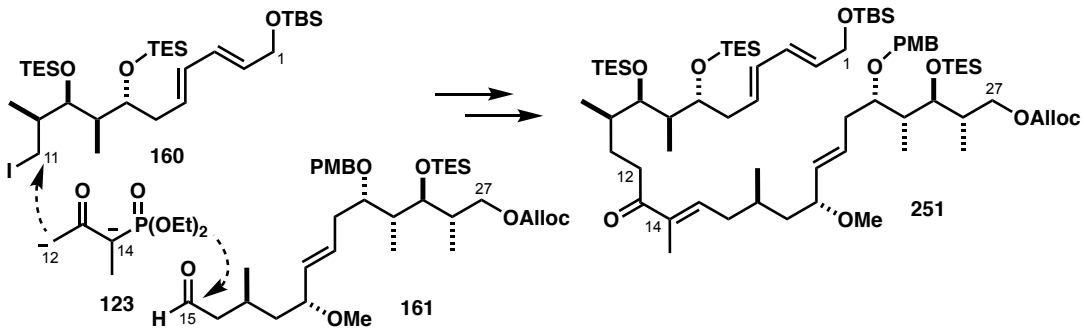

Scheme 115 Linkage of the northern and southern fragments **160** and **161** *via* the C_{12}–C_{14} **123** β-ketophosphonate

Synthesis of the C_{12}–C_{14} linker **123** entails the alkylation of the lithium anion of diethyl ethylphosphonate with ethyl acetate to attach the acetyl group. Deprotonation with ^{n}BuLi forms the lithiated species, which undergoes a single addition into the ester (**Scheme 116**). The product was isolated in 61% yield by distillation under reduced pressure and the process was highly amenable to scale-up, producing in excess of 15 g of fragment **123** in a single batch.

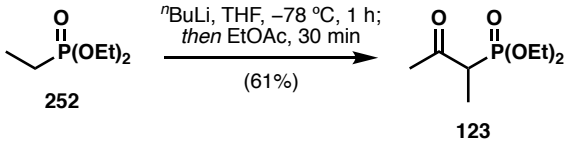

Scheme 116 Synthesis of the C_{12}–C_{14} fragment **123** by acetylation

Alkylation at C_{11} requires the β-ketophosphonate **123** to act as a nucleophile at the less hindered γ-terminus. Due to negative charge stabilisation at C_{14}, γ-deprotonation can only be achieved once the most acidic proton has been removed first. Treatment of **123** with sodium hydride in THF produces an insoluble monoanion, which is subsequently metallated with ^{n}BuLi at –78 °C to generate a pale yellow solution of the dianion (**Scheme 117**), ready to react with the iodide.

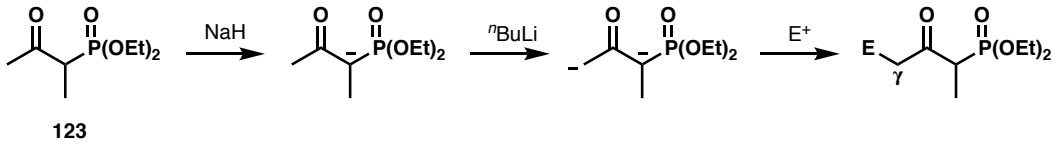

Scheme 117 Formation of the dianion of **123** by double deprotonation

The reaction was expected to proceed with virtually no stereoselectivity at C_{14} to produce a 1:1 mixture of diastereomers **253** at that position. However, a regioisomeric alkylation product **254** (**Scheme 118**) constituted a significant component (20–30%) of the isolated product mixture and the selectivity had previously been found to be highly dependent on the nature of the electrophile (**Scheme 118**).[162] The branched regioisomer **254** is inseparable by chromatography, though it does not interfere with the subsequent HWE step due to the lack of α-protons on the phosphonate and can thus be carried through the olefination step. Nevertheless, the unproductive pathway causes unnecessary loss of advanced material and every effort must be made to prevent it.

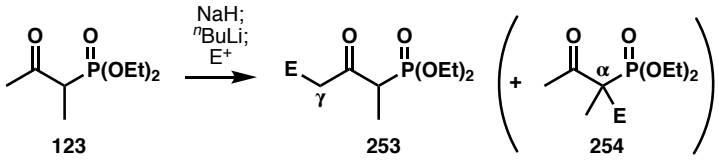

Scheme 118 Observed mixture of products in the alkylation reaction of iodide **160**

Housden's preliminary work towards the alkylation of the *bis*-TES iodide **160** indicated that no reaction occurs below 0 °C. The addition of hexamethylphosphoramide (HMPA) with the intention of deaggregating the dianion did not affect the outcome. The product distributions of regioisomers **253** and **254** (**Scheme 119**) varied in the range of 2:1 up to 4:1 by ^{1}H NMR analysis. The highest yield (85%, 3:1 **253**:**254**) was obtained with 50-fold excess of the dianion. This was clearly not a practicable solution on scale but it could be replicated by reverse addition of the iodide **160** into a solution of the anion.

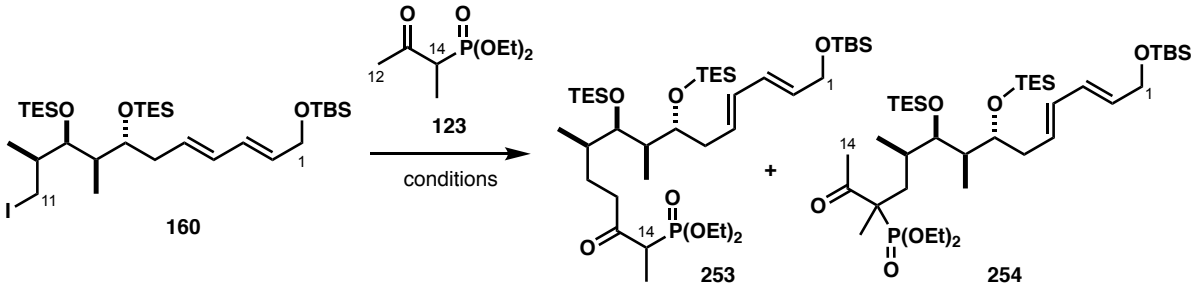

Scheme 119 Alkylation of iodide **160** with phosphonate **123**

Optimisation efforts by the author are presented in **Table 10**. Standard conditions were taken to be 50 mg **160**, 6 eq. **123**, 7 eq. NaH, 6 eq. ^{n}BuLi, THF, 0 °C (entries 1–3) where full conversion as judged by TLC was achieved after 1.5–2 h reaction time. It became immediately apparent that the reaction yields and selectivities drop progressively with increasing scale. Reducing the speed of addition, either adding the iodide into the dianion (entry 4) or *vice versa* (entry 5) produced similar yields and it was not possible to account for the remaining mass balance.

One potentially important parameter was the reaction solvent. Replacing THF with a different ethereal solvent could change the aggregation and hence the reactivity of the dianion. By this logic, a larger solvation cage around the metallated species should encourage reaction through the less hindered γ-terminus, though it may also preclude any alkylation entirely. This was indeed the case when using TBME (entry 6), and, more surprisingly, 1,2-dimethoxyethane (DME, entry 7), which was expected to more strongly bind the lithium cation and increase the dianion nucleophilicity. Even warming both reactions to room temperature and adding HMPA only returned recovered substrate. Conducting the experiments in Et_2O (entries 8–11) was met with slight success, though there was no noteworthy improvement. Increasing the equivalents of HMPA (entries 9–10) gave a more favourable isomer ratio but also diminished the yield.

Table 10 Screening of conditions for alkylation of iodide **160**

Entry	Variation from standard conditions	Solvent	Ratio[a] (**253**:**254**)	Combined yield
1	/	THF	4.6:1	86%
2	**400 mg 160**	**THF**	**3.0:1**	**75%**
3	1.00 g **160**	THF	2.7:1	68%
4	syringe pump addition over 30 min	THF	3.4:1	70%
5	dianion added to **160** by syringe pump over 30 min	THF	5.5:1	66%
6	0 ° C → rt, 100 µL HMPA	TBME	no reaction	
7	0 ° C → rt, 100 µL HMPA	DME	no reaction	
8	/	Et_2O	no reaction	
9	2 eq. HMPA, −78 ° C → −30 ° C	Et_2O	1.5:1	66%
10	6 eq. HMPA, −78 ° C → −30 ° C	Et_2O	2.2:1	56%
11	300 mg **160**, 50 eq. HMPA	Et_2O	3.3:1	54%

[a] Determined by ^{1}H NMR analysis of the isolated product mixture.

One final attempt at upgrading the selectivity was to perform a modified alkylation. Instead of forming the β-ketophosphonate **253**, the iodide can be homologated with EtOAc, followed by a single addition of the lithiated diethyl ethylphosphonate into the resulting ester **255** (**Scheme 120**). This would add a step to the longest linear sequence but on the other hand completely prevent the formation of the undesired regioisomer **254** by virtue of the mechanism.

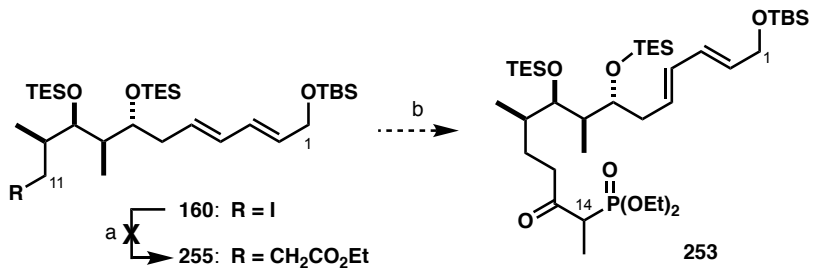

(a) LDA, EtOAc, THF; *then* **160**; (b) ^{n}BuLi, diethyl ethylphosphonate, THF; *then* **255**

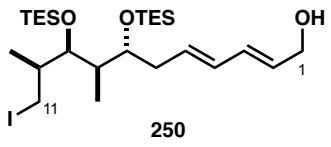

Scheme 120 Alternative sequence from iodide **160** to phosphonate **253** and the observed byproduct **250**

What seemed like a relatively straightforward transformation ultimately lead to none of the desired ester **255**. No conversion was observed below 0 °C even with HMPA additive and at room temperature. In

each case the TBS-deprotected material was the only recovered product. This option was not pursued further and instead the attention was turned on the more pressing C_1–C_{14} phosphonate **253** linkage to the C_{15}–C_{27} aldehyde **161** with the intention of removing the undesired regioisomers at this stage.

The mechanism of a HWE olefination is illustrated in **Scheme 121**. Construction of a trisubstituted olefin in an HWE reaction is generally more challenging but the $Ba(OH)_2$ variant of this methodology has been applied to highly functionalised substrates in the syntheses of numerous natural products. Due to the similar complexity of both components, the aldehyde to phosphonate ratio was kept as close to 1:1 as possible, also taking into account the presence of the unreactive regioisomer **254**.

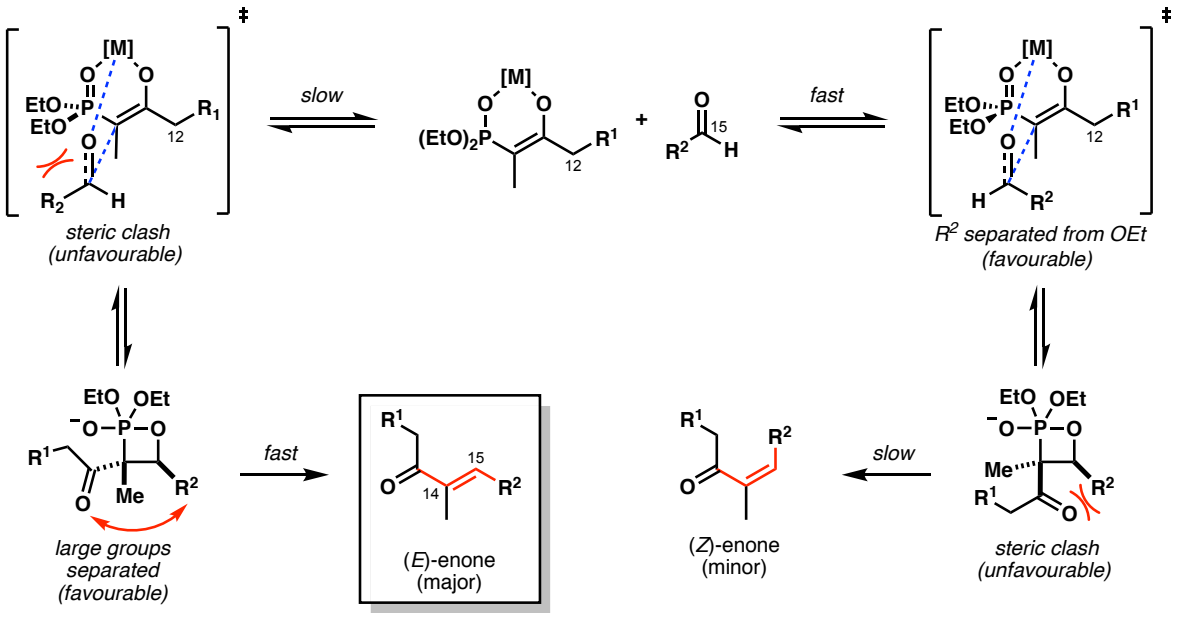

Scheme 121 The origin of selectivity in the Horner–Wadsworth–Emmons olefination with aldehyde **161** and β-ketophosphonate **253**

β-Ketophosphonate **253** (1.05 eq. of **253**, used as a mixture with **254**[‡]) was deprotonated with $Ba(OH)_2$ in anhydrous THF followed by the addition of aldehyde **161** in aqueous THF (THF/H_2O, 40:1) which forged enone **251** in 96% yield. No undesired (*Z*)-isomer was detected in the ^{1}H NMR of the crude product, indicating superb *E*/*Z* selectivity (>20:1). The aldehyde was largely consumed in the first 24 h (determined by TLC analysis) and although the progress was slower on larger scales (up to 1 g of aldehyde **161**), extended reaction times did not negatively impact the outcome. Any unreacted southern fragment **161** was easily separated from the product **251** by chromatography on silica and recovered. Pleasingly, no loss of the allylic carbonate functionality at C_{27} occurred.

[‡] Ratio of **253** to **254** determined by ^{1}H NMR integration

This result constitutes the most efficient and selective method of constructing the C_{14}–C_{15} trisubstituted double bond to date. Kigoshi's publication on a second-generation route to aplyronine A[112] presents an improvement in the NHK coupling step as part of their overall strategy, yet the need to simultaneously introduce the C_{13} chiral centre reduces the overall yield due to the more challenging nature of the asymmetric reaction variant.

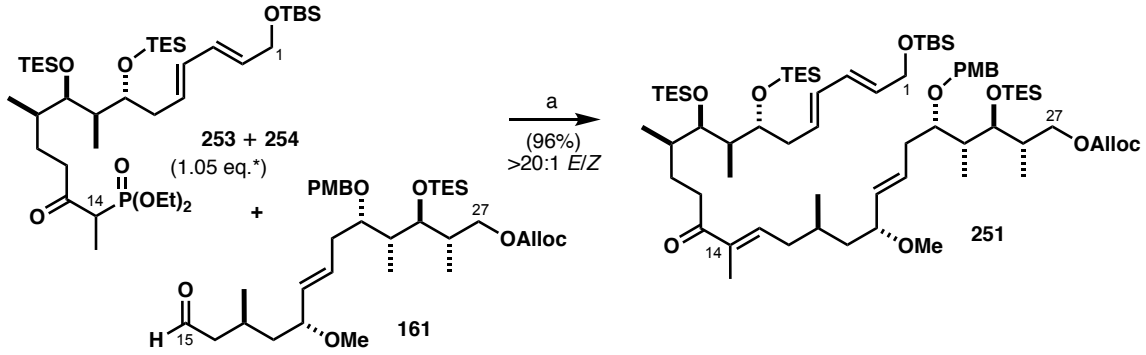

(a) $Ba(OH)_2$, THF, **253**, rt, 1.5 h; *then* **161**, THF/H_2O (40:1), rt, 20 h

Scheme 122 HWE reaction between the northern and southern fragments **161** and **253**

4.1.2. Elaboration of Enone 251

The final, C_{13} allylic stereocentre was installed in an analogous manner to C_{19} on the southern fragment, using the enantiomeric (*R*)-Me-CBS oxazaborolidine **140** in stoichiometric quantities to ensure complete conversion and prevent unwanted hydroboration of the alkenes in the molecule. Alcohol **256** was generated in an excellent 93% yield and 15:1 *dr*.

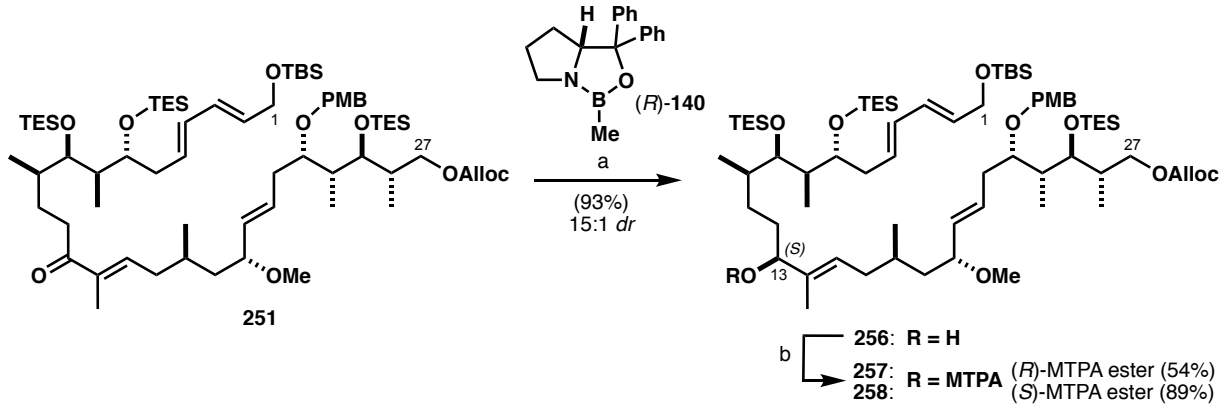

(a) (*R*)-**140** (1.3 eq.), $BH_3 \cdot SMe_2$, THF, –20 °C → –10 °C, 3 h; (b) (*R*)- or (*S*)-MTPA, DCC, DMAP, CH_2Cl_2, rt, 3 h

Scheme 123 CBS reduction of the C_{13} carbonyl and synthesis of Mosher esters **257** and **258**

Mosher ester derivatives **257** and **258** were synthesised to confirm the absolute configuration, however, a lack of distinct signals near the C_{13} oxymethine gave an inconsistent result in the analysis. Due to the

structural similarity to the analogous allylic alcohol from the first-generation route (**Figure 31**), the new stereocentre was assumed to be (13*S*) without further investigation.

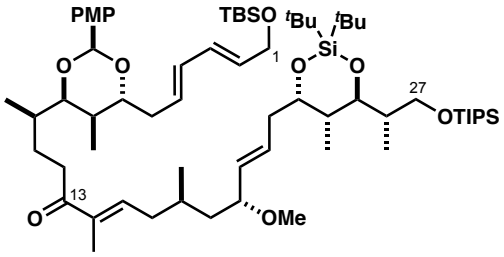

Figure 31 CBS reduction substrate from the first-generation Paterson synthesis of the aplyronine

Methylation of the newly formed allylic alcohol under previously established conditions (NaH, MeI) was predicted to proceed without difficulties. Employing sodium hydride as a strong, non-nucleophilic base should facilitate irreversible deprotonation of the free hydroxyl at C_{13}, which can then be alkylated by excess electrophile to produce the methyl ether.

This was unfortunately not the case as the starting material was converted into unexpected new products by TLC analysis, of which four main components were isolated (**Scheme 124**). Beside the desired methyl ether **162** the compounds can be attributed to the cleavage of Alloc group which first yields alcohol **259**, followed by either methylation at C_{27} or migration of the C_{25} TES group onto the less hindered primary hydroxyl.

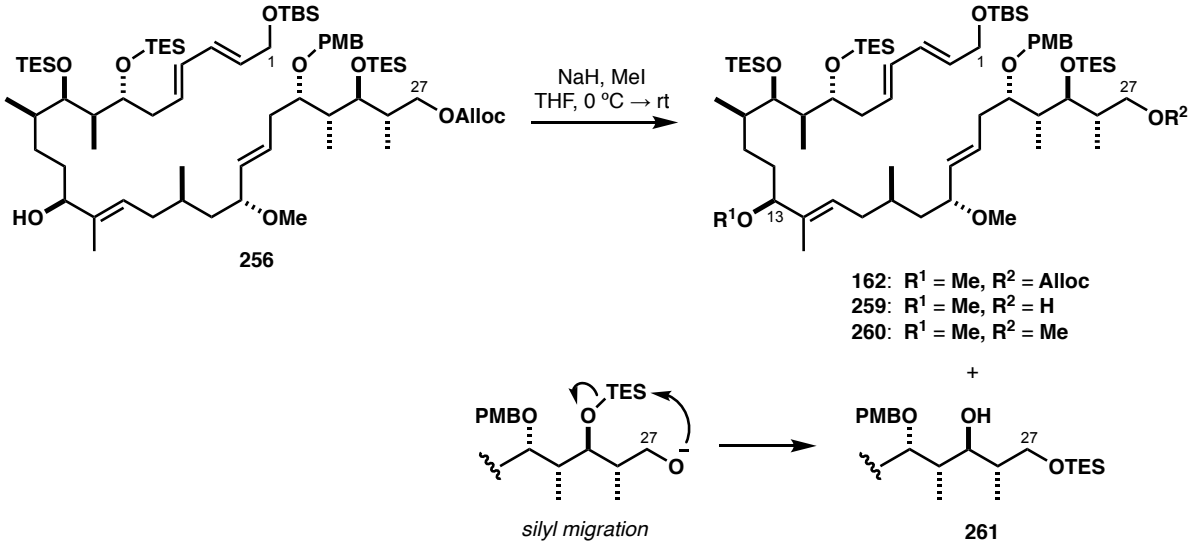

Scheme 124 Multiple byproduct formation in the methylation of alcohol **256** with NaH and MeI

Upon prolonged storage, sodium hydride reacts with atmospheric moisture and is hydrolysed into nucleophilic sodium hydroxide, which is a threat to the allyl carbonate group. Despite employing strictly

anhydrous conditions and using a new bottle of sodium hydride the byproduct formation could not be prevented. It became apparent that a screen of alternative methylation conditions would be required in order to complete this transformation in a high yielding and reproducible manner.

Model substrate **240** was revisited as a suitable substrate to first establish which combination of bases and methylating agents would leave the Alloc intact before optimising for higher yields (**Table 11**). Lee's conditions (NaH, MeI, 0 °C → rt) in entry 1 served as a reference for the rate of deprotection and lowering the temperature (entry 2) gave a similar outcome. Changing the solvent to *N*,*N*-dimethylformamide (DMF) (entries 3 and 4) still facilitated carbonate removal and also promoted rapid methylation of the resulting alcohol, possibly as a consequence of poor oxyanion solvation and greater nucleophilicity towards MeI. Gratifyingly, prolonged treatment with either Meerwein salt ($Me_3O{\cdot}BF_4$) or methyl triflate (MeOTf) (entries 5–8) returned only recovered starting material suggesting that using a milder base may prove beneficial.

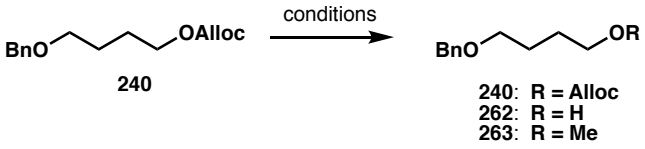

Table 11 Screen of methylation conditions on model substrate **240**

Entry	Base and methylating agent	Solvent	Temperature	Major product
1	NaH, MeI	THF	rt	**262**
2	NaH, MeI	THF	0 °C	**262**
3	NaH, MeI	DMF	rt	**263**
4	NaH, MeI	DMF	0 °C	**263**
5	Meerwein salt, Proton-sponge®	CH_2Cl_2	rt	**240**
6	Meerwein salt, Proton-sponge®	CH_2Cl_2	0 °C	**240**
7	MeOTf, *di*-^{t}Bu-pyr	CH_2Cl_2	rt	**240**
8	MeOTf, *di*-^{t}Bu-pyr	CH_2Cl_2	0 °C	**240**

(*Reactions performed on 5 mg of substrate **240** at 16–24 h reaction time*)

To lend further confidence to the new conditions a second model system was investigated which would match the more sterically congested stereocentre at C_{13}. **265** was synthesised in an analogous manner to the C_1–C_{27} substrate **256** using a simple Alloc-protected aldehyde **264** (derived from octane-1,8-diol in

two steps) and β-ketophosphonate **123**, which underwent an HWE reaction and subsequent CBS reduction (**Scheme 125**). Note that all yields are unoptimised.

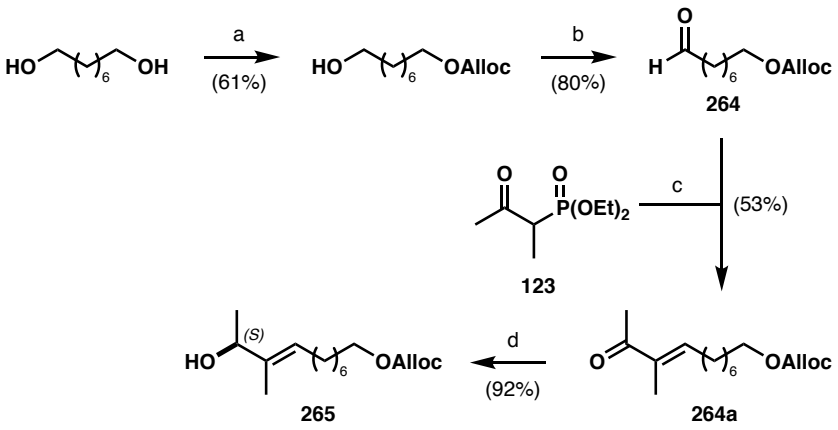

(a) allylOC(O)Cl (1 eq.), CH_2Cl_2/pyr (1:1), 0 ºC → rt, 2 h; (b) Dess–Martin periodinane, $NaHCO_3$, CH_2Cl_2, 0 ºC → rt, 15 min; (c) $Ba(OH)_2$, THF, **123**, rt, 45 min; *then* **264**, THF/H_2O (40:1), rt, 16 h; (d) (*R*)-2-Me-CBS **140**, $BH_3 \cdot SMe_2$, THF, –10 ºC, 1 h

Scheme 125 Synthesis of a model methylation substrate **265**

With allylic alcohol **265** in hand, methylation experiments were carried out on small scale to monitor progression and any additional side reactions over time (**Scheme 126**). 10 eq. of both Meerwein salt and Proton-sponge® gave clean and rapid conversion within the first few hours. Unfortunately, it proved difficult to push the reaction to completion. Despite the addition extra portions of the Meerwein reagent, the crude mixture consisted of 40% recovered alcohol **265** after 2 days at room temperature, judging by ^{1}H NMR analysis. Alternatively, using 10 eq. of MeOTf as the electrophile in presence of *di*-^{t}Bu-pyridine base gave near-quantitative conversion but with a significantly longer reaction time (3 days).

(proportion of **265** *and* **266** *estimated by ^{1}H NMR analysis)*

a:	60%	40%
b:	66%	34%

(a) Meerwein salt (10 eq.), Proton-sponge® (10 eq.), CH_2Cl_2, rt, 2 days; (b) MeOTf (10 eq.), *di*-^{t}Bu-pyr (10 eq.), CH_2Cl_2, 2 or 3 days

Scheme 126 Methylation studies on model alcohol **265**

MeOTf was a highly promising option on the model system, yet gave somewhat disappointing results on the C_1–C_{27} substrate **256** (**Table 12**, entries 1–3). Conversion stalled even at mildly elevated temperature (30 °C) or prolonged reaction times and appearance of unidentified byproducts was clearly seen by TLC.

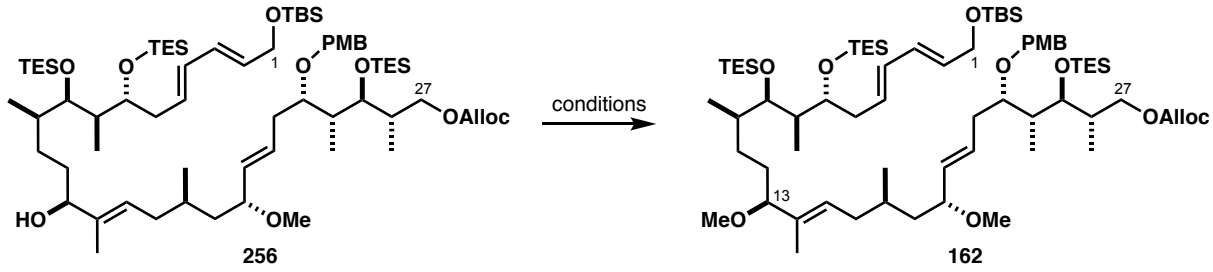

Table 12 Methylation of the C_1–C_{27} allylic alcohol

Entry	Base and methylating agent	Temperature	Reaction time	Isolated yield
1[a]	MeOTf (10 eq.), *di*-^{t}Bu-pyr (20 eq.)	rt	24 h	58% (95% BRSM)
2[a]	MeOTf (15 eq.), *di*-^{t}Bu-pyr (20 eq.)	30 °C	24 h	70%
3[a]	MeOTf (15 eq.), *di*-^{t}Bu-pyr (20 eq.)	30 °C	3 days	69%
4[a]	Meerwein salt (20 eq.), Proton-sponge® (20 eq.)	rt	24 h	72% (100% BRSM)
5	Meerwein salt (5 eq.), Proton-sponge® (5 eq.)	rt	7 h	69% (77% BRSM)
6	**Meerwein salt (5 eq.), Proton-sponge® (5 eq.)**	**rt**	**16 h**	**78% (85% BRSM)**
7[b]	Meerwein salt (10 eq.), Proton-sponge® (10 eq.)	rt	16 h	74%
8[b]	Meerwein salt (7 eq.), Proton-sponge® (7 eq.)	rt	16 h	76%

[a] Reactions performed on more than 50 mg **256**. [b] Reactions performed on more than 1 g **256**.

Meerwein methylation proved to be the safer option and produced more consistent results. Using a large excess of reagent on small scale (entry 4) indicated that the majority of **162** was produced in the first 1–2 hours and the substrate was never fully consumed. Other optimisation experiments were aimed towards reducing the excess of the electrophile and finding the optimal reaction time (entries 5 and 6) Despite investigating several conditions the yields remained uniform across a range of scales up to more than a gram of alcohol **256** (entries 7 and 8). Over the course of this project, more than 3 g of compound **162** were prepared.

With plentiful stocks of the C_1–C_{27} methyl ether **162** in hand, the planned sequence continued by revealing the macrolactonisation sites in a single oxidative step. Firstly, PMB cleavage at the C_{23} hydroxyl was anticipated to occur without difficulty. The second transformation, perhaps one of the most

elegant features of the Paterson strategy, was the conversion of the allylic TBS moiety into the corresponding aldehyde in a DDQ-mediated oxidation.

This serendipitous discovery in the early stages of the aplyronine project was later identified to be a more general transformation for electron-rich silyl ethers.[164] The mechanism commences with substrate oxidation at the allylic position and hydrogen radical transfer to the quinone. The resulting intermediate is stabilised by the silyloxy group, which leaves the Si–O bond weakened and subject to facile cleavage to reveal the carbonyl (**Scheme 127**). As with other oxidative processes in presence of DDQ, the mechanism likely involves SET steps, indicated by the distinctly coloured charge-transfer complex.

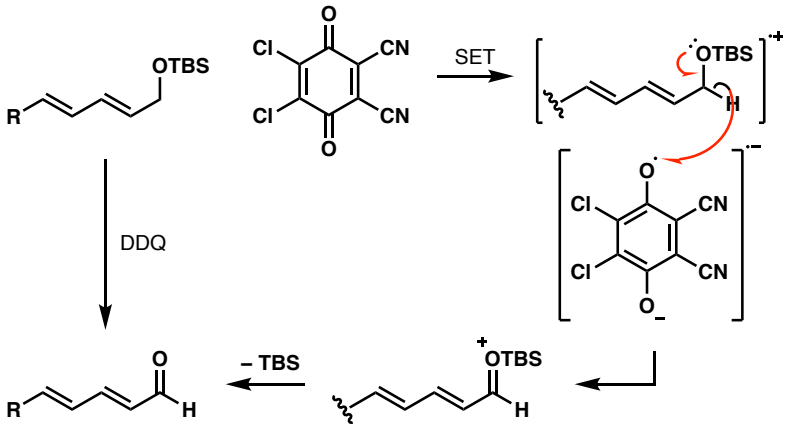

Scheme 127 Mechanism of allylic TBS ether oxidation to aldehyde with DDQ

Methyl ether **162** was treated with DDQ in CH_2Cl_2/pH 7 buffer (1:1) at 0 °C and gradual oxidation of initially the allylic, followed by the benzylic methylene was observed to afford aldehyde **163** in 82% yield as illustrated in **Scheme 128**. The preferentially allylic oxidation was confirmed by the isolation of the intermediate enal **267** with with the PMB group still intact. **267** could be separated from the crude mixture and subjected to further deprotection to yield the desired aldehyde **163** though it was generally carried out as a one-step double transformation. The reaction is rapid, often complete within 10 min.

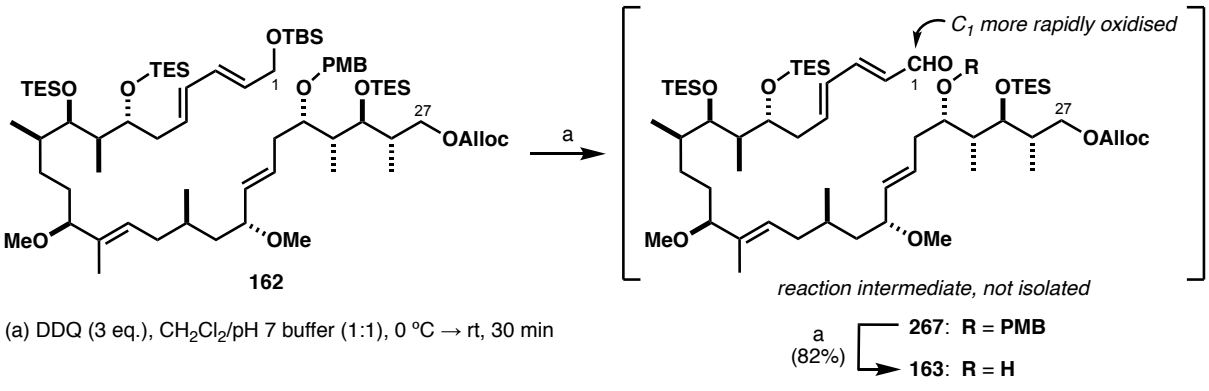

(a) DDQ (3 eq.), CH_2Cl_2/pH 7 buffer (1:1), 0 °C → rt, 30 min

Scheme 128 One-step DDQ-mediated double deprotection and C_1 oxidation to yield dienal **163**

Adding further portions of DDQ (0.5–1 eq.) to achieve full double deprotection must be done with great care to avoid the formation of overoxidation byproduct, tentatively assigned to be **268**. The supporting argument for it is the loss of the C_{19} OMe signal in the ^{1}H NMR and a downfield shift of the H_{20}/H_{21} olefinic peaks, which can be attributed to the undesired oxidation of the allylic methyl ether to the corresponding enone (**Figure 32**). No such occurence was observed for the C_{13} methyl ether.

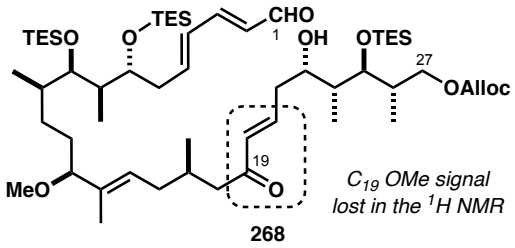

Figure 32 Enone overoxidation byproduct **268**

Another unexpected event was occasional diminishing of signals for the H_2–H_5 protons in comparison to other olefinic peaks (**Figure 33**).

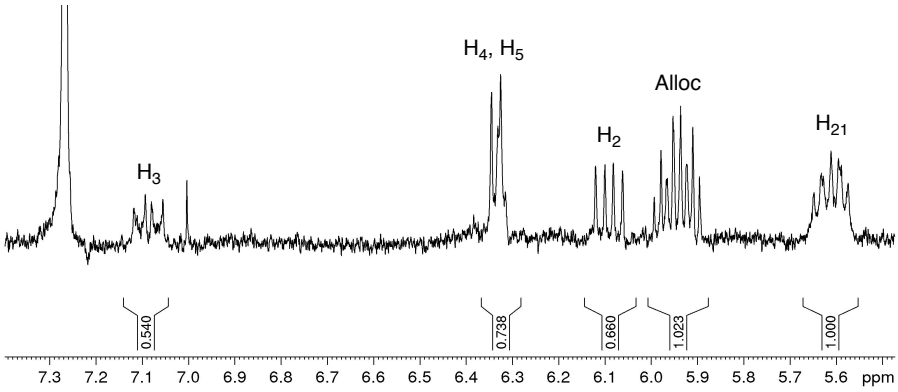

Figure 33 Olefinic region of the ^{1}H NMR spectrum of a mixture of aldehyde **163** an an unidentified byproduct, lacking H_2–H_5 protons

This observation was particularly puzzling as no other distinct additional protons appeared and this was not observed in the spectrum of the preceding compound **162**. The byproduct was to some extent separable by column chromatography, though it was not possible to isolate it as a single compound and was thus never fully characterised. One hypothesis is that the electron-poor nature of the dienal may cause the moiety to become light-sensitive or susceptible to reaction with radicals. PMB removal with DDQ undergoes two SET steps and may inadvertently facilitate other radical-mediated processes. Similar issues have been encountered in the Paterson synthetic efforts towards the total synthesis of hemicalide.[227] Light sensitivity was probed by exposing the solution of compound **163** in $CDCl_3$ to sunlight and monitoring the presence of the peaks in question by ^{1}H NMR over time. The rate of diene signal

disappearance was slow over several days and it was not clear whether this was due to UV exposure or storage at room temperature. Ultimately, the most effective method of avoiding this unwanted side process was carrying out the transformation in the absence of light, the addition of DDQ in sub-stoichiometric portions and with minimal excess, keeping the reaction time as short as possible and the temperature at 0 °C.

The *seco*-acid for the macrolactonisation can be furnished by chemoselective oxidation of the C_1 aldehyde precursor under Pinnick conditions.[169] A general mechanism for this process is depicted in **Scheme 129**. In the mildly acidic, dihydrogenphosphate-buffered reaction medium, sodium chlorite ($NaClO_2$) is converted into chlorous acid ($HClO_2$). This species is thought to be the active oxidant, which forms an adduct with the aldehyde and facilitates hydride abstraction in a pericyclic transition state. Products of this step are the corresponding carboxylic acid and hypochlorous acid (HOCl). The latter is a highly electrophilic byproduct, which can either react with free chlorite ions (ClO_2^-) or with any olefins to give a halohydrin. For this purpose, 2-methyl-2-butene is added in excess as a HOCl scavenger.

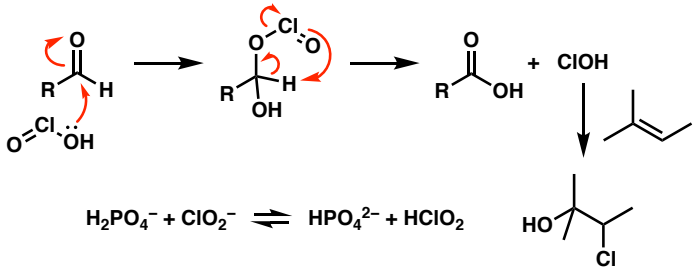

Scheme 129 Mechanism of the Pinnick oxidation

When aldehyde **163** was subjected to the mixture of Pinnick reagents at room temperature, gradual conversion into the ensuing *seco*-acid **164** occurred in excellent yield (96%) as shown in **Scheme 130**. The reaction often stalled and additional oxidant was needed before all starting material was consumed. An important caveat to mention is that more 2-methyl-2-butene must also be added before further portions of $NaClO_2$ to prevent the formation of byproducts. As was the case with the aldehyde formation step, the H_2–H_5 proton signals were seen to diminish if this protocol was not followed.

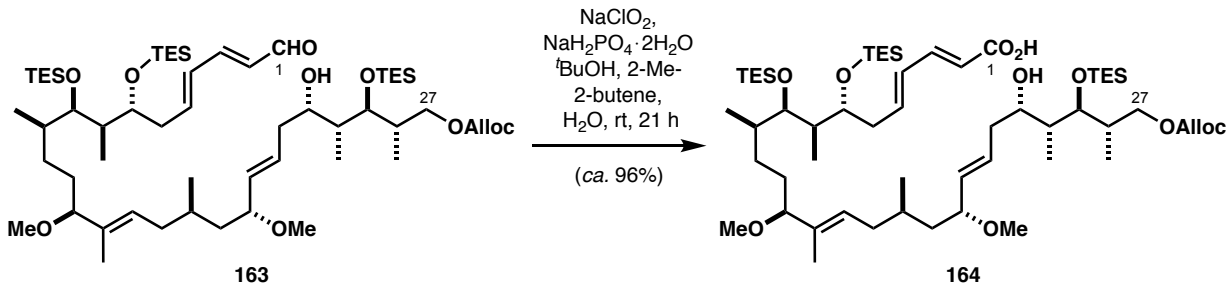

Scheme 130 Pinnick oxidation of dienal **163** to produce *seco*-acid **164**

While it may seem convenient to attribute the changes in the diene to the reactive nature of the HOCl byproduct, there are other more electron-rich olefins present, which should in theory attack HOCl preferentially, though they seemingly remained unaffected (as judged bt ^{1}H NMR analysis). The *seco*-acid **164** was generally found to be suitably pure after a simple aqueous work up and could be used in the macrolactonisation without further purification. Due to the high solubility of the carboxylic acid in the aqueous phase it proved tricky to fully wash out the residual ^{t}BuOH. Column chromatography enabled clean separation of any unwanted residues and byproducts, though this incurred some loss of material, which is likely a consequence of the polar acid being partially retained on the silica.

4.2. Macrolactonisation and Formal Second-Generation Total Synthesis

With the required *seco*-acid **164** in hand, the pivotal site-specific macrolactonisation could be attempted. There is still a lack of extensive methodological studies investigating the optimal conditions to apply to a particular substrate due to precious nature of the intermediates which are usually subjected to macrocyclisation.[228] The initial method of choice here was the Yamaguchi protocol as this previously gave the best result in forming the C_1–C_{27} macrocycle **121** (**Section 2.3.3.**).

Substrate **164** was first activated at the carboxylic acid through formation of a mixed anhydride with superstoichiometric 2,4,6-trichlorobenzoyl chloride (TCBC, 10 eq.) and Et_3N (20 eq.) in THF in the absence of light (**Scheme 131**). The latter was a precautionary measure to minimise further disappearance of the H_2–H_5 protons in the delicate dienoate. The resulting anhydride **269** was diluted with PhMe and added to a solution of DMAP in PhMe. By keeping the addition rate low and dilution high, the risk of unproductive oligomerisation occurring instead of intramolecular attack was kept at a minimum.

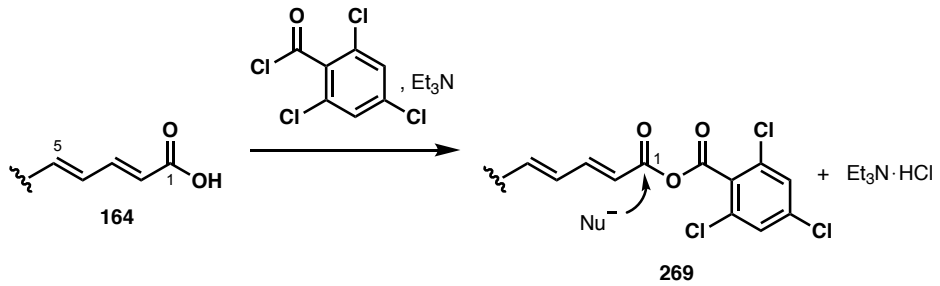

Scheme 131 Activation of the C_1 carbonyl towards nucleophilic attack through the mixed anhydride **269**

Beside the expected macrolactone **165**, several unidentified byproducts were isolated from the crude mixture. Their predominant distinguishing features by ^{1}H NMR were substantial loss of the H_2–H_5, H_7 and H_9 protons. In addition, some of the mass balance was thought to consist of unwanted oligomeric species. This conclusion is based on the characteristic shift of the C_{23} hydroxyl to the ester methine region in the ^{1}H NMR whereas other peaks, particularly in the olefinic range, remained aligned with the spectrum of the open-chain *seco*-acid substrate **164**. The lack of more obvious shifts in that region is very much unlike the major spectral changes observed for cyclic product **165**. The loss of H_7 and H_9 signals is more difficult to rationalise, particularly as both TES groups in those positions remained intact. This occurred particularly frequently at temperatures upwards of 50 °C and prolonged reaction times. Gentle heating just above ambient temperature (30 °C) was tolerated but did not greatly improve the outcome, yielding around 40% of product **165** at best.

In an attempt to suppress oligomerisation, for Shiina macrolactonisation[229] using 2-methyl-6-nitrobenzoic anhydride (MNBA, **Figure 34**) to activate the carboxylic acid was tested as an alternative, albeit without much success. Starting material was being consumed but only trace product was detected amongst a complex mixture of byproducts. This was clearly not a satisfying solution either and attention was turned back to improving the Yamaguchi conditions as this had shown initial promise.

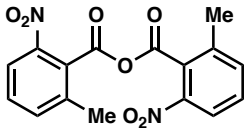

Figure 34 Structure of MNBA

A relevant factor was found to be the purity of *seco*-acid **164**. In most cases, the crude product of Pinnick oxidation appeared sufficiently pure to be carried through the next step. Pleasingly, when the carboxylic acid was purified by column chromatography prior to the Yamaguchi step, the yield increased to 65–70% for the macrolactonisation step alone (**Scheme 132**). In this particular case, addition of the anhydride to

DMAP in PhMe could be performed either fairly rapidly (< 1 h) or over an extended period of time (12 h) and produced a very similar outcome.

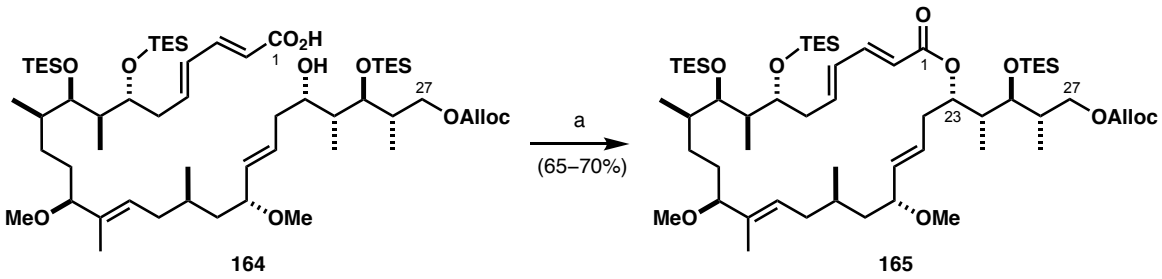

(a) TCBC (20 eq.), Et_3N (40 eq.), THF, rt, 1 h; *then* PhMe, addition into DMAP (60 eq.), PhMe over 12 h; *then* rt, 3 h

Scheme 132 Macrolactonisation of *seco*-acid **164** under Yamaguchi conditions

The very last step towards the known macrocyclic intermediate **159** was the Alloc deprotection at C_{27} with a source of Pd(0). Mechanistically, this proceeds *via* a oxidative addition of Pd(0) into the allylic carbonate to form a Pd(II) π-allyl complex (**Scheme 133**). In the process, the carbonate anion is liberated and can undergo spontaneous decarboxylation to reveal the primary alcohol. Pd(II) can be reduced by the attack of dimedone on the π-allyl species, which regenerates Pd(0) and closes the catalytic cycle.

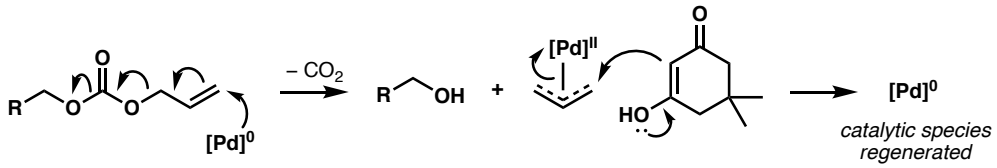

Scheme 133 Mechanism for Pd(0)-catalysed Alloc deprotection

Protected macrolactone **165** was treated with catalytic tetrakis(triphenylphosphine)-palladium(0) ($Pd(PPh_3)_4$) in THF in the absence of light and with dimedone as the allyl scavenger (**Scheme 134**). The reaction was complete after stirring at room temperature for 1 h and alcohol **159** was isolated in excellent yield (99%). Gratifyingly, NMR spectra of **159** were in complete agreement with those previously reported.[108] This achievement marks the finish line of the second-generation formal total synthesis of the aplyronines by meeting one of the key goals set out at the beginning of this work.

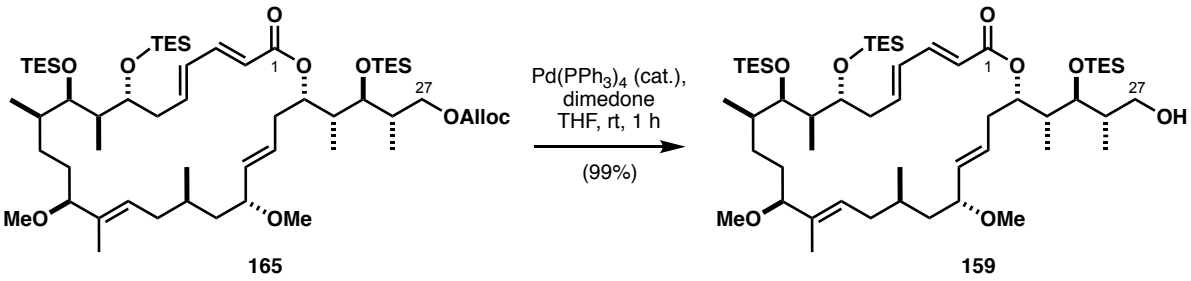

Scheme 134 C_{27} Alloc deprotection of macrolactone **165** with catalytic Pd(0)

4.3. Summary

Chapter 4 concludes the final, most challenging part of the campaign towards a sustainable supply of the aplyronine macrocycle. The strategic features of the revised strategy introduced new hurdles to overcome and while not every step could be perfected in the given time frame, none of the difficulties proved to be unsurmountable.

The Paterson strategy for the assembly of the C_1–C_{27} backbone once again served well to unite two complex fragments in an excellent yield and selectivity, thereby paving the way towards the planned endgame (**Scheme 135**). Several late-stage intermediates containing the C_1–C_5 dienal were unexpectedly delicate and it was difficult to ascertain the underlying reasons for this. Perhaps the most pleasant surprise during this study was the largely dormant behaviour of the Alloc protecting group, which had been introduced with much scepticism as there are very limited examples of its use in a multi-step synthesis of a complex natural product. The only unexpected difficulty pertaining to this decision was observed in the C_{13} methyl ether formation, a generally trivial transformation.

After significant efforts to synthesise the *seco*-acid **164** for the site-specific macrolactonisation and the orthogonal unmasking of the C_{27} position, these reaction indeed proceeded as planned. The first-generation route was hence intercepted at intermediate **159**, thereby eliminating several time-consuming steps after macrocycle closure. Following the new sequence, alcohol **159** was prepared in 21 steps and 6% yield from (*S*)-ethyl ketone **170**.

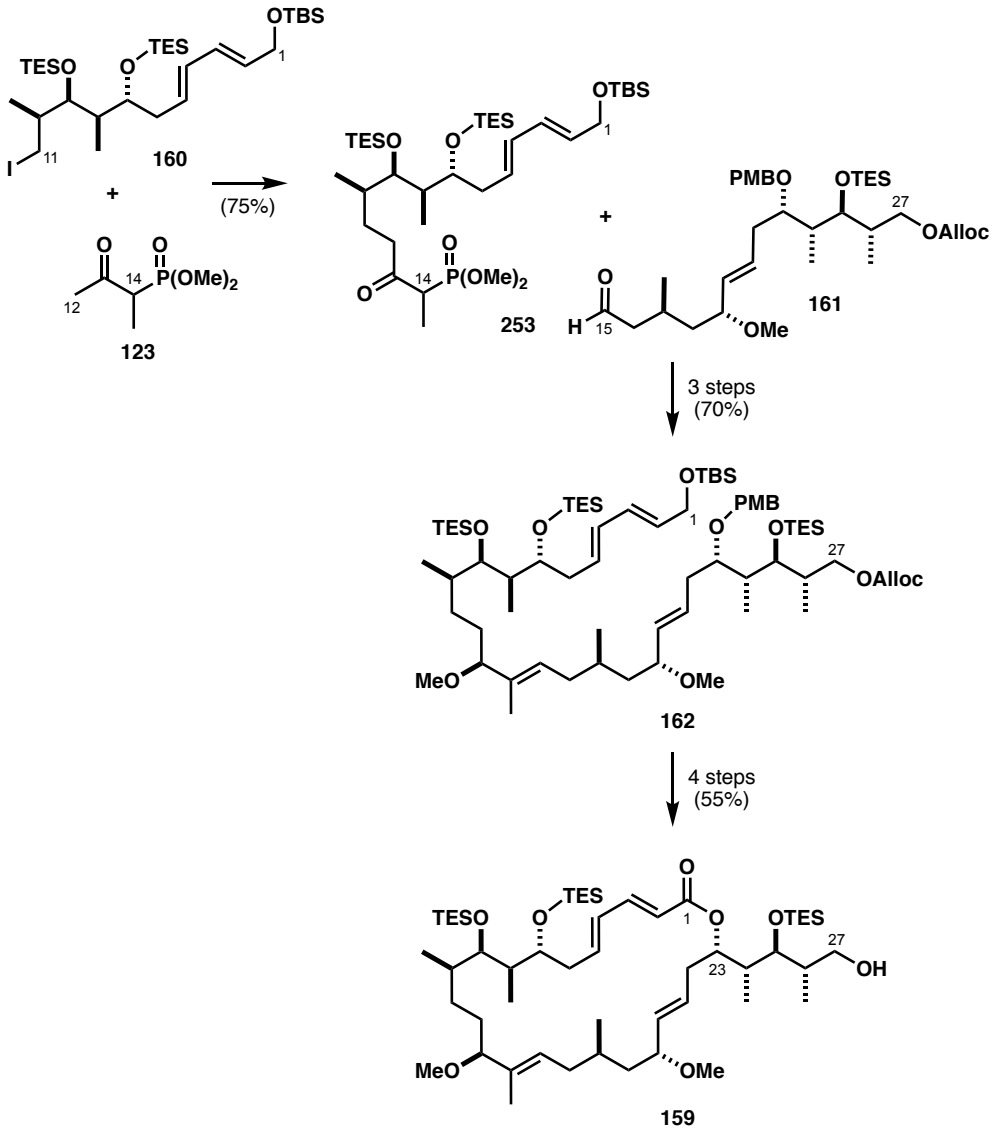

Scheme 135 Summary of the fragment coupling and steps towards the C_1–C_{27} macrocycle **159**

Chapter 5

Results and Discussion – Part III

C_{28}–C_{34} Side Chain Synthesis and Linkage to the Macrocycle

5.1. Synthesis of C_{28}–C_{34} Side Chain 118

5.1.1. Retrosynthesis

Synthesis of the third-generation ketone coupling partner **118** had been devised by Fink (as presented in **Section 2.3.4**). In the process of replenishing stocks of **118** for the purposes of the aplyronine campaign, the 1,3-*syn*-3,4-*syn* C_{29}–C_{32} stereotetrad was constructed by utilising titanium aldol reaction as the only deviation from the original sequence. This alteration was inspired by the success of this methodology in the earlier stages of this project (as seen in **Section 3.3.3.**). The carbon atom bearing the *N*-vinylformamide functionality was appended under modified Wittig conditions, followed by isomerisation to the (*E*)-olefin.

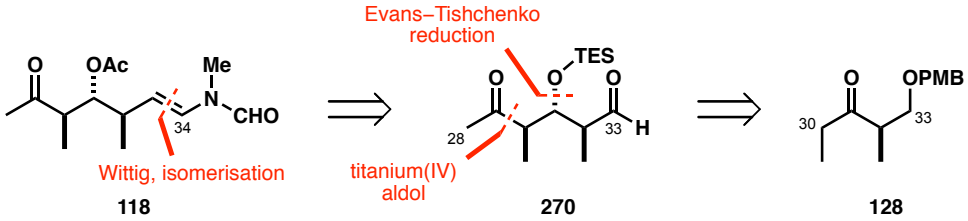

Scheme 136 Retrosynthetic analysis of the C_{28}–C_{34} ketone **118**

5.1.2. Preparation of the *N*-Vinylformamide from PMB Ether 274

Side chain scale-up, undertaken by the author, commenced from stocks of material which had been kindly provided by another Paterson group member working on the aplyronine project, Talia Pettigrew. For completeness, her contribution is summarised below.

Chiral ketone **128** was prepared *via* the familiar sequence (seen in **Section 3.3.2.**), this time starting from the (*R*)- enantiomer of commercially available Roche ester **126** (**Scheme 137**). The hydroxyl was protected with PMBTCA and catalytic acid (PPTS) before the ester functionality was converted into the corresponding Weinreb amide with *N*,*O*-dimethylhydroxylamine hydrochloride and ^{i}PrMgCl. Carefully controlled single addition of ethylmagnesium bromide to amide **272** afforded ethyl ketone **128** in 72% yield over three steps, ready for the following aldol condensation.

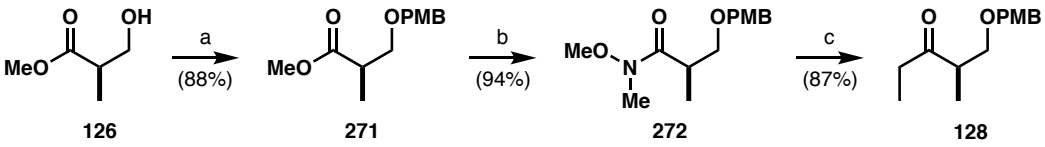

(a) PMBTCA, PPTS (cat.), CH_2Cl_2, 0 °C → rt, 16 h; (b) MeNH(OMe)·HCl, ^{i}PrMgCl, THF, –30 °C → –15 °C, 3.5 h; (c) EtMgBr, THF, –5 °C, 1.5 h

Scheme 137 Synthesis of the (*R*)-Roche ester ethyl ketone **128** by Pettigrew

The pre-existing stereocentre on ketone **128** exerted good levels of enantioselectivity in the aldol reaction with excess acetaldehyde in presence of (^{i}PrO)$TiCl_3$ Lewis acid, forging β-hydroxyketone **149** with an all-*syn* stereotriad in an isolated yield of 85% yield and 11:1 *dr*. As expected, the electron-rich PMB group aids the stereoinduction by imposing a chelated transition state (**TS 9**), facilitated by the oxophilic titanium centre (**Scheme 138**). This reaction represents further exploration of the titanium aldol methodology as part of the aplyronine project and has now superseded Fink's original protocol with $Sn(OTf)_2$ as the preferred method for constructing the C_{29}–C_{30} bond. Pettigrew noted that under optimal conditions, *dr* values up to 15:1 can be obtained.

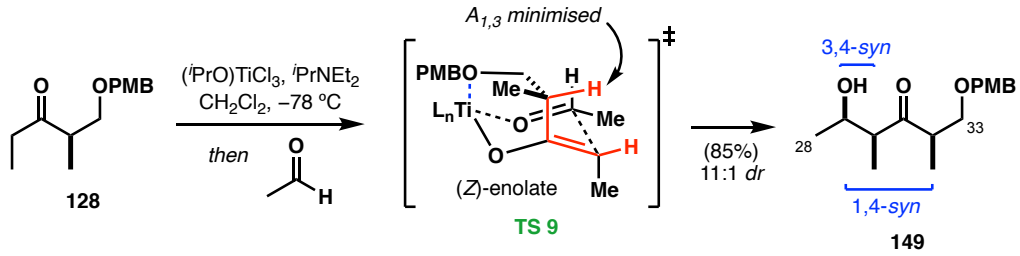

Scheme 138 Pettigrew's titanium aldol to form the C_{28}–C_{33} β-hydroxyketone **149**

Reduction of the remaining C_{31} carbonyl occurred smoothly under the Evans–Tishchenko conditions (**Scheme 139**), relaying the stereochemical information from the existing C_{29} hydroxyl to forge a 1,3-*anti* motif in **273** with excellent control (96%, >20:1 *dr*). Finally, differential protection of the C_{31} secondary alcohol as TES ether was achieved with TESOTf and 2,6-lutidine to provide **274** in 94% yield.

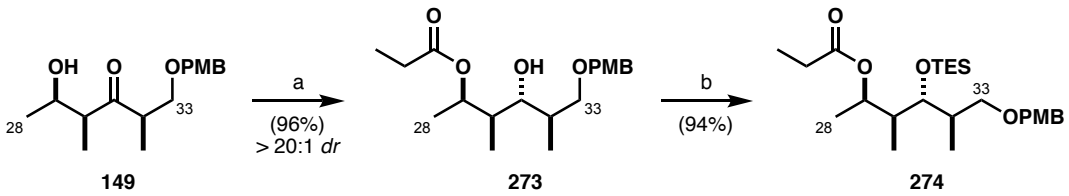

(a) SmI_2 (10 mol%), EtCHO (6 eq.), THF, –20 ºC, 1 h; (b) TESOTf, 2,6-lut., CH_2Cl_2, –78 ºC, 1.5 h

Scheme 139 Elaboration of the aldol adduct **149** to the PMB ether **274**

Synthetic efforts described hereupon had been undertaken solely by the author. The PMB ether was oxidatively cleaved with DDQ in CH_2Cl_2/pH 7 buffer (4:1) biphasic solvent mixture as indicated in **Scheme 140**. Careful purification by column chromatography in toluene/EtOAc enabled removal of any remaining minor isomers from the aldol and Evans–Tishchenko reactions as insufficient polarity difference rendered them inseparable in the previous stages. Diastereomerically pure alcohol **275** was isolated in 92% yield and was reacted further with DIBALH to rapidly cleave the residual propionate ester and provide diol **151** (94%).

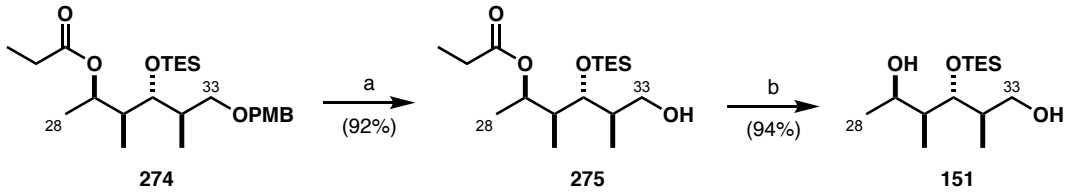

(a) DDQ, CH_2Cl_2/pH 7 buffer (4:1), 0 ºC → rt, 75 min; (b) DIBALH, CH_2Cl_2 –78 ºC, 2.5 h

Scheme 140 Sequential deprotection of the C_{29} and C_{33} hydroxyls

Adjusting the C_{29} oxidation level could be carried out in the same step as converting the C_{33} terminus into the aldehyde, ready for a Wittig reaction to append the delicate *N*-vinylformamide. Kinetically, oxidation of C_{33} is likely to be more rapid, which would leave the newly formed carbonyl susceptible to the attack of the C_{29} hydroxyl and formation of a cyclic byproduct **276** (**Scheme 141**).

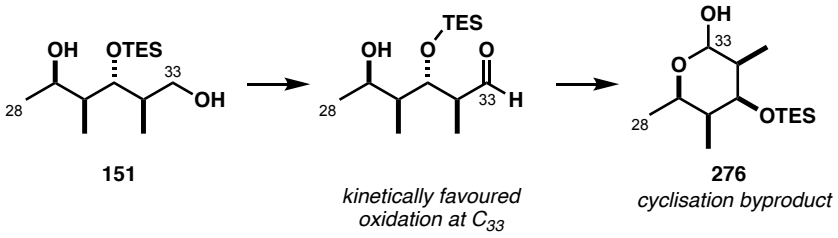

Scheme 141 Formation of a cyclic byproduct as a result of kinetically favoured oxidation of the C_{33} alcohol

The method which can circumvent this issue by virtue of its mechanism is Swern oxidation (**Scheme 142**). Addition of the triethylamine base, which triggers the carbonyl formation, is done only after both alcohols had been activated as the alkoxysulfonium salt and can no longer act as nucleophiles at the

oxygen atom. The sensitive keto aldehyde **277** was formed with no detectable epimerisation of the α-stereocentres (**Scheme 143**) and to prevent this occurring during chromatography on silica, crude material was used in the next step without further purification.

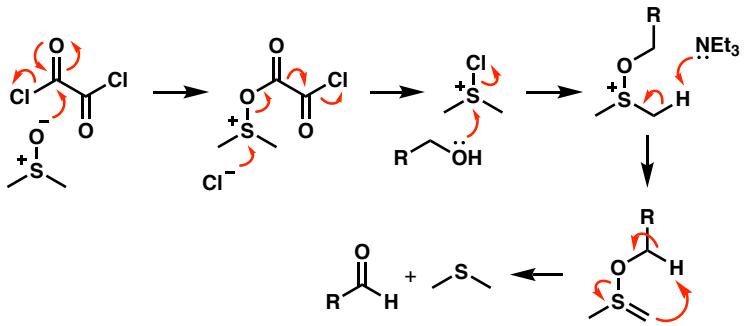

Scheme 142 Proposed mechanism of the Swern oxidation

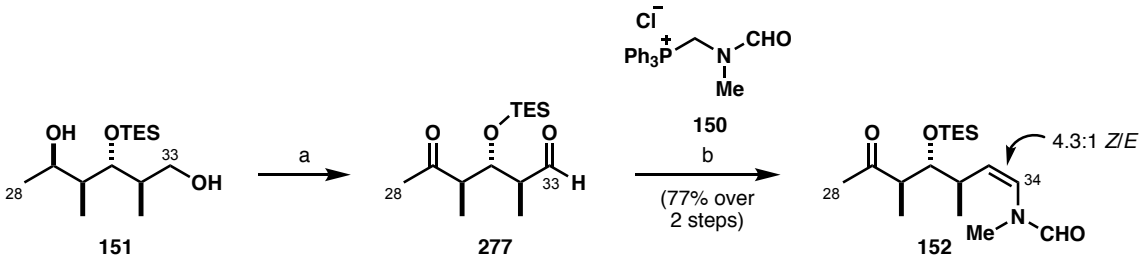

(a) $(COCl)_2$, DMSO, CH_2Cl_2, –78 °C, 15 min, *then* **151**, 15 min, *then* Et_3N, 1 h; (b) LiHMDS, **150**, THF, –78 °C → 0 °C, 45 min, *then* **277**, –78 °C, 1.5 h

Scheme 143 Double Swern oxidation of diol **151** and modified Wittig reaction to install the (*Z*)-vinylformamide

The C_{33}–C_{34} double bond was forged following a modified Wittig protocol developed in the Paterson group in the earlier stages of the aplyronine project[173] and used with great success in a previous synthesis of the reidispongiolide A side chain containing this exact functionality.[230,231] Phosphonium salt **150** (prepared in two steps from *N*-methylformamide and paraformaldehyde by Pettigrew) was deprotonated with lithium hexamethyldisilazane (LiHMDS) to form the corresponding ylid and reacted at the more electrophilic aldehyde terminus of **277**. *N*-Vinylformamide **152** was isolated as a 4.3:1 mixture of *Z*/*E* isomers in 70% yield over two steps on more than 1.5 g of crude aldehyde.

Next, TES ether **152** was first treated with AcOH-buffered TBAF to reveal the secondary alcohol under neutral conditions (**Scheme 144**), followed by acetylation with acetic anhydride, triethylamine and catalytic DMAP. Minimising acetate loss *via* E_1cb was achieved by strictly keeping the reaction temperature below 0 °C and only a small amount (< 5%) of enone elimination byproduct was observed even after purification on silica. Regardless, the crude acetate **279** was typically subjected to the isomerisation without the need for chromatography beforehand.

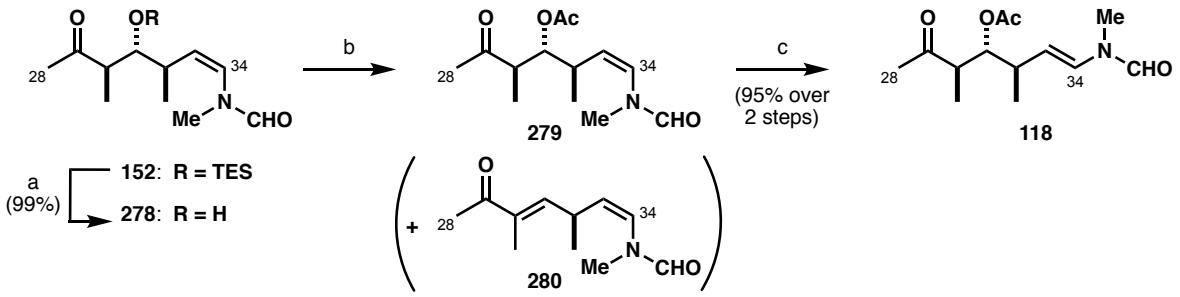

(a) TBAF/AcOH (1:1), THF, 0 °C, 4 h; (b) Ac_2O, Et_3N, DMAP (cat.), 0 °C, 1 h; (c) I_2, CH_2Cl_2 (dark), 22 h

Scheme 144 Deprotection/acetylation sequence on the C_{31} hydroxyl and isomerisation of the *N*-vinylformamide

Finally, the *Z*/*E* olefin mixture at the *N*-vinylformamide **279** was fully converted into the thermodynamically favoured (*E*)-isomer with molecular iodine in CH_2Cl_2. In the absence of light, the reaction is thought to proceed *via* an ionic mechanism (**Scheme 145**). Theoretically, iodine should only be required in catalytic quantities as it is regenerated in the final elimination step. However, in order to obtain satisfactory reaction rates, a stoichiometric amount was added instead. Williams also observed that the success of the isomerisation is dependant upon the concentration of substrate. The C_{28}–C_{34} side chain **118** was thus isolated in excellent yield (95%) over two steps from alcohol **278**.

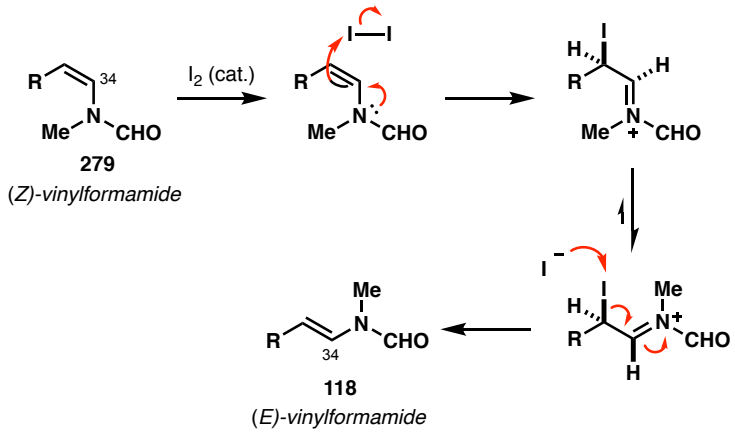

Scheme 145 Iodine-mediated ionic mechanism for the (*Z*)- to (*E*)- isomerisation of the vinylformamide

In summary, nearly 1 g of ketone **118** was prepared in seven steps and 63% yield from the stocks of intermediate **274**, confirming once again that Fink had devised a reliable route to the aplyronine side chain.

5.2. Boron Aldol Coupling to the C_1–C_{27} Macrocyclic Aldehyde 120

With a replenished supply of the macrocycle **159** and side chain **118** in hand, the synthesis could be advanced towards the full aplyronine skeleton. A Swern oxidation at C_{27} successfully delivered the C_{27} aldehyde **120** and the risk of epimerisation at the α-stereocentre was mitigated by avoiding aldehyde **120** purification by flash chromatography. Triethylamine hydrochloride salts were removed in the mildly acidic workup and and the crude material was used immediately in the subsequent boron aldol reaction to complete the carbon backbone of the aplyronines.

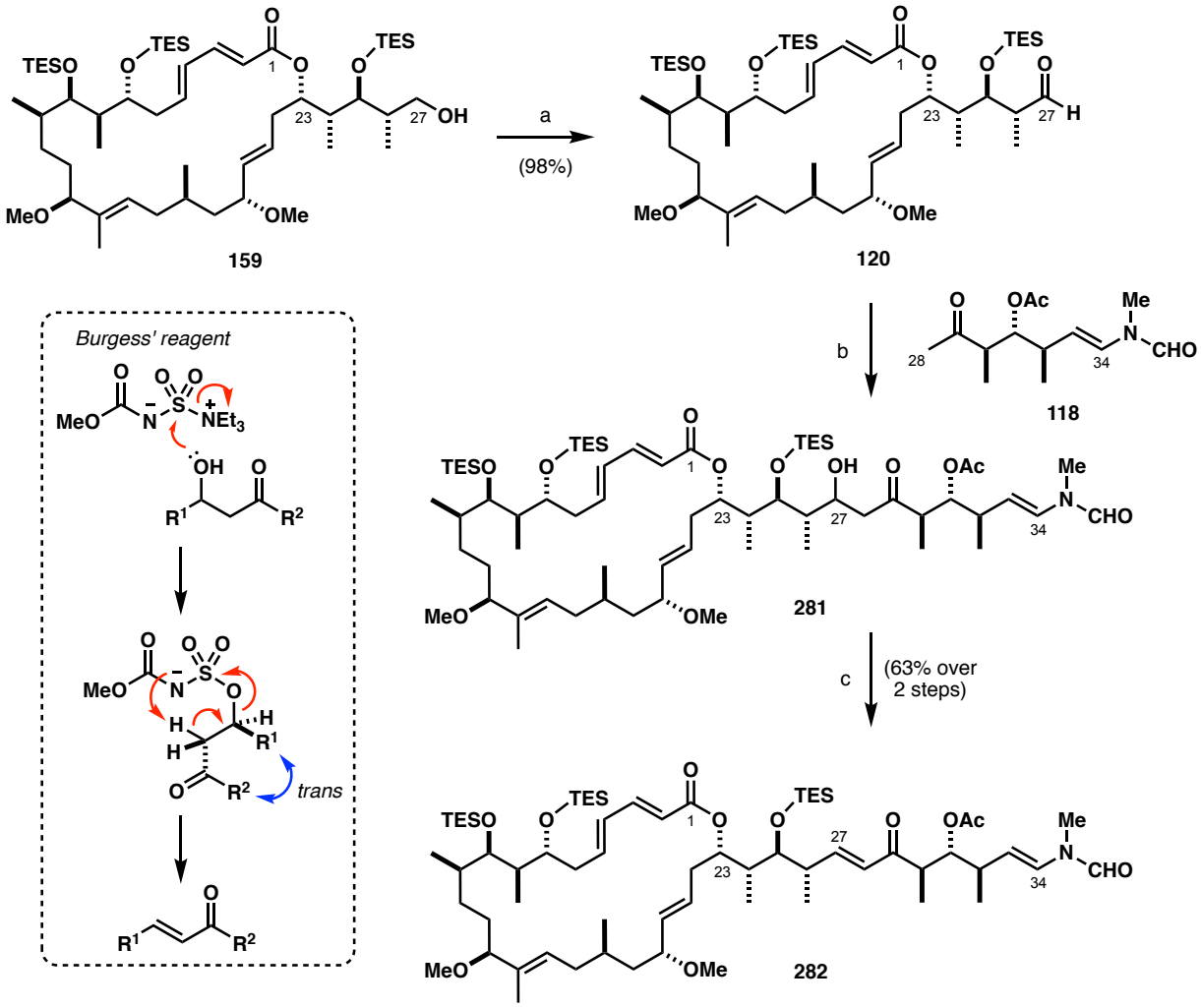

(a) $(COCl)_2$, DMSO, CH_2Cl_2, –78 °C, 30 min, *then* **159**, 30 min, *then* Et_3N, 0 °C → rt, 45 min; (b) **118**, Cy_2BCl, Et_3N, Et_2O, 0 °C, 30 min, *then* **120**, –78 °C, 1 h, *then* –40 °C, 1 h, *then* –10 °C, 1 h; (c) Burgess' reagent, THF, rt, 17 h

Scheme 146 Swern oxidation of the macrocyclic alcohol **159** and side chain attachment through aldol reaction of **118** and **120**

The less precious side chain **118**, relatively speaking, is used in excess to ensure complete consumption of the valuable aldehyde **120**. Ketone **118** was enolised with Cy_2BCl Lewis acid and Et_3N at 0 °C, making

every effort to rigorously exclude moisture. After addition of aldehyde **120** at −78 °C, the reaction was gradually warmed up to −40 °C then −10 °C over 2 h until complete. No substantial byproducts were observed in the crude ^{1}H NMR and the aldehyde was consumed entirely within a relatively short reaction time. The typical boron-mediated aldol oxidative workup with hydrogen peroxide[232] was avoided due to the potentially sensitive nature of this advanced fragment and was replaced by MeOH/pH 7 buffer.

At this stage, excess unreacted side chain **118** was carried forward as a mixture with the aldol adduct **281** as chromatographic separation proved to be very difficult. Dehydration to the enone **282** was achieved by using Burgess' reagent[174] (*N*-(triethylammoniumsulfonyl)carbamate), avoiding the risk of elimination of the delicate C_{31} acetate. This reaction proceeds *via* an initial attack of the C_{27} hydroxyl on the electrophilic sulfur which enables an intramolecular *syn* elimination *via* a 6-membered transition state as illustrated in **Scheme 146**. Use of fresh reagent was crucial in order to reach full conversion, though unreacted material can be easily resubjected if the reaction stalls.

5.3. Summary

The Paterson second-generation route to the known macrocyclic alcohol **159** constitutes a total of 53 steps and 20 steps in the longest linear sequence (**Scheme 147**). The cornerstone of fragment assembly remained the efficient $Ba(OH)_2$-mediated olefination to forge the C_{14}–C_{15} and C_{20}–C_{21} (*E*)-olefins and the stereotetrads were constructed in a series of highly stereocontrolled aldol reaction, followed by 1,3-*anti* reductions, showcasing the impressive selectivity of these transformations.

The most pivotal strategic revision was the alteration of the overall protecting group strategy to accommodate the planned site-specific macrocyclisation. To facilitate this goal, the synthesis of the C_{21}–C_{27} **168** was revisited to introduce the necessary orthogonal protecting groups as well as produce a more scalable and robust synthesis of the C_{23}–C_{26} stereotetrad. Replacing the capricious $Sn(OTf)_2$ aldol methodology with a titanium variant produced excellent results and is one of the most impactful improvements in this project. A similarly fruitful venture was the investigation into the synthesis of chiral acid **137** from achiral starting materials. Pig liver esterase-mediated desymmetrisation has been established as the protocol of choice to reliably afford the C_{15}–C_{20} phosphonate fragment **167** in more than 95% *ee* of the isolated (17*R*) methyl stereocentre with high material throughput. Adjustments of silyl groups in the C_{15}–C_{27} region were introduced stepwise with great caution, though some of the initial reservations regarding their stability transpired to be unnecessary. Overall, the C_{15}–C_{27} aldehyde **161** was prepared in a total of 20 steps (14 steps LLS). As every step of the sequence was carried out on multi-grams of substrate, the route can be relied upon to deliver the necessary quantities of material for a substantial scale-up of the macrocycle.

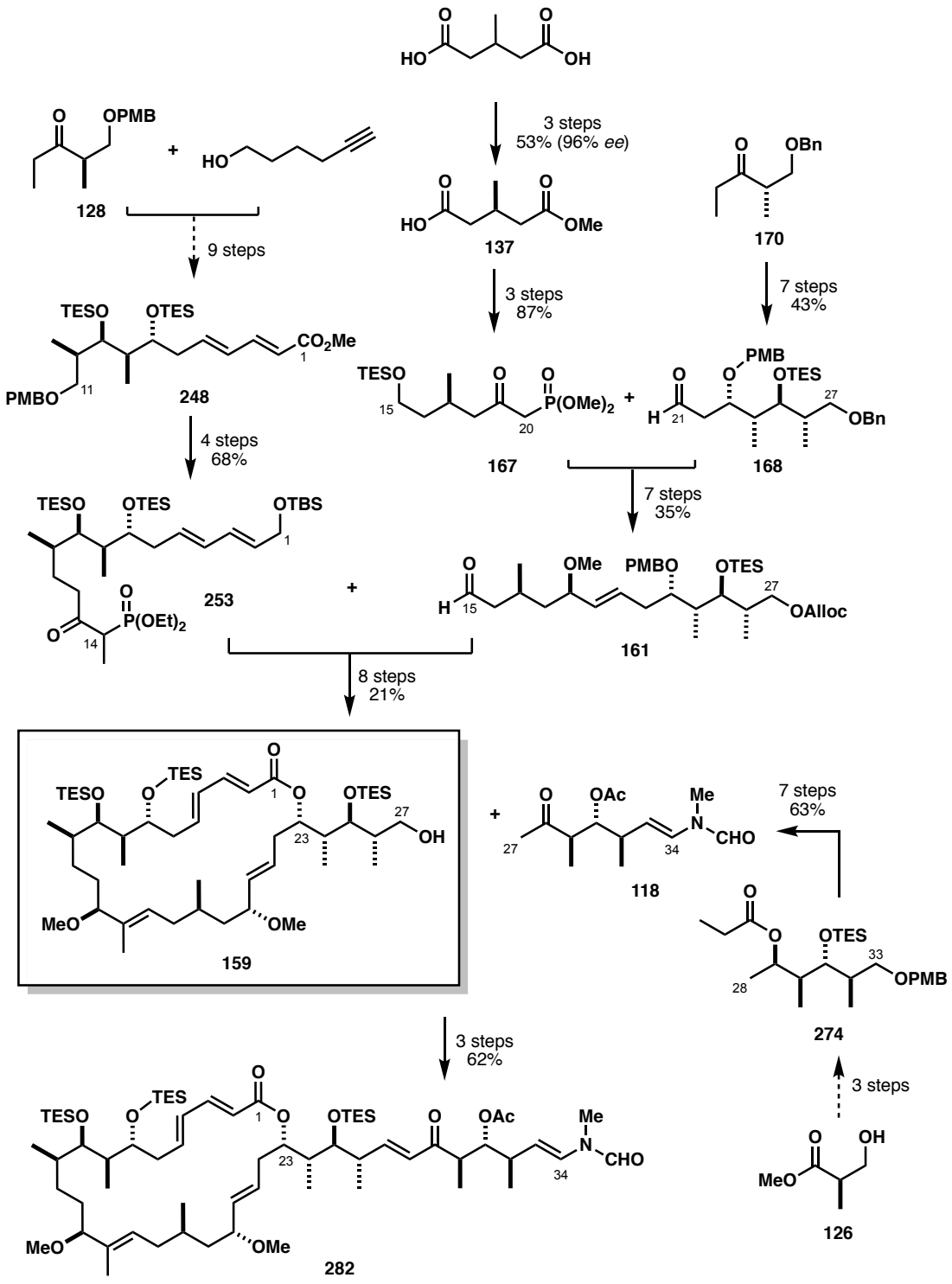

Scheme 147 Summary of the second-generation synthesis of the aplyronines

The C_1–C_{11} part of the macrocyclic skeleton was aligned with the new protecting group strategy to place a *bis*-TES moiety on the 1,3-*anti* diol early on. Alkylation at C_{11} to form the β-ketophosphonate **253** remained somewhat of a bottleneck as brief optimisation studies did not yield the desired increase in regioselectivity for that step. Nevertheless, union of the northern and southern fragments assembled the C_1–C_{27} framework with great efficiency (96%) and paved the way towards the advanced intermediates. In the later stages, the concise one-step allylic TBS oxidation/PMB deprotection, site-specific macrolide formation and palladium-catalysed Alloc deprotection replaced a rather laborious sequence of protecting group manipulations. This had been one of the major goals set out at the beginning and it was pleasing to see that the adventurous plan lead to a reduced overall step count.

Finally, stocks of the C_{28}–C_{34} ketone **118** were also replenished for the purposes of late-stage intermediate scale-up. The troublesome tin aldol step to construct the C_{29}–C_{32} stereotetrad has now been superseded, which has improved the scalability of the otherwise efficient route. Shortly after coupling of the macrocycle **120** to the side chain **118**, studies by the author were concluded.

5.4. Future Work

Notionally, this project was devised to address the issues in the original Paterson synthesis of the aplyronine core and to start afresh with the existing experience as a guideline. While many improvements have been made, there remains several steps which could be further optimised. The most pressing matters to be examined in the future endeavours are summarised below.

5.4.1. Improvements to the C_1–C_{27} Macrocycle Synthesis

The route towards the C_1–C_{14} northern fragment **253** has been highly optimised at all stages except for the alkylation of iodide **160**. In the event, at least 25% of material half way through the LLS of the aplyronine synthesis is lost in a single operation on a medium scale (a few hundred mg). This remains a highly frustrating bottleneck and stems from the lack of understanding of the nature of the dianion in solution with regards to the complex electrophile. Experiments carried out in different ethereal solvents (Et_2O, TBME, DME) gave a preliminary indication that perhaps the phosphonate solvation plays a key role in the reactivity profile. There is scope to probethis hypothesis further, including using additives to de-aggregate the species other than HMPA such as DMPU or tetraalkylureas.

The peculiar loss of proton signals observed at a late stage in the synthesis prior to forming the macrolactone must be further investigated before the precious late-stage material is brought to a point where these issues seem to appear. By considering the case of the C_1–C_{11} iodide **160**, where storage even

at low temperatures over prolonged time periods causes degradation, the suspected problematic intermediates could be put to the test by altering either storage conditions or rigorously excluding light when carrying out the DDQ allylic TBS oxidation/PMB removal or the Pinnick oxidation of **162** and **163**, respectively. With the supply of material in excess of 2 g currently stored at the methyl ether **162** stage, approximately 1 g of the macrocycle should still be accessible if the reactions are carefully performed on small scale even before further optimisation is undertaken.

The macrocyclisation of **164** has not yet been explored in great detail. Blakey and Lee found the Yamaguchi–Yonemitsu and Keck macrolactonisation procedures to be inferior in comparison to the Yamaguchi and Shiina variant. That being said, due to the unique behaviour of each cyclisation substrate, results and speculations based on merely structurally similar examples should not be taken as conclusive. This is especially relevant for examples where particular protecting groups assert major conformational bias of the compound in solution. The extensive choice of esterification methodology available nowadays which has been applied to macrolacronisations in particular[233] provides plenty of scope to experiment beyond the select few fallback options.

The Yamaguchi protocol could be altered by variation of solvent (e.g. $CHCl_3$ or THF) as well as higher temperatures at reduced reaction times to prevent substrate degradation upon heating. On the other hand, use of the highly basic DMAP, especially in large excess, is one of the main drawbacks of the Yamaguchi procedure as it has been shown to sometimes lead to isomerisation of double bonds out of conjugation at the mixed anhydride stage (**Scheme 148**). This occurrence has not been confirmed for *seco*-acid **164** specifically but closer inspection of the residues isolated from column chromatography may indicate whether this is a potentially problematic event. Such isomerisations were observed by Evans during the synthesis of oasomycin A[234] and addition of $^{i}PrNEt_2$ to the macrolactonisation substrate was vital to the successful ring formation when treating with TCBC.

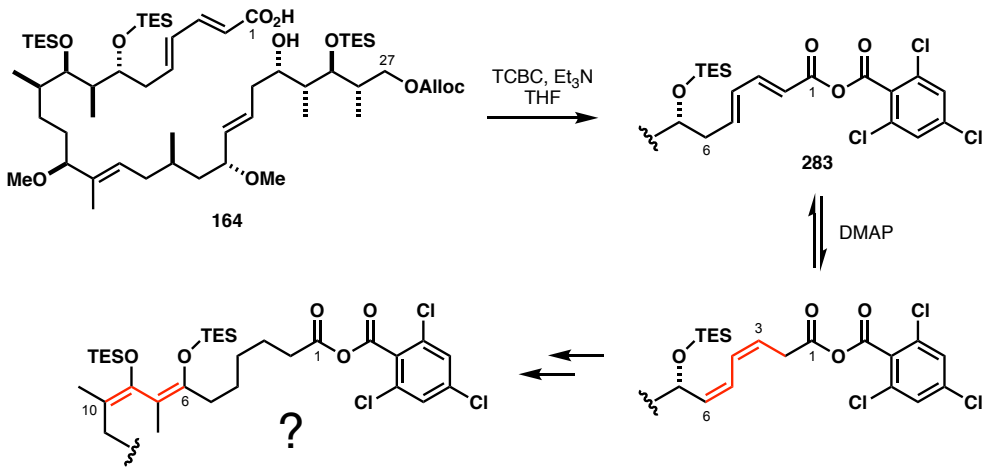

Scheme 148 Speculative deconjugation of the C_2–C_5 diene after formation of the mixed anhydride **283**

5.4.2. Synthesis of Linker-Modified Derivatives for ADC Development

Williams had devised a route towards the enantiopure isomers of *N*,*N*,*O*-trimethylserine but did not manage to prepare any natural aplyronine congeners with each of them attached. These highly interesting targets for biological testing should be accessible with further stocks of aplyronine C prepared by the established endgame following a scale-up of the macrocycle **159**. Each of the diastereomers is expected to have a unique biological profile due to subtle differences in the key pharmacophore on the northern portion of the macrocycle with regards to tubulin binding, which has to date not been fully elucidated. It is likely that one of the serine enantiomers forms stronger interactions than the other and the observed binding affinity is the average of the two as the natural material was collected as a scalemic mixture. If this theory is proven correct, there may be scope to increase potency by simply appending enantiopure amino acids at C_7. Williams has already demonstrated that under Yonemitsu conditions, no racemisation of the stereocentre is seen in reaction with a linker-modified alcohol **284** (**Scheme 149**), hence it is predicted that this would not occur upon reaction with any structurally similar intermediates either.

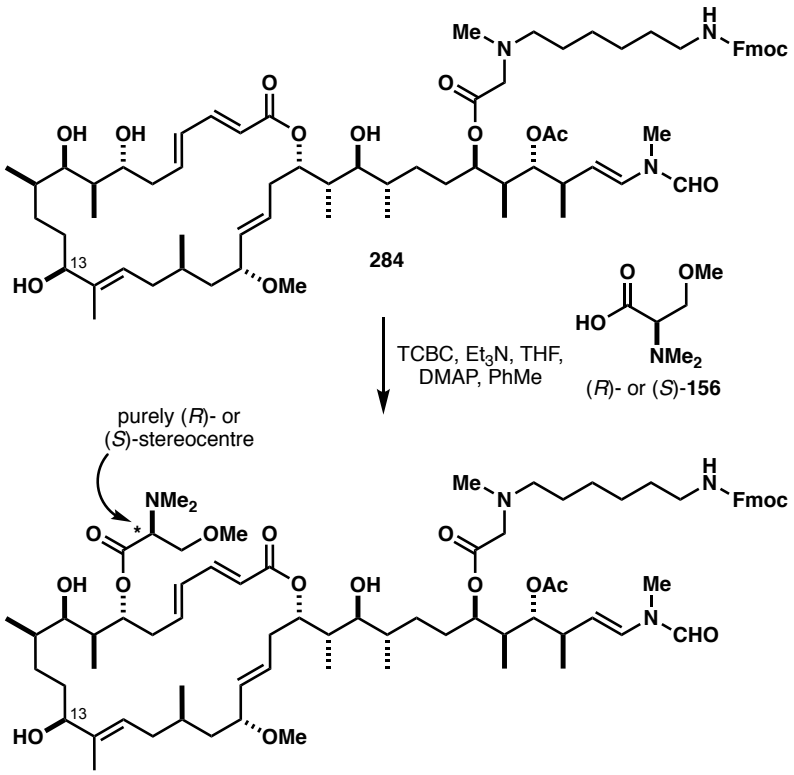

Scheme 149 Williams' esterification studies with enantiopure (*R*)- or (*S*)-*N*,*N*,*O*-trimethylserine **156**

In the context of the aplyronines as ADC payloads, the pendant amino acids may be compatible with the recent linkage technology developed by Genentech (**Scheme 150**).[235] Starting with a commercially available valine-citrulline linker **285** with a maleimide handle and a PABC spacer, the benzylic alcohol is converted the chloride, then reacted with a tertiary amine on the payload to form a quaternary ammonium

linkage by an S_N2 displacement of the halide (**286**). Conjugation through a cysteine on the mAb affords the ADC in a highly efficient three-step sequence without the use of protecting groups. Release of the toxin is triggered by the action of lysosome proteases to cleave the linker peptide bond, followed by a traceless elimination of the spacer. Genentech have achieved successful preparation of ADCs with a variety of tertiary amine-containing drugs as warheads and an additional disulfide-based linker which operates by the same basic principle.

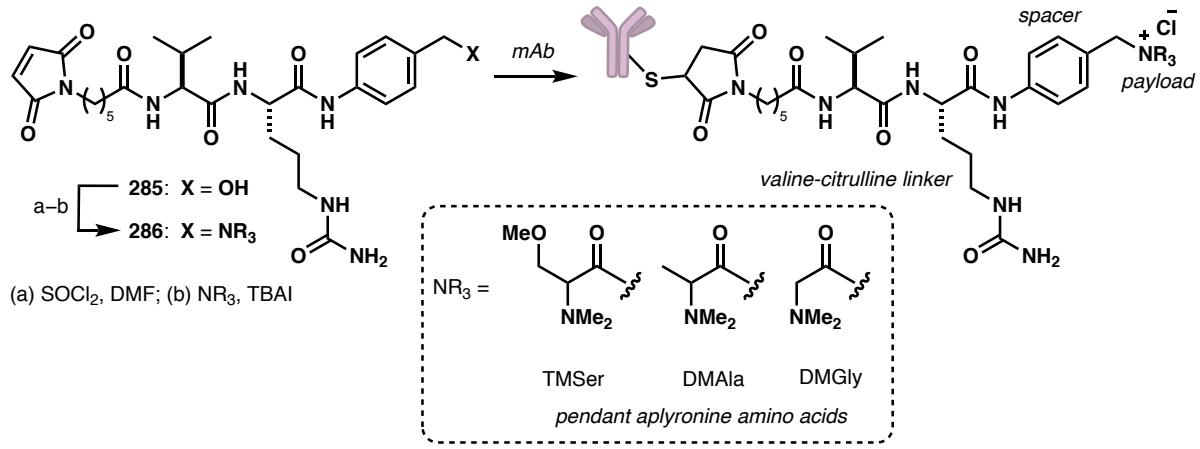

Scheme 150 Application of Genentech's quaternary ammonium linkage technology in the context of aplyronines as ADC payloads

The major advantage of this technology is the formation of charged species, which decreases the risk of ADC aggregation as well as freeing the drug without any remnants of the linker which could impede target binding. The latter is especially relevant for the aplyronines when binding to two large biomolecules (actin and tubulin) at the same time. As the amino acids in aplyronines are appended late-stage and have a profound effect of binding, a number of ADC variations could easily be prepared from a late-stage precursor.

The future goal of combining the apylronines with ADCs to develop anticancer agents which are highly specific for cancer cells could lead to a huge breakthrough in modern medicine for the treatment of a variety of different cancers. The development of a scalable synthesis towards these natural products represents one step to this prospect becoming a reality.

Chapter 6

Experimental

6.1. General Prodecures

Except where stated otherwise, all reactions were performed under anhydrous conditions under an atmosphere of argon at room temperature, using oven-dried glassware and standard techniques for handling air-sensitive materials.

Purification of reagents and solvents was carried out by standard means.[§] Benzene (PhH), toluene (PhMe), dichloromethane (CH_2Cl_2) and dimethyl sulfoxide (DMSO) were distilled from calcium hydride (CaH_2) and stored under an atmosphere of argon. THF and Et_2O were distilled from benzophenone ketyl radical / potassium or sodium wire, respectively, and stored under an atmosphere of argon. Solvents used for chromatography and extraction were distilled.

Et_3N, pyridine (pyr), 2,6-lutidine, dimethyl methylphosphonate and diethyl ethylphosphonate were distilled from and stored over CaH_2 under an argon atmosphere. $^{i}Pr_2NEt$ was first distilled from ninhydrin, then from KOH and stored over CaH_2 under an atmosphere of argon. EtOAc, 1,2-dimethoxyethane (DME), crotonaldehyde and methyl vinyl ether were distilled from CaH_2. TCBC, $TiCl_4$ and oxalyl chloride were distilled and stored under an argon atmosphere. Propionaldehyde was distilled from anhydrous $CaCl_2$ and used immediately. AcOH was distilled from chromium trioxide and stored under an atmosphere of argon. 4 Å molecular sieves were activated by heating in a microwave oven and dried under vacuum. DDQ was recrystallised from distilled $CHCl_3$. Proton-Sponge® was recrystallized from MeOH. Anhydrous barium hydroxide ($Ba(OH)_2$) was generated by drying barium hydroxide

[§] W.L.F. Armarego and D.D. Perrin, *Purification of Laboratory Chemicals*, 4th edition, Butterworth-Heinemann, **1996**

octahydrate ($Ba(OH)_2 \cdot 8H_2O$) at 130 ºC under vacuum overnight and stored in the glove box. Unless stated otherwise, all other chemicals were used as received.

Solutions of ammonium chloride (NH_4Cl), sodium hydrogencarbonate ($NaHCO_3$), sodium/potassium (Na^+/K^+) tartrate, brine (NaCl) and sodium thiosulfate ($Na_2S_2O_3$) were saturated and aqueous. Buffer solutions were prepared from stock tablets as directed.

Flash column chromatography was conducted on Merck Kieselgel 60 (230–400 mesh) silica gel under a positive pressure. Preparative thin layer chromatography was carried out using Merck Kieselgel 60 F254 plates. All solvent mixtures are reported as volume ratios.

6.2. Analytical Procedures

Analytical thin layer chromatography (TLC) was carried out on Merck Kieselgel 60 F254 plates, coated with 0.25 mm of silica gel, using phosphomolybdic acid/cerium (IV) sulphate dip, potassium permanganate dip, bromocresol green dip and/or ultraviolet light (254 nm) for visualisation.

Spectra were recorded on the following machines: Bruker Avance 500 BB (500 MHz) and Bruker Avance TCI Cryoprobe (500 MHz) and Bruker Avance DRX 400 (400 MHz).

^{1}H nuclear magnetic resonance (NMR) spectra were recorded at ambient probe temperature (298 K) using an internal deuterium lock for $CDCl_3$ (δ_H = 7.26 ppm). ^{1}H NMR data are presented as: chemical shift (in ppm, δ scale relative to tetramethylsilane, δ_{TMS} = 0 ppm), integration, multiplicity (s = singlet, d = doublet, t = triplet, q = quartet, quin = quintet, sext = sextet, m = multiplet, br = broad, obs = obscured), coupling constants (*J* in Hz). Assignments of protons were based on unambiguous chemical shifts and coupling patterns with the aid of 2D spectra, and by analogy to fully interpreted spectra for structurally related compounds. Proton-decoupled ^{13}C NMR spectra were recorded at at ambient probe temperature (298 K) and an internal deuterium lock for $CDCl_3$ (δ_C = 77.14 ppm). Data are listed by chemical shift (in ppm, δ scale relative to tetramethylsilane, δ_{TMS} = 0 ppm).

Fourier transform infrared (FT-IR) spectra were recorded as a thin film using a Perkin–Elmer Spectrum One spectrometer. Maximum absorbance frequencies (ν_{max}) are reported in wavenumbers (cm^{-1}).

Optical rotation measurements were performed on the Perkin-Elmer 343 polarimeter at the sodium D-line (589 nm) and reported in the following format: $[\alpha]_{20}^{D}$, concentration of solution (*c* in g / 100 mL) and solvent.

High resolution mass spectrometry (HRMS) spectra were recorded by the EPRSC National Mass Spectrometry facility (Swansea, UK) or the departmental Mass spectrometry service (University Chemical Laboratories, Cambridge) using the electrospray ionisation (ESI) or the atmospheric solids analysis (ASAP) technique. The parent ion is quoted with the indicated ion: $[M+H]^+$, $[M+Na]^+$, $[M+NH_4]^+$ or $[M-H_2O]$.

GC analysis was performed using a 6890N Network GC system (Agilent Technologies Inc., Palo Alto, CA, USA), equipped with a Varian CP7502, CHIRASIL DEX CB (25.0 m x 250 μm x 0.25 μL nominal) capillary column.

Melting points are uncorrected.

6.3. Preparation of Reagents

Tin(II) Triflate ($Sn(OTf)_2$)[162]

Tin granules (2.64 g, 22.2 mmol) were stirred *in vacuo* for 3 days with occasional heating to melt. Triflic acid (10.0 g, 66.6 mmol) was added dropwise under an argon atmosphere and the mixture was heated to 85 °C for 3 days. After cooling to room temperature, the light grey foam was broken up by washing with anhydrous Et_2O without exposure to air until the filtrate appeared colourless. The residue was dried *in vacuo* with vigorous stirring for 16 hours. Tin triflate (6.75 g, 16.2 mmol, 73%) was obtained as a white-grey powder and stored under a strictly anhydrous argon atmosphere.

Samarium Diiodide (SmI_2)

Method A:[236] THF (23.7 mL) was added to a mixture of samarium metal (745 mg, 4.95 mmol) and iodine (697 mg, 2.47 mmol) under Ar, rigorously excluding oxygen. The resulting suspension was sonicated at rt for 45 min and the resulting deep blue solution of SmI_2 (*ca.* 0.1 M in THF) was used immediately.

Method B:[237] Samarium metal (448 mg, 2.98 mmol) and iodine (684 mg, 2.69 mmol) were suspended in anhydrous THF (27 mL) under Ar and refluxed for 3 h, taking care to exclude oxygen. The resulting deep blue solution of SmI_2 (*ca.* 0.1 M in THF) was cooled to rt and used immediately.

Raney Nickel[238]

Ni/Al alloy powder (15.0 g) was added portion-wise to a solution of NaOH (19.0 g) in H_2O (75 mL) at 0 °C, controlling the exotherm by maintaining the reaction temperature below 20 °C. The mixture was then let to warm to rt at which point evolution of hydrogen gas and a temperature rise to 30 °C were observed.

Once effervescence became slow, the reaction was warmed to 80 °C and stirred at this temperature for 4 h. The mixture was then cooled to rt and the liquid phase decanted away. The residual slurry was transferred to a beaker and stirred with 10% NaOH solution (125 mL). The liquid phase was then decanted and the washing repeated with H_2O (20 x 50 mL) until the pH of the decanted solution became pH 7. The black solid was finally washed with EtOH (5 x 50 mL) and stored under EtOH in an airtight container.

Lithium di-*tert*-Butylbiphenyl (LiDBB)[223]

Freshly cut Li wire (320 mg, 46.1 mmol) was rinsed with hexane, cut into 1 cm strips and added to a solution of di-*tert*-butylbiphenyl (13.7 g, 51.3 mmol) in THF (48 mL), rigorously excluding oxygen. The resulting mixture was sonicated for 4 h at 0 °C to give a dark green solution of LiDBB (1 M in THF), which was used immediately.

2-Iodoxybenzoic Acid (IBX)[239]

2-Iodobenzoic acid (50.0 g, 202 mmol) was added in one portion to a stirred solution of Oxone™ (181 g, 689 mmol) in H_2O (650 mL) and the resulting suspension heated to 80 °C for 3.5 h during which a white foam had formed. The mixture was cooled to rt and left to stand for 16 h. The precipitate was collected by filtration, washed with H_2O (6 x 100 mL) and acetone (2 x 100 mL), then dried *in vacuo* to give IBX (45.8 g, 164 mmol, 81%) as a white powder.

Dess−Martin Periodinane (DMP)[239]

A mixture of IBX (44.2 g, 158 mmol) and $TsOH{\cdot}H_2O$ (311 mg, 1.58 mmol) in acetic anhydride (220 mL) was heated to 85 °C for 1.5 h, then at 90 °C for a further 2 h. The resulting yellow solution was cooled to rt then to 0 °C for 2 h to give a precipitate. The mixture was filtered and the solids washed with Et_2O (5 x 50 mL), then dried under vacuum to give DMP (62.7 g, 148 mmol, 94%) as a white solid.

Lithium hexamethyldisilazane (LiHMDS)[240]

^{n}BuLi (4.43 mL, 1.6 M in hexanes, 7.00 mmol) was added dropwise over 10 min to a stirred solution of hexamethyldisilazane (1.61 mL, 7.69 mmol) in THF (2.56 mL) at 0 °C and stirred at this temperature for an additional 1 h. The resulting solution of LiHMDS (1.0 M in THF) was used immediately.

6.4. Experimental Procedures for Chapter 3

Ethyl ketone 171

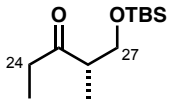

EtMgBr (12.8 mL, 3.0 M in Et_2O, 38.2 mmol) was added dropwise to a solution of Weinreb amide **172** (4.98 g, 19.1 mmol) in Et_2O (75 mL) at 0 °C. The mixture was stirred at this temperature for 2 h then warmed to rt for a further 13 h. After cooling to 0 °C, the reaction was quenched by careful addition of NH_4Cl solution (45 mL). The phases were separated and the aqueous layer was extracted with Et_2O (3 × 75 mL). Combined organic phases were washed with brine (75 mL), dried ($MgSO_4$) and concentrated *in vacuo*. Purification by flash column chromatography (gradient elution: EtOAc/40–60 PE, 1:10 → 1:5) afforded ketone **171** (3.80 g, 16.5 mmol, 86%) as a colourless oil.

R_f 0.72 (EtOAc/40–60 PE, 1:5); **^{1}H NMR** (400 MHz, $CDCl_3$): δ_H 3.73–3.69 (1H, m, H_{27a}), 3.59 (1H, dd, J = 9.6, 5.6 Hz, H_{27b}), 2.76 (1H, m, H_{26}), 2.56–2.44 (2H, m, H_{24} × 2), 1.05–0.99 (6H, m, Me_{24}, Me_{26}), 0.85 (9H, s, $SiC(C\underline{H}_3)_3$), 0.02 (3H, s, $SiC\underline{H}_3$), 0.00 (3H, s, $SiC\underline{H}_3$).

The data is in accordance with that reported by Denmark.[241]

3-((4-Methoxybenzyl)oxy)propan-1-ol (174)

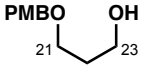

Powdered KOH (1.27 g, 22.6 mmol) was added portion-wise to a cold slurry of propane-1,3-diol (16.7 g, 21.9 mmol) in DMSO (80 mL), carefully cooled using an ice bath. On warming to rt, a clear solution formed. The mixture was cooled to 0 °C and PMBCl (2.98 mL, 22.0 mmol) was added dropwise. The reaction was warmed to rt and stirred for 3.5 h until complete, then cooled to 0 °C and quenched with 3 M HCl (40 mL). The quenching mixture was stirred for 30 min while warming to rt, then diluted with EtOAc (100 mL). The phases were separated and the aqueous layer was extracted with EtOAc (5 × 50 mL). Combined organic phases were washed with H_2O (50 mL) and brine (50 mL), dried ($MgSO_4$) and concentrated *in vacuo*. Purification by flash column chromatography (gradient elution: EtOAc/40–60 PE, 1:4 → 1:0) yielded alcohol **174** (3.62 g, 18.5 mmol, 84%) as a pale yellow oil.

R_f 0.10 (EtOAc/40–60 PE, 1:3); **^{1}H NMR** (500 MHz, $CDCl_3$): δ_H 7.28 (2H, d, J = 8.7 Hz, Ar$\underline{H}$), 6.91 (2H, d, J = 8.7 Hz, Ar$\underline{H}$), 4.48 (2H, s, $ArC\underline{H}_2O$), 3.83 (3H, s, $ArOC\underline{H}_3$), 3.80 (2H, t, J = 5.6 Hz, H_{23} × 2),

3.67 (2H, t, J = 5.6 Hz, H_{21} × 2), 2.24 (1H, br s, O<u>H</u>), 1.88 (2H, quin, J = 5.6 Hz, H_{22} x 2).

The data is in accordance with that reported by Menche.[242]

3-((4-Methoxybenzyl)oxy)propanal (169)

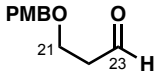

DMSO (3.83 mL, 54.0 mmol) was added dropwise to a solution of oxalyl chloride (3.48 mL, 40.5 mmol) in CH_2Cl_2 (60 mL) at −78 °C and stirred for 1 h. A solution of alcohol **174** (5.30 g, 27.0 mmol) in CH_2Cl_2 (40 mL) was added *via* cannula and the mixture was stirred for 30 min before addition of Et_3N (11.3 mL, 81.0 mmol). The resulting bright yellow reaction mixture was warmed to rt and stirred for 15 h, then quenched with H_2O (40 mL). The phases were separated and the aqueous layer was extracted with CH_2Cl_2 (3 × 200 mL). The combined organic phases were washed with $NaHCO_3$ solution (3 × 200 mL) and brine (200 mL), dried ($MgSO_4$) and concentrated *in vacuo*. Aldehyde **169** (5.16 g, 26.6 mmol, 98%) was obtained as a pungent yellow oil and used without further purification.

R_f 0.38 (EtOAc/40–60 PE, 1:3); **^{1}H NMR** (500 MHz, $CDCl_3$): δ_H 9.81 (1H, t, J = 1.9 Hz, H_{23}), 7.27 (2H, d, J = 8.7 Hz, Ar<u>H</u>), 6.90 (2H, d, J = 8.7 Hz, Ar<u>H</u>), 4.48 (2H, s, ArC<u>H</u>$_2$O), 3.83 (3H, s, ArOC<u>H</u>$_3$), 3.81 (2H, t, J = 6.2 Hz, H_{21} × 2), 2.70 (2H, td, J = 6.2, 1.8 Hz, H_{22} × 2).

The data is in accordance with that reported by Menche.[243]

Aldol adduct 175

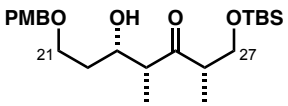

Et_3N (180 μL, 1.29 mmol) was added dropwise to a suspension of $Sn(OTf)_2$ (479 mg, 1.15 mmol) in CH_2Cl_2 (1 mL) at −78 °C to form a bright yellow mixture. A solution of ketone **171** (204 mg, 0.885 mmol, dried azeotropically from PhH and stirred over CaH_2 immediately prior to use) in CH_2Cl_2 (1.5 mL) was added *via* cannula and the reaction mixture was stirred at −78 °C for 2 h. Aldehyde **169** (255 mg, 1.31 mmol, dried azeotropically from PhH and stirred over CaH_2 immediately prior to use) in CH_2Cl_2 (1 mL) was added slowly *via* cannula. The reaction was stirred at −78 °C for 15 h and quenched with pH 7 buffer (2.5 mL) and Na^+/K^+ tartrate solution (2.5 mL). The resulting emulsion was vigorously stirred for 2 h while warming to rt. The organic phase was separated and filtered through Celite® and the aqueous layer was extracted with Et_2O (3 × 20 mL). The combined organic extracts were dried ($MgSO_4$) and concentrated *in vacuo*. The crude material was subjected to a Pinnick oxidation to remove unreacted

aldehyde **169**:

A solution of $NaClO_2$ (354 mg, 3.91 mmol) and $NaH_2PO_4 \cdot 2H_2O$ (809 mg, 5.19 mmol) in H_2O (3.0 mL) was added to the solution of the crude mixture in 2-methyl-2-butene (0.3 mL) and *t*-BuOH (3 mL) at 0 °C. The reaction was warmed to rt and stirred for 16 h. The mixture was diluted with brine (3 mL) and extracted with Et_2O (3 × 3 mL). The combined organic extracts were dried ($MgSO_4$) and concentrated *in vacuo*. Purification by flash column chromatography (gradient elution: EtOAc/40–60 PE, 1:30 → 1:10) yielded aldol adduct **175** (273 mg, 0.643 mmol, 74% over 2 steps, 8:1 *dr*) as a pale yellow oil.

R_f 0.59 (EtOAc/40–60 PE, 1:3); **$[\alpha]_{20}^{D}$** = +15.6 (*c* 1.0, $CHCl_3$); **IR** (thin film, ν_{max} / cm^{-1}): 3483, 2930, 2858, 1702, 1613, 1513, 1463, 1362, 1302, 1248, 1173, 1091, 1035, 105, 835, 777; **^{1}H NMR** (500 MHz, $CDCl_3$): δ_H 7.27 (2H, d, *J* = 8.8 Hz, Ar<u>H</u>), 6.90 (2H, d, *J* = 8.8 Hz, Ar<u>H</u>), 4.47 (1H, d, *J* = 11.5 Hz, ArC<u>H</u>$_a$H$_b$O), 4.45 (1H, d, *J* = 11.5 Hz, ArC<u>H</u>$_a$H$_b$O), 4.19 (1H, m, H_{23}), 3.83 (3H, s, ArOC<u>H</u>$_3$), 3.80 (1H, dd, *J* = 9.4, 8.6 Hz, H_{27a}), 3.64 (2H, app q, *J* = 6.1 Hz, H_{21} x 2), 3.59 (1H, dd, *J* = 9.4, 5.1 Hz, H_{27b}), 3.27 (1H, d, *J* = 2.8 Hz, O<u>H</u>), 3.09–3.00 (1H, m, H_{26}), 2.76 (1H, dq, *J* = 7.0, 3.9 Hz, H_{24}), 1.83–1.76 (1H, m, H_{22a}), 1.71–1.65 (1H, m, H_{22b}), 1.15 (3H, d, *J* = 7.0 Hz, Me_{24}), 1.01 (3H, d, *J* = 7.1 Hz, Me_{26}), 0.89 (9H, s, SiC(C<u>H</u>$_3$)$_3$), 0.06 (3H, s, SiC<u>H</u>$_3$), 0.05 (3H, s, SiC<u>H</u>$_3$); **^{13}C NMR** (125 MHz, $CDCl_3$): δ_C 218.3, 159.2, 130.3, 129.3, 113.9, 72.9, 69.4, 68.1, 66.1, 55.3, 51.2, 47.3, 34.0, 25.9, 18.4, 13.6, 10.1, −5.5, −5.6; **HRMS** calculated for $C_{23}H_{44}O_5NSi$ $[M+NH_4]^+$ 442.2983, found 442.2981.

(*R*)-Mosher ester 178

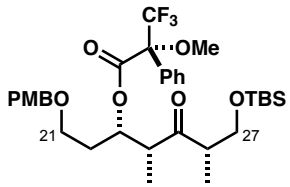

DCC (60 µL, 1.0 M in CH_2Cl_2, 60.0 µmol) and DMAP (8.2 mg, 67.1 µmol) were added sequentially to a solution of β-hydroxy ketone **175** (6.2 mg, 14.6 µmol) and (*R*)-(+)-α-methoxy-α-(trifluoromethyl)-phenylacetic acid (14.9 mg, 63.6 µmol) in CH_2Cl_2 (1 mL) and the mixture was stirred at rt for 17 h. The white suspension was concentrated *in vacuo* and the residue was purified by flash column chromatography (gradient elution: EtOAc/40–60 PE, 1:20 → 1:10) to afford (*R*)-Mosher ester **178** as an inseparable mixture with DCC (11.1 mg, *ca.* 70%).

R_f 0.62 (EtOAc/40–60 PE, 1:3); **^{1}H NMR** (500 MHz, $CDCl_3$): δ_H 7.62–7.54 (2H, m, Ph<u>H</u>), 7.47–7.37 (3H, m, Ph<u>H</u>), 7.25 (2H, d, *J* = 8.5 Hz, Ar<u>H</u>), 6.88 (2H, d, *J* = 8.5 Hz, Ar<u>H</u>), 5.60–5.57 (1H, m, H_{23}), 4.37 (1H, d, *J* = 11.6 Hz, ArC<u>H</u>$_a$H$_b$O), 4.33 (1H, d, *J* = 11.6 Hz, ArCH$_a$<u>H</u>$_b$O), 3.82 (3H, s, ArOC<u>H</u>$_3$), 3.74 (1H,

dd, J = 9.8, 7.5 Hz, H_{27a}), 3.53 (3H, s, OC$\underline{H}_3$), 3.52 (1H, dd, J = 9.7, 6.0 Hz, H_{27b}), 3.49–3.40 (2H, m, H_{21} x 2), 2.96 (1H, qd, J = 7.1, 5.6 Hz, H_{24}), 2.83 (1H, m, H_{26}), 1.95 (1H, obs m, H_{22a}), 1.89 (1H, obs m, H_{22b}), 1.06 (3H, d, J = 7.1 Hz, Me_{24}), 0.97 (3H, d, J = 7.0 Hz, Me_{26}), 0.88 (9H, s, SiC(C$\underline{H}_3$)$_3$), 0.05 (3H, s, SiC$\underline{H}_3$), 0.03 (3H, s, SiC$\underline{H}_3$).

(*S*)-Mosher ester 179

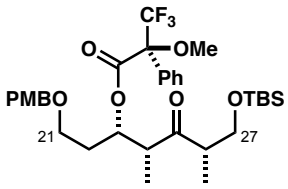

DCC (60 μL, 1.0 M in CH_2Cl_2, 60.0 μmol) and DMAP (7.4 mg, 60.6 μmol) were added sequentially to a solution of β-hydroxy ketone **175** (5.3 mg, 11.8 μmol) and (*S*)-(−)-α-methoxy-α-(trifluoromethyl)-phenylacetic acid (15.0 mg, 64.0 μmol) in CH_2Cl_2 (1 mL) and the mixture was stirred at rt for 17 h. Upon completion, the mixture was quenched with $NaHCO_3$ solution (2 mL) and diluted with CH_2Cl_2 (2 mL). Phases were separated and the aqueous layer was extracted with CH_2Cl_2 (3 × 1 mL). The combined organic layers were washed with $NaHCO_3$ solution (2 mL), dried over $MgSO_4$ and concentrated *in vacuo*. The crude product was purified by flash column chromatography (gradient elution: EtOAc/40–60 PE, 1:20) to yield (*S*)-Mosher ester **179** (6.9 mg, 10.8 μmol, 86%) as a colourless oil.

R_f 0.72 (EtOAc/40–60 PE, 1:3); **^{1}H NMR** (400 MHz, $CDCl_3$): δ_H 7.59–7.53 (2H, m, Ph$\underline{H}$), 7.45-7.35 (3H, m, Ph$\underline{H}$), 7.23 (2H, d, J = 8.6 Hz, Ar$\underline{H}$), 6.87 (2H, d, J = 8.6 Hz, Ar$\underline{H}$), 5.63–5.59 (1H, m, H_{23}), 4.35 (1H, d, J = 11.6 Hz, ArC$\underline{H}_a$H$_b$O), 4.33 (1H, d, J = 11.6 Hz, ArCH$_a\underline{H}_b$O), 3.81 (3H, s, ArOC$\underline{H}_3$), 3.75 (1H, dd, J = 9.7, 7.2 Hz, H_{27a}), 3.54 (1H, dd, J = 9.7, 6.2 Hz, H_{27b}), 3.50 (3H, s, OC$\underline{H}_3$), 3.39–3.28 (2H, m, H_{21} × 2), 2.99 (1H, qd, J = 7.1, 4.7 Hz, H_{24}), 2.97-2.89 (1H, m, H_{26}), 1.91 (1H, obs m, H_{22a}), 1.88 (1H, obs m, H_{22b}), 1.14 (3H, d, J = 7.2 Hz, Me_{24}), 1.03 (3H, d, J = 7.0 Hz, Me_{26}), 0.88 (9H, s, SiC(C$\underline{H}_3$)$_3$), 0.05 (3H, s, SiC$\underline{H}_3$), 0.04 (3H, s, SiC$\underline{H}_3$).

Ethyl ketone 170

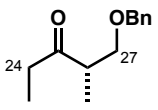

EtMgBr (60.0 mL, 3.0 M in Et_2O, 180 mmol) was added over 1.5 h to a solution of Weinreb amide **182** (14.1 g, 60.0 mmol) in Et_2O (150 mL) at 0 °C. The grey suspension was stirred at this temperature for 18 h then quenched by careful addition of NH_4Cl solution (150 mL). The mixture was warmed to rt and the aqueous layer was extracted with Et_2O (3 × 100 mL). Combined organic phases were dried ($MgSO_4$),

concentrated *in vacuo* and purified by flash column chromatography (gradient elution: EtOAc/40–60 PE, 1:20 → 1:2). Ketone **170** (7.28 g, 35.3 mmol, 59%, 83% BRSM) was obtained as a colourless oil.

R_f 0.43 (EtOAc/40–60 PE, 1:10); **^{1}H NMR** (500 MHz, $CDCl_3$): δ_H 7.38–7.35 (2H, m, PhH), 7.32–7.30 (3H, m, PhH), 4.53 (1H, d, J = 12.1 Hz, PhCH_aH_bO), 4.49 (1H, d, J = 12.1 Hz, PhCH_aH_bO), 3.66 (1H, dd, J = 9.0, 7.9 Hz, H_{27a}), 3.49 (1H, dd, J = 9.0, 5.5 Hz, H_{27b}), 2.95–2.88 (1H, m, H_{26}), 2.54 (2H, q, J = 7.2 Hz, H_{24} × 2), 1.10 (3H, d, J = 7.2 Hz, Me_{26}), 1.07 (3H, d, J = 7.2 Hz, Me_{24}).

The data is in accordance with that reported by Paterson.[244]

Aldol adduct 183

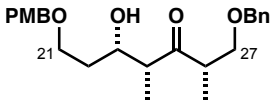

Ti(^{i}PrO)$_4$ (4.10 mL, 13.9 mmol) was added dropwise to a solution of $TiCl_4$ (4.55 mL, 41.4 mmol) in CH_2Cl_2 (100 mL) at 0 °C. The mixture was stirred for 10 min, then warmed to rt and stirred for a further 20 min. The resulting colourless solution was added dropwise to a solution of ketone **170** (9.51 g, 46.1 mmol, dried azeotropically from PhH and stirred over CaH_2 immediately prior to use) in CH_2Cl_2 (210 mL) at −78 °C and a gradual colour change from colourless through yellow and finally bright orange was observed as well as evolution of gas. The mixture was stirred for 10 min before ^{i}Pr$_2$NEt (8.83 mL, 50.7 mmol) was added dropwise and a colour change to dark red was observed. Aldehyde **169** (12.1 g, 62.1 mmol, dried azeotropically from PhH and stirred over CaH_2 immediately prior to use) in CH_2Cl_2 (210 mL) was then added dropwise *via* syringe down the side of the reaction flask over 30 min. The mixture was stirred at −78 °C for a further 16 h before being quenched with MeOH (2 mL), warmed to rt and Na^+/K^+ tartrate solution (25 mL) added. The biphasic mixture was stirred at rt for a further 2 h before extracting with CH_2Cl_2 (3 x 250 mL). The combined organic phases were dried ($MgSO_4$) and concentrated *in vacuo*.

The crude product was dissolved in ^{t}BuOH/2-Me-but-2-ene (88 mL, 10:1) at 0 °C. A solution of $NaClO_2$ (4.65 g, 51.5 mmol) and $NaH_2PO_4{\cdot}2H_2O$ (16.2 g, 103 mmol) in H_2O (80 mL) was added portionwise and a colour change to bright yellow was observed. The mixture was warmed to rt and stirred for 64 h during which the colour had dissipated. The reaction was diluted with brine (100 mL), extracted with Et_2O (6 x 100 mL), dried (Na_2SO_4) and concentrated *in vacuo*. The residue was purified by flash column chromatography (gradient elution: EtOAc/40–60 PE, 1:8 → 1:4) to yield aldol adduct **183** (15.1 g, 37.7 mmol, 82%, 12:1 *dr*) as a colourless oil.

The title compound can also be accessed *via* the following protocol:

Et_3N (190 μL, 1.36 mmol) was added dropwise to a suspension of $Sn(OTf)_2$ (525 mg, 1.26 mmol) in CH_2Cl_2 (1.5 mL) at −78 °C to form a bright yellow mixture. A solution of ketone **170** (200 mg, 0.969 mmol, dried azeotropically from PhH and stirred over CaH_2 immediately prior to use) in CH_2Cl_2 (1.5 mL) was added *via* cannula and the reaction mixture was stirred at −78 °C for 2 h. Aldehyde **169** (270 mg, 1.39 mmol, dried azeotropically from PhH and stirred over CaH_2 immediately prior to use) in CH_2Cl_2 (1 mL) was added *via* cannula. The reaction mixture was stirred at −78 °C for 75 min and quenched by the addition of pH 7 buffer solution (5 mL) The resulting emulsion was filtered through Celite®, washing with CH_2Cl_2. Phases were separated and the aqueous layer was extracted with CH_2Cl_2 (3 × 5 mL). The combined organic extracts were dried ($MgSO_4$) and concentrated *in vacuo*. ^{1}H NMR analysis of the crude product mixture indicated an 8:1 diastereomeric ratio.

The crude material was subjected to Pinnick oxidation to remove unreacted aldehyde. A solution of $NaClO_2$ (62.9 mg, 0.684 mmol) and $NaH_2PO_4{\cdot}2H_2O$ (213 mg, 1.37 mmol) in H_2O (2 mL) was added to the solution of the crude reaction product in 2-methyl-2-butene (0.2 mL) and ^{t}BuOH (2 mL) at 0 °C. The reaction was warmed to rt and stirred for 16 h. The mixture was diluted with brine (3 mL) and extracted with Et_2O (3 × 3 mL). The combined organic extracts were dried ($MgSO_4$) and concentrated *in vacuo*. Purification by flash column chromatography (gradient elution: EtOAc/40–60 PE, 1:15 → 1:5) yielded aldol adduct **183** (227 mg, 0.591 mmol, 61%, 9:1 *dr*) as a colourless oil.

R_f 0.29 (EtOAc/40–60 PE, 1:3); **$[\alpha]_{20}^{D}$** = −2.9 (*c* 1.0, $CHCl_3$); **IR** (thin film, ν_{max} / cm^{-1}): 3495, 2935, 2861, 1709, 1613, 1513, 1455, 1363, 1302, 1247, 1174, 1094, 1032, 821, 739, 699; **^{1}H NMR** (400 MHz, $CDCl_3$): δ_H 7.35–7.22 (7H, m, PhH, ArH), 6.87 (2H, d, *J* = 8.7 Hz, ArH), 4.48 (2H, d, *J* = 11.8 Hz, $ArCH_aH_bO$), 4.45 (2H, d, *J* = 11.8 Hz, $ArCH_aH_bO$), 4.42 (2H, s, $PhCH_2O$), 4.19–4.15 (1H, m, H_{23}) 3.80 (3H, s, $ArOCH_3$), 3.66 (1H, t, *J* = 8.8 Hz, H_{21a}), 3.59–3.52 (2H, m, H_{27} × 2), 3.45 (1H, dd, *J* = 8.8, 5.0 Hz, H_{21b}), 3.21 (1H, d, *J* = 3.2 Hz, OH), 3.17 (1H, obs qt, *J* = 7.0, 1.9 Hz, H_{26}), 2.77 (1H, qd, *J* = 6.9, 4.0 Hz, H_{24}), 1.78–1.61 (2H, m, H_{22} × 2), 1.11 (3H, d, *J* = 7.0 Hz, Me_{26}), 1.03 (3H, d, *J* = 7.0 Hz, Me_{24}); **^{13}C NMR** (125 MHz, $CDCl_3$): δ_C 217.2, 159.2, 137.8, 130.3, 129.3, 128.5, 127.8, 127.7, 113.8, 73.4, 73.0, 72.8, 69.7, 68.0, 55.3, 51.3, 45.2, 33.8, 13.7, 10.2; **HRMS** calculated for $C_{24}H_{36}O_5N$ $[M+NH_4]^+$ 418.2588, found 418.2588.

(*R*)-Mosher ester 185

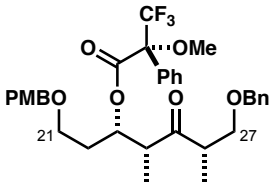

DCC (62 μL, 1.0 M in CH_2Cl_2, 62.0 μmol) and DMAP (8.0 mg, 65.5 μmol) were added sequentially to a solution of β-hydroxy ketone **183** (5.4 mg, 13.5 μmol) and (*R*)-(+)-α-methoxy-α-(trifluoromethyl)-phenylacetic acid (14.0 mg, 59.8 μmol) in CH_2Cl_2 (1 mL). The mixture was stirred at rt for 17 h, then quenched by the addition of $NaHCO_3$ solution (2 mL). Layers were separated and the aqueous phase was extracted with CH_2Cl_2 (2 × 2 mL). The combined organic phases were dried ($MgSO_4$) and concentrated *in vacuo*. The crude product was purified by flash column chromatography (gradient elution: EtOAc/40–60 PE, 1:25 → 1:15) to yield (*S*)-Mosher ester **185** as an inseparable mixture with DCC (5.0 mg, *ca.* 50% yield).

R_f 0.71 (EtOAc/40–60 PE, 1:3); **^{1}H NMR** (500 MHz, $CDCl_3$): δ_H 7.66–7.62 (2H, m, PhH), 7.59–7.54 (3H, m, PhH), 7.42–7.30 (5H, m, PhH), 7.23 (2H, d, *J* = 8.6 Hz, ArH), 6.87 (2H, d, *J* = 8.6 Hz, ArH), 5.61-5.57 (1H, m, H_{23}), 4.46 (1H, d, *J* = 11.9 Hz, $ArCH_aCH_bO$), 4.41 (1H, d, *J* = 11.8 Hz, $ArCH_aCH_bO$), 4.35 (2H, s, $PhCH_2O$), 3.81 (3H, s, $ArOCH_3$), 3.59 (1H, dd, *J* = 8.9, 8.2 Hz, H_{27a}), 3.52 (3H, s, OCH_3), 3.39 (1H, dd, *J* = 8.9, 5.8 Hz, H_{27b}), 3.40 (1H, obs m, H_{21a}), 3.38 (1H, obs m, H_{21b}), 2.98 (1H, obs m, H_{26}), 2.95 (1H, obs m, H_{24}), 1.98–1.90 (2H, m, H_{22} × 2), 1.05 (3H, d, *J* = 7.1 Hz, Me_{26}), 0.98 (3H, d, *J* = 7.1 Hz, Me_{24}).

(*S*)-Mosher ester 186

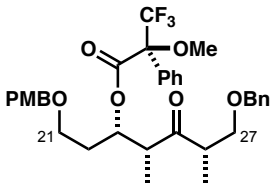

DCC (62 μL, 1.0 M in CH_2Cl_2, 62.0 μmol) and DMAP (8.0 mg, 65.5 μmol) were added sequentially to a solution of β-hydroxy ketone **183** (5.5 mg, 13.7 μmol) and (*S*)-(−)-α-methoxy-α-(trifluoromethyl)-phenylacetic acid (15.6 mg, 66.6 μmol) in CH_2Cl_2 (1 mL) and the mixture was stirred at rt for 17 h. The reaction was quenched with $NaHCO_3$ solution (2 mL) and diluted with CH_2Cl_2 (2 mL). The phases were separated and the aqueous layer was extracted with CH_2Cl_2 (2 × 2 mL). The combined organic phases were dried ($MgSO_4$) and concentrated *in vacuo*. The crude product was purified by flash column chromatography (gradient elution: EtOAc/40–60 PE, 1:25 → 1:15) to yield (*S*)-Mosher ester **186** (8.4 mg,

13.6 μmol, 98%) as a colourless oil.

R_f 0.72 (EtOAc/40–60 PE, 1:3); **^{1}H NMR** (500 MHz, $CDCl_3$): δ_H 7.58–7.55 (2H, m, PhH), 7.42–7.37 (3H, m, PhH), 7.34–7.26 (5H, m, PhH), 7.26 (2H, d, *J* = 8.6 Hz, ArH), 6.87 (2H, d, *J* = 8.7 Hz, ArH), 5.66–5.62 (1H, m, H_{23}), 4.48 (1H, d, *J* = 12.0 Hz, $ArCH_aCH_bO$), 4.41 (1H, d, *J* = 12.0 Hz, $ArCH_aCH_bO$), 4.32 (2H, ABq, *J* = 11.4 Hz, $PhCH_2O$), 3.81 (3H, s, $ArOCH_3$), 3.62 (1H, dd, *J* = 9.0, 7.9 Hz, H_{27a}), 3.51 (3H, s, OCH_3), 3.43 (1H, dd, *J* = 9.0, 5.9 Hz, H_{27b}), 3.36 (1H, dt, *J* = 9.7, 5.9 Hz, H_{21a}), 3.31 (1H, dt, *J* = 9.7, 6.8 Hz, H_{21b}), 3.12–3.04 (1H, m, H_{26}), 3.04 (1H, qd, *J* = 7.1, 4.8 Hz, H_{24}), 1.92–1.85 (2H, m, H_{22} × 2), 1.13 (3H, d, *J* = 7.1 Hz, Me_{24}), 1.05 (3H, d, *J* = 7.1 Hz, Me_{26}).

Propionate 188

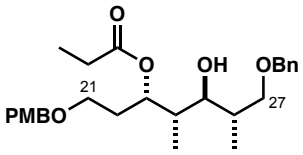

Freshly prepared SmI_2 (25.6 mL, 0.1 M in THF, 2.56 mmol) was added dropwise to a solution of propionaldehyde (freshly distilled from $CaCl_2$, 8.36 mL, 116 mmol) in THF (200 mL) at 0 °C. The mixture was stirred for 5 min until the dark blue colour no longer persisted and cooled to −20 °C. A solution of aldol adduct **183** (10.2 g, 25.6 mmol) in THF (70 mL) was added *via* cannula and the green/yellow reaction mixture was stirred at −20 °C for 16 h. The reaction was then warmed up to −10 °C and stirred for a further 65 h before quenching with $NaHCO_3$ solution (200 mL) and warming to rt. The mixture was extracted with EtOAc (3 × 150 mL) and the combined organic extracts were washed with brine (10 mL), dried ($MgSO_4$) and concentrated *in vacuo*. The crude product was purified by flash column chromatography (gradient elution: EtOAc/40–60 PE, 1:12 → 1:8) to afford ester **188** (11.0 g, 23.9 mmol, 93%, >20:1 *dr*) as a colourless oil.

R_f 0.66 (EtOAc/40–60 PE, 1:2); **$[\alpha]_{20}^{D}$** = −13.2 (*c* 1.0, $CHCl_3$); **IR** (thin film, ν_{max} / cm^{-1}): 3513, 2859, 1712, 1612, 1513, 1455, 1363, 1247, 1200, 1083, 1034, 1002, 820, 737, 698; **^{1}H NMR** (500 MHz, $CDCl_3$): δ_H 7.36–7.26 (5H, m, PhH), 7.25 (2H, d, *J* = 8.7 Hz, ArH), 6.87 (2H, d, *J* = 8.7 Hz, ArH), 5.46 (1H, ddd, *J* = 9.3, 4.0, 1.7 Hz, H_{23}), 4.48 (2H, s, $PhCH_2O$), 4.41 (1H, d, *J* = 11.5 Hz, $ArCH_aH_bO$), 4.39 (1H, d, *J* = 11.5 Hz, $ArCH_aH_bO$), 3.80 (3H, s, $ArOCH_3$), 3.58 (1H, dd, *J* = 9.2, 5.2 Hz, H_{27a}), 3.49–3.42 (3H, m, H_{21} × 2, H_{27b}), 3.39 (1H, d, *J* = 5.7 Hz, OH), 3.12 (1H, ddd, *J* = 9.1, 5.7, 3.4 Hz, H_{25}), 2.30 (1H, dq, *J* = 15.9, 7.8 Hz, $H_{2a'}$), 2.29 (1H, dq, *J* = 15.9, 7.5 Hz, $H_{2b'}$), 2.10-1.96 (2H, m, H_{22a}, H_{26}), 1.85–1.72 (2H, m, H_{22b}, H_{24}), 1.12 (2H, t, *J* = 7.6 Hz, $H_{3'}$ × 3), 1.08 (3H, d, *J* = 7.1 Hz, Me_{26}), 0.90 (3H, d, *J* = 7.0 Hz, Me_{24}); **^{13}C NMR** (125 MHz, $CDCl_3$): δ_C 175.2, 159.2, 138.4, 130.4, 129.3, 128.4, 127.6, 127.5, 113.8,

76.3, 73.3, 72.8, 72.1, 71.2, 67.0, 55.3, 40.8, 34.8, 33.2, 27.8, 16.4, 10.3, 9.3; **HRMS** calculated for $C_{27}H_{39}O_6$ $[M+NH_4]^+$ 459.2741, found 459.2738.

TES ether 191

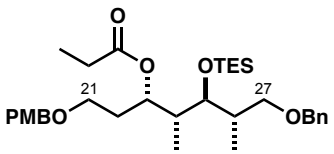

TESOTf (6.48 mL, 28.7 mmol) was added dropwise to a solution of alcohol **188** (11.0 g, 23.9 mmol) and 2,6-lutidine (5.53 mL, 47.8 mmol) in CH_2Cl_2 (500 mL) at −78 °C. The reaction mixture was stirred for 2 h, then quenched by the addition of $NaHCO_3$ solution (300 mL) and warmed to rt. The phases were separated and the organic layer was extracted with CH_2Cl_2 (2 x 300 mL). The combined organic phases were dried ($MgSO_4$), concentrated *in vacuo* and purified by flash column chromatography (gradient elution: EtOAc/40–60 PE, 1:50 → 1:15) to afford TES ether **191** (13.2 g, 22.9 mmol, 96%) as a colourless oil.

$\mathbf{R}_f$ 0.59 (EtOAc/40–60 PE, 1:5); $[\alpha]_{20}^{D}$ = −14.0 (*c* 1.0, $CHCl_3$); **IR** (thin film, ν_{max} / cm^{-1}): 2956, 2873, 1728, 1609, 1510, 1459, 1362, 1302, 1251, 1189, 1096, 1038, 1005, 820, 737, 700; **^{1}H NMR** (500 MHz, $CDCl_3$): δ_H 7.38–7.34 (4H, m, PhH), 7.31–7.29 (1H, m, PhH), 7.28 (2H, d, *J* = 8.8 Hz, ArH), 6.89 (2H, d, *J* = 8.8 Hz, ArH), 5.22 (1H, ddd, *J* = 7.6, 5.5, 3.1, H_{23}), 4.50 (2H, s, $PhCH_2O$), 4.43 (1H, d, *J* = 11.3 Hz, $ArCH_aH_bO$), 4.40 (1H, d, *J* = 11.3 Hz, $ArCH_aH_bO$), 3.82 (3H, s, $ArOCH_3$), 3.59 (1H, dd, *J* = 9.3, 4.6 Hz, H_{27a}), 3.57 (1H, dd, *J* = 7.0, 3.9 Hz, H_{25}), 3.51–3.44 (2H, m, H_{21} × 2), 3.33 (1H, dd, *J* = 9.2, 7.9 Hz, H_{27b}), 2.30 (2H, q, *J* = 7.5 Hz, $H_{2'}$ x 2), 2.12–2.07 (1H, m, H_{26}), 2.00–1.93 (1H, m, H_{22a}), 1.90–1.83 (2H, m, H_{22b}, H_{24}), 1.14 (3H, t, *J* = 7.5 Hz, $H_{3'}$ x 3), 1.05 (3H, d, *J* = 7.1 Hz, Me_{26}), 0.96 (9H, t, *J* = 8.0 Hz, $SiCH_2CH_3$ x 3), 0.96 (3H, d, *J* = 7.0 Hz, Me_{24}), 0.63 (6H, q, *J* = 8.0 Hz, $SiCH_2CH_3$ x 3); **^{13}C NMR** (125 MHz, $CDCl_3$): δ_C 174.0, 159.1, 138.8, 130.5, 129.3, 128.3, 127.5, 127.4, 113.7, 76.9, 73.0, 72.7, 72.1, 71.9 67.2, 55.3, 41.1, 36.9, 33.5, 27.9, 15.9, 11.1, 9.2, 7.1, 5.4; **HRMS** calculated for $C_{33}H_{53}O_6Si$ $[M+H]^+$ 573.3606, found 573.3609.

Alcohol 198

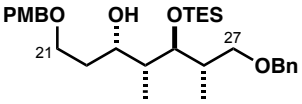

DIBALH (29.8 mL, 1.0 M in hexanes, 29.8 mmol) was added dropwise to a solution of TES ether **191** (13.2 g, 22.9 mmol) in CH_2Cl_2 (350 mL) at −78 °C and the mixture was stirred at this temperature for 2 h.

An additional portion of DIBALH (4.58 mL, 4.58 mmol) was added and the reaction stirred for a further 30 min. Upon completion, the mixture was quenched by the addition of Na^+/K^+ tartrate solution (500 mL), warmed to rt and stirred vigorously for 16 h. The layers were separated and the aqueous phase extracted with EtOAc (5 x 200 mL). Combined organic extracts were dried (Na_2SO_4) and concentrated *in vacuo* to give alcohol **198** (11.8 g, 22.9 mmol, 99%) as a colourless oil which was used without further purification.

R_f 0.50 (EtOAc/40–60 PE, 1:4); **$[\alpha]_{20}^{D}$** = −10.7 (*c* 1.0, $CHCl_3$); **IR** (thin film, ν_{max} / cm^{-1}): 2952, 2881, 1617, 1514, 1455, 1413, 1368, 1300, 1247, 1169, 1094, 1037, 1001, 819, 737, 696; **^{1}H NMR** (500 MHz, $CDCl_3$): δ_H 7.39–7.34 (4H, m, PhH), 7.32–7.29 (1H, m, PhH), 7.27 (2H, d, *J* = 8.6 Hz, ArH), 6.89 (2H, d, *J* = 8.6 Hz, ArH), 4.54 (1H, d, *J* = 12.0 Hz, $ArCH_aH_bO$), 4.48 (1H, d, *J* = 12.0 Hz, $ArCH_aH_bO$), 4.46 (1H, d, *J* = 11.5 Hz, $PhCH_aH_bO$), 4.44 (1H, d, *J* = 11.5 Hz, $PhCH_aH_bO$), 4.22 (1H, dd, *J* = 8.9, 3.9, H_{23}), 3.82 (3H, s, $ArOCH_3$), 3.76 (1H, dd, *J* = 7.4, 3.2 Hz, H_{25}), 3.59 (2H, t, *J* = 6.4 Hz, H_{21} x 2), 3.52 (1H, dd, *J* = 9.0, 4.4 Hz, H_{27a}), 3.41 (1H, dd, *J* = 8.8, 6.4 Hz, H_{27b}), 2.12 (1H, ddd, *J* = 11.5, 6.8, 4.7 Hz, H_{26}), 1.91–1.84 (1H, m, H_{22a}), 1.70–1.64 (1H, m, H_{24}), 1.61–1.55 (1H, m, H_{22b}), 1.02 (3H, d, *J* = 7.0 Hz, Me_{24}), 1.00 (3H, d, *J* = 7.0 Hz, Me_{26}), 0.97 (9H, t, *J* = 8.0 Hz, $SiCH_2CH_3$ x 3), 0.66 (6H, q, *J* = 7.8 Hz, $SiCH_2CH_3$ x 3); **^{13}C NMR** (125 MHz, $CDCl_3$): δ_C 159.1, 138.6, 130.6, 129.3, 128.3, 127.6, 127.5, 113.8, 80.1, 73.1, 72.8, 72.6, 68.5, 68.0, 55.3, 38.1, 38.1, 35.1, 14.8, 11.6, 7.0, 5.3; **HRMS** calculated for $C_{30}H_{49}O_5Si$ $[M+H]^+$ 517.3344, found 517.3333.

Diol 189

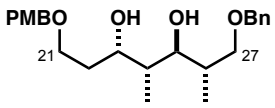

$Me_4NBH(OAc)_3$ (1.79 g, 6.82 mmol) was dissolved in MeCN/AcOH (2:1, 9 mL) and the cloudy solution was stirred at rt for 1 h before being cooled to −30 °C. A solution of aldol adduct **183** (275 mg, 0.687 mmol, 9:1 *dr*) in MeCN (2 mL) was added *via* cannula. The mixture was stirred for 24 h before being quenched by pouring into Na^+/K^+ tartrate / $NaHCO_3$ solution (1:1, 15 mL) at 0 °C. The solution was stirred for 3 h whilst being warmed to rt. The phases were separated and the aqueous layer was extracted with CH_2Cl_2 (3 × 10 mL). The combined organics were washed with brine (10 mL), dried ($MgSO_4$) and concentrated *in vacuo*. The crude product was purified by flash column chromatography (gradient elution: EtOAc/40–60 PE, 1:4 → 1:3) to afford diol **189** as a colourless oil (232 mg, 0.576 mmol, 84%, 18:1 *dr*).

The title compound can also be accessed *via* the following protocol from ester **188**:

Potassium carbonate (2.00 g, 14.4 mmol) was added to a solution of ester **188** (3.31 g, 7.22 mmol) in MeOH (72 mL) and stirred at rt for 20 h. Upon completion, the reaction mixture was poured into brine (40 mL) and extracted with EtOAc (3 × 100 mL). The combined organic extracts were dried ($MgSO_4$) and concentrated *in vacuo* to afford diol **189** (2.66 g, 6.61 mmol, 92%), which was used without further purification.

R_f 0.31 (EtOAc/40–60 PE, 1:2); **$[\alpha]_{20}^{D}$** = +0.85 (*c* 2.0, $CHCl_3$); **IR** (thin film, ν_{max} / cm^{-1}): 3417, 2863, 1613, 1586, 1514, 1455, 1363, 1303, 1248, 1174, 1093, 1034, 975, 820, 739, 699; **^{1}H NMR** (500 MHz, $CDCl_3$): δ_H 7.40–7.30 (5H, m, PhH), 7.27 (2H, d, *J* = 8.7 Hz, ArH), 6.89 (2H, d, *J* = 8.7 Hz, ArH), 4.55 (2H, s, $PhCH_2O$), 4.47 (2H, s, $ArCH_2O$), 4.28 (2H, d, *J* = 3.5 Hz, OH_{25}), 4.20–4.16 (1H, m, H_{23}), 3.87 (1H, d, *J* = 1.6 Hz, OH_{23}), 3.82 (3H, s, $ArOCH_3$), 3.69–3.61 (3H, m, H_{27a}, H_{25}, H_{21a}), 3.59–3.54 (2H, m, H_{27b}, H_{21b}), 2.14 (1H, app qd, *J* = 6.8, 4.7 Hz, H_{26}), 1.97–1.89 (1H, m, H_{24}), 1.79–1.73 (1H, m, H_{22a}), 1.64–1.58 (1H, m, H_{22b}), 1.04 (3H, d, *J* = 7.2 Hz, Me_{24}), 0.90 (3H, d, *J* = 6.8 Hz, Me_{26}); **^{13}C NMR** (125 MHz, $CDCl_3$): δ_C 159.3, 137.8, 130.5, 129.4, 128.4, 127.8, 127.6, 113.9, 81.1, 75.1, 73.6, 73.0, 70.2, 68.3, 55.2, 38.5, 36.0, 34.2, 14.4, 11.6; **HRMS** calculated for $C_{24}H_{35}O_5$ $[M+H]^+$ 403.2479, found 403.2480.

Acetonide 192

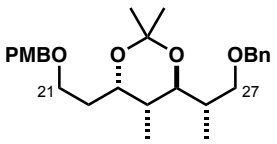

PPTS (1 crystal) was added to a solution of diol **189** (22.0 mg, 54.7 μmol) in 2,2-dimethoxypropane (1 mL) at rt. The reaction mixture was stirred at rt for 17 h then concentrated *in vacuo*. The crude product was purified by flash column chromatography (gradient elution: EtOAc/40–60 PE, 1:20 → 1:1) to yield acetonide **192** (21.0 mg, 47.4 μmol, 87%) as a colourless oil.

R_f 0.73 (EtOAc/40–60 PE, 1:3); **$[\alpha]_{20}^{D}$** = −8.6 (*c* 1.0, $CHCl_3$); **IR** (thin film, ν_{max} / cm^{-1}): 2858, 1613, 1587, 1513, 1455, 1379, 1302, 1247, 1224, 1174, 1143, 1098, 1037, 989, 820, 736, 698; **^{1}H NMR** (500 MHz, $CDCl_3$): δ_H 7.36 (4H, m, PhH), 7.32–7.27 (3H, m, PhH, ArH), 6.90 (2H, d, *J* = 8.7 Hz, ArH), 4.46 (1H, ABq, *J* = 12.0 Hz, $PhCH_aH_b$), 4.44 (1H, ABq, *J* = 12.0 Hz, $PhCH_aH_b$), 4.45 (2H, ABq, *J* = 11.6 Hz, $ArCH_2O$), 4.00 (1H, dt, *J* = 10.2, 4.0 Hz, H_{23}), 3.83 (3H, s, $ArOCH_3$), 3.61 (1H, dd, 9.2, 4.6 Hz, H_{27a}), 3.57–3.50 (2H, m, H_{21} × 2), 3.38 (1H, dd, *J* = 9.2, 6.9 Hz, H_{27b}), 3.27 (1H, dd, *J* = 7.3, 5.5 Hz, H_{25}), 2.01–1.93 (1H, m, H_{26}), 1.86–1.80 (1H, m, H_{24}), 1.75–1.61 (2H, m, H_{22} × 2), 1.32 (3H, s, $C(CH_3)_a(CH_3)_b$), 1.30 (3H, s, $C(CH_3)_a(CH_3)_b$), 1.05 (3H, d, *J* = 6.9 Hz, Me_{26}), 0.88 (3H, d, *J* = 6.9 Hz, Me_{24}); **^{13}C NMR** (125 MHz, $CDCl_3$): δ_C 159.2, 138.8, 130.6, 129.4, 128.3, 127.6, 127.4, 113.8, 100.3,

76.6, 73.1, 72.9, 72.3, 66.9, 66.0, 55.3, 37.8, 36.9, 31.1, 25.3, 23.5, 14.4, 12.6; **HRMS** calculated for $C_{27}H_{38}O_5Na$ $[M+Na]^+$ 465.2600, found 465.2611.

PMP acetal 195

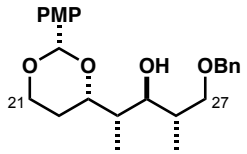

A mixture of activated 4 Å molecular sieves (388 mg) and PMB ether **189** (302 mg, 0.750 mmol, dried azeotropically from PhH) in CH_2Cl_2 (5 mL) was cooled to 0 °C. A solution of DDQ (157 mg, 0.692 mmol) in CH_2Cl_2 (10 mL) was added slowly *via* syringe and immediate colour change to dark green/blue was observed. The mixture was stirred at this temperature for a further 2 h before being warmed to rt and quenched by filtering through a pad of Celite® onto $NaHCO_3$ solution (15 mL). The layers were separated and the aqueous phase extracted with CH_2Cl_2 (3 × 10 mL). The combined organic extracts were washed with brine (30 mL), dried ($MgSO_4$) and concentrated *in vacuo*. The residue was purified by flash column chromatography (gradient elution: EtOAc/40–60 PE, 1:7 → 1:0) to yield PMP acetal **195** (211 mg, 0.527 mmol, 77%) as a colourless oil.

$\mathbf{R}_f$ 0.52 (EtOAc/40–60 PE, 1:2); $[\boldsymbol{\alpha}]_{\mathbf{20}}^{\boldsymbol{D}}$ = −20.5 (*c* 1.0, $CHCl_3$); **IR** (thin film, ν_{max} / cm^{-1}): 3507, 2963, 2857, 1615, 1517, 1362, 1303, 1247, 1100, 981, 827, 749, 697, 595 ; **^{1}H NMR** (400 MHz, $CDCl_3$): δ_H 7.38 (2H, d, *J* = 8.7 Hz, Ar$\underline{H}$), 7.36–7.28 (5H, m, Ph$\underline{H}$), 6.88 (2H, d, *J* = 8.7 Hz, Ar$\underline{H}$), 5.48 (1H, s, ArC$\underline{H}O_2$), 5.12 (1H, d, *J* = 12.0 Hz, PhC$\underline{H}_aH_b$), 5.10 (1H, d, *J* = 12.0 Hz, PhC$H_a\underline{H}_b$), 4.31–4.25 (2H, m, H_{21a}, H_{23}), 3.98 (1H, td, *J* = 12.0, 2.6 Hz, H_{21b}), 3.80 (3H, s, ArOC$\underline{H}_3$), 3.66 (1H, dd, *J* = 9.0, 4.0 Hz, H_{27a}), 3.54 (1H, dd, *J* = 9.1, 5.7 Hz, H_{27b}), 3.50 (1H, dd, *J* = 7.0, 5.2 Hz, H_{25}), 3.23 (1H, d, *J* = 6.9 Hz, O$\underline{H}$), 2.12 (1H, dddd, *J* = 12.5, 12.2, 5.0, 4.8 Hz, H_{22a}), 2.04–1.94 (1H, m, H_{26}), 1.82 (1H, ddq, *J* = 7.2, 2.5 Hz, H_{24}), 1.35–1.30 (1H, m, H_{22b}), 1.11 (3H, d, *J* = 6.9 Hz, Me_{26}), 1.02 (3H, d, *J* = 7.0 Hz, Me_{24}); **^{13}C NMR** (125 MHz, $CDCl_3$): δ_C 156.0, 138.4, 131.2, 128.4, 128.4, 127.6, 127.4, 113.6, 101.3, 78.1, 76.8, 73.5, 72.5, 67.3, 55.3, 40.0, 36.0, 27.7, 15.7, 11.9; **HRMS** calculated for $C_{24}H_{33}O_5$ $[M+H]^+$ 401.2325, found 401.2323.

PMP acetal 190

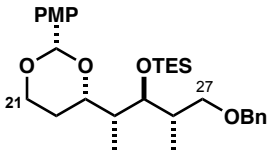

DDQ (7.80 g, 34.3 mmol) was added in one portion to a stirred slurry of alcohol **198** (11.8 g, 22.9 mmol) and activated 4 Å molecular sieves (~20 g) in CH_2Cl_2 (500 mL) at 0 °C. The resulting dark blue mixture was stirred at this temperature for 30 min before being warmed to rt and stirred for a further 1.5 h during which the colour had gradually changed to brown. The mixture was filtered through a plug of Celite® onto $NaHCO_3$ solution (300 mL) and rinsed with CH_2Cl_2 (200 mL). The aqueous phase was extracted with CH_2Cl_2 (3 x 300 mL), the combined organic extracts were dried ($MgSO_4$) and the crude product was purified by flash column chromatography (gradient elution: EtOAc/40–60 PE, 1:30 → 1:20) to afford PMP acetal **190** (9.54 g, 18.5 mmol, 81%) as a colourless oil.

$\mathbf{R}_f$ 0.69 (EtOAc/40–60 PE, 1:4); $[\alpha]_{20}^{D}$ = +19.6 (*c* 1.0, $CHCl_3$); **IR** (thin film, ν_{max} / cm^{-1}): 2957, 2876, 1616, 1518, 1456, 1393, 1302, 1249, 1171, 1093, 1038, 1011, 827, 735, 698; **^{1}H NMR** (400 MHz, $CDCl_3$): δ_H 7.40 (2H, d, *J* = 8.6 Hz, ArH), 7.35–7.27 (5H, m, PhH), 6.88 (2H, d, *J* = 8.6 Hz, ArH), 5.46 (1H, s, ArCHO$_2$), 4.51 (1H, d, *J* = 12.4 Hz, PhCH$_a$H$_b$O), 4.47 (1H, d, *J* = 12.4 Hz, PhCH$_a$H$_b$O), 4.27 (1H, dd, *J* = 11.2, 4.7, Hz, H_{21a}), 4.10–4.07 (1H, m, H_{23}), 3.94 (1H, br t, *J* = 11.2 Hz, H_{21b}), 3.80 (3H, s, ArOCH$_3$), 3.72 (1H, dd, *J* = 10.3, 8.3 Hz, H_{25}), 3.64 (1H, dd, *J* = 9.2, 4.9 Hz, H_{27a}), 3.29 (1H, dd, *J* = 9.2 Hz, H_{27b}), 2.13–1.98 (2H, m, H_{22a}, H_{26}), 1.73–1.66 (1H, m, H_{24}), 1.31–1.27 (1H, m, H_{22b}), 1.05 (3H, d, *J* = 7.0 Hz, Me_{26}), 0.99 (3H, d, *J* = 7.0 Hz, Me_{24}), 0.94 (9H, t, *J* = 7.8 Hz, SiCH$_2$CH$_3$ x 3), 0.63 (6H, q, *J* = 7.8 Hz, SiCH$_2$CH$_3$ x 3); **^{13}C NMR** (125 MHz, $CDCl_3$): δ_C 159.8, 138.9, 131.8, 128.3, 127.5, 127.4, 127.3, 113.5, 101.0, 76.6, 76.2, 73.0, 71.8, 67.3, 55.3, 42.7, 36.5, 29.2, 16.3, 11.0, 7.2, 5.6; **HRMS** calculated for $C_{30}H_{47}O_5Si$ $[M+H]^+$ 515.3187, found 515.3182.

PMP acetal 202

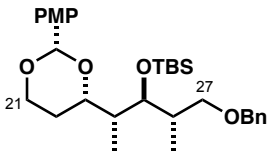

TBSOTf (106 μL, 0.460 mmol) was added dropwise to a stirred solution of alcohol **195** (123 mg, 0.307 mmol) and 2,6-lutidine (71 μL, 0.614 mmol) in CH_2Cl_2 (0.5 mL) at −78 °C. The reaction was stirred at this temperature for 2 h, then quenched with MeOH (0.5 mL) and $NaHCO_3$ solution (2 mL). The mixture was warmed to rt and the layers were separated. The aqueous phase was extracted with CH_2Cl_2 (3 × 2

mL) and the combined organic extracts dried ($MgSO_4$) and concentrated *in vacuo*. The residue was purified by flash column chromatography (EtOAc/40–60 PE, 1:20) to yield TBS ether **202** (150 mg, 0.291 mmol, 95%) as a colourless oil.

R_f 0.80 (EtOAc/40–60 PE, 1:3); $[\alpha]_{20}^{D}$ = +14.8 (*c* 1.0, $CHCl_3$); **IR** (thin film, ν_{max} / cm^{-1}): 2955, 2857, 1615, 1518, 1463, 1390, 1361, 1302, 1249, 1170, 1094, 1037, 832, 774, 698; **^{1}H NMR** (400 MHz, $CDCl_3$): δ_H 7.41 (2H, d, *J* = 8.7 Hz, ArH), 7.35–7.27 (5H, m, PhH), 6.88 (2H, d, *J* = 8.7 Hz, ArH), 5.46 (1H, s, ArCHO$_2$), 4.50 (1H, d, *J* = 12.4 Hz, PhCH$_a$H$_b$), 4.46 (1H, d, *J* = 12.4 Hz, PhCH$_a$H$_b$), 4.26 (1H, ddd, *J* = 11.4, 4.9, 1.2 Hz, H$_{21a}$), 4.04 (1H, ddd, *J* = 11.4, 3.8, 2.5 Hz, H$_{23}$), 3.93 (1H, ddd, *J* = 12.0, 11.4, 2.4 Hz, H$_{21b}$), 3.80 (3H, s, ArOCH$_3$), 3.71 (1H, dd, *J* = 7.0, 3.1 Hz, H$_{25}$), 3.64 (1H, dd, *J* = 9.3, 4.8 Hz, H$_{27a}$), 3.30 (1H, dd, *J* = 9.3, 8.2 Hz, H$_{27b}$), 2.14–2.05 (1H, m, H$_{26}$), 1.99 (1H, dddd, *J* = 12.0, 12.0, 5.0, 4.9 Hz, H$_{22a}$), 1.73 (1H, qdd, *J* = 7.0, 7.9, 3.8 Hz, H$_{24}$), 1.35 (1H, m, H$_{22b}$), 1.04 (3H, d, *J* = 7.0 Hz, Me$_{26}$), 1.01 (3H, d, *J* = 7.0 Hz, Me$_{24}$), 0.90 (9H, s, SiC(CH$_3$)$_3$) 0.07 (3H, s, SiCH$_3$), 0.06 (3H, s, SiCH$_3$); **^{13}C NMR** (100 MHz, $CDCl_3$): δ_C 159.5, 138.4, 131.4, 128.0, 127.1, 127.0, 126.9, 113.2, 100.5, 76.0, 75.5, 72.6, 71.9, 66.8, 54.9, 42.8, 36.7, 29.1, 25.8, 18.1, 15.8, 10.8, −4.0, −4.5; calculated for $C_{30}H_{47}O_5Si$ $[M+H]^+$ 515.3187, found 515.3182.

Alcohol 199

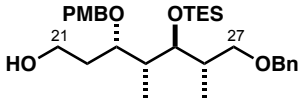

DIBALH (12.2 mL, 1.0 M in hexanes, 12.2 mmol) was added dropwise over 30 min to a solution of PMP acetal **190** (2.11 g, 4.10 mmol) in CH_2Cl_2 (40 mL) at −78 °C and stirred at this temperature for 1 h. The reaction mixture was warmed to −30 °C for 1 h, during which a yellow colour gradually appeared. The solution was allowed to warm to 0 °C and stirred for a further 1 h before quenching with Na^+/K^+ tartrate solution (100 mL). The biphasic mixture was stirred vigorously for 16 h, then extracted with CH_2Cl_2 (3 x 100 mL). The combined organic phases were dried (Na_2SO_4) and concentrated *in vacuo*. The crude product was purified by flash column chromatography (gradient elution: PhMe/CH_2Cl_2, 1:1 → 0:1, then EtOAc/40–60 PE, 1:4) to give alcohol **199** (1.67 g, 3.23 mmol, 79%) as a colourless oil.

The title compound can also be accessed *via* the following protocol:

TESOTf (264 μL, 1.23 mmol) was added dropwise to a solution of *bis*-alcohol **200** (165 mg, 0.410 mmol) and 2,6-lutidine (286 μL, 2.46 mmol) in CH_2Cl_2 (10 mL) at −78 °C. The reaction was stirred for 1 h before quenching with $NaHCO_3$ solution (10 mL). Phases were separated and the aqueous layer was extracted with CH_2Cl_2 (3 x 20 mL). Combined organic extracts were dried (Na_2SO_4), concentrated *in*

vacuo and the crude product was purified by flash column chromatography (gradient elution, EtOAc/40–60, 1:50 → 1:40).

The *Bis*-TES ether product (253 mg, 0.401 mmol) was dissolved in THF/H_2O/AcOH (5:2:1, 5 mL) and stirred at rt for 5 h before being cooled to 0 °C and quenched with $NaHCO_3$ solution (10 mL) and stirred for 15 min until bubbling had ceased. The phases were separated and the aqueous layer was extracted with EtOAc (3 x 10 mL). The combined organic phases were dried (Na_2SO_4) and alcohol **199** (191 mg, 0.369 mmol, 90% over 2 steps) was obtained as a colourless oil.

R_f 0.15 (EtOAc/40–60 PE, 1:5); **$[\alpha]_{20}^{D}$** = −12.6 (*c* 1.0, $CHCl_3$); **IR** (thin film, ν_{max} / cm^{-1}): 3428, 2955, 2876, 1613, 1514, 1455, 1413, 1301, 1247, 1173, 1039, 1011, 821, 735, 698; **^{1}H NMR** (400 MHz, $CDCl_3$): δ_H 7.35–7.33 (4H, m, PhH), 7.31–7.28 (1H, m, PhH), 7.26 (2H, d, *J* = 8.7 Hz, ArH), 6.87 (2H, d, *J* = 8.7 Hz, ArH), 4.51 (2H, s, $PhCH_2O$), 4.49 (2H, s, $ArCH_2O$), 3.80 (3H, s, $ArOCH_3$), 3.79–3.69 (4H, m, H_{21} x 2, H_{23}, H_{25}), 3.62 (1H, dd, *J* = 9.2, 4.6 Hz, H_{27a}), 3.30 (1H, dd, *J* = 9.2, 8.0 Hz, H_{27b}), 2.11–2.01 (2H, m, H_{26}, OH), 1.90–1.76 (3H, m, H_{22} x 2, H_{24}), 1.03 (3H, d, *J* = 7.0 Hz, Me_{26}), 1.00 (3H, d, *J* = 7.2 Hz, Me_{24}), 0.95 (9H, t, *J* = 7.9 Hz, $SiCH_2CH_3$ x 3), 0.62 (6H, q, *J* = 7.9 Hz, $SiCH_2CH_3$ x 3); **^{13}C NMR** (125 MHz, $CDCl_3$): δ_C 159.0, 138.7, 130.8, 129.1, 128.2, 127.4, 127.3, 113.7, 78.2, 77.1, 73.0, 72.3, 71.8, 60.7, 55.2, 42.2, 37.1, 35.5, 15.9, 11.7, 7.0, 5.4; **HRMS** calculated for $C_{30}H_{49}O_5Si$ $[M+H]^+$ 517.3344, found 517.3335.

Aldehyde 168

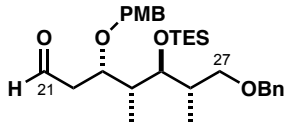

Dess–Martin periodinane (6.16 g, 14.5 mmol) was added portion-wise to a stirred slurry of alcohol **199** (5.00 g, 9.68 mmol) and $NaHCO_3$ (2.44 g, 29.0 mmol) in CH_2Cl_2 (150 ml) at 0 °C. The reaction mixture was stirred at this temperature for 1 h, then warmed to rt and stirred for a further 75 min until complete. The suspension was quenched with $Na_2S_2O_3$ solution (300 mL) and stirred for 45 min before extracting with CH_2Cl_2 (2 x 200 mL). The combined organic extracts were dried ($MgSO_4$), concentrated *in vacuo* and purified by flash column chromatography (gradient elution: EtOAc/40–60 PE, 0:1 → 1:5) to afford aldehyde **168** (4.57 g, 8.88 mmol, 92%) as a colourless oil.

R_f 0.49 (EtOAc/40–60 PE, 1:5); **$[\alpha]_{20}^{D}$** = −5.2 (*c* 1.0, $CHCl_3$); **IR** (thin film, ν_{max} / cm^{-1}): 2956, 2876, 1725, 1613, 1514, 1455, 1302, 1248, 1173, 1087, 1039, 1011, 821, 736, 698; **^{1}H NMR** (400 MHz, $CDCl_3$): δ_H 9.79 (1H, br t, *J* = 2.2 Hz, CHO), 7.35-7.32 (4H, m, PhH), 7.30–7.27 (1H, m, PhH), 7.23 (2H, d, *J* = 8.6

Hz, ArH), 6.87 (2H, d, *J* = 8.6 Hz, ArH), 4.49 (2H, s, ArCH_2O), 4.46 (2H, s, PhCH_2O), 4.23−4.19 (1H, m, H_{23}), 3.80 (3H, s, ArOCH_3), 3.75 (1H, dd, *J* = 6.7, 3.8 Hz, H_{25}), 3.59 (1H, dd, *J* = 9.2, 4.9 Hz, H_{27a}), 3.30 (1H, dd, *J* = 9.2, 7.8 Hz, H_{27b}), 2.78 (1H, ddd, *J* = 16.4, 6.9, 2.4 Hz, H_{22a}), 2.61 (1H, ddd, *J* = 16.4, 5.0, 1.9 Hz, H_{22b}), 2.12–2.06 (1H, m, H_{26}), 1.78 (1H, qdd, *J* = 7.0, 4.3, 3.7 Hz, H_{24}), 1.04 (3H, d, *J* = 6.9 Hz, Me_{26}), 0.99–0.94 (12H, m, Me_{24}, $SiCH_2CH_3$ x 3), 0.64 (6H, q, *J* = 7.9 Hz, $SiCH_2CH_3$ x 3); **^{13}C NMR** (100 MHz, $CDCl_3$): δ_C 201.1, 158.7, 138.4, 130.3, 128.6, 127.9, 127.1, 127.0, 113.4, 76.8, 74.0, 72.7, 71.7, 71.2, 54.9, 47.8, 42.3, 36.9, 15.4, 11.5, 6.8, 5.2; **HRMS** calculated for $C_{30}H_{47}O_5Si$ $[M+H]^+$ 515.3187, found 515.3180.

Alcohol 203

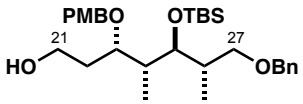

DIBALH (790 µL, 1.0 M in hexanes, 0.787 mmol) was added dropwise to a solution of PMP acetal **202** (135 mg, 0.262 mmol) in CH_2Cl_2 (3 mL) at −78 °C. The mixture was stirred at this temperature for 30 min and warmed to rt for a further 3.5 h. The reaction was quenched with Na^+/K^+ tartrate solution (3 mL) and stirred vigorously for 18 h. The layers were separated and the aqueous phase was extracted with CH_2Cl_2 (3 × 5 mL). The combined organic extracts were dried ($MgSO_4$) and concentrated *in vacuo*. The crude product was purified by flash column chromatography (gradient elution: EtOAc/40–60 PE, 1:8 → 1:5) to yield alcohol **203** (104 mg, 0.201 mmol, 77%) as a colourless oil.

$\mathbf{R}_f$ 0.35 (EtOAc/40–60 PE, 1:3); $[\alpha]_{20}^{D}$ = −16.5 (*c* 1.0, $CHCl_3$); **IR** (thin film, ν_{max} / cm^{-1}): 3390, 2928, 1612, 1513, 1462, 1360, 1301, 1247, 1173, 1035, 833, 772, 735, 697; **^{1}H NMR** (500 MHz, $CDCl_3$): δ_H 7.38–7.34 (4H, m, PhH), 7.32–7.28 (3H, m, PhH, ArH × 2), 6.89 (2H, d, *J* = 8.6 Hz, ArH), 4.52 (2H, s, ArCH_2O), 4.50 (2H, s, PhCH_2O), 3.82 (3H, s, ArOCH_3), 3.81–3.71 (4H, m, H_{21} × 2, H_{23}, H_{25}), 3.67 (1H, dd, *J* = 9.3, 4.5 Hz, H_{27a}), 3.31 (1H, dd, *J* = 9.3, 8.3 Hz, H_{27b}), 2.16–2.12 (1H, m, OH), 2.09–2.02 (1H, m, H_{26}), 1.93–1.87 (2H, m, H_{22a}, H_{24}), 1.83–1.77 (1H, m, H_{22b}), 1.06 (3H, d, *J* = 7.0 Hz, Me_{26}), 1.06 (3H, d, *J* = 7.0 Hz, Me_{24}), 0.90 (9H, s, $SiC(CH_3)_3$) 0.09 (3H, s, $SiCH_3$), 0.07 (3H, s, $SiCH_3$); **^{13}C NMR** (125 MHz, $CDCl_3$): δ_C 159.2, 138.8, 130.8, 129.4, 128.3, 127.6, 127.5, 113.9, 79.2, 76.5, 73.0, 73.6, 72.2, 60.0, 55.3, 43.2, 37.1, 35.1, 26.1, 18.4, 16.4, 11.8, −3.8, −4.3; **HRMS** calculated for $C_{30}H_{49}O_5Si$ $[M+H]^+$ 517.3344, found 517.3338.

Aldehyde 204

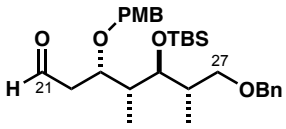

DMSO (14 μL, 0.193 mmol) was added dropwise to a solution of oxalyl chloride (12 μL, 0.145 mol) in CH_2Cl_2 (1 mL) at −78 °C and the mixture was stirred for 1 h. A solution of alcohol **203** (51.0 mg, 98.7 μmol) in CH_2Cl_2 (0.5 mL) was added *via* cannula and stirred for a further 45 min. Et_3N (41 μL, 0.30 mmol) was added and the cloudy mixture was warmed to rt for 2 h. The reaction was quenched by the addition of NH_4Cl solution (2 mL). The phases were separated and the aqueous layer was extracted with CH_2Cl_2 (3 × 3 mL). The combined organic phases were dried ($MgSO_4$) and concentrated *in vacuo*. The residue was purified by flash column chromatography (EtOAc/40–60 PE, 1:10) to afford aldehyde **204** (48.0 mg, 93.2 μmol, 95%) as a colourless oil.

R_f 0.39 (EtOAc/40–60 PE, 1:5); $[\alpha]_{20}^{D}$ = −8.4 (*c* 1.0, $CHCl_3$); **IR** (thin film, ν_{max} / cm^{-1}): 2929, 1724, 1613, 1514, 1463, 1249, 1038, 835, 774, 698; **^{1}H NMR** (500 MHz, $CDCl_3$): δ_H 9.83 (1H, m, C<u>H</u>O), 7.39–7.29 (5H, m, Ph<u>H</u>), 7.25 (2H, d, *J* = 8.6 Hz, Ar<u>H</u>), 6.89 (2H, d, *J* = 8.6 Hz, Ar<u>H</u>), 4.50 (2H, s, ArC<u>H</u>$_2$O), 4.50 (1H, d, *J* = 11.1 Hz, PhC<u>H</u>$_a$H$_b$O), 4.48 (1H, d, *J* = 11.1 Hz, PhCH$_a$<u>H</u>$_b$O), 4.15 (1H, dd, *J* = 5.1, 4.9 Hz, H_{23}), 3.82 (3H, s, ArOC<u>H</u>$_3$), 3.77 (1H, dd, *J* = 5.9, 3.7 Hz, H_{25}), 3.64 (1H, dd, *J* = 9.2, 4.9 Hz, H_{27a}), 3.32 (1H, dd, *J* = 9.2, 8.0 Hz, H_{27b}), 2.76 (1H, ddd, *J* = 16.4, 6.8, 2.6 Hz, H_{22a}), 2.68 (1H, ddd, *J* = 16.4, 5.0, 1.8 Hz, H_{22b}), 2.15–2.06 (1H, m, H_{26}), 1.88–1.82 (1H, m, H_{24}), 1.06 (3H, d, *J* = 7.0 Hz, Me_{26}), 1.04 (3H, d, *J* = 7.0 Hz, Me_{24}), 0.92 (9H, s, SiC(C<u>H</u>$_3$)$_3$) 0.10 (3H, s, SiC<u>H</u>$_3$), 0.09 (3H, s, SiC<u>H</u>$_3$); **^{13}C NMR** (125 MHz, $CDCl_3$): δ_C 201.5, 159.2, 138.7, 130.5, 129.1, 128.3, 127.5, 127.4, 113.8, 76.5, 74.9, 73.0, 72.4, 71.7, 55.3, 47.9, 43.3, 37.4, 26.2, 18.4, 15.8, 11.9, −3.8, −4.1; **HRMS** calculated for $C_{30}H_{47}O_5Si$ $[M+H]^+$ 515.3187, found 515.3181.

Dimethyl 3-methylglutarate (205)

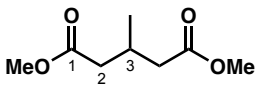

Acetyl chloride (29.3 mL, 411 mmol) was added dropwise to a solution of 3-methylglutaric acid (15.0 g, 103 mmol) in MeOH (200 mL) at 0 °C. The mixture was heated at reflux for 16 h, then cooled to rt. The solvent was removed under reduced pressure and the residue was neutralised by careful addition of $NaHCO_3$ solution (200 mL). Once gas evolution had ceased, the residue was extracted with CH_2Cl_2 (3 × 50 mL). The combined organic extracts were dried ($MgSO_4$) and concentrated *in vacuo* to afford diester **205** (15.9 g, 90.7 mmol, 89% yield) as a yellow oil, which was used without further purification.

R_f 0.61 (EtOAc/40–60 PE, 1:2); **^{1}H NMR** (400 MHz, $CDCl_3$): δ_H 3.68 (6H, s, OC$\underline{H}_3$ x 2), 2.52–2.42 (1H, m, H_1), 2.40 (2H, dd, J = 15.0, 6.0 Hz, H_{2a} × 2), 2.25 (2H, dd, J = 15.0, 7.3 Hz, H_{2b} × 2), 1.03 (3H, d, J = 6.5 Hz, Me_3).

Data in agreement with that presented by Jones.[211]

(*R*)-Methyl-3-methylglutarate (137)

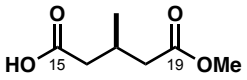

Dimethyl 3-methylglutarate (**205**) (17.8 g, 102 mmol) was dissolved in KH_2PO_4/Na_2PO_4 buffer solution (480 mL, 0.1 M, pH 7) and MeOH (120 mL). The solution was cooled to −10 °C and pig liver esterase (370 mg, 6660 U) was added. Aqueous NaOH (1.0 M, 102 mL, 102 mmol) was added dropwise at such a rate as to maintain the pH between 6.0 and 7.5. After 10 hours the addition was complete, the light brown suspension was filtered through a pad of Celite® and the residue was rinsed with H_2O (200 mL). The pH of the combined filtrates was adjusted to 3 with 3 N HCl solution and the mixture extracted with Et_2O (8 × 400 mL). The combined organic phases were dried (Na_2SO_4) and concentrated *in vacuo* to give monoester **137** (15.9 g, 99.0 mmol, 97%) as a colourless liquid.

(−)-Cinchonidine (29.1 g, 99.0 mmol) was added to a solution of enantioenriched monoester **137** in acetone (280 mL). The white suspension was heated to 40 °C. H_2O (35 mL) was added dropwise to the rapidly stirring mixture until a clear pale yellow solution formed. The solution was cooled to rt, then left to stand at −5 °C for 16 h to give off-white, needle-like crystals. The solid was collected by filtration, washed with ice-cold acetone (50 mL) and dried *in vacuo*. An additional crop of product was obtained from the mother liquor by leaving it to stand at −10 °C for 16 h, filtering and washing the solids with acetone (20 mL). The combined collected solids were dissolved 2 N HCl solution (200 mL), then extracted with Et_2O (5 × 200 mL). The organic extracts were dried (Na_2SO_4) and concentrated *in vacuo* to yield monoester **137** as a colourless oil (9.90 g, 61.8 mmol, 62%, 96% *ee*).

The GC analyses were carried out in split mode (ratio 50:1) using helium as a carrier gas at a flow rate of 134 mL min^{-1} 25.00 psi. The injection port temperature was 250 °C and the oven was maintained at 97 °C. The FID detector was at 250 °C, using H_2 flow at 40.00 mL min^{-1}, air at 450 mL min^{-1} and helium makeup flow at 45.0 mL min^{-1}. R_T (R) 165.6 min, R_T (*S*) 172.0 min, total run time 240 min.

R_f 0.24 (EtOAc/40–60 PE, 1:1); **^{1}H NMR** (500 MHz, $CDCl_3$): δ_H 3.70 (3H, s, OC$\underline{H}_3$), 2.53–2.42 (3H, m, H_{16a}, H_{17}, H_{18a}), 2.35–2.27 (2H, m, H_{16b}, H_{18b}), 1.08 (3H, d, J = 6.5 Hz, Me_{17}).

Data in agreement with that presented by Fürstner.[214]

Methyl (*R*)-5-hydroxy-3-methylpentanoate (206)

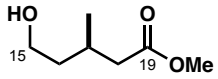

Borane–dimethylsulfide complex (3.41 mL, 35.9 mmol) was added dropwise to a solution of (*R*)-methyl-3-methylglutarate **137** (4.79 g, 29.9 mmol) in THF (200 mL) at 0 °C. The solution was stirred at 0 °C for 1 h, then warmed to rt and stirred for a further 2 h. Upon completion, the reaction mixture was cooled to 0 °C and quenched by the dropwise addition of $NaHCO_3$ solution (10 mL). The mixture was diluted with H_2O (50 mL) and extracted with Et_2O (6 x 200 mL). The combined organic phases were dried (Na_2SO_4), concentrated *in vacuo* and the residue was purified by flash column chromatography (gradient elution: EtOAc/40–60 PE, 1:4 → 1:1). Alcohol **206** (4.28 g, 29.3 mmol, 98%) was obtained as a colourless oil.

$\mathbf{R}_f$ 0.31 (EtOAc/40–60 PE, 1:3); **^{1}H NMR** (400 MHz, $CDCl_3$): δ_H 3.70–3.65 (2H, m, H_{15} x 2), 3.68 (3H, s, OC$\underline{H}_3$), 2.35 (1H, dd, J = 14.9, 6.5 Hz, H_{18a}), 2.21 (1H, dd, J = 14.9, 7.1 Hz, H_{18b}), 2.20–2.11 (1H, m, H_{17}), 1.66 (1H, br s, O$\underline{H}$), 1.63−1.47 (2H, m, H_{16} x 2), 0.99 (3H, d, J = 6.6 Hz, Me_{17}).

Data in agreement with that presented by Tamm.[166]

TES ester 208

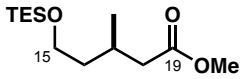

TESCl (2.45 mL, 14.6 mmol) was added dropwise to a solution of alcohol **206** (1.78 g, 12.2 mmol) and imidazole (1.24 g, 18.2 mmol) in CH_2Cl_2 (100 mL) at 0 °C. The reaction mixture was warmed to rt and stirred for 1 h before being cooled to 0 °C, then quenched by addition of $NaHCO_3$ solution (100 mL). The mixture was warmed to rt and diluted with H_2O (50 mL). The phases were separated and the aqueous layer extracted with CH_2Cl_2 (2 x 100 mL). The combined organic phases were dried ($MgSO_4$) and concentrated *in vacuo*. Purification by flash column chromatography (gradient elution: EtOAc/40–60 PE, 1:50 → 1:20) yielded ester **208** (2.99 g, 11.5 mmol, 94%) as a colourless oil.

$\mathbf{R}_f$ 0.76 (EtOAc/40–60 PE, 1:4); **^{1}H NMR** (500 MHz, $CDCl_3$): δ_H 3.70–3.64 (2H, m, H_{15} × 2), 3.69 (3H, s, OC$\underline{H}_3$), 2.38 (1H, dd, J = 14.1, 5.2 Hz, H_{18a}), 2.17–2.09 (1H, m, H_{17}), 2.16 (1H, dd, J = 14.1, 8.2 Hz, H_{18b}), 1.64–1.57 (1H, m, H_{16a}), 1.50–1.43 (1H, m, H_{16b}), 0.98 (9H, t, J = 8.0 Hz, $SiCH_2C\underline{H}_3$ x 3), 0.98 (3H, d, J = 6.5 Hz, Me_{17}), 0.62 (6H, q, J = 8.0 Hz, $SiC\underline{H}_2CH_3$ x 3).

Data in agreement with that presented by Lee.[245]

TES phosphonate 167

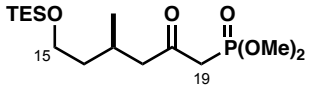

^{n}BuLi (58.4 mL, 1.6 M in hexanes, 93.4 mmol) was added to a solution of dimethyl methylphosphonate (13.9 g, 112 mmol) in THF (350 mL) at −78 °C and the mixture was stirred for 45 min. A solution of ester **208** (9.72 g, 37.3 mmol) in THF (50 mL) was added *via* cannula and the reaction mixture was stirred for 2.5 h. Upon completion, the mixture was quenched with NH_4Cl solution (200 mL), warmed to rt and diluted with water (200 mL). The aqueous phase was extracted with EtOAc (4 x 300 mL), the combined organic layers dried ($MgSO_4$) and concentrated *in vacuo*. The crude product was purified by flash column chromatography (gradient elution: EtOAc/40–60 PE, 1:4 → 3:1) to yield phosphonate **167** (12.4 g, 35.1 mmol, 94%) as a colourless oil.

The title compound can also be accessed *via* the following protocol:

NaH (251 mg, 60% in mineral oil, 6.30 mmol) was suspended in THF (15 mL) at 0 °C. Lactol **221** (500 mg, 2.10 mmol) was dissolved in THF (10 mL) and added *via* cannula. The reaction mixture was stirred at this temperature for 1 h, followed by the dropwise addition of TESCl (0.704 mL, 4.20 mmol). The resulting mixture was warmed to rt and stirred for a further 45 min before being cooled to 0 °C and quenched with NH_4Cl solution (20 mL). Layers were separated and the aqueous phase was extracted with EtOAc (5 x 15 mL). Combined organic phases were dried ($MgSO_4$) and condentrated *in vacuo*. Purification by flash column chromatography (gradient elution: EtOAc/40–60 PE, 1:4 → 3:2) afforded phosphonate **167** (632 mg, 1.79 mmol, 85%) as a colourless oil.

R_f 0.31 (EtOAc/40–60 PE, 1:1); **$[\alpha]_{20}^{D}$** = +4.5 (*c* 1.0, $CHCl_3$); **IR** (thin film, ν_{max} / cm^{-1}): 2956, 2873, 1713, 1457, 1261, 1185, 1088, 1033, 807, 741; **^{1}H NMR** (500 MHz, $CDCl_3$): δ_H 3.76 (6H, d, *J* = 11.2 Hz, P(OC$\underline{H}_3$) x 2), 3.64–3.56 (2H, m, H_{15} x 2), 3.06 (1H, dd, *J* = 18.2, 13.6 Hz, H_{20a}), 3.02 (1H, dd, *J* = 18.2, 13.6 Hz, H_{20b}), 2.60 (1H, dd, *J* = 17.0, 5.4 Hz, H_{18a}), 2.44 (1H, dd, *J* = 17.0, 8.0 Hz, H_{18b}), 2.18–2.09 (1H, m, H_{17}), 1.54–1.47 (1H, m, H_{16a}), 1.41–1.34 (1H, m, H_{16b}), 0.93–0.89 (12H, $SiCH_2C\underline{H}_3$ x 3, Me_{17}), 0.55 (6H, q, *J* = 8.1 Hz, $SiC\underline{H}_2CH_3$ x 3); **^{13}C NMR** (125 MHz, $CDCl_3$): δ_C 201.4, 77.3, 60.6, 51.4, 41.0, 39.3, 25.9, 19.7, 6.7, 4.3; **HRMS** calculated for $C_{15}H_{34}O_5PSi_3$ $[M+H]^+$ 353.1908, found 353.1910.

TBS ester 209

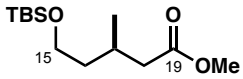

TBSCl (262 mg, 1.74 mmol) was added to a solution of alcohol **206** (182 mg, 1.24 mmol) and imidazole (127 mg, 1.87 mmol) in CH_2Cl_2 (20 mL). A white precipitate formed gradually and the resulting suspension was stirred at rt for 16 h. Upon completion, the reaction was cooled to 0 °C and quenched with NH_4Cl solution (10 mL). The mixture was warmed to rt and stirred for 20 min. The organic phase was separated and the aqueous layer was extracted with CH_2Cl_2 (3 × 5 mL). The combined organic extracts were dried ($MgSO_4$) and concentrated *in vacuo*. The crude product was purified by flash column chromatography (EtOAc/40–60 PE, 1:50) to yield ester **209** (233 mg, 89.5 μmol, 72%) as a colourless oil.

$\mathbf{R}_f$ 0.81 (EtOAc/40–60 PE, 1:4); **^{1}H NMR** (500 MHz, $CDCl_3$): δ_H 3.70–3.65 (2H, m, H_{15} x 2), 3.69 (3H, s, OC$\underline{H}_3$), 2.38 (1H, dd, J = 14.1, 5.1 Hz, H_{18a}), 2.17 (1H, dd, J = 14.1, 8.2 Hz, H_{18b}), 2.16–2.09 (1H, m, H_{17}), 1.62–1.56 (1H, m, H_{16a}), 1.45 (1H, ddd, J = 13.5, 7.0, 6.5 Hz, H_{16b}), 0.98 (3H, d, J = 6.5 Hz, Me_{17}), 0.91 (9H, s, SiC(C$\underline{H}_3$)$_3$), 0.07 (6H, s, Si(C$\underline{H}_3$)$_2$).

Data in agreement with that presented by Lee.[162]

TBS phosphonate 210

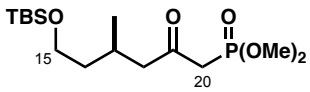

^{n}BuLi (480 μL, 1.6 M in hexanes, 0.768 mmol) was added dropwise to a solution of distilled dimethyl methylphosphonate (100 μL, 0.921 mmol) in THF (3 mL) at −78 °C and the mixture was stirred for 1 h. A solution of ester **209** (79.0 mg, 0.303 mmol) in THF (1 mL) was added *via* cannula and the reaction was stirred at this temperature for 3 h. Upon completion, the mixture was quenched with NH_4Cl solution (3 mL). Layers were separated and the aqueous phase was extracted with CH_2Cl_2 (3 × 3 mL). The combined organic extracts were washed with brine (5 mL), dried ($MgSO_4$) and concentrated *in vacuo*. The crude product was purified by flash column chromatography (gradient elution: EtOAc/40–60 PE, 1:6 → 1:0) to afford phosphonate **210** (91.0 mg, 25.8 μmol, 85% yield) as a colourless oil.

$\mathbf{R}_f$ 0.24 (EtOAc/40–60 PE, 1:3); **^{1}H NMR** (400 MHz, $CDCl_3$): δ_H 3.79 (6H, d, J = 11.2 Hz, P(OC$\underline{H}_3$) x 2), 3.69–3.58 (2H, m, H_{15} x 2), 3.10 (1H, dd, J = 16.1, 13.8 Hz, H_{20a}), 3.04 (1H, dd, J = 16.1, 13.8 Hz, H_{20b}), 2.63 (1H, dd, J = 17.0, 5.4 Hz, H_{18a}), 2.47 (1H, dd, J = 17.0, 8.0 Hz, H_{18b}), 2.23–2.12 (1H, m, H_{17}), 1.58–1.49 (1H, m, H_{16a}), 1.45–1.36 (1H, m, H_{16b}), 0.93 (3H, d, J = 6.7 Hz, Me_{17}), 0.89 (9H, s,

$SiC(C\underline{H}_3)_3$), 0.05 (6H, s, $SiC\underline{H}_3$ x 2).

Data in agreement with that presented by Lee.[162]

2-(1-Adamantanyl)-4-methylphenol (216)

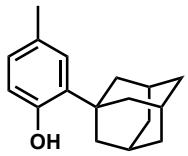

Adamantan-1-ol (5.00 g, 3.28 mmol) was added to a solution of *p*-cresol (3.38 g, 31.3 mmol) in CH_2Cl_2 (30 mL), followed by addition of conc. H_2SO_4 (1.83 mL) over 20 min. The resulting cloudy mixture was stirred for 20 min then diluted with H_2O and slowly neutralised to pH 10 by addition of 10% aqueous NaOH solution (30 mL). The mixture was extracted with CH_2Cl_2 (3 x 100 mL), the combined organic phases dried (Na_2SO_4) and concentrated *in vacuo*. Crude material was triturated with MeOH (30 mL), heated to reflux then cooled to rt and filtered. The solid was washed with MeOH (2 x 50 mL) and the filtrate concentrated *in vacuo* to yield phenol **216** (5.44 g, 22.4 mmol, 72%) as white crystals.

$\mathbf{R}_f$ 0.46 (EtOAc/40–60 PE, 1:5); **^{1}H NMR** (500 MHz, $CDCl_3$): δ_H 7.02 (1H, d, J = 1.9 Hz, Ar$\underline{H}$), 6.87 (1H, dd, J = 8.0, 1.9 Hz, Ar$\underline{H}$), 6.55 (1H, dd, J = 8.0 Hz, Ar$\underline{H}$), 4.53 (1H, s, O$\underline{H}$), 2.28 (3H, s, $ArC\underline{H}_3$), 2.14–2.12 (6H, m, $C\underline{H}_2$ x 3), 2.08–2.06 (3H, m, C$\underline{H}$ x 3), 1.78 (6H, t, J = 3.1 Hz, $C\underline{H}_2$ x 3).

Data in agreement with that presented by Jacobsen.[217]

3-(1-Adamantanyl)-2-hydroxy-5-methylbenzaldehyde (217)

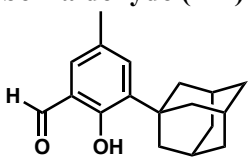

$SnCl_4$ (97 μL, 82.6 μmol) was added dropwise to a stirred solution of phenol **216** (1.00 g, 4.13 mmol) and 2,6-lutidine (382 μL, 3.30 mmol) in PhMe (13 mL) and a yellow precipitate was observed. The bright yellow mixture was stirred at rt for 1.5 h before paraformaldehyde (701 mg, 23.4 mmol) was added in one portion. The reaction was heated to reflux for 4 h, then cooled to rt and filtered through a short pad of silica gel, eluting with EtOAc (50 mL). The filtrate was washed with H_2O (30 mL), 1 N HCl solution (30 mL) and brine (30 mL) and dried (Na_2SO_4). The organic phase was concentrated *in vacuo* to afford aldehyde **217** (1.05 g, 3.88 mmol, 94%) as a yellow solid.

$\mathbf{R}_f$ 0.71 (EtOAc/40–60 PE, 1:5); **^{1}H NMR** (400 MHz, $CDCl_3$): δ_H 11.65 (1H, s, C$\underline{H}$O), 9.83 (1H, s, O$\underline{H}$), 7.28 (1H, d, J = 2.1 Hz, Ar$\underline{H}$), 7.17 (1H, d, J = 2.1 Hz, Ar$\underline{H}$), 2.33 (3H, s, $ArC\underline{H}_3$), 2.16–2.12 (6H, m,

C<u>H</u>$_2$ x 3) 2.11–2.08 (3H, m, C<u>H</u> x 3), 1.79 (6H, t, J = 2.9 Hz, C<u>H</u>$_2$ x 3).

Data in agreement with that presented by Jacobsen.[217]

Imine 219

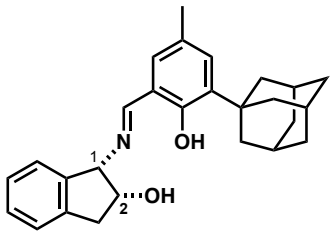

Aldehyde **217** (5.05 g, 18.7 mmol) was suspended in EtOH (200 proof, 75 mL) and the mixture heated to 80 °C until a clear solution was obtained. (1*S*,2*R*)-Aminoindanol (2.93 g, 19.6 mmol) was added and the reaction heated to reflux for 1 h during which a bright yellow precipitate had formed. The mixture was then cooled to rt and left to stand for 16 h. The solid was collected by filtration, washed with cold EtOH (200 proof, 150 mL) and dried *in vacuo* to obtain imine **219** (5.83 g, 14.5 mmol, 78%) as yellow crystals.

R$_f$ 0.49 (EtOAc/40–60 PE, 1:5); **^{1}H NMR** (500 MHz, $CDCl_3$): δ_H 13.07 (1H, s, ArO<u>H</u>), 8.57 (1H, s, C<u>H</u>=N), 7.34–7.17 (4H, m, Ar<u>H</u>), 7.12 (1H, d, J = 2.1 Hz, Ar<u>H</u>), 6.99 (1H, d, J = 2.1 Hz, Ar<u>H</u>), 4.80 (1H, d, J = 5.4 Hz, H_1), 4.70 (1H, dq, J = 7.0, 5.4 Hz, H_2), 3.26 (1H, dd, J = 16.2, 6.0 Hz, H_{3a}), 3.14 (1H, dd, J = 16.2, 5.1 Hz, H_{3b}), 2.31 (3H, s, ArC<u>H</u>$_3$), 2.16–2.12 (6H, m, C<u>H</u>$_2$ x 3), 2.10–2.03 (3H, m, C<u>H</u> x 3), 1.77 (6H, br s, C<u>H</u>$_2$ x 3).

Data in agreement with that presented by Jacobsen.[217]

(1*S*,2*R*)-Jacobsen catalyst 213

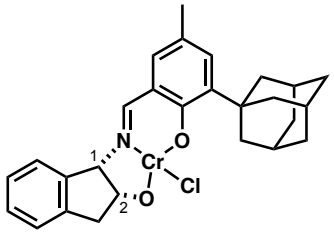

Chromium(II) chloride (2.02 g, 17.4 mmol) was added to imine **219** (5.83 g, 14.5 mmol) in the glove box. The solids were suspended in THF (200 mL) under Ar and stirred at rt for 3 h, then exposed to air and stirred for a further 14 h. The flask was put under an Ar atmosphere followed by addition of 2,6-lutidine (4.04 mL, 34.9 mmol) and the reaction stirred at rt for 3 h during which a colour change to brown was observed. The mixture was diluted with Et_2O (150 mL) and washed with NH_4Cl solution (2 x 200

mL) and brine (2 x 200 mL). The organic phase was dried (Na_2SO_4) and concentrated *in vacuo* to yield catalyst **213** (7.05 g, 14.4 mmol, 99%) as a brown powder.

IR (ν_{max} / cm^{-1}): 2900, 2846, 1615,1536, 1432, 1339, 1308, 1228, 1169, 1081.

Dihydropyran 214

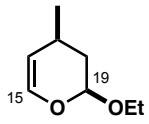

Crotonaldehyde (2.83 mL, 34.2 mmol) and ethyl vinyl ether (16.4 mL, 171 mmol) were added to a flask containing (1*S*,2*R*)-catalyst **213** (416 mg, 0.855 mmol) and activated powdered 4 Å molecular sieves (2.50 g). The resulting brown suspension was stirred for 3 days at rt, then diluted with 30–40 PE (20 mL) and filtered through Celite®, eluting with 30–40 PE (2 x 10 mL). The solvent was removed under reduced pressure (400 mmHg) and the residue was fractionally distilled under reduced pressure (15 mmHg) into a cooled flask (−78 °C). Dihydropyran **214** was obtained as a mixture with crotonaldehyde and was transferred into the next step without further purification.

$\mathbf{R_f}$ 0.87 (EtOAc/40–60 PE, 1:4); **^{1}H NMR** (400 MHz, $CDCl_3$): δ_H 6.24 (1H, dd, *J* = 6.2, 2.2 Hz, H_{15}), 4.92 (1H, dd, *J* = 8.8, 2.2 Hz, H_{19}), 4.65 (1H, ddd, *J* = 6.1, 2.2, 1.4 Hz, H_{16}), 3.93 (1H, dq, *J* = 9.6 Hz, 7.0 Hz, $OC\underline{H}_aH_bCH_3$), 3.58 (1H, dq, *J* = 9.6, 7.0 Hz, $OCH_a\underline{H}_bCH_3$), 2.47–2.37 (1H, m, H_{17}), 2.02 (1H, dddd, *J* = 13.0, 6.2, 2.1, 1.4 Hz, H_{18a}), 1.50 (1H, ddd, *J* = 13.1, 10.0, 8.8 Hz, H_{18b}), 1.25 (3H, t, *J* = 7.1 Hz, $OCH_aH_bC\underline{H}_3$), 1.04 (3H, d, *J* = 7.0 Hz, Me_{17}).

Data in agreement with that presented by Jacobsen.[217]

Mixed acetal 220

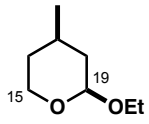

A mixture of dihydropyran **214** and crotonaldehyde was dissolved in Et_2O (30 mL) and Pd/C (1.60 g, 1.50 mmol, 10 wt%) was added. The reaction mixture was placed under an atmosphere of hydrogen (balloon pressure) and stirred for 2 days at rt. Upon completion, the catalyst was removed by filtration through Celite®, eluting with Et_2O (2 x 5 mL). The solvent was removed under reduced pressure (400 mmHg) to give mixed acetal **220** (3.16 g, 21.9 mmol, 74% over 2 steps) as a colourless oil.

R_f 0.82 (EtOAc/40–60 PE, 1:4); **^{1}H NMR** (500 MHz, $CDCl_3$): δ_H 4.35 (1H, dd, *J* = 9.4, 2.2 Hz, H_{19}), 4.00 (1H, ddd, *J* = 11.6, 4.6, 1.7 Hz, H_{15a}), 3.92 (1H, dq, *J* = 9.5, 7.2 Hz, $OC\underline{H}_aH_bCH_3$), 3.53 (1H, dq, *J* = 9.5, 7.0 Hz, $OCH_a\underline{H}_bCH_3$), 3.43 (1H, app td, *J* = 12.0, 2.4 Hz, H_{15b}), 1.82–1.79 (1H, m, *J* = 12.7 Hz, H_{18a}), 1.72–1.59 (1H, m, H_{17}), 1.51–1.48 (1H, m, *J* = 13.2 Hz, H_{16a}), 1.23 (3H, t, *J* = 7.1 Hz, $OCH_aH_bC\underline{H}_3$), 1.23–1.17 (1H, m, H_{18b}), 1.11 (1H, ddd, *J* = 12.7, 12.1, 9.5 Hz, H_{16b}), 0.97 (3H, d, *J* = 6.6 Hz, Me_{17}).

Data in agreement with that presented by Jacobsen for the enantiomer of mixed acetal **220**.[217]

Lactone 207

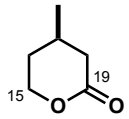

Mixed acetal **220** was dissolved in H_2O/acetone (1:1, 30 mL) and $TsOH{\cdot}H_2O$ (300 mg, 1.58 mmol) was added. The reaction mixture was stirred at rt for 24 h before being quenched with $NaHCO_3$ solution. The layers were separated and the aqueous phase was extracted with Et_2O (3 x 80 mL). Combined organic extracts were dried (Na_2SO_4) and carefully concentrated under reduced pressure (200 torr).

The residue was dissolved in CH_2Cl_2 (450 mL) at rt and PCC (31.9 g, 148 mmol) was added portion-wise. A colour change from orange to dark brown was observed and the reaction mixture was stirred at rt for 20 h. The mixture was diluted with 30–40 PE (50 mL) and filtered through Celite®, eluting with 30–40 PE (2 x 15 mL). The solvent was removed under reduced pressure (430 mmHg) and the residue was purified by flash column chromatography (gradient elution: Et_2O/30–40 PE, 1:5 → 1:0) and fractions containing product **207** were combined. The solvent was removed by careful fractional distillation at ambient pressure to yield lactone **207** as a colourless oil (1.83 g, 16.0 mmol, 64% yield over 2 steps).

R_f 0.22 (EtOAc/40–60 PE, 1:4); $[\alpha]_{20}^{D}$ = +20.0 (*c* 1.0, $CHCl_3$); **^{1}H NMR** (500 MHz, $CDCl_3$): δ_H 4.44 (1H, ddd, *J* = 11.3, 4.7, 4.0 Hz, H_{15a}), 4.29 (1H, ddd, *J* = 11.3, 10.8, 3.8 Hz, H_{15b}), 2.74–2.67 (1H, m, H_{18a}), 2.17–2.07 (2H, m, H_{16a}, H_{18b}), 1.94 (1H, dqd, *J* = 14.2, 4.0, 1.7 Hz, H_{16b}), 1.59–1.51 (1H, m H_{17}), 1.09 (3H, d, *J* = 6.3 Hz, Me_{17}).

Data in agreement with that presented by Evans.[220]

Lactol 221

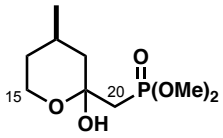

^{n}BuLi (9.86 mL, 1.6 M in hexanes, 6.16 mmol) was added dropwise to a solution of dimethyl methylphosphonate (2.18 g, 17.5 mmol) in THF (30 mL) at −78 °C and the bright yellow mixture was stirred at this temperature for 45 min. Lactone **207** (1.00 g, 8.76 mmol) was dissolved in THF (10 mL) and added to the solution of the anion *via* cannula. The reaction mixture was stirred at −78 °C for 1.5 h until complete, then quenched by the addition of NH_4Cl solution (30 mL) while warming to rt. The phases were separated and the aqueous layer was extracted with EtOAc (3 x 50 mL). Combined organic phases were dried (Na_2SO_4) and the crude product was purified by flash column chromatography (gradient elution: EtOAc/40–60 PE, 1:4 → 1:0). Lactol **221** (1.83 g, 7.68 mmol, 87%) was obtained as a colourless oil which crystallised to a white solid upon standing.

R_f 0.26 (EtOAc); **m.p.** 32–34 °C; **IR** (thin film, ν_{max} / cm^{-1}): 3383, 2953, 1442, 1218, 1183, 1091, 1024, 986, 929, 905, 859, 845, 820, 801, 771, 728; **^{1}H NMR** (500 MHz, $CDCl_3$): δ_H 5.16 (1H, br s, O<u>H</u>), 3.86 (1H, dd, *J* = 12.7, 11.3 Hz, H_{15a}), 3.74 (3H, d, *J* = 11.4 Hz, P(OC<u>H</u>$_3$)), 3.66 (3H, d, *J* = 11.4 Hz, P(OC<u>H</u>$_3$)), 3.61 (1H, dd, *J* = 11.3, 4.7 Hz, H_{15b}), 2.11 (1H, br s, H_{20a}), 2.07 (1H, br s, H_{20b}), 2.03–1.94 (1H, m, H_{17}), 1.79–1.76 (1H, m, H_{18a}), 1.51–1.47 (1H, m, H_{16a}), 1.13 (1H, dddd, *J* = 12.7, 12.7, 12.7, 4.7 Hz, H_{16b}), 1.00 (1H, dd, *J* = 12.9, 12.3 Hz, H_{18b}), 0.84 (3H, d, *J* = 7.1 Hz, Me_{17}); **^{13}C NMR** (125 MHz, $CDCl_3$): δ_C 94.6, [94.5], 60.9, 53.3, 51.6, 44.6, 38.2, [37.2], 33.5, 25.1, [25.0], 22.0; **HRMS** calculated for $C_9H_{18}O_4P$ [M−H_2O] 221.0943, found 221.0947.

Distinguishable resonances of the diastereomers in the ^{13}C NMR spectrum are given in brackets.

Enone 223

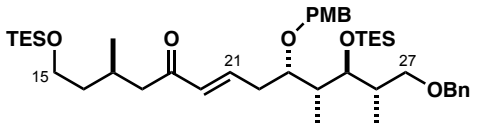

A solution of phosphonate **167** (7.26 g, 20.6 mmol) in THF (80 mL) was added *via* cannula to a suspension of $Ba(OH)_2$ (4.71 g, 27.4 mmol) in THF (60 mL) and the mixture stirred at rt for 1 h. A solution of aldehyde **168** (10.1 g, 19.6 mmol) in THF/H_2O (40:1, 120 mL) was added *via* cannula and the reaction stirred for 16 h. Upon completion, the mixture was quenched with NH_4Cl solution (200 mL) and diluted with H_2O (150 mL). The aqueous phase was extracted with EtOAc (3 x 300 mL), dried ($MgSO_4$)

and concentrated *in vacuo*. Crude material was purified by flash column chromatography (gradient elution: EtOAc/40–60 PE, 1:30 → 1:20) to yield enone **223** (12.2 g, 16.5 mmol, 85%, > 20:1 *E*/*Z*) as a colourless oil.

R_f 0.54 (EtOAc/40–60 PE, 1:10); **$[\alpha]_{20}^{D}$** = −14.4 (*c* 1.0, $CHCl_3$); **IR** (thin film, ν_{max} / cm^{-1}): 2948, 2913, 2877, 1669, 1613, 1514, 1457, 1415, 1376, 1298, 1243, 1169, 1092, 1041, 1009, 973, 822, 737, 694; **^{1}H NMR** (500 MHz, $CDCl_3$): δ_H 7.38–7.34 (4H, m, PhH), 7.32–7.28 (1H, m, PhH), 7.26 (2H, d, *J* = 8.5 Hz, ArH), 6.88 (2H, d, *J* = 8.5 Hz, ArH), 6.82 (1H, dt, *J* = 15.8, 7.3 Hz, H_{21}), 6.17 (1H, d, *J* = 15.8 Hz, H_{20}), 4.53 (1H, d, *J* = 11.1 Hz, ArCH_aH_bO), 4.50 (2H, ABq, *J* = 12.2 Hz, PhCH_2O), 4.44 (1H, d, *J* = 11.1 Hz, ArCH_aH_bO), 3.82 (3H, s, ArOCH_3), 3.78–3.71 (2H, m, H_{23}, H_{25}), 3.70–3.61 (3H, m, H_{15} x 2, H_{27a}), 3.31 (1H, app t, *J* = 8.6 Hz, H_{27b}), 2.60–2.51 (2H, m, H_{18a}, H_{22a}), 2.49–2.44 (1H, m, H_{22b}), 2.36 (1H, dd, *J* = 15.4, 8.5 Hz, H_{18b}), 2.22–2.16 (1H, m, H_{17}), 2.11–2.05 (1H, m, H_{26}) 1.79–1.72 (1H, m, H_{24}), 1.62–1.56 (1H, m, H_{16a}), 1.49–1.42 (1H, m, H_{16b}), 1.05 (3H, d, *J* = 7.0 Hz, Me_{26}), 1.00–0.93 (24H, m, Me_{17}, Me_{24}, $SiCH_2CH_3$ x 6), 0.66–0.60 (12H, m, $SiCH_2CH_3$ x 6); **^{13}C NMR** (125 MHz, $CDCl_3$): δ_C 199.9, 159.1, 143.7, 138.8, 132.5, 130.9, 128.9, 128.3, 127.5, 127.4, 113.8, 78.3, 77.1, 73.0, 72.2, 71.5, 60.9, 55.3, 47.6, 42.1, 39.9, 37.0, 36.0, 26.7, 20.0, 16.1, 11.1, 7.2, 6.8, 5.6, 4.4; **HRMS** calculated for $C_{43}H_{73}O_6Si_2$ $[M+H]^+$ 741.4940, found 741.4935.

Allylic alcohol 224

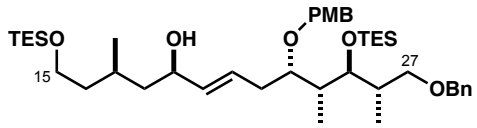

(*S*)-Me-CBS catalyst **138** (673 μL, 1.0 M in PhMe, 0.673 mmol) was added to a solution of enone **223** (4.99 g, 6.73 mmol) in THF (100 mL) at –20 °C and stirred for 10 min. $BH_3{\cdot}SMe_2$ (761 μL, 15.4 mmol) was added dropwise, the reaction warmed to –10 °C and stirred for 1.5 h before being carefully quenched with MeOH (20 mL). The mixture was warmed to rt and stirred for a further 15 min before concentrating *in vacuo*. The residue was redissolved in MeOH (20 mL), then concentrated *in vacuo* and the procedure repeated three times. Purification by flash column chromatography (gradient elution: EtOAc/40–60 PE, 1:30 → 1:10) afforded allylic alcohol **224** (4.97 g, 6.69 mmol, 99%, 13:1 *dr*) as a colourless oil.

R_f 0.44 (EtOAc/40–60 PE, 1:5); **$[\alpha]_{20}^{D}$** = −5.2 (*c* 1.0, $CHCl_3$); **IR** (thin film, ν_{max} / cm^{-1}): 2956, 2869, 1616, 1518, 1454, 1378, 1301, 1244, 1171, 1082, 1033, 996, 963, 820, 808, 729, 696; **^{1}H NMR** (500 MHz, $CDCl_3$): δ_H 7.34–7.35 (4H, m, PhH), 7.32–7.28 (1H, m, PhH), 7.27 (2H, d, *J* = 8.4 Hz, ArH), 6.88 (2H, d, *J* = 8.4 Hz, ArH), 5.64 (1H, ddd, *J* = 15.2, 8.0, 7.0 Hz, H_{21}), 5.54 (1H, dd, *J* = 15.2, 6.8 Hz, H_{20}), 4.57 (1H, d, *J* = 11.1 Hz, ArCH_aH_bO), 4.52 (1H, d, *J* = 12.2 Hz, PhCH_aH_bO), 4.49 (1H, d, *J* = 12.2 Hz,

$PhCH_aH_bO$), 4.41 (1H, d, J = 11.1 Hz, $ArCH_aH_bO$), 4.21–4.14 (1H, m, H_{19}) 3.82 (3H, s, $ArOCH_3$), 3.74 (1H, dd, J = 7.0, 3.2 Hz, H_{25}), 3.72–3.63 (4H, m, H_{15} x 2, H_{23}, H_{27b}), 3.32 (1H, dd, J = 8.8, 8.8 Hz, H_{27b}), 2.44 (1H, ddd, J = 14.2, 7.3, 6.0 Hz, H_{22a}), 2.29 (1H, ddd, J = 14.2, 7.2, 7.2 Hz, H_{22b}), 2.13–2.05 (1H, m, H_{26}), 1.83–1.63 (4H, m, H_{16a}, H_{17}, H_{24}, OH) 1.50–1.37 (3H, m, H_{16b}, H_{18} x 2), 1.06 (3H, d, J = 7.0 Hz, Me_{26}), 1.01–0.94 (24H, m, Me_{17}, Me_{24}, $SiCH_2CH_3$ x 6), 0.63 (12H, J = 7.9 Hz, $SiCH_2CH_3$ x 6); **^{13}C NMR** (125 MHz, $CDCl_3$): δ_C 158.8, 138.8, 135.4, 131.3, 128.7, 128.2, 128.0, 127.3, 127.2, 113.5, 78.6, 77.1, 72.9, 72.1, 70.9, 70.7, 60.9, 55.2, 44.4, 41.4, 39.4, 36.7, 35.1, 26.3, 20.3, 16.1, 10.6, 7.1, 6.7, 5.5, 4.3; **HRMS** calculated for $C_{43}H_{78}O_6Si_2N$ $[M+NH_4]^+$ 760.5362, found 760.5360.

(*R*)-Mosher ester 225

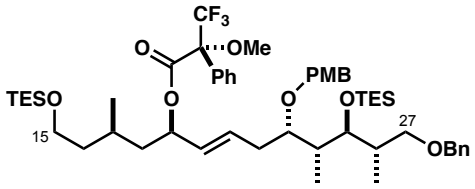

DCC (67 µL, 1.0 M in CH_2Cl_2, 67.0 µmol) and DMAP (8.0 mg, 67.0 µmol) were added sequentially to a solution of allylic alcohol **224** (10.4 mg, 14.0 µmol) and (*R*)-(+)-α-methoxy-α-(trifluoromethyl)-phenylacetic acid (16.0 mg, 68.3 µmol) in CH_2Cl_2 (2 mL) and the mixture was stirred at rt for 17 h. The white suspension was concentrated *in vacuo* and the residue was purified by flash column chromatography (gradient elution: EtOAc/40–60 PE, 0:1 → 1:30) to afford (*R*)-Mosher ester **225** as a colourless oil (10.2 mg, 10.6 µmol, 76%).

R_f 0.66 (EtOAc/40–60 PE, 1:8); **^{1}H NMR** (400 MHz, $CDCl_3$): δ_H 7.53–7.48 (2H, m, PhH), 7.40–7.35 (3H, m, PhH), 7.34–7.29 (4H, m, PhH), 7.29–7.27 (1H, m, PhH), 7.24 (2H, d, J = 8.6 Hz, ArH), 6.85 (2H, d, J = 8.6 Hz, ArH), 5.80 (1H, dt, J = 15.2, 7.0 Hz, H_{21}), 5.55–5.48 (1H, m, H_{19}), 5.39 (1H, dd, J = 15.2, 7.9 Hz, H_{20}), 4.50 (1H, d, J = 11.0 Hz, $ArCH_aH_bO$), 4.48 (1H, d, J = 12.0 Hz, $PhCH_aH_bO$), 4.44 (1H, d, J = 12.0 Hz, $PhCH_aH_bO$), 4.37 (1H, dd, J = 11.0 Hz, $ArCH_aH_bO$), 3.80 (3H, s, $ArOCH_3$), 3.70 (1H, dd, J = 7.1, 3.3 Hz, H_{25}), 3.65–3.57 (4H, m, H_{15} x 2, H_{23}, H_{27a}), 3.53 (3H, s, OCH_3), 3.29 (1H, dd, J = 8.9, 8.5 Hz, H_{27b}), 2.39 (1H, dt, J = 14.2, 6.5 Hz, H_{22a}), 2.25 (1H, dt, J = 14.2, 7.1 Hz, H_{22b}), 2.11–2.08 (1H, m, H_{26}), 1.75–1.60 (4H, m, H_{16a}, H_{17}, H_{18a}, H_{24}), 1.42–1.28 (2H, m, H_{16b}, H_{18b}), 1.02 (3H, d, J = 6.8 Hz, Me_{26}), 0.97–0.91 (24H, m, Me_{17}, Me_{24}, $SiCH_2CH_3$ x 6), 0.62–0.55 (12H, m, $SiCH_2CH_3$ x 6).

(*S*)-Mosher ester 226

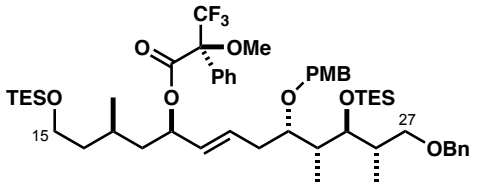

DCC (67 μL, 1.0 M in CH_2Cl_2, 67.0 μmol) and DMAP (8.0 mg, 67.0 μmol) were added sequentially to a solution of allylic alcohol **224** (9.8 mg, 13.2 μmol) and (*S*)-(+)-α-methoxy-α-(trifluoromethyl)-phenylacetic acid (16.0 mg, 68.3 μmol) in CH_2Cl_2 (2 mL) and the mixture was stirred at rt for 17 h. The white suspension was concentrated *in vacuo* and the residue was purified by flash column chromatography (gradient elution: EtOAc/40–60 PE, 0:1 → 1:30) to afford (*R*)-Mosher ester **226** as a colourless oil (6.2 mg, 6.5 μmol, 49%).

R_f 0.64 (EtOAc/40–60 PE, 1:8); **^{1}H NMR** (400 MHz, $CDCl_3$): δ_H 7.55–7.50 (2H, m, PhH), 7.39–7.35 (3H, m, PhH), 7.34–7.31 (4H, m, PhH), 7.29–7.27 (1H, m, PhH), 7.24 (2H, d, *J* = 8.5 Hz, ArH), 6.85 (2H, d, *J* = 8.5 Hz, ArH), 5.86 (1H, dt, *J* = 14.2, 7.0 Hz, H_{21}), 5.56–5.47 (2H, m, H_{19}, H_{20}), 4.51 (1H, d, *J* = 11.0 Hz, PhCH_aH_bO), 4.48 (1H, d, *J* = 12.1 Hz, ArCH_aH_bO), 4.43 (1H, d, *J* = 12.1 Hz, ArCH_aH_bO), 4.38 (1H, d, *J* = 11.0 Hz, PhCH_aH_bO), 3.80 (3H, s, ArOCH_3), 3.71 (1H, dd, *J* = 6.9, 3.3 Hz, H_{25}), 3.65–3.57 (4H, m, H_{12} x 2, H_{23}, H_{27a}), 3.52 (3H, s, OCH_3), 3.28 (1H, dd, *J* = 8.7, 8.7 Hz, H_{27b}), 2.43 (1H, dt, *J* = 14.3, 6.3 Hz, H_{22a}), 2.28 (1H, dt, *J* = 14.3, 6.9 Hz, H_{22b}), 2.09–2.00 (1H, m, H_{26}), 1.74–1.65 (1H, m, H_{24}), 1.63–1.51 (3H, m, H_{16a}, H_{17}, H_{18a}), 1.37–1.27 (2H, m, H_{16b}, H_{18b}), 1.02 (3H, d, *J* = 6.9 Hz, Me_{26}), 0.97–0.90 (21H, m, Me_{24}, $SiCH_2CH_3$ x 6), 0.85 (3H, d, *J* = 6.2 Hz, Me_{17}), 0.63–0.56 (12H, m, $SiCH_2CH_3$ x 6).

Methyl ether 227

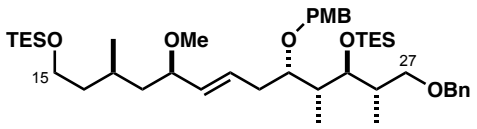

Sodium hydride (3.99 g, 60% dispersion in mineral oil) was washed with hexane (2 x 20 mL) and dried *in vacuo* before adding THF (50 mL). The suspension was cooled to 0 °C and a solution of allylic alcohol **224** (10.6 g, 14.2 mmol) in THF (70 mL) was added *via* cannula. The mixture was left to stir for 1 h before adding MeI (7.09 mL, 114 mmol) and warming to rt. The reaction was stirred for 4 h until complete and carefully quenched with MeOH (50 mL) at 0 °C. The mixture was warmed to rt, poured into brine (200 mL), diluted with H_2O (100 mL) and extracted with EtOAc (2 x 250 mL). Combined organic phases were dried ($MgSO_4$), concentrated *in vacuo* and purified by flash column chromatography

(gradient elution: EtOAc/40–60 PE, 0:1 → 1:22) to give methyl ether **227** (9.57 g, 12.6 mmol, 89%) as a colourless oil.

R_f 0.79 (EtOAc/40–60 PE, 1:8); **$[\alpha]_{20}^{D}$** = +3.6 (*c* 1.0, $CHCl_3$); **IR** (thin film, ν_{max} / cm^{-1}): 2956, 2875, 1613, 1514, 1455, 1248, 1091, 1041, 1011, 971, 818, 738; **^{1}H NMR** (400 MHz, $CDCl_3$): δ_H 7.35–7.33 (4H, m, PhH), 7.31–7.27 (1H, m, PhH), 7.26 (2H, d, *J* = 8.3 Hz, ArH), 6.87 (2H, d, *J* = 8.3 Hz, ArH), 5.58 (1H, dt, *J* = 15.2, 7.4 Hz, H_{21}), 5.29 (1H, dd, *J* = 15.2, 8.6 Hz, H_{20}), 4.58 (1H, d, *J* = 11.1 Hz, $ArCH_aH_bO$), 4.51 (1H, d, *J* = 12.2 Hz, $PhCH_aH_bO$), 4.46 (1H, d, *J* = 12.2 Hz, $PhCH_aH_bO$), 4.40 (1H, *J* = 11.1 Hz, $ArCH_aH_bO$), 3.81 (3H, s, $ArOCH_3$), 3.74 (1H, dd, *J* = 7.8, 2.4 Hz, H_{25}), 3.72–3.59 (4H, m, H_{15} × 2, H_{23}, H_{27a}), 3.56 (1H, app q, *J* = 7.4 Hz, H_{19}), 3.29 (1H, app t, *J* = 8.9 Hz, H_{27b}), 3.22 (3H, s, OMe), 2.48 (1H, dt, *J* = 14.2, 5.4 Hz, H_{22a}), 2.29 (1H, dt, *J* = 14.2, 7.8 Hz, H_{22b}), 2.13–2.06 (1H, m, H_{26}), 1.83–1.75 (1H, m, H_{24}), 1.72–1.58 (2H, m, H_{16a}, H_{17}), 1.51–1.33 (3H, m, H_{16b}, H_{18} x 2), 1.05 (3H, d, *J* = 6.9 Hz, Me_{26}), 0.99–0.93 (21H, m, Me_{24}, $SiCH_2CH_3$ x 6), 0.89 (3H, d, *J* = 6.7 Hz, Me_{17}), 0.65–0.58 (12H, m, $SiCH_2CH_3$ x 6); **^{13}C NMR** (100 MHz, $CDCl_3$): δ_C 158.6, 138.5, 132.7, 131.0, 130.3, 128.3, 127.9, 127.1, 127.0, 113.3, 80.4, 78.1, 76.8, 72.7, 71.7, 70.6, 60.6, 55.4, 54.9, 42.7, 40.8, 39.7, 36.5, 34.8, 25.8, 19.6, 15.7, 10.0, 6.8, 6.5, 5.3, 4.1; **HRMS** calculated for $C_{44}H_{76}O_6Si_2Na$ $[M+Na]^+$ 779.5073, found 779.5057.

Alcohol 238

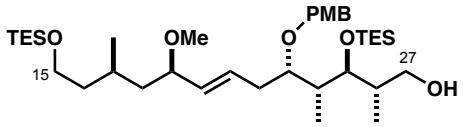

A solution of LiDBB (20.0 mL, 1.0 M in THF, 20.0 mmol) was added to a solution of methyl ether **227** (3.03 g, 4.00 mmol) in degassed THF (145 mL) at −78 °C. The reaction was stirred for 20 min before being quenched by addition of NH_4Cl solution and warming to rt. The phases were separated and the aqueous layer extracted with EtOAc (3 x 100 mL). Combined organic extracts were dried (Na_2SO_4), concentrated *in vacuo* and purified by flash column chromatography (gradient elution: EtOAc/40–60 PE, 1:50 → 1:8) to yield alcohol **238** (2.04 g, 3.20 mmol, 77%, 96% BRSM) as a colourless oil.

R_f 0.51 (EtOAc/40–60 PE, 1:3); **$[\alpha]_{20}^{D}$** = +11.0 (*c* 1.0, $CHCl_3$); **IR** (thin film, ν_{max} / cm^{-1}): 3452, 2960, 2877, 1615, 1514, 1459, 1417, 1378, 1302, 1251, 1169, 1088, 1038, 1011, 969, 820, 747; **^{1}H NMR** (400 MHz, $CDCl_3$): δ_H 7.24 (2H, d, *J* = 8.6 Hz, ArH), 6.88 (2H, d, *J* = 8.6 Hz, ArH), 5.59 (1H, dt, *J* = 15.2, 6.6 Hz, H_{21}), 5.33 (1H, dd, *J* = 15.2, 8.2 Hz, H_{20}), 4.59 (1H, d, *J* = 11.1 Hz, $ArCH_aH_bO$), 4.50, (1H, *J* = 11.1 Hz, $ArCH_aH_bO$), 3.81 (3H, s, $ArOCH_3$), 3.82–3.77 (2H, m, H_{25}, H_{27a}), 3.69–3.52 (5H, m, H_{15} × 2, H_{19}, H_{23}, H_{27b}), 3.24 (3H, s, OCH_3), 2.66 (1H, dd, *J* = 7.3, 4.0 Hz, OH), 2.51 (1H, dt, *J* = 14.1, 5.4 Hz, H_{22a}), 2.38 (1H, dt, *J* = 14.1, 7.9 Hz, H_{22b}), 1.91–1.85 (2H, m, H_{24}, H_{26}), 1.71–1.55 (2H, m, H_{16a}, H_{18a}),

1.52–1.33 (3H, m, H_{16b}, H_{17}, H_{18b}), 1.07 (3H, d, J = 6.9 Hz, Me_{26}), 0.99–0.94 (21H, m, Me_{24}, $SiCH_2C\underline{H}_3$ x 6), 0.89 (3H, d, J = 6.5 Hz, Me_{17}), 0.69–0.57 (12H, m, $SiC\underline{H}_2CH_3$ x 6); **^{13}C NMR** (125 MHz, $CDCl_3$): δ_C 159.0, 133.5, 131.1, 130.0, 128.6, 113.7, 80.7, 79.8, 78.4, 70.7, 65.3, 61.0, 55.9, 55.3, 43.1, 42.0, 40.0, 36.2, 34.9, 26.2, 20.0, 16.6, 9.9, 7.0, 6.8, 5.4, 4.5; **HRMS** calculated for $C_{37}H_{74}O_6Si_2N$ $[M+NH_4]^+$ 684.5049, found 684.5048.

Allyl carbonate 241

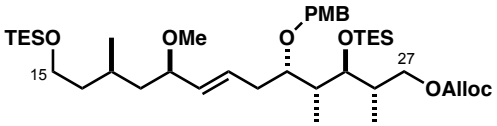

Allyl chloroformate (5.00 mL, 47.2 mmol) was added dropwise to a solution of alcohol **238** (3.16 g, 4.72 mmol) in CH_2Cl_2/pyr (1:1, 60 mL) at −60 °C and a white precipitate was observed. The resulting suspension was let to gradually warm to −20 °C and stirred at this temperature for 3 h before being quenched with $NaHCO_3$ solution (30 mL) and stirred until bubbling had ceased. The aqueous phase was extracted with CH_2Cl_2 (3 x 100 mL) and the combined organic extracts dried (Na_2SO_4), concentrated *in vacuo* and purified by flash column chromatography (gradient elution: EtOAc/40–60 PE, 1:50 → 1:15). Allyl carbonate **241** (3.12 g, 4.15 mmol, 88%) was obtained as a colourless oil.

$\mathbf{R}_f$ 0.45 (EtOAc/40–60 PE, 1:10); $[\boldsymbol{\alpha}]_{\boldsymbol{20}}^{\boldsymbol{D}}$ = +5.0 (*c* 1.0, $CHCl_3$); **IR** (thin film, ν_{max} / cm^{-1}): 2960, 2877, 1746, 1514, 1461, 1294, 1253, 1090, 1037, 1009, 969, 737, 727; **^{1}H NMR** (500 MHz, $CDCl_3$): δ_H 7.26 (2H, d, J = 8.5 Hz, Ar$\underline{H}$), 6.89 (2H, d, J = 8.5 Hz, Ar$\underline{H}$), 6.00–5.92 (1H, m, C$\underline{H}$=CH_2), 5.62–5.56 (1H, m, H_{21}), 5.38 (1H dd, J = 17.1, 1.2 Hz, CH=C$\underline{H}_a$$H_b$), 5.34 (1H, dd, J = 15.5, 7.1 Hz, H_{20}), 5.29 (1H, dd, J = 10.3, 1.2 Hz, CH=$CH_a\underline{H}_b$), 4.64 (2H, d, J = 5.7 Hz, OC$\underline{H}_2$), 4.60 (1H, d, J = 11.1 Hz, ArC$\underline{H}_a$$H_b$O), 4.40 (1H, J = 11.1 Hz, Ar$CH_a\underline{H}_b$O), 4.32 (1H, dd, J = 10.6, 4.1 Hz, H_{27a}), 3.97 (1H, dd, J = 10.6, 9.3 Hz, H_{27b}), 3.82 (3H, s, ArOC$\underline{H}_3$), 3.74 (1H, dd, J = 7.4, 2.6 Hz, H_{25}), 3.70–3.62 (3H, m, H_{15} × 2, H_{23}), 3.60–3.55 (1H, m, H_{19}), 3.25 (3H, s, OC$\underline{H}_3$), 2.51 (1H, dt, J = 14.0, 5.5 Hz, H_{22a}), 2.31 (1H, dt, J = 14.0, 7.9 Hz, H_{22b}), 2.16–2.11 (1H, m, H_{26}), 1.84–1.77 (1H, m, H_{24}), 1.71–1.60 (2H, m, $H_{17,}$ H_{18a}), 1.51–1.36 (2H, m, H_{16a} x 2, H_{18b}), 1.06 (3H, d, J = 6.9 Hz, Me_{26}), 1.00–0.96 (21H, m, Me_{24}, $SiCH_2C\underline{H}_3$ x 6), 0.91 (3H, d, J = 6.9 Hz, Me_{17}), 0.67–0.59 (12H, m, $SiC\underline{H}_2CH_3$ x 6); **^{13}C NMR** (125 MHz, $CDCl_3$): δ_C 158.9, 155.2, 133.3, 131.8, 131.3, 130.3, 128.7, 118.8, 113.7, 80.8, 78.4, 77.0, 70.9, 69.9, 68.3, 61.0, 55.8, 55.3, 43.1, 41.3, 40.0, 35.7, 35.0, 26.2, 20.0, 16.0, 10.1, 7.1, 6.8, 5.6, 4.5; **HRMS** calculated for $C_{41}H_{78}O_8Si_2N$ $[M+NH_4]^+$ 768.5260, found 768.5253.

Alcohol 242

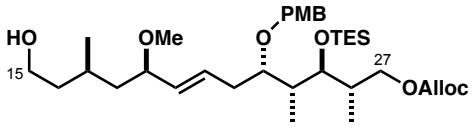

Acetic acid (10 mL) was added dropwise to a solution of TES ether **241** (4.95 g, 6.58 mmol) in THF/H_2O (3:1, 10 mL) at 0 °C. The mixture was warmed to rt and stirred for 3.5 h. Upon completion, the reaction mixture was cannulated into $NaHCO_3$ solution (250 mL) at 0 °C and stirred until bubbling had ceased. The layers were separated and the aqueous phase extracted with EtOAc (3 x 300 mL). The combined organic extracts were dried (Na_2SO_4), concentrated *in vacuo* and purified by flash column chromatography (gradient elution: EtOAc/40–60 PE, 1:8 → 1:3) to afford alcohol **242** (3.41 g, 5.35 mmol, 81%, 89% BRSM) as a colourless oil.

R_f 0.24 (EtOAc/40–60 PE, 1:2); **$[\alpha]_{20}^{D}$** = +2.0 (*c* 1.0, $CHCl_3$); **IR** (thin film, ν_{max} / cm^{-1}): 3464, 2956, 2877, 1742, 1512, 1457, 1395, 1376, 1292, 1253, 1167, 1092, 1041, 1009, 969, 822, 791, 735; **^{1}H NMR** (500 MHz, $CDCl_3$): δ_H 7.26 (2H, d, *J* = 8.6 Hz, ArH), 6.89 (2H, d, *J* = 8.6 Hz, ArH), 6.00–5.92 (1H, m, CH=CH_2), 5.64–5.58 (1H, m, H_{21}), 5.38 (1H, dd, *J* = 17.1, 1.4 Hz, CH=CH_aH_b), 5.34 (1H, dd, *J* = 15.4, 8.3 Hz, H_{20}), 5.29 (1H, dd, *J* = 10.4, 1.4 Hz, CH=CH_aH_b), 4.64 (2H, d, *J* = 5.7 Hz, OCH_2), 4.59 (1H, d, *J* = 11.1 Hz, ArCH_aH_bO), 4.40 (1H, *J* = 11.1 Hz, ArCH_aH_bO), 4.32 (1H, dd, *J* = 10.6, 4.1 Hz, H_{27a}), 3.96 (1H, dd, *J* = 10.5, 8.9 Hz, H_{27b}), 3.83 (3H, s, ArOCH_3), 3.74 (1H, dd, *J* = 7.5, 2.6 Hz, H_{25}), 3.72–3.64 (3H, m, H_{15} x 2, H_{23}), 3.62–3.58 (1H, m, H_{19}), 3.26 (3H, s, OCH_3), 2.52 (1H, dt, *J* = 14.1, 7.0 Hz, H_{22a}), 2.32 (1H, dt, *J* = 14.1, 7.8 Hz, H_{22b}), 2.17–2.10 (1H, m, H_{26}), 1.82–1.77 (1H, m, H_{24}), 1.75–1.69 (1H, m, H_{17}), 1.67–1.61 (1H, m, H_{18a}), 1.56–1.49 (1H, m, H_{16a}), 1.47–1.40 (2H, m, $H_{16b,}$ H_{18b}), 1.06 (3H, d, *J* = 6.8 Hz, Me_{26}), 0.97 (9H, t, *J* = 8.0 Hz, $SiCH_2CH_3$ x 3), 0.97 (3H, d, *J* = 7.0 Hz, Me_{24}), 0.94 (3H, d, *J* = 6.7 Hz, Me_{17}), 0.65 (6H, q, *J* = 8.0 Hz, $SiCH_2CH_3$ x 3); **^{13}C NMR** (125 MHz, $CDCl_3$): δ_C 158.9, 155.3, 133.1, 131.7, 131.2, 130.4, 128.6, 118.8, 113.7, 80.7, 78.3, 77.0, 70.8, 69.8, 68.3, 61.0, 55.8, 55.3, 42.8, 41.2, 39.8, 35.6, 34.9, 26.2, 20.2, 16.1, 10.2, 7.1, 5.6; **HRMS** calculated for $C_{35}H_{64}O_8SiN$ $[M+NH_4]^+$ 654.4396, found 654.4393.

Aldehyde 161

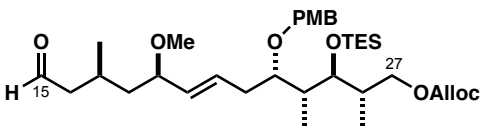

Dess–Martin periodinane (3.19 g, 7.52 mmol) was added portion-wise to a stirred mixture of alcohol **242** (3.99 g, 6.27 mmol) and $NaHCO_3$ (2.11 g, 25.1 mmol) in CH_2Cl_2 (130 mL) at 0 °C. The bright yellow

reaction slurry was stirred at this temperature for 1 h until complete. The mixture was quenched with $Na_2S_2O_3$ solution (150 mL) and stirred for 45 min until the yellow colour had dissipated. After diluting with H_2O (100 mL), the phases were separated and the aqueous layer was extracted with CH_2Cl_2 (5 x 100 mL). Combined organic phases were dried ($MgSO_4$), concentrated *in vacuo* and purified by flash column chromatography (gradient elution: EtOAc/40–60 PE, 1:20 → 1:4) to yield aldehyde **161** (3.39 g, 5.34 mmol, 85%) as a colourless oil.

R_f 0.58 (EtOAc/40–60 PE, 1:2); **$[\alpha]_{20}^{D}$** = +1.1 (*c* 1.0, $CHCl_3$); **IR** (thin film, ν_{max} / cm^{-1}): 2956, 2873, 1750, 1726, 1609, 1510, 1463, 1399, 1378, 1294, 1247, 1175, 1098, 1037, 1013, 969, 822, 791, 739; **^{1}H NMR** (500 MHz, $CDCl_3$): δ_H 9.74 (1H, t, *J* = 2.0 Hz, C<u>H</u>O), 7.26 (2H, d, *J* = 8.6 Hz, Ar<u>H</u>), 6.89 (2H, d, *J* = 8.6 Hz, Ar<u>H</u>), 6.00–5.92 (1H, m, C<u>H</u>=CH_2), 5.65–5.59 (1H, m, H_{21}), 5.38 (1H, dd, *J* = 17.2, 1.2, Hz, CH=C<u>H_a</u>H_b), 5.34 (1H, dd, *J* = 15.5, 7.1 Hz, H_{20}), 5.29 (1H, dd, *J* = 10.4, 1.2 Hz, CH=CH_a<u>H_b</u>), 4.64 (2H, d, *J* = 5.7 Hz, OC<u>H_2</u>), 4.59 (1H, d, *J* = 10.9 Hz, ArC<u>H_a</u>H_bO), 4.41 (1H, *J* = 10.9 Hz, ArCH_a<u>H_b</u>O), 4.32 (1H, dd, *J* = 10.6, 4.2 Hz, H_{27a}), 3.96 (1H, dd, *J* = 10.6, 9.1 Hz, H_{27b}), 3.82 (3H, s, ArOC<u>H_3</u>), 3.74 (1H, dd, *J* = 7.6, 2.6 Hz, H_{25}), 3.70–3.67 (1H, m, H_{23}), 3.57–3.53 (1H, m, H_{19}), 3.24 (3H, s, OC<u>H_3</u>), 2.54–2.42 (2H, m, H_{16a}, H_{22a}), 2.35–2.22 (3H, m, H_{16b}, H_{17}, H_{22b}), 2.17–2.10 (1H, m, H_{26}), 1.83–1.76 (1H, m, H_{24}), 1.63–1.57 (1H, m, H_{18a}), 1.42 (1H, dt, *J* = 13.9, 6.1 Hz, H_{18b}), 1.06 (3H, d, *J* = 6.9 Hz, Me_{26}), 1.00–0.96 (15H, m, Me_{17}, Me_{24}, $SiCH_2C$<u>H_3</u> x 3), 0.67–0.62 (6H, m, SiC<u>H_2</u>CH_3 x 3); **^{13}C NMR** (125 MHz, $CDCl_3$): δ_C 202.8, 159.0, 155.2, 132.8, 131.8, 131.2, 130.8, 128.6, 118.8, 113.7, 80.2, 78.3, 77.1, 70.8, 69.8, 68.3, 55.7, 55.3, 50.8, 42.7, 41.4, 35.6, 35.0, 24.8, 20.5, 16.0, 10.2, 7.1, 5.6; **HRMS** calculated for $C_{35}H_{58}O_8SiNa$ $[M+Na]^+$ 657.3793, found 657.3774.

Enone 229

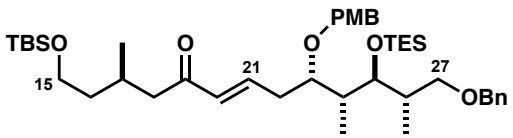

THF (0.8 mL) was added to a flask containing $Ba(OH)_2$ (34.8 mg, 0.203 mmol) and sonicated for 5 min. A solution of phosphonate **210** (58.0 mg, 0.165 mmol) in THF (1.2 mL) was added *via* cannula to the resulting white suspension and the mixture stirred at rt for 45 min. A solution of aldehyde **168** (81.0 mg, 0.157 mmol) in THF/H_2O (40:1, 2 mL) was added *via* cannula and the reaction stirred for 16 h. Upon completion, the mixture was diluted with THF (2 mL) and quenched with NH_4Cl solution (3 mL). The aqueous phase was extracted with Et_2O (3 x 5 mL), dried ($MgSO_4$) and concentrated *in vacuo*. Crude material was purified by flash column chromatography (EtOAc/40–60 PE, 1:10) to yield enone **229** (110 mg, 0.148 mmol, 94%, > 20:1 *E*/*Z*) as a pale yellow oil.

R_f 0.69 (EtOAc/40–60 PE, 1:5); **$[\alpha]_{20}^{D}$** = −13.2 (*c* 1.0, $CHCl_3$); **IR** (thin film, ν_{max} / cm^{-1}): 2952, 2929, 2877, 2849, 1699, 1675, 1627, 1615, 1516, 1459, 1365, 1296, 1250, 1172, 1092, 1037, 1009, 977, 830, 778, 737, 699; **^{1}H NMR** (500 MHz, $CDCl_3$): δ_H 7.34–7.33 (4H, m, PhH), 7.30–7.26 (1H, m, PhH), 7.24 (2H, d, *J* = 8.6 Hz, ArH), 6.87 (2H, d, *J* = 8.6 Hz, ArH), 6.80 (1H, dt, *J* = 15.8, 7.4 Hz, H_{21}), 6.15 (1H, d, *J* = 15.8 Hz, H_{20}), 4.51 (1H, d, *J* = 11.0 Hz, $PhCH_aH_bO$), 4.50 (1H, d, *J* = 12.2 Hz, $ArCH_aH_b$), 4.46 (1H, d, *J* = 12.2 Hz, $ArCH_aH_b$), 4.42 (1H, d, *J* = 11.0 Hz, $PhCH_aH_bO$), 3.80 (3H, s, $ArOCH_3$), 3.76–3.70 (2H, m, H_{23}, H_{25}), 3.68–3.59 (3H, m, H_{15} x 2, H_{27a}), 3.29 (1H, dd, *J* = 8.6, 7.8 Hz, H_{27b}), 2.59–2.41 (3H, m, H_{18a}, H_{22} × 2), 2.33 (1H, dd, *J* = 15.5, 8.3 Hz, H_{18b}), 2.22–2.13 (1H, m, H_{17}), 2.09–2.03 (1H, m, H_{26}), 1.76–1.71 (1H, m, H_{24}), 1.60–1.51 (1H, m, H_{16a}), 1.45–1.37 (1H, m, H_{16b}), 1.03 (3H, d, *J* = 6.9 Hz, Me_{26}), 0.97–0.90 (24H, m, Me_{17}, Me_{24}, $SiC(CH_3)_3$, $SiCH_2CH_3$ x 3), 0.61 (6H, q, *J* = 8.0 Hz, $SiCH_2CH_3$ x 3), 0.05 (6H, s, $SiCH_3$ x 2); **^{13}C NMR** (125 MHz, $CDCl_3$): δ_C 199.5, 158.7, 143.3, 138.4, 132.1, 130.5, 128.5, 127.9, 127.1, 127.0, 113.4, 77.9, 76.7, 72.7, 71.8, 71.1, 60.8, 54.9, 47.2, 41.7, 39.4, 36.7, 35.6, 26.3, 25.6, 19.6, 17.9, 15.7, 10.7, 6.8, 5.2, −5.6 x 2; **HRMS** calculated for $C_{43}H_{76}O_6NSi_2$ $[M+NH_4]^+$ 758.5206, found 758.5194.

Allylic alcohol 231

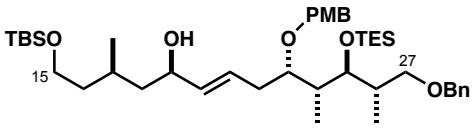

(*S*)-Me-CBS catalyst (209 μL, 1.0 M in PhMe, 0.209 mmol) and $BH_3{\cdot}SMe_2$ (198 μL, 2.09 mol) were added sequentially to a solution of enone **229** (776 mg, 1.05 mmol) in THF (35 mL) at –20 °C. The reaction was stirred at this temperature for 2.5 h, then quenched with MeOH (30 mL). After warming to rt, solvent was removed under reduced pressure. The residue was dissolved in MeOH (15 mL), then concentrated *in vacuo* and the procedure repeated three times. Crude product was purified by flash column chromatography (gradient elution: EtOAc/40–60 PE, 1:15 → 1:5) afforded allylic alcohol **231** (700 mg, 0.942 mmol, 90%, 10:1 *dr*) as a colourless oil.

R_f 0.48 (EtOAc/40–60 PE, 1:4); **$[\alpha]_{20}^{D}$** = −3.8 (*c* 1.0, $CHCl_3$); **IR** (thin film, ν_{max} / cm^{-1}): 3404, 2956, 2931, 2876, 1613, 1514, 1462, 1361, 1302, 1249, 1172, 1092, 1039, 1008, 970, 836, 776, 736, 697; **^{1}H NMR** (500 MHz, $CDCl_3$): δ_H 7.36–7.35 (4H, m, PhH), 7.32-7.28 (1H, m, PhH), 7.27 (2H, d, *J* = 8.2 Hz, ArH), 6.88 (2H, d, *J* = 8.2 Hz, ArH), 5.64 (1H, dt, *J* = 15.2, 7.2 Hz, H_{21}), 5.53 (1H, dd, *J* = 15.2, 6.8 Hz, H_{20}), 4.56 (1H, d, *J* = 11.2 Hz, $ArCH_aH_bO$), 4.52 (1H, d, *J* = 11.9 Hz, $PhCH_aH_bO$), 4.49 (1H, d, *J* = 11.9 Hz, $PhCH_aH_bO$), 4.41 (1H, d, *J* = 11.2 Hz, $ArCH_aH_bO$), 4.20–4.14 (1H, m, H_{19}) 3.82 (3H, s, $ArOCH_3$), 3.74–3.62 (5H, m, H_{15} × 2, H_{23}, H_{25}, H_{27a}), 3.31 (1H, dd, *J* = 8.7, 8.7 Hz, H_{27b}), 2.44 (1H, dt, *J* = 7.5, 6.5

Hz, H_{22a}), 2.31–2.25 (1H, m, H_{22b}), 2.11–2.06 (1H, m, H_{26}), 1.81–1.76 (1H, m, H_{17}), 1.75–1.70 (1H, m, H_{24}), 1.67–1.62 (2H, m, H_{16a}, O<u>H</u>), 1.45 (2H, t, *J* = 6.8 Hz, H_{18} x 2), 1.42–1.35 (1H, m, H_{16b}), 1.05 (3H, d, *J* = 6.8 Hz, Me_{26}), 0.98–0.92 (15H, m, $SiCH_2C\underline{H}_3$ x 3, Me_{17}, Me_{24}), 0.92 (9H, s, $SiC(C\underline{H}_3)_3$), 0.63 (6H, q, *J* = 8.0 Hz, $SiC\underline{H}_2CH_3$ x 3), 0.08 (6H, s, $SiC\underline{H}_3$ x 2); **^{13}C NMR** (125 MHz, $CDCl_3$): δ_C 158.8, 135.5, 131.2, 128.7, 128.2, 128.0, 127.4, 127.3, 113.6, 78.6, 77.1, 76.9, 72.9, 72.1, 71.0, 70.9, 61.3, 55.2, 44.4, 41.4, 39.4, 36.7, 35.2, 26.2, 25.9, 20.3, 18.2, 16.2, 10.6, 7.1, 5.5, −5.4 x 2; **HRMS** calculated for $C_{43}H_{78}O_6NSi_2$ $[M+NH_4]^+$ 760.5362, found 760.5356.

Methyl ether 233

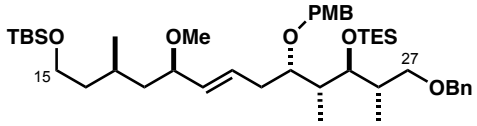

Sodium hydride (377 mg, 60% dispersion in mineral oil, 9.42 mmol) was washed with hexane (3 x 5 mL), dried *in vacuo* and suspended in THF (10 mL) at 0 °C. A solution of allylic alcohol **231** (700 mg, 0.942 mmol) in THF (10 mL) was added *via* cannula and the white suspension was stirred at this temperature for 1 h. MeI (754 µl, 11.3 mmol) was added dropwise and the reaction was warmed to rt and stirred for 20 h. The mixture was quenched with MeOH (15 mL), then poured into brine (20 mL) and extracted with Et_2O (3 x 20 mL). Combined organic phases were dried ($MgSO_4$), concentrated *in vacuo* and purified by flash column chromatography (gradient elution: EtOAc/40–60, 1:25 → 1:18) to afford methyl ether **233** (639 mg, 0.844 mmol, 90%) as a colourless oil.

$\mathbf{R}_f$ 0.52 (EtOAc/40–60 PE, 1:8); $[\alpha]_{20}^{D}$ = +4.2 (*c* 1.0, $CHCl_3$); **IR** (thin film, ν_{max} / cm^{-1}): 2952, 2929, 2877, 1613, 1512, 1463, 1360, 1298, 1251, 1173, 1094, 1044, 1007, 969, 836, 777, 731, 696; **^{1}H NMR** (500 MHz, $CDCl_3$): δ_H 7.36–7.35 (4H, m, Ph<u>H</u>), 7.31–7.29 (1H, m, Ph<u>H</u>), 7.27 (2H, d, *J* = 8.2 Hz, Ar<u>H</u>), 6.88 (2H, d, *J* = 8.2 Hz, Ar<u>H</u>), 5.62–5.56 (1H, m, H_{21}), 5.30 (1H, dd, *J* = 15.4, 8.4 Hz, H_{20}), 4.58 (1H, d, *J* = 11.0 Hz, $ArC\underline{H}_aH_bO$), 4.49 (2H, ABq, *J* = 11.9 Hz, $PhC\underline{H}_2O$), 4.41 (1H, *J* = 11.0 Hz, $ArCH_a\underline{H}_bO$), 3.82 (3H, s, $ArOC\underline{H}_3$), 3.76–3.74 (1H, m, H_{23}), 3.71–3.60 (4H, m, H_{15} × 2, H_{25}, H_{27a}), 3.56 (1H, app q, *J* = 7.4 Hz, H_{19}), 3.30 (1H, app t, *J* = 8.8 Hz, H_{27b}), 3.23 (3H, s, $OC\underline{H}_3$), 2.49 (1H, dt, *J* = 14.0, 5.3 Hz, H_{22a}), 2.30 (1H, dt, *J* = 14.0, 7.9 Hz, H_{22b}), 2.13–2.07 (1H, m, H_{26}), 1.82–1.76 (1H, m, H_{24}), 1.70 (1H, app sext, *J* = 6.7 Hz, H_{17}), 1.63–1.57 (1H, m, H_{16a}), 1.50–1.33 (3H, m, H_{16b}, H_{18} x 2), 1.06 (3H, d, *J* = 6.9 Hz, Me_{26}), 0.98–0.90 (24H, m, Me_{17}, Me_{24}, $SiC(C\underline{H}_3)_3$, $SiCH_2C\underline{H}_3$ x 3), 0.63 (6H, q, *J* = 7.8 Hz, $SiC\underline{H}_2CH_3$ x 3), 0.07 (6H, s, $SiC\underline{H}_3$ x 2); **^{13}C NMR** (125 MHz, $CDCl_3$): δ_C 158.8, 138.7, 132.9, 131.3, 130.5, 128.5, 128.2, 127.4, 127.3, 113.6, 80.7, 78.4, 77.0, 72.9, 71.9, 70.8, 61.1, 55.7, 55.2, 42.9, 41.0, 40.0, 36.8, 35.1, 26.0, 25.9, 19.9, 18.2, 16.0, 10.3, 7.0, 5.5 −5.3, −5.4; **HRMS** calculated for $C_{44}H_{80}O_6NSi_2$ $[M+NH_4]^+$ 774.5519, found 774.5518.

Enone 228

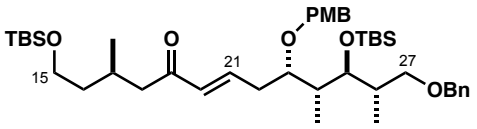

Anhydrous $Ba(OH)_2$ (9.6 mg, 56.0 μmol) in THF (0.8 mL) was sonicated for 5 min to form a white suspension. A solution of phosphonate **210** (35.2 mg, 99.7 μmol) in THF (1.2 mL) was added *via* cannula. The reaction mixture was stirred at rt for 1 h before a solution of aldehyde **204** (47.9 mg, 93.2 μmol) in THF/H_2O (40:1, 2 mL) was added. The cloudy mixture was stirred for a further 16 h, diluted with THF (2 mL) and poured into NH_4Cl solution (5 mL). The phases were separated and the aqueous layer was extracted with Et_2O (3 × 5 mL). The combined organic phases were washed with brine (5 mL), dried ($MgSO_4$) and concentrated *in vacuo*. The crude product was purified by flash column chromatography (EtOAc/40–60 PE, 1:20) to give enone **228** (48.0 mg, 64.8 μmol, 69%) as a colourless oil.

R_f 0.61 (EtOAc/40–60 PE, 1:5); $[\alpha]_{20}^{D}$ = −15.5 (*c* 1.0, $CHCl_3$); **IR** (thin film, ν_{max} / cm^{-1}): 2927, 2855, 1696, 1614, 1514, 1462, 1361, 1248, 1173, 1091, 1037, 834, 774, 698; **^{1}H NMR** (500 MHz, $CDCl_3$): δ_H 7.38–7.29 (5H, m, PhH), 7.26 (2H, d, *J* = 8.5 Hz, ArH), 6.88 (2H, d, *J* = 8.5 Hz, ArH), 6.84 (1H, dt, *J* = 15.8, 7.9 Hz, H_{21}), 6.17 (1H, d, *J* = 15.8 Hz, H_{20}), 4.51 (1H, d, *J* = 10.9 Hz, PhCH_aH_bO), 4.50 (1H, d, *J* = 12.1 Hz, ArCH_aH_bO), 4.48 (1H, d, *J* = 12.1 Hz, ArCH_aH_bO), 4.43 (1H, d, *J* = 10.9 Hz, PhCH_aH_bO), 3.81 (3H, s, ArOCH_3), 3.73–3.63 (5H, m, H_{15} × 2, H_{23}, H_{25}, H_{27a}), 3.30 (1H, app t, *J* = 8.7 Hz, H_{27b}), 2.57–2.49 (3H, m, H_{18a}, H_{22} × 2), 2.36 (1H, dd, *J* = 15.2, 8.4 Hz, H_{18b}), 2.23–2.15 (1H, m, H_{17}), 2.10–2.03 (1H, m, H_{26}) 1.83–1.76 (1H, m, H_{24}), 1.60–1.54 (1H, m, H_{16a}), 1.47–1.40 (1H, m, H_{16b}), 1.05 (3H, d, *J* = 7.0 Hz, Me_{26}), 1.01 (3H, d, *J* = 7.0 Hz, Me_{24}), 0.93 (3H, d, *J* = 7.0 Hz, Me_{17}), 0.92 (9H, s, SiC(CH_3)$_3$), 0.89 (9H, s, SiC(CH_3)$_3$), 0.07 (6H, s, SiCH_3), 0.06 (3H, s, SiCH_3), 0.04 (3H, s, SiCH_3); **^{13}C NMR** (125 MHz, $CDCl_3$): δ_C 199.8, 159.1, 143.3, 138.7, 132.6, 130.6, 129.0, 128.2, 127.4, 127.3, 113.7, 78.7, 76.3, 72.9, 72.4, 71.5, 61.1, 55.1, 47.3, 42.7, 39.7, 37.0, 35.6, 26.6, 26.0, 25.9, 19.9, 18.2, 18.2, 16.2, 11.1, −4.0, −4.3, −5.4, −5.4; **HRMS** calculated for $C_{43}H_{76}O_6NSi_2$ $[M+NH_4]^+$ 758.5206, found 758.5227.

Allylic alcohol 230

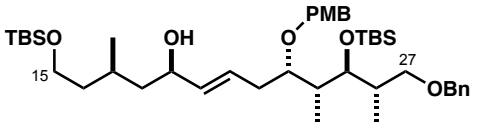

(*S*)-Me-CBS catalyst (3 μL, 1.0 M in PhMe, 3.0 μmol) was added to a solution of enone **228** (22.0 mg, 29.7 mmol) in THF (0.5 mL) at −20 °C, followed by $BH_3{\cdot}SMe_2$ (2 μL, 19.3 mmol). The reaction was

warmed to −10 °C and stirred for 1.5 h before being carefully quenched with MeOH (1 mL). The mixture was warmed to rt and stirred for a further 30 min before concentrating *in vacuo*. The residue was redissolved in MeOH (1 mL), then concentrated *in vacuo* and the procedure repeated three times. Purification by flash column chromatography (gradient elution: EtOAc/40–60 PE, 1:15 → 1:10) afforded allylic alcohol **230** (18.0 mg, 24.2 mmol, 82%, 15:1 *dr*) as a colourless oil.

R_f 0.40 (EtOAc/40–60 PE, 1:5); **$[\alpha]_{20}^{D}$** = −6.7 (*c* 1.0, $CHCl_3$); **IR** (thin film, ν_{max} / cm^{-1}): 3465, 2953, 2927, 2854, 1514, 1463, 1361, 1302, 1248, 1172, 1090, 1037, 1005, 969, 939, 899, 834, 773, 734, 698; **^{1}H NMR** (500 MHz, $CDCl_3$): δ_H 7.35–7.33 (4H, m, PhH), 7.30–7.27 (1H, m, PhH), 7.26 (2H, d, *J* = 8.7 Hz, ArH), 6.86 (2H, d, *J* = 8.7 Hz, ArH), 5.66 (1H, dt, *J* = 15.4, 7.0 Hz, H_{21}), 5.54 (1H, dd, *J* = 15.4, 6.9 Hz, H_{20}), 4.53 (1H, d, *J* = 11.0 Hz, $ArCH_aH_bO$), 4.49 (1H, d, *J* = 12.0 Hz, $PhCH_aH_bO$), 4.45 (1H, d, *J* = 12.0 Hz, $PhCH_aH_bO$), 4.39 (1H, d, *J* = 11.0 Hz, $ArCH_aH_bO$), 4.19−4.14 (1H, m, H_{19}), 3.80 (3H, s, $ArOCH_3$), 3.72–3.61 (4H, m, H_{15} × 2, H_{25}, H_{27a}), 3.58–3.55 (1H, m, H_{23}), 3.30 (1H, dd, *J* = 8.9, 8.6 Hz, H_{27b}), 2.39–2.30 (2H, m, H_{22} × 2), 2.10–2.02 (1H, m, H_{26}) 1.85–1.78 (1H, m, H_{24}), 1.75–1.69 (1H, m, H_{17}), 1.65–1.58 (2H, m, OH, H_{16a}), 1.44 (2H, t, *J* = 6.9 Hz, H_{18} x 2), 1.40–1.33 (1H, m, H_{16b}), 1.04 (3H, d, *J* = 6.9 Hz, Me_{26}), 0.98 (3H, d, *J* = 7.1 Hz, Me_{24}), 0.92 (3H, d, *J* = 6.7 Hz, Me_{17}), 0.91 (9H, s, $SiC(CH_3)_3$), 0.88 (9H, s, $SiC(CH_3)_3$), 0.06 (6H, s, $SiCH_3$ x 2), 0.05 (3H, s, $SiCH_3$), 0.04 (3H, s, $SiCH_3$); **^{13}C NMR** (125 MHz, $CDCl_3$): δ_C 159.0, 138.9, 135.7, 131.2, 129.0, 128.3, 127.8, 127.5, 127.4, 113.7, 79.3, 76.7, 73.0, 72.6, 71.2, 70.9, 61.4, 55.3, 44.6, 42.4, 39.5, 36.9, 35.1, 29.7, 26.1, 26.0, 20.4, 18.4, 18.4, 16.5, 10.8, −3.8, −4.2, −5.3, −5.3; **HRMS** calculated for $C_{43}H_{78}O_6NSi_2$ $[M+NH_4]^+$ 760.5362, found 760.5361.

Methyl ether 232

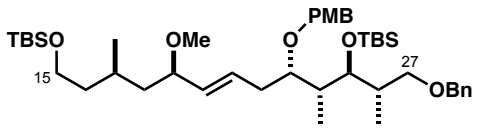

Sodium hydride (11.0 mg, 60% dispersion in mineral oil, 275 μmol) was washed with hexane (3 x 1 mL) and dried *in vacuo*. THF (0.2 mL) was added and the suspension was cooled to 0 °C. A solution of allylic alcohol **230** (9.1 mg, 12.2 mmol) in THF (0.35 mL) was added *via* cannula and the pale yellow mixture was stirred at this temperature for 30 min before addition of MeI (15 μl, 245 μmol). The reaction was warmed to rt and stirred for 18 h before being quenched with MeOH (0.5 mL). The quenched mixture was poured into brine (2 mL) and extracted with Et_2O (3 x 2 mL). Combined organic phases were dried ($MgSO_4$), concentrated *in vacuo* and purified by flash column chromatography (gradient elution: EtOAc/40–60, 1:20 → 1:10) to afford methyl ether **232** (9.5 mg, 12.5 μmol, 94%) as a colourless oil.

R_f 0.65 (EtOAc/40–60 PE, 1:5); **$[\alpha]_{20}^{D}$** = −2.5 (*c* 0.53, $CHCl_3$); **IR** (thin film, ν_{max} / cm^{-1}): 2926, 2855, 1514, 1462, 1249, 1093, 835, 773, 698; **^{1}H NMR** (500 MHz, $CDCl_3$): δ_H 7.37–7.33 (4H, m, PhH), 7.30–7.28 (1H, m, PhH), 7.26 (2H, d, *J* = 8.5 Hz, ArH), 6.87 (2H, d, *J* = 8.5 Hz, ArH), 5.64–5.58 (1H, m, H_{21}), 5.31 (1H, dd, *J* = 15.4, 8.3 Hz, H_{20}), 4.56 (1H, d, *J* = 11.1 Hz, $ArCH_aH_bO$), 4.50 (1H, ABq, *J* = 11.7 Hz, $PhCH_aH_bO$), 4.46 (1H, ABq, *J* = 11.7 Hz, $PhCH_aH_bO$), 4.41 (1H, *J* = 11.1 Hz, $ArCH_aH_bO$), 3.81 (3H, s, $ArOCH_3$), 3.75 (1H, dd, *J* = 6.4, 2.5 Hz, H_{25}), 3.69–3.61 (4H, m, H_{15} × 2, H_{23}, H_{27a}), 3.58–3.54 (1H, m, H_{19}), 3.31 (1H, app t, *J* = 9.0 Hz, H_{27b}), 3.23 (3H, s, OCH_3), 2.46–2.41 (1H, m, H_{22a}), 2.37–2.30 (1H, m, H_{22b}), 2.14–2.07 (1H, m, H_{26}), 1.86–1.80 (1H, m, H_{24}), 1.75–1.67 (1H, m, H_{17}), 1.63–1.57 (1H, m, H_{16a}), 1.50–1.22 (3H, m, H_{16b}, H_{18} x 2), 1.05 (3H, d, *J* = 6.8 Hz, Me_{26}), 0.97 (3H, d, *J* = 6.9 Hz, Me_{24}), 0.91–0.89 (21H, m, Me_{17}, $SiC(CH_3)_3$ x 2), 0.07 (12H, s, $SiCH_3$ x 4); **^{13}C NMR** (125 MHz, $CDCl_3$): δ_C 158.9, 138.8, 133.1, 131.3, 130.3, 128.8, 128.3, 127.5, 127.4, 113.7, 80.8, 79.0, 76.6, 73.0, 72.5, 71.1, 61.3, 55.8, 55.3, 43.1, 41.9, 39.9, 37.1, 35.1, 29.7, 26.2, 26.0, 20.0, 18.4, 18.3, 16.1, 10.6, −3.8, −4.0, −5.2, −5.3; **HRMS** calculated for $C_{44}H_{80}O_6NSi_2$ $[M+NH_4]^+$ 774.5519, found 774.5518.

***Bis*-TES alcohol 248**

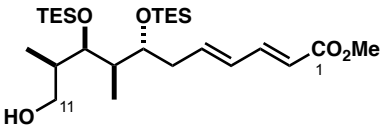

DDQ (5.48 g, 24.2 mmol) was added in one portion to a solution of PMB ether **247** (10.0 g, 16.1 mmol) in CH_2Cl_2/pH 7 buffer (2:1, 300 ml) at 0 °C. The resulting dark green mixture was warmed to rt and stirred for 1 h until completion before quenching with $NaHCO_3$ solution (300 mL) and diluting with CH_2Cl_2 (200 mL). The emulsion was stirred for a further 1 h before being diluted with H_2O (600 mL). The layers were separated and the aqueous phase was extracted with EtOAc (3 x 500 mL). Combined organic extracts were dried (Na_2SO_4), concentrated *in vacuo* and purified by flash column chromatography (PhMe, then gradient elution: EtOAc/40–60 PE, 1:7 → 1:5) to yield alcohol **248** (7.27 g, 14.5 mmol, 90%) as a pale yellow oil.

R_f 0.31 (EtOAc/40–60 PE, 1:10); **$[\alpha]_{20}^{D}$** = −11.1 (*c* 1.6, $CHCl_3$); **IR** (thin film, ν_{max} / cm^{-1}): 3456, 2953, 2912, 2877, 1722, 1703, 1644, 1617, 1458, 1436, 1415, 1303, 1240, 1174, 1139, 1063, 1003, 867, 804, 725; **^{1}H NMR** (500 MHz, $CDCl_3$): δ_H 7.29 (1H, dd, *J* = 15.4, 10.0 Hz, H_3), 6.23 (1H, dd, *J* = 15.4, 10.0 Hz, H_4), 6.17 (1H, ddd, *J* = 15.4, 6.9, 6.0 Hz, H_5), 5.83 (1H, d, *J* = 15.3 Hz, H_2), 3.80–3.76 (2H, m, H_9, H_{11a}), 3.77 (3H, s, CO_2CH_3), 3.74 (1H, ddd, *J* = 6.4, 3.7 Hz, H_7), 3.59–3.55 (1H, m, H_{11b}), 2.65 (1H, t, *J* = 5.1 Hz, OH), 2.37–2.32 (1H, m, H_{6a}), 2.28 (1H, ddd, *J* = 14.7, 6.2, 3.9 Hz, H_{6b}), 1.88–1.81 (1H, m, H_8), 1.81–1.75 (1H, m, H_{10}), 1.03 (3H, d, *J* = 7.1 Hz, Me_{10}), 1.00 (9H, t, *J* = 7.9 Hz, $SiCH_2CH_3$ x 3), 0.98 (9H,

t, J = 7.9 Hz, $SiCH_2C\underline{H}_3$ x 3), 0.91 (3H, d, J = 6.9 Hz, Me_8), 0.68 (6H, t, J = 7.9 Hz, $SiC\underline{H}_2CH_3$ x 3), 0.62 (6H, t, J = 7.9 Hz, $SiC\underline{H}_2CH_3$ x 3); **^{13}C NMR** (125 MHz, $CDCl_3$): δ_C 167.7, 144.8, 140.6, 130.5, 119.3, 77.6, 73.4, 65.3, 51.5, 42.5, 39.2, 36.7, 14.7, 11.0, 7.1, 7.0, 5.5, 5.3; **HRMS** calculated for $C_{26}H_{53}O_5Si_2$ $[M+H]^+$ 501.3426, found 501.3418.

Iodide 249

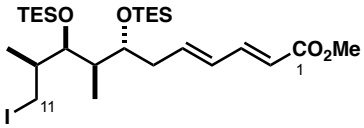

PPh_3 (4.22 g, 16.1 mmol) and imidazole (1.34 g, 19.6 mmol) were added sequentially to a solution of alcohol **248** (4.47 g, 8.93 mmol) in Et_2O/MeCN (1:1, 100 mL) at 0 °C, followed by portion-wise addition of I_2 (4.07 g, 16.1 mmol). The reaction mixture was warmed up to rt and stirred for 2 h before being quenched by addition of $NaHCO_3$ solution (100 mL). The mixture was extracted with Et_2O (3 x 100 mL), the combined organic phases dried ($MgSO_4$) and concentrated *in vacuo*. Purification by flash column chromatography (gradient elution: EtOAc/40–60 PE, 1:50 → 1:10) yielded iodide **249** (4.18 g, 6.84 mmol, 77%, 92% BRSM) as a colourless oil.

R_f 0.58 (EtOAc/40–60 PE, 1:10); **$[\alpha]_{20}^{D}$** = –10.0 (*c* 2.0, $CHCl_3$); **IR** (thin film, ν_{max} / cm^{-1}): 2955, 2911, 2877, 1722, 1645, 1617, 1458, 1434, 1415, 1300, 1264, 1241, 1140, 1102, 1064, 1003, 739, 723; **^{1}H NMR** (500 MHz, $CDCl_3$): δ_H 7.27 (1H, dd, J = 15.4, 10.0 Hz, H_3), 6.21 (1H, dd, J = 15.0, 9.9 Hz, H_4), 6.15 (1H, ddd, J = 15.0, 6.9, 6.4 Hz, H_5), 5.81 (1H, d, J = 15.4 Hz, H_2), 3.74 (3H, s, $CO_2C\underline{H}_3$), 3.69 (1H, ddd, J = 6.7, 5.3, 4.1 Hz, H_7), 3.66 (1H, dd, J = 4.2, 3.8 Hz, H_9), 3.29 (1H, dd, J = 9.9, 4.2 Hz, H_{11a}), 2.99 (1H, dd, J = 9.9, 9.0 Hz, H_{11b}), 2.32–2.25 (2H, m, H_6 x 2), 1.86–1.79 (1H, m, H_{10}), 1.72–1.66 (1H, m, H_8), 1.05 (3H, d, J = 6.8 Hz, Me_{10}), 0.96 (9H, t, J = 7.8 Hz, $SiCH_2C\underline{H}_3$ x 3), 0.95 (9H, t, J = 7.8 Hz, $SiCH_2C\underline{H}_3$ x 3), 0.85 (3H, d, J = 6.8 Hz, Me_8), 0.68 (6H, t, J = 7.8 Hz, $SiC\underline{H}_2CH_3$ x 3), 0.59 (6H, t, J = 7.8 Hz, $SiC\underline{H}_2CH_3$ x 3); **^{13}C NMR** (125 MHz, $CDCl_3$): δ_C 167.6, 144.8, 141.0, 130.3, 119.2, 76.1, 73.7, 51.4, 42.1, 41.6, 36.7, 17.7, 11.5, 10.2, 7.0, 6.9, 5.5, 5.2; **HRMS** calculated for $C_{26}H_{52}O_4ISi_2$ $[M+H]^+$ 611.2443, found 611.2435.

Alcohol 250

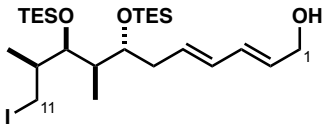

DIBALH (38.7 mL, 1.0 M in hexanes, 38.7 mmol) was added dropwise to a solution of ester **249** (7.87 g, 12.9 mmol) in CH_2Cl_2 (250 mL) at −78 °C and the mixture stirred for 1.5 h. Upon completion, the mixture was quenched by addition of Na^+/K^+ tartrate solution (300 mL) and water (100 mL), then warmed to rt and stirred vigorously for 1.5 h. The phases were separated and the aqueous layer extracted with CH_2Cl_2 (3 x 200 mL). The combined organic extracts were dried (Na_2SO_4), concentrated *in vacuo* and purified by flash column chromatography (gradient elution: EtOAc/40–60 PE, 1:20 → 1:15) to give alcohol **250** (7.31 g, 12.5 mmol, 97%) as a colourless oil.

$\mathbf{R}_f$ 0.33 (EtOAc/40–60 PE, 1:5); $[\boldsymbol{\alpha}]_{20}^{D}$ = −10.6 (*c* 0.8, $CHCl_3$); **IR** (thin film, ν_{max} / cm^{-1}): 3357, 2956, 2909, 2881, 1461, 1415, 1378, 1237, 1140, 1102, 1068, 1009, 993, 741, 727; **^{1}H NMR** (500 MHz, $CDCl_3$): δ_H 6.23 (1H, dd, *J* = 15.3, 10.7 Hz, H_3), 6.08 (1H, dd, *J* = 15.3, 10.7 Hz, H_4), 5.77–5.69 (2H, m, H_2, H_5), 4.18 (2H, br d, *J* = 4.9 Hz, H_1 x 2), 3.67–3.64 (2H, m, H_7, H_9), 3.32 (1H, dd, *J* = 9.9, 3.7 Hz, H_{11a}), 2.98 (1H, dd, *J* = 9.9, 9.1 Hz, H_{11b}), 2.22–2.20 (2H, m, H_6 x 2), 1.87–1.79 (1H, m, H_{10}), 1.72–1.65 (1H, m, H_8), 1.33 (1H, t, *J* = 5.3 Hz, O<u>H</u>), 1.05 (3H, d, *J* = 6.9 Hz, Me_{10}), 0.96 (18H, t, *J* = 7.8 Hz, $SiCH_2C\underline{H}_3$ x 6), 0.84 (3H, d, *J* = 6.8 Hz, Me_8), 0.63 (6H, q, *J* = 7.8 Hz, $SiC\underline{H}_2CH_3$ x 3), 0.60 (6H, q, *J* = 7.8 Hz, $SiC\underline{H}_2CH_3$ x 3); **^{13}C NMR** (125 MHz, $CDCl_3$): δ_C 132.0, 131.6, 131.4, 129.8, 76.2, 73.9, 63.4, 42.0, 41.6, 36.3, 17.8, 11.8, 10.5, 7.0, 6.9, 5.5, 5.2; **HRMS** calculated for $C_{25}H_{52}O_3ISi_2$ $[M+H]^+$ 583.2494, found 583.2486.

TBS ether 160

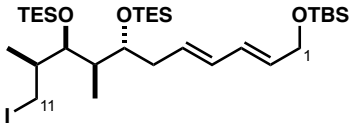

Imidazole (1.71 g, 25.1 mmol) and TBSCl (2.84 g, 18.8 mmol) were added sequentially to a solution of alcohol **250** (7.31 g, 12.5 mmol) in CH_2Cl_2 (250 mL) and the resulting mixture stirred for 30 min until completion. The reaction was quenched with NH_4Cl solution (200 mL), the phases separated and the aqueous layer extracted with CH_2Cl_2 (2 x 200 mL). The combined organic extracts were dried ($MgSO_4$), concentrated *in vacuo* and the residue purified by flash column chromatography (EtOAc/40–60 PE, 1:50). TBS ether **160** (8.63 g, 12.4 mmol, 99% yield) was obtained as a colourless oil.

R_f 0.72 (40–60 PE); **$[\alpha]_{20}^{D}$** = –6.0 (*c* 1.2, $CHCl_3$); **IR** (thin film, ν_{max} / cm^{-1}): 2952, 2873, 1459, 1413, 1378, 1260, 1255, 1241, 1104, 1062, 1007, 963, 836, 777, 737, 727; **^{1}H NMR** (500 MHz, $CDCl_3$): δ_H 6.19 (1H, dd, *J* = 15.1, 10.4 Hz, H_3), 6.06 (1H, dd, *J* = 15.1, 10.9 Hz, H_4), 5.69–5.63 (2H, m, H_2, H_5), 4.21 (2H, d, *J* = 5.6 Hz, H_1 x 2), 3.66–3.64 (2H, m, H_7, H_9), 3.32 (1H, dd, *J* = 9.7, 3.7 Hz, H_{11a}), 2.98 (1H, dd, *J* = 9.7, 9.1 Hz, H_{11b}), 2.21–2.18 (2H, m, H_6 x 2), 1.88–1.81 (1H, m, H_{10}), 1.73–1.66 (1H, m, H_8), 1.05 (3H, d, *J* = 6.8 Hz, Me_{10}), 0.96 (18H, t, *J* = 7.8 Hz, $SiCH_2C\underline{H}_3$ x 6), 0.91 (9H, s, $SiC(C\underline{H}_3)_3$), 0.85 (3H, d, *J* = 6.9 Hz, Me_8), 0.62 (6H, q, *J* = 7.8 Hz, $SiC\underline{H}_2CH_3$ x 3), 0.61 (6H, q, *J* = 7.8 Hz, $SiC\underline{H}_2CH_3$ x 3), 0.07 ($SiC\underline{H}_3$ x 2); **^{13}C NMR** (125 MHz, $CDCl_3$): δ_C 131.7, 131.5 x 2, 130.0, 76.3, 74.0, 63.5, 42.1, 41.5, 36.3, 25.9, 18.3, 17.9, 11.7, 10.5, 7.0, 6.9, 5.5, 5.2, –5.3; **HRMS** calculated for $C_{31}H_{66}O_3ISi_3$ $[M+H]^+$ 697.3359, found 697.3357.

6.5. Experimental Procedures for Chapter 4

Phosphonate 123

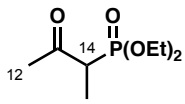

^{n}BuLi (100 mL, 1.6M in hexanes, 160 mmol) was added to a solution of diethyl ethylphosphonate (23.6 mL, 146 mmol) in THF (200 mL) at –78 °C and stirred for 1 h. EtOAc (14.3 mL, 146 mmol) was added dropwise and the reaction stirred at this temperature for a further 30 min before being quenched with NH_4Cl solution (100 mL) and warmed to rt. Phases were separated and the aqueous layer extracted with EtOAc (5 x 250 mL). Combined organic extracts were dried ($MgSO_4$), concentrated *in vacuo* and the residue purified by distillation under reduced pressure (95 °C, 0.5 mm Hg). Phosphonate **123** (18.5 g, 88.7 mmol, 61%) was obtained as a colourless oil.

R_f 0.24 (EtOAc); **^{1}H NMR** (500 MHz, $CDCl_3$): δ_H 4.19–4.13 (4H, m, $P(OC\underline{H}_2CH_3)$ x 2), 3.23 (1H, dq, *J* = 25.5, 7.1 Hz, H_{14}), 2.36 (3H, s, Me_{12}), 1.38 (3H, dd, *J* = 16.5, 7.1 Hz, Me_{14}), 1.35 (6H, td, *J* = 7.1, 2.1 Hz, $P(OCH_2C\underline{H}_3)$ x 2).

Data in agreement with that presented by Lee.[162]

Phosphonate 253

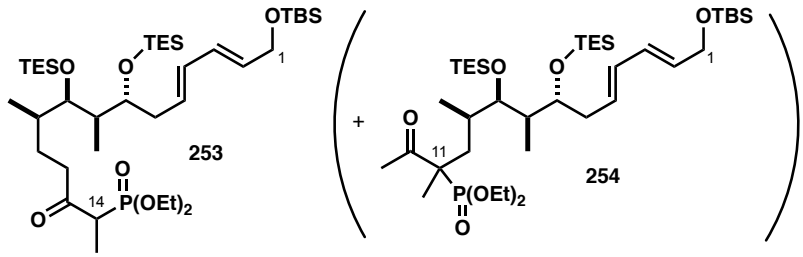

Phosphonate **123** (715 mg, 3.44 mmol) was added to a suspension of NaH (160 mg, 60% dispersion in mineral oil, 4.02 mmol) in THF (10 mL) at 0 °C and stirred at this temperature for 30 min, followed by dropwise addition of ^{n}BuLi (2.15 mL, 1.6 M in hexanes, 3.44 mmol). After stirring for a further 30 min, during which a clear pale yellow solution of the dianion was formed, the mixture was cooled to −10 °C and a solution of iodide **160** (400 mg, 0.574 mmol) in THF (5 mL) was added *via* cannula over 10 min. The reaction mixture was stirred for 2 h, gradually developing a bright yellow colour, then quenched by addition of NH_4Cl solution (100 mL) and warmed to rt. The aqueous phase was extracted with EtOAc (3 x 20 mL), dried ($MgSO_4$) and the crude product purified by flash column chromatography (gradient elution: EtOAc/40–60 PE, 1:20 → 1:3). Phosphonate **253** was obtained as an inseparable mixture with the undesired regioisomer **254** (336 mg, 0.432 mmol, 75%, 88% BRSM) in a 3:1 ratio.

$\mathbf{R}_f$ 0.23 (EtOAc/40–60 PE, 1:2); **^{1}H NMR** (500 MHz, $CDCl_3$): δ_H 6.19 (1H, dd, J = 15.1, 10.6 Hz, H_3), 6.05 (1H, dd, J = 15.1, 10.6 Hz, H_4), 5.72–5.62 (2H, m, H_2, H_5), 4.21 (2H, d, J = 5.5 Hz, H_1 x 2), 4.17–4.08 (4H, m, P(OC$\underline{H}_2$CH$_3$) x 2), 3.67–3.57 (1H, m, H_7), 3.55–3.52 (1H, m, H_9), 3.23 (0.80H, dq, J = 25.1, 7.2 Hz, H_{14}), 2.88 (0.40H, ddd, J = 17.5, 9.9, 4.9 Hz, H_{12a}), 2.77–2.60 (0.80H, m, H_{12a}, H_{12b}), 2.47 (0.40H, ddd, J = 17.5, 9.5, 6.1 Hz, H_{12b}), [2.36] (0.75H, s, Me_{14}*), [1.89–1.81] (0.25H, m, H_{11b}*), 1.78–1.63 (2H, m, H_8, H_{11a}, H_{11b}), 1.55–1.48 (1H, m, H_{10}), 1.42–1.31 (10H, m, H_{11a}, H_{11b}, Me_{14}, P(OCH$_2$C$\underline{H}_3$) x 2), 1.00–0.85 (33H, m, Me_8, Me_{10}, Me_{14}*, SiCH$_2$C$\underline{H}_3$ x 6, C(C$\underline{H}_3$)$_3$), [0.72] (0.75H, d, J = 6.7 Hz, Me_8*), 0.64–0.55 (12H, m, SiC$\underline{H}_2$CH$_3$ x 6), 0.08 (6H, s, SiC$\underline{H}_3$ x 2); **HRMS** calculated for $C_{39}H_{85}NO_7PSi_3$ $[M+NH_4]^+$ 794.5366, found 794.5362.

Distinguishable resonances of the minor regioisomer are given in brackets and marked with an asterisk. Note that the diastereomeric ratio of **253** at C_{14} is approximately 1:1.

Allyl (4-(benzyloxy)butyl) carbonate (240)

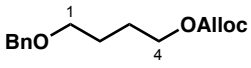

Allyl chloroformate (176 μL, 1.81 mmol) was added to a solution of alcohol **262** (100 mg, 0.555 mmol)

in CH_2Cl_2/pyr (1:1, 6 mL) at 0 °C. The reaction was warmed to rt and stirred for 16 h before being recooled to 0 °C and quenched with $NaHCO_3$ solution (5 mL). Phases were separated and the aqueous layer extracted with EtOAc (3 x 10 mL). Combined organic extracts were dried (Na_2SO_4), concentrated *in vacuo* and purified by flash column chromatography (gradient elution: EtOAc/40–60 PE, 1:50 → 1:20) to give allyl carbonate **240** (101 mg, 0.382 mmol, 69%) as a coulourless oil.

R_f 0.73 (EtOAc/40–60 PE, 1:3); **IR** (thin film, ν_{max} / cm^{-1}): 2952, 2853, 1744, 1450, 1393, 1362, 1247, 1094, 1025, 991, 949, 931, 789, 737, 694; **^{1}H NMR** (400 MHz, $CDCl_3$): δ_H 7.37–7.27 (5H, m, PhH), 5.94 (1H, ddt, *J* = 17.1, 10.4, 5.7 Hz, CH=CH_2), 5.36 (1H, dq, *J* = 17.1, 1.4 Hz, CH=C$H_a$$CH_b$), 5.27 (1H, dq, *J* = 10.4, 1.4 Hz, CH=$CH_a$$H_b$), 4.62 (2H, dt, *J* = 5.7, 1.4 Hz, OCH_2), 4.50 (2H, s, PhCH_2O), 4.18 (2H, t, *J* = 6.5 Hz, H_1 x 2), 3.50 (2H, t, *J* = 6.2 Hz, H_4 x 2), 1.83–1.76 (2H, m, H_2 x 2), 1.74–1.67 (2H, m, H_3 x 2); **^{13}C NMR** (125 MHz, $CDCl_3$): δ_C 154.7, 138.1, 131.3, 128.0, 127.2 x 2, 118.5, 72.6, 69.2, 68.0, 67.6, 25.7, 25.3; **HRMS** calculated for $C_{15}H_{21}O_4$ $[M+H]^+$ 264.1434, found 264.1438.

Allyl (8-hydroxyoctyl) carbonate

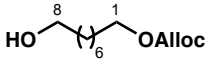

1,8-Octanediol (303 mg, 2.07 mmol) was added in small portions to a solution of allyl chloroformate (45 μL, 0.423 mmol) in CH_2Cl_2/pyr (1:1, 3 mL) at 0 °C, then warmed to rt. After stirring for 2 h the reaction was quenched by addition of $NaHCO_3$ solution (5 mL) and extracted with EtOAc (3 x 3 mL). Combined organic layers were dried (Na_2SO_4) and concentrated *in vacuo*. Crude product was purified by flash column chromatography (gradient elution: EtOAc/40–60 PE, 1:10 → 1:4) to afford allyl (8-hydroxyoctyl) carbonate (59.0 mg, 0.256 mmol, 61%) as a colourless oil.

R_f 0.35 (EtOAc/40–60 PE, 1:2); **IR** (thin film, ν_{max} / cm^{-1}): 3369, 2937, 2865, 1742, 1459, 1393, 1362, 1249, 1056, 1025, 997, 955, 933, 789; **^{1}H NMR** (400 MHz, $CDCl_3$): δ_H 5.97–5.89 (1H, m, CH=CH_2), 5.35 (1H, br d, *J* = 17.2 Hz, CH=C$H_a$$CH_b$), 5.26 (1H, br d, *J* = 10.4 Hz, CH=$CH_a$$H_b$), 4.61 (2H, ddd, *J* = 5.9, 2.6, 1.5 Hz, OCH_2), 4.13 (2H, t, *J* = 6.6 Hz, H_1 x 2), 3.61 (2H, t, *J* = 6.6 Hz, H_8 x 2), 1.82–1.69 (1H, m, OH), 1.66 (2H, quin, *J* = 7.0 Hz, H_2 x 2), 1.55 (2H, quin, *J* = 6.9 Hz, H_7 x 2), 1.39–1.28 (8H, m, H_3 x 2, H_4 x 2, H_5 x 2, H_6 x 2); **^{13}C NMR** (125 MHz, $CDCl_3$): δ_C 155.1, 131.7, 118.8, 68.3, 68.2, 62.9, 32.7, 29.2, 29.1, 28.6, 25.6 x 2; **HRMS** calculated for $C_{12}H_{23}O_4$ $[M+H]^+$ 231.1591, found 231.1593.

Allyl (8-oxoxyoctyl) carbonate (264)

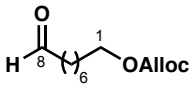

Dess–Martin periodinane (157 mg, 0.371 mmol) was added to a suspension of allyl (8-hydroxyoctyl) carbonate (57.0 mg, 0.248 mmol) and $NaHCO_3$ (104 mg, 1.24 mmol) in CH_2Cl_2 (5 mL) at 0 °C and stirred for 5 min. The mixture was then warmed to rt and stirred for a further 15 min until complete. The reaction was quenched with $Na_2S_2O_3$ solution (10 mL) and the biphasic mixture stirred rapidly for 20 min. Phases were separated and the aqueous layer extracted with EtOAc (3 x 5 mL). Combined organic layers were dried ($MgSO_4$), concentrated *in vacuo* and the residue was purified by flash column chromatography (EtOAc/40–60 PE, gradient elution: 1:20 → 1:10). Aldehyde **264** (45.1 mg, 0.197 mmol, 80%) was obtained as a colourless oil.

$\mathbf{R}_f$ 0.70 (EtOAc/40–60 PE, 1:3); **IR** (thin film, ν_{max} / cm^{-1}) 2929, 2857, 1742, 1722, 1461, 1397, 1362, 1245, 993, 955, 937, 795; **^{1}H NMR** (400 MHz, $CDCl_3$): δ_H 9.77 (1H, br t, J = 1.7 Hz, C<u>H</u>O), 5.94 (1H, ddt, J = 17.1 Hz, 10.8 Hz, 5.7 Hz, C<u>H</u>=CH_2), 5.36 (1H, dd, J = 17.1, 1.3 Hz, CH=C<u>H</u>$_a$H$_b$), 5.27 (1H, dd, J = 10.8, 0.9 Hz, CH=CH$_a$<u>H</u>$_b$), 4.62 (2H, br d, J = 5.7 Hz, OC<u>H</u>$_2$), 4.14 (2H, t, J = 6.6 Hz, H_1 x 2), 2.43 (2H, td, J = 7.3, 1.6 Hz, H_8 x 2), 1.71–1.60 (4H, m, H_2 x 2, H_7 x 2), 1.42–1.31 (8H, m, H_3 x 2, H_4 x 2, H_5 x 2, H_6 x 2); **^{13}C NMR** (125 MHz, $CDCl_3$): δ_C 202.7, 155.1, 131.7, 118.8, 68.3, 68.1, 43.8, 29.0, 28.9, 28.6, 25.5, 21.9; **HRMS** calculated for $C_{12}H_{21}O_4$ $[M+H]^+$ 229.1434, found 229.1435.

Enone 264a

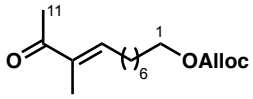

A solution of phosphonate **123** (80.0 mg, 0.385 mmol) in THF (2 mL) was added *via* cannula to a flask containing of $Ba(OH)_2$ (83.0 mg, 0.482 mmol) in THF (2 mL). The resulting suspension was stirred at rt for 45 min before adding a solution of aldehyde **264** (44.0 mg, 0.193 mmol) in THF/H_2O (40:1, 2 mL). The reaction was stirred for 16 h during which a pale yellow colour developed. The mixture was quenched by addition of NH_4Cl solution (5 mL) and extracted with EtOAc (3 x 5 mL). Combined organic phases were dried ($MgSO_4$), concentrated *in vacuo* and purified by flash column chromatography (gradient elution: EtOAc/40–60 PE, 1:15 → 1:10) to yield enone **264a** (29.0 mg, 0.103 mmol, 53%, >20:1 *E*/*Z*) as a colourless oil.

$\mathbf{R}_f$ 0.71 (EtOAc/40–60 PE, 1:3); **IR** (thin film, ν_{max} / cm^{-1}) 2925, 2853, 1746, 1667, 1637, 1459, 1393, 1366, 1249, 1082, 957, 935, 789; **^{1}H NMR** (400 MHz, $CDCl_3$): δ_H 6.60 (1H, t, J = 7.3 Hz, H_8), 5.92 (1H

ddt, J = 17.1, 10.4, 5.9 Hz, C<u>H</u>=CH$_2$), 5.34 (1H, br d, J = 17.1 Hz, CH=C<u>H$_a$</u>H$_b$), 5.25 (1H, br d, J = 10.4, CH=CH$_a$<u>H$_b$</u>), 4.61 (2H, d, J = 5.8 Hz, OC<u>H$_2$</u>), 4.13 (2H, t, J = 6.7 Hz, H$_1$ x 2), 2.29 (3H, s, Me$_{11}$), 2.22 (2H, dt, J = 7.4, 7.0 Hz, H$_7$ x 2), 1.74 (3H, s, Me$_9$), 1.70–1.63 (2H, m, H$_2$ x 2), 1.49–1.42 (2H, m, H$_6$ x 2), 1.45–1.31 (6H, m, H$_3$ x 2, H$_4$ x 2, H$_5$ x 2); **^{13}C NMR** (100 MHz, $CDCl_3$): δ_C 199.6, 154.8, 143.4, 137.3, 131.4, 118.6, 68.0, 67.7, 28.9, 28.7, 28.6, 28.2 x 2, 25.2, 25.0, 10.8; **HRMS** calculated for $C_{16}H_{27}O_4$ $[M+Na]^+$ 283.1904, found 283.1906.

Allylic alcohol 265

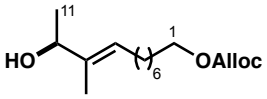

(*R*)-Me-CBS catalyst (149 μL, 0.149 mmol) and $BH_3{\cdot}SMe_2$ (11 μL, 0.119 mmol) were added sequentially to a solution of enone **264a** (28.4 mg, 0.100 mmol) in THF (2 mL) at –10 °C. The reaction was stirred at this temperature for 1 h, then quenched by dropwise addition of MeOH. The mixture was warmed to rt and stirred for 15 minutes before being concentrated *in vacuo*. The residue was redissolved in MeOH (2 mL), followed by concentration *in vacuo*, which was repeated twice. Crude product was purified by flash column chromatography (gradient elution: EtOAc/40–60 PE, 1:15 → 1:10) to give allylic alcohol **265** (26.0 mg, 91.4 μmol, 92%) as a colourless oil.

R$_f$ 0.38 (EtOAc/40–60 PE, 1:3); **IR** (thin film, ν_{max} / cm^{-1}); 3424, 2924, 2849, 1742, 1460, 1395, 1361, 1252, 1078, 1034, 963, 935, 889, 796; **^{1}H NMR** (500 MHz, $CDCl_3$): δ_H 5.95 (1H, ddt, J = 17.2, 10.5 Hz, C<u>H</u>=CH$_2$), 5.42–5.39 (1H, m, H$_8$), 5.37 (1H, dq, J = 17.2, 1.5 Hz, CH=C<u>H$_a$</u>H$_b$), 5.82 (1H, dq, J = 10.5, 1.2 Hz, CH=H$_a$<u>H$_b$</u>), 4.64 (2H, dt, J = 5.8, 1.3 Hz, OC<u>H$_2$</u>), 4.22 (1H, q, J = 6.4 Hz, H$_{10}$), 4.15 (2H, t, J = 6.8 Hz, H$_1$ x 2), 2.03–1.99 (2H, m, H$_7$ x 2), 1.71–1.65 (2H, m, H$_2$ x 2), 1.63 (3H, s, Me$_9$), 1.41–1.31 (8H, m, H$_3$ x 2, H$_4$ x 2, H$_5$ x 2, H$_6$ x 2), 1.26 (3H, d, J = 6.4 Hz, Me$_{11}$); **^{13}C NMR** (125 MHz, $CDCl_3$): δ_C 155.1, 138.4, 131.7, 125.2, 118.8, 73.4, 68.3, 68.2, 29.4, 29.1 x 2, 28.6, 27.4, 25.6, 21.6, 11.4; **HRMS** calculated for $C_{16}H_{28}O_4Na$ $[M+Na]^+$ 307.1880, found 307.1883.

Enone 251

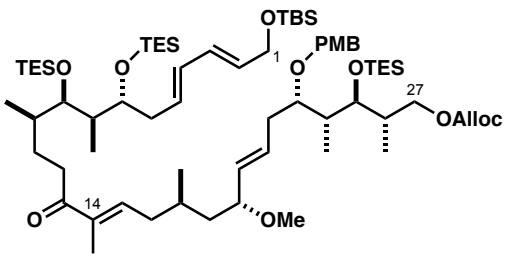

A suspension of $Ba(OH)_2$ (47.0 mg, 0.275 mmol) in THF (2 mL) was sonicated for 5 min before a solution of **253** and **254** (3:1, 336 mg, 0.324 mmol) in THF (2 mL) was added. The mixture was stirred at rt for 1.5 h before a solution of aldehyde **161** (166 mg, 0.262 mmol) in THF/H_2O (40:1, 2 mL) was added *via* cannula. The reaction mixture was stirred for 20 h before being quenched with NH_4Cl solution (5 mL) and diluted with H_2O (2 mL). The layers were separated and the aqueous phase was extracted with EtOAc (3 x 10 mL). Combined organic extracts were dried ($MgSO_4$), concentrated *in vacuo* and the crude material purified by flash column chromatography (gradient elution: EtOAc/40–60 PE, 1:30 → 1:5). Enone **251** (315 mg, 0.250 mmol, 96%) was obtained as a colourless oil.

R_f 0.53 (EtOAc/40–60 PE, 1:5); **$[\alpha]_{20}^{D}$** = +1.1 (*c* 1.0, $CHCl_3$); **IR** (thin film, ν_{max} / cm^{-1}): 2953, 2876, 1746, 1670, 1514, 1459, 1377, 1292, 1247, 1169, 1092, 1038, 1006, 969, 835, 776, 736, 735, 723; **^{1}H NMR** (500 MHz, $CDCl_3$): δ_H 7.26 (2H, d, *J* = 8.4 Hz, Ar$\underline{H}$), 6.89 (2H, d, *J* = 8.4 Hz, Ar$\underline{H}$), 6.64 (1H, t, *J* = 6.9 Hz, H_{15}), 6.21 (1H, dd, *J* = 15.0, 10.5 Hz, H_3), 6.07 (1H, dd, *J* = 15.0, 10.5 Hz, H_4), 6.00–5.92 (1H, m, C$\underline{H}$=CH_2), 5.71 (1H, dt, *J* = 15.2, 7.5 Hz, H_2), 5.66 (1H, dt, *J* = 15.2, 5.5 Hz, H_5), 5.64–5.58 (1H, m, H_{21}), 5.38 (1H, dd, *J* = 17.2, 1.4 Hz, CH=C$\underline{H}_a$$H_b$), 5.33 (1H, dd, *J* = 15.5, 8.5 Hz, H_{20}), 5.28 (1H, dd, *J* = 10.4, 1.3 Hz, CH=$CH_a\underline{H}_b$), 4.64 (2H, d, *J* = 5.7 Hz, OC$\underline{H}_2$), 4.59 (1H, d, *J* = 11.1 Hz, ArC$\underline{H}_a$$H_b$O), 4.40 (1H, d, *J* = 11.1 Hz, Ar$CH_a\underline{H}_b$O), 4.32 (1H, dd, *J* = 10.8, 4.3 Hz, H_{27a}), 4.22 (2H, d, *J* = 5.6 Hz, H_1 x 2), 3.96 (1H, dd, *J* = 10.5, 9.0 Hz, H_{27b}), 3.82 (3H, s, ArOC$\underline{H}_3$), 3.74 (1H, dd, *J* = 7.5, 2.8 Hz, H_{25}), 3.71–3.63 (2H, m, H_7, H_{23}), 3.61–3.56 (2H, m, H_9, H_{19}), 3.26 (3H, s, OC$\underline{H}_3$), 2.76 (1H, ddd, *J* = 15.3, 9.8, 5.3 Hz, H_{12a}), 2.62–2.50 (2H, m, H_{12b}, H_{22a}), 2.35–2.28 (2H, m, H_{16a}, H_{22b}), 2.20–2.05 (4H, m, H_6 x 2, H_{16b}, H_{26}), 1.84–1.73 (4H, m, H_8, H_{11a}, H_{17}, H_{24}), 1.79 (3H, s, Me_{14}), 1.60–1.53 (2H, m, H_{10}, H_{18a}), 1.46–1.39 (2H, m, H_{11b}, H_{18b}), 1.06 (3H, d, *J* = 6.9 Hz, Me_{26}), 1.00–0.92 (36H, m, Me_8, Me_{17}, Me_{24}, $SiCH_2C\underline{H}_3$ x 9), 0.93 (9H, s, $SiC(C\underline{H}_3)_3$), 0.88 (3H, d, *J* = 6.9 Hz, Me_{10}), 0.66–0.57 (18H, m, $SiC\underline{H}_2CH_3$ x 9), 0.09 (6H, s, $SiC\underline{H}_3$ x 2); **^{13}C NMR** (125 MHz, $CDCl_3$): δ_C 201.9, 159.0, 155.2, 140.4, 138.1, 133.0, 131.7, 131.4, 131.2, 130.6, 130.4, 130.3, 128.6 x 2, 118.8, 113.7, 80.5, 78.3, 77.5, 74.5, 70.8, 69.8, 68.3, 63.7, 55.8, 55.3, 42.9, 41.8, 41.3, 38.1, 36.1 x 2, 35.6, 35.4, 34.9, 29.6, 26.8, 26.0 x 2, 20.0, 18.4, 16.2, 16.0, 11.6, 10.5, 10.2, 7.2, 7.1, 7.0, 5.6 x 2, 5.3, –5.2; **HRMS** calculated for $C_{70}H_{132}NO_{11}Si_4$ $[M+NH_4]^+$ 1274.8872, found 1274.8855.

Allylic alcohol 256

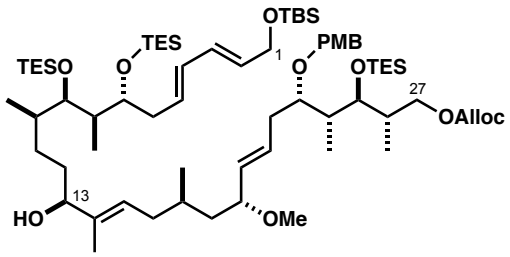

(*R*)-Me-CBS catalyst (1.62 mL, 1.0 M in PhMe, 1.61 mmol) was added to a solution of enone **251** (1.56 g, 1.24 mmol) in THF (50 mL) at –20 °C, followed by dropwise addition of $BH_3{\cdot}SMe_2$ (141 μL, 1.48 mmol). The mixture was warmed to –10 °C and stirred for 3 h before being slowly quenched with $NaHCO_3$ solution (10 mL), warmed to rt and stirred for a further 20 min until bubbling had ceased. The mixture was diluted with H_2O (20 mL), extracted with EtOAc (3 x 40 mL), dried (Na_2SO_4) and concentrated *in vacuo*. Purification by flash column chromatography (gradient elution: EtOAc/40–60 PE, 1:15 → 1:8) yielded allylic alcohol **256** (1.45 g, 1.15 mmol, 93%, 20:1 *dr*) as a colourless oil.

R_f 0.44 (EtOAc/40–60 PE, 1:5); **$[\alpha]_{20}^{D}$** = +6.3 (*c* 1.0, $CHCl_3$); **IR** (thin film, ν_{max} / cm^{-1}): 2952, 2873, 1748, 1516, 1460, 1415, 1379, 1299, 1248, 1100, 1042, 1006, 969, 834, 778, 741; **^{1}H NMR** (500 MHz, $CDCl_3$): δ_H 7.26 (2H, d, *J* = 8.5 Hz, Ar$\underline{H}$), 6.89 (2H, d, *J* = 8.5 Hz, Ar$\underline{H}$), 6.21 (1H, dd, *J* = 15.0, 10.5 Hz, H_3), 6.06 (1H, dd, *J* = 15.0, 10.4 Hz, H_4), 5.96 (1H, ddt, *J* = 17.1, 10.4, 5.8 Hz, C$\underline{H}$=CH_2), 5.70 (1H, dt, *J* = 15.1, 7.5 Hz, H_2), 5.66 (1H, dt, *J* = 15.1, 5.3 Hz, H_5), 5.63–5.57 (1H, m, H_{21}), 5.40–5.36 (2H, m, H_{15}, CH=C$\underline{H_a}H_b$), 5.32–5.27 (2H, m, H_{20}, CH=C$H_a\underline{H_b}$), 4.65–4.63 (2H, m, O$C\underline{H_2}$), 4.60 (1H, d, *J* = 11.2 Hz, ArC$\underline{H_a}H_bO$), 4.40 (1H, d, *J* = 11.2 Hz, ArC$H_a\underline{H_b}$O), 4.32 (1H, dd, *J* = 10.6, 4.2 Hz, H_{27a}), 4.23 (2H, d, *J* = 5.1 Hz, H_1 x 2), 3.98–3.94 (2H, m, H_{13}, H_{27b}), 3.82 (3H, s, ArOC$\underline{H_3}$), 3.74 (1H, dd, *J* = 7.7, 2.7 Hz, H_{25}), 3.69 (1H, ddd, *J* = 7.7, 5.3, 2.7 Hz, H_{23}), 3.64–3.61 (1H, m, H_7), 3.58–3.53 (1H, m, H_{19}), 3.52 (1H, dd, *J* = 5.0, 3.4 Hz, H_9), 3.25 (3H, s, OC$\underline{H_3}$), 2.52 (1H, dd, *J* = 14.1, 5.4 Hz, H_{22a}), 2.32 (1H, dd, *J* = 14.1, 7.9 Hz, H_{22b}), 2.22 (4H, m, H_6 x 2, H_{16a}, H_{26}), 1.87–1.74 (3H, m, H_8, H_{16b}, H_{24}), 1.68–1.60 (2H, m, H_{12a}, H_{18a}), 1.61 (3H, s, Me_{14}), 1.57–1.39 (6H, m, H_{10}, H_{11} x 2, H_{12b}, H_{17}, H_{18b}), 1.06 (3H, d, *J* = 6.9 Hz, Me_{26}), 0.99–0.95 (33H, m, Me_{10}, Me_{24}, $SiCH_2C\underline{H_3}$ x 9), 0.94 (9H, s, $SiC(C\underline{H_3})_3$), 0.91 (3H, d, *J* = 6.8 Hz, Me_{17}), 0.88 (6H, d, *J* = 6.8 Hz, Me_8), 0.67–0.57 (18H, m, $SiC\underline{H_2}CH_3$ x 9), 0.10 (6H, s, $SiC\underline{H_3}$ x 2); **^{13}C NMR** (125 MHz, $CDCl_3$): δ_C 158.9, 155.2, 138.0, 133.3, 131.7, 131.6, 131.4, 131.2, 130.3 x 2, 128.6, 125.8, 118.8, 113.7, 80.8, 79.0, 78.3, 77.7, 77.2, 74.6, 70.8, 69.8, 68.3, 63.7, 55.8, 55.2, 42.9, 41.9, 41.3, 38.5, 35.9, 35.6, 35.0, 34.9, 33.1, 29.9, 27.8, 26.0 x 2, 19.8, 18.5, 16.5, 16.1, 11.0, 10.4, 10.2, 7.2, 7.1, 7.0, 5.7, 5.6, 5.2, –5.1; **HRMS** calculated for $C_{70}H_{134}NO_{11}Si_4$ $[M+NH_4]^+$ 1276.9028, found 1276.9018.

(*R*)-Mosher ester 257

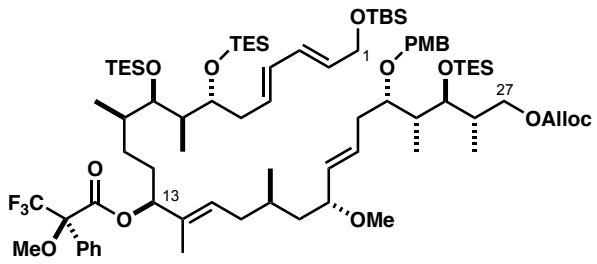

DCC (80 μL, 1.0 M in CH_2Cl_2, 80 μmol) was added to a solution of allylic alcohol **256** (10.9 mg, 8.6 μmol), (*R*)-(−)-α-methoxy-α-(trifluoromethyl)-phenylacetic acid (19.0 mg, 81.1 μmol) and DMAP (10.0 mg, 81.9 μmol) in CH_2Cl_2 (1 mL). The cloudy reaction mixture was stirred at rt for 3 h until complete. Solvent was removed *in vacuo*, the residue dissolved in Et_2O and filtered through cotton wool. The solution was concentrated *in vacuo* and the crude mixture purified by flash column chromatography (gradient elution: EtOAc/40–60 PE, 1:25 → 1:20) to yield (*R*)-Mosher ester **257** (9.8 mg, 6.6 μmol, 54%) as a colourless oil.

R_f 0.51 (EtOAc/40–60 PE, 1:10); **^{1}H NMR** (500 MHz, $CDCl_3$): δ_H 7.52–7.50 (2H, m, PhH), 7.41–7.38 (3H, m, PhH), 7.26 (2H, d, *J* = 8.5 Hz, ArH), 6.89 (2H, d, *J* = 8.5 Hz, ArH), 6.21 (1H, dd, *J* = 14.9, 10.1 Hz, H_3), 6.06 (1H, dd, *J* = 14.9, 10.4 Hz, H_4), 5.96 (1H, ddt, *J* = 17.1, 10.4, 5.8 Hz, CH=CH_2), 5.69–5.67 (2H, m, H_2, H_5), 5.62–5.54 (2H, m, H_{13}, H_{21}), 5.40–5.31 (3H, m, H_{15}, H_{20}, CH=CH_aH_b), 5.29 (1H, br d, *J* = 10.4 Hz, CH=CH_aH_b), 4.64 (1H, d, *J* = 5.6 Hz, OCH_2), 4.60 (1H, d, *J* = 11.1 Hz, ArCH_aCH_bO), 4.40 (1H, d, *J* = 11.1 Hz, ArC$H_a$$H_b$O), 4.32 (1H, dd, *J* = 10.6, 4.0 Hz, H_{27a}), 4.23 (2H, d, *J* = 5.3 Hz, H_1 x 2), 3.97 (1H, dd, *J* = 10.5, 9.3 Hz, H_{27b}), 3.82 (3H, s, ArOCH_3), 3.75 (1H, dd, *J* = 7.6, 2.4 Hz, H_{25}), 3.70–3.65 (1H, m H_{23}), 3.62–3.55 (2H, m, H_7, H_{19}), 3.58 (3H, s, OCH_3), 3.51 (1H, dd, *J* = 4.9, 3.2 Hz, H_9), 3.25 (3H, s, OMe_{19}), 2.52 (1H, dt, *J* = 14.0, 5.3 Hz, H_{22a}), 2.31 (1H, dt, *J* = 14.0, 8.2 Hz, H_{22b}), 2.22–2.09 (4H, m, H_6 x 2, H_{12a}, H_{26}), 1.84–1.75 (3H, m, H_{12b}, H_{16a}, H_{24}), 1.73–1.69 (1H, m, H_8), 1.67–1.60 (2H, m, H_{16b}, H_{17}), 1.55–1.47 (2H, m, H_{10}, H_{18a}), 1.43 (3H, s, Me_{14}), 1.43–1.37 (2H, m, H_{11a}, H_{18b}), 1.06 (3H, d, *J* = 6.8 Hz, Me_{26}), 0.99–0.91 (34H, m, H_{11b}, Me_{10}, Me_{24}, $SiCH_2CH_3$ x 9), 0.93 (9H, s, $SiC(CH_3)_3$), 0.87 (3H, d, *J* = 6.8 Hz, Me_8), 0.87 (3H, d, *J* = 6.8 Hz, Me_{17}), 0.67–0.56 (18H, m, $SiCH_2CH_3$ x 9), 0.10 (6H, s, $SiCH_3$ x 2); **HRMS** calculated for $C_{80}H_{141}F_3O_{13}NSi_4$ $[M+NH_4]^+$ 1492.9427, found 1492.9418.

(*S*)-Mosher ester 258

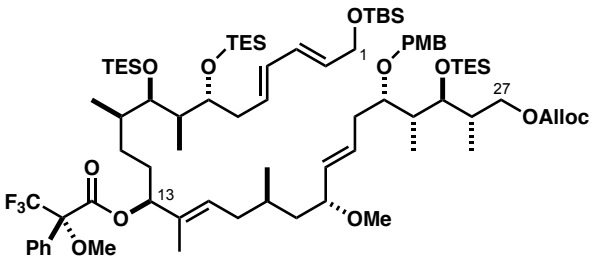

DCC (80 μL, 1.0 M in CH_2Cl_2, 80 μmol) was added to a solution of allylic alcohol **256** (10.6 mg, 8.4 μmol), (*S*)-(+)-α-methoxy-α-(trifluoromethyl)-phenylacetic acid (19.0 mg, 81.1 μmol) and DMAP (10.0 mg, 81.9 μmol) in CH_2Cl_2 (1 mL). The cloudy reaction mixture was stirred at rt for 3 h until complete. Solvent was removed *in vacuo*, the residue dissolved in Et_2O and filtered through cotton wool. The solution was concentrated *in vacuo* and the crude mixture purified by flash column chromatography (gradient elution: EtOAc/40–60 PE, 1:25 → 1:20) to yield (*S*)-Mosher ester **258** (11.0 mg, 7.5 μmol, 89%) as a colourless oil.

R_f 0.47 (EtOAc/40–60 PE, 1:10); **^{1}H NMR** (500 MHz, $CDCl_3$): δ_H 7.53–7.49 (2H, m, PhH), 7.41–7.38 (3H, m, PhH), 7.26 (2H, d, *J* = 8.4 Hz, ArH), 6.89 (2H, d, *J* = 8.4 Hz, ArH), 6.20 (1H, dd, *J* = 14.9, 10.3 Hz, H_3), 6.06 (1H, dd, *J* = 14.9, 10.9 Hz, H_4), 5.96 (1H, ddt, *J* = 17.1, 10.6, 5.7 Hz, CH=CH_2), 5.72–5.65 (2H, m, H_2, H_5), 5.63–5.56 (2H, m, H_{13}, H_{21}), 5.41–5.28 (4H, m, H_{15}, H_{20}, CH=C$H_a$$H_b$, CH=$CH_a$$H_b$), 4.64 (2H, d, *J* = 5.7 Hz, OCH_2), 4.59 (1H, d, *J* = 10.8 Hz, ArC$H_a$$CH_b$O), 4.40 (1H, d, *J* = 10.8 Hz, Ar$CH_a$$H_b$O), 4.32 (1H, dd, *J* = 10.6, 4.2 Hz, H_{27a}), 4.23 (2H, d, *J* = 5.4 Hz, H_1 x 2), 3.97 (1H, dd, *J* = 10.4, 9.3 Hz, H_{27b}), 3.82 (3H, s, ArOCH_3), 3.74 (1H, dd, *J* = 7.5, 2.5 Hz, H_{25}), 3.69–3.64 (1H, m, H_{23}), 3.62–3.56 (2H, m, H_7, H_{19}), 3.54 (3H, s, OCH_3), 3.49 (1H, dd, *J* = 4.7, 3.4 Hz, H_9), 3.24 (3H, s, OMe_{19}), 2.51 (1H, dt, *J* = 14.0, 5.5 Hz, H_{22a}), 2.33–2.27 (1H, m, H_{22b}), 2.20–2.10 (4H, m, H_6 x 2, H_{12a}, H_{26}), 1.86–1.76 (3H, m, H_{12b}, H_{16a}, H_{24}), 1.75–1.65 (2H, m, H_8, H_{10}), 1.61 (3H, s, Me_{14}), 1.62–1.48 (3H, m, H_{16b}, H_{17}, H_{18a}), 1.43–1.19 (2H, m, H_{11a}, H_{18b}), 1.05 (3H, d, *J* = 6.7 Hz, Me_{26}), 0.99–0.92 (31H, m, H_{11b}, Me_{24}, $SiCH_2CH_3$ x 9), 0.93 (9H, s, $SiC(CH_3)_3$), 0.90–0.85 (9H, m, Me_8, Me_{10}, Me_{17}), 0.67–0.56 (18H, m, $SiCH_2CH_3$ x 9), 0.09 (6H, s, $SiCH_3$ x 2); **HRMS** calculated for $C_{80}H_{141}F_3O_{13}NSi_4$ $[M+NH_4]^+$ 1492.9427, found 1492.9413.

Methyl ether 162

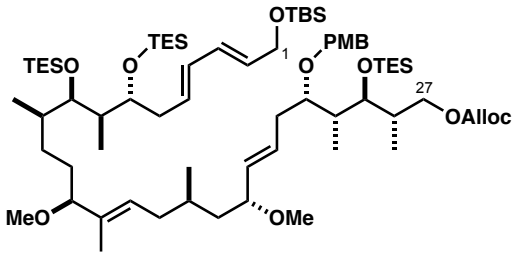

A solution of allylic alcohol **256** (1.66 g, 1.32 mmol) in CH_2Cl_2 (20 mL) was added *via* cannula to a flask containing trimethyloxonium tetrafluoroborate (1.36 g, 9.25 mmol) and Proton-Sponge® (1.98 g, 9.25 mmol). The resulting mixture was stirred for 4 h during which a colour change from pale yellow to orange was observed, then quenched by addition of NH_4Cl solution (50 mL). Phases were separated and the aqueous layer extracted with CH_2Cl_2 (3 x 50 mL). Combined organic extracts were dried (Na_2SO_4) and concentrated *in vacuo* to give a yellow solid. Crude product was purified by flash column chromatography (gradient elution: EtOAc/40–60 PE, 1:40 → 1:5) to give methyl ether **162** (1.28 g, 0.278 mmol, 76%) as a pale yellow oil.

R_f 0.64 (EtOAc/40–60 PE, 1:5); **$[\alpha]_{20}^{D}$** = +5.6 (*c* 1.0, $CHCl_3$); **IR** (thin film, ν_{max} / cm^{-1}): 2960, 2933, 2873, 1746, 1514, 1461, 1380, 1296, 1251, 1098, 1041, 1011, 989, 973, 843, 776, 739, 725; **^{1}H NMR** (500 MHz, $CDCl_3$): δ_H 7.25 (2H, d, *J* = 8.5 Hz, ArH), 6.89 (2H, d, *J* = 8.5 Hz, ArH), 6.20 (1H, dd, *J* = 15.1, 10.5 Hz, H_3), 6.06 (1H, dd, *J* = 15.1, 10.5 Hz, H_4), 5.96 (1H, ddt, *J* = 17.1, 10.5, 5.8 Hz, CH=CH_2), 5.70 (1H, dt, *J* = 15.1, 7.5 Hz, H_2), 5.66 (1H, dt, *J* = 15.1, 5.4 Hz, H_5), 5.59 (1H, ddd, *J* = 14.8, 7.9, 6.3 Hz, H_{21}), 5.37–5.31 (1H, m, CH=CH_aH_b), 5.37–5.31 (2H, m, H_{15}, H_{20}), 5.30–5.27 (1H, m, CH=CH_aH_b), 4.64 (2H, d, *J* = 5.9 Hz, OCH_2), 4.60 (1H, d, *J* = 11.0 Hz, ArCH_aH_bO), 4.40 (1H, d, *J* = 11.0 Hz, ArCH_aH_bO), 4.32 (1H, dd, *J* = 10.6, 4.3 Hz, H_{27a}), 4.23 (2H, d, *J* = 5.2 Hz, H_1 x 2), 3.96 (1H, dd, *J* = 10.6, 9.0 Hz, H_{27b}), 3.83 (3H, s, ArOCH_3), 3.75 (1H, dd, *J* = 7.5, 2.6 Hz, H_{25}), 3.71–3.67 (1H, m, H_{23}), 3.64–3.57 (2H, m, H_7, H_{19}), 3.51 (1H, dd, *J* = 4.3, 3.4 Hz, H_9), 3.38 (1H, dd, *J* = 7.0, 6.9 Hz, H_{13}), 3.26 (3H, s, OMe_{19}), 3.17 (3H, s, OMe_{13}), 2.52 (1H, ddd, *J* = 14.1, 5.5, 5.3 Hz, H_{22a}), 2.31 (1H, ddd, *J* = 14.1, 8.0, 7.3 Hz, H_{22b}), 2.20–2.12 (4H, m, H_6 x 2, H_{16a}, H_{26}), 1.89–1.74 (3H, m, H_8, H_{16b}, H_{24}), 1.68–1.63 (1H, m, H_{17}), 1.58–1.48 (4H, m, H_{10}, H_{11a}, H_{12} x 2), 1.52 (3H, s, Me_{14}), 1.46–1.40 (2H, m, H_{11b}, H_{18b}), 1.06 (3H, d, *J* = 6.9 Hz, Me_{26}), 0.99–0.96 (30H, m, Me_{24}, $SiCH_2CH_3$ x 9), 0.94 (9H, s, $SiC(CH_3)_3$), 0.91–0.87 (9H, m, Me_8, Me_{10}, Me_{17}), 0.67–0.58 (18H, m, $SiCH_2CH_3$ x 9), 0.10 (6H, s, $SiCH_3$ x 2); **^{13}C NMR** (125 MHz, $CDCl_3$): δ_C 159.0, 155.2, 135.1, 133.4, 131.8 x 2, 131.4, 131.2, 130.3 x 2, 130.2, 128.7, 127.8, 118.8, 113.7, 88.5, 80.9, 78.4, 77.7, 77.1, 74.7, 70.8, 69.8, 68.2, 63.8, 55.9, 55.6, 55.3, 42.9, 41.7, 41.3, 38.6, 35.8, 35.6, 35.0, 34.8, 32.0, 29.9, 27.9, 26.0, 19.8, 18.4, 16.3, 15.9, 10.3, 10.2, 10.1, 7.2, 7.1, 7.0, 5.7, 5.6, 5.2, –5.2; **HRMS** calculated for $C_{71}H_{136}NO_{11}Si_4$ $[M+NH_4]^+$ 1290.9185, found 1290.9173.

Aldehyde 163

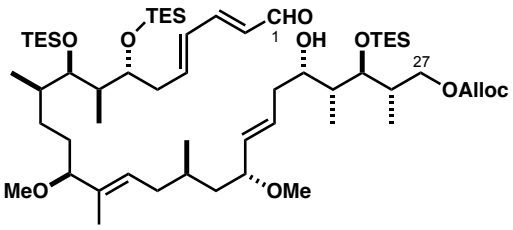

DDQ (107 mg, 0.471 mmol) was added to a stirred solution of TBS ether **162** (201 mg, 0.158 mmol) in CH_2Cl_2/pH 7 buffer solution (3:1, 10 mL) at 0 °C and a colour change to dark blue was observed. The mixture was warmed to rt and stirred for 30 min during which a gradual colour change to red was seen. An additional portion of DDQ (18.0 mg, 79.0 μmol) was added and the mixture stirred for an additional 30 min until complete. The reaction was quenched with $NaHCO_3$ solution (10 mL), warmed to rt and stirred for 30 min. Phases were separated and the aqueous layer extracted with CH_2Cl_2 (3 x 10 mL). Combined organic extracts were dried (Na_2SO_4), concentrated *in vacuo* and purified by flash column chromatography (gradient elution: EtOAc/40–60 PE, 1:15 → 1:8). Aldehyde **163** (133 mg, 0.128 mmol, 82%) was obtained as a pale yellow oil.

R_f 0.33 (EtOAc/40–60 PE, 1:5); **$[\alpha]_{20}^{D}$** = +3.0 (*c* 1.0, $CHCl_3$); **IR** (thin film, ν_{max} / cm^{-1}): 2948, 2873, 1752, 1683, 1637, 1461, 1376, 1251, 1156, 1094, 1006, 967, 801, 795, 737, 723; **^{1}H NMR** (500 MHz, $CDCl_3$): δ_H 9.57 (1H, d, *J* = 7.9 Hz, C<u>H</u>O), 7.10 (1H, dd, *J* = 15.3, 10.0 Hz, H_3), 6.38–6.30 (2H, m, H_4 H_5), 6.10 (1H, dd, *J* = 15.2, 7.9 Hz, H_2), 5.95 (1H, ddt, *J* = 17.1, 10.4, 5.8 Hz, C<u>H</u>=CH_2), 5.62 (1H, ddd, *J* = 15.1, 8.3, 5.9 Hz, H_{21}), 5.38 (1H, ddt, *J* = 17.1, 1.3, 1.3 Hz, CH=C<u>H_a</u>H_b), 5.36–5.31 (2H, m, H_{15}, H_{20}), 5.29 (1H, ddt, *J* = 10.4, 1.2, 1.2 Hz, CH=CH_a<u>H_b</u>), 4.67 (1H, dddd, *J* = 13.0, 5.9, 1.2, 1.2 Hz, OC<u>H_a</u>H_b), 4.62 (1H, dddd, *J* = 13.0, 5.9, 1.2, 1.2 Hz, OCH_a<u>H_b</u>), 4.28 (1H, dd, *J* = 10.5, 3.9 Hz, H_{27a}), 4.09–4.05 (2H, m, H_{23}, H_{27b}), 3.74 (1H, dd, *J* = 7.7, 2.9 Hz, H_{25}), 3.70–3.67 (1H, m, H_7), 3.58–3.53 (1H, m, H_{19}), 3.51 (1H, dd, *J* = 4.0, 3.9 Hz, H_9), 3.37 (1H, dd, *J* = 6.9, 6.8 Hz, H_{13}), 3.24 (3H, s, OMe_{19}), 3.16 (3H, s, OMe_{13}), 2.37–2.27 (3H, m, H_6 x 2, H_{22a}), 2.19–2.12 (3H, m, H_{16a}, H_{22b}, H_{26}), 1.89–1.83 (1H, m, H_{16b}), 1.79–1.70 (2H, m, H_8, H_{24}), 1.66–1.60 (1H, m, H_{17}), 1.57–1.39 (7H, m, H_{10}, H_{11} x 2, H_{12} x 2, H_{18} x 2), 1.51 (3H, s, Me_{14}), 1.04 (3H, d, *J* = 7.1 Hz, Me_{24}), 1.01–0.95 (30H, m, Me_{26}, $SiCH_2C$<u>H_3</u> x 9), 0.90–0.88 (9H, m, Me_8, Me_{10}, Me_{17}), 0.69 (6H, q, *J* = 7.9 Hz, SiC<u>H_2</u>CH_3 x 3), 0.64–0.58 (12H, m, SiC<u>H_2</u>CH_3 x 6); **^{13}C NMR** (125 MHz, $CDCl_3$): δ_C 194.0, 155.1, 152.4, 144.8, 135.1, 133.2, 131.6, 130.3 x 2, 130.2, 127.7, 119.0, 88.4, 80.8, 79.9, 77.4, 74.3, 70.3, 70.2, 68.4, 55.8, 55.7, 42.7, 41.6, 38.9, 37.9, 36.9 x 2, 36.4, 34.9, 32.0, 29.9, 29.7, 28.3, 19.9, 16.0, 14.4, 11.2, 10.4, 10.0, 7.1, 7.0, 5.6, 5.2 x 2; **HRMS** calculated for $C_{57}H_{112}NO_{10}Si_3$ $[M+NH_4]^+$ 1054.7589, found 1054.7586.

***Seco* acid 164**

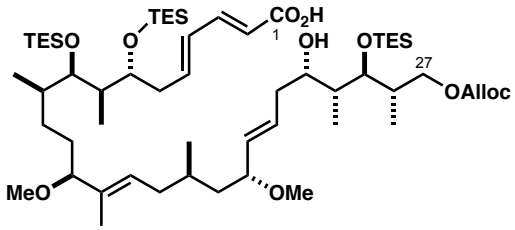

A solution of $NaClO_2$ (367 mg, 4.06 mmol) and $NaH_2PO_4{\cdot}H_2O$ (845 mg, 5.42 mmol) in H_2O (8.3 mL) was added dropwise to a solution of aldehyde **163** (281 mg, 0.271 mmol) in ^{t}BuOH/2-methyl-but-2-ene (10:1, 16.7 mL) at rt and stirred for 21 h. The mixture was diluted with H_2O (30 mL) and EtOAc (30 mL) and the phases were separated. The organic layer was washed with H_2O (3 x 20 mL) and back-extracted with EtOAc (2 x 10 mL). Combined organic phases were dried (Na_2SO_4) and concentrated *in vacuo*. Crude *seco*-acid **164** (274 mg, 0.260 mmol, 96% yield) was used in the next step without additional purification.

R_f 0.37 (EtOAc/40–60 PE, 1:2); **$[\alpha]_{20}^{D}$** = –1.3 (*c* 1.0, $CHCl_3$); **IR** (thin film, ν_{max} / cm^{-1}): 2952, 2916, 2880, 1746, 1722, 1692, 1639, 1460, 1417, 1395, 1377, 1252, 1092, 1034, 1004, 965, 743, 727; **^{1}H NMR** (500 MHz, $CDCl_3$): δ_H 7.35–7.29 (1H, m, H_3), 6.27–6.16 (2H, m, H_4, H_5), 5.94 (1H, ddt, *J* = 17.1, 10.4, 5.8 Hz, C<u>H</u>=CH_2), 5.80 (1H, d, *J* = 15.3 Hz, H_2), 5.61 (1H, ddd, *J* = 14.9, 8.0, 6.4 Hz, H_{21}), 5.37 (1H, ddt, *J* = 17.2, 1.4, 1.4 Hz, CH=C<u>H</u>$_a$H$_b$), 5.36–5.29 (2H, m, H_{15}, H_{20}), 5.28 (1H, ddt, *J* = 10.4, 1.2, 1.2 Hz, CH=CH$_a$<u>H</u>$_b$), 4.69–4.59 (2H, m, OC<u>H</u>$_2$), 4.27 (1H, dd, *J* = 10.4, 3.7 Hz, H_{27a}), 4.12–4.04 (2H, m, H_{23}, H_{27b}), 3.74 (1H, dd, *J* = 7.8, 2.7 Hz, H_{25}), 3.67–3.63 (1H, m, H_7), 3.60–3.53 (2H, m, H_9, H_{19}), 3.36 (1H, dd, *J* = 6.9, 6.8 Hz, H_{13}), 3.23 (3H, s, OMe_{19}), 3.15 (3H, s, OMe_{13}), 2.38–2.27 (3H, m, H_6 x 2, H_{22a}), 2.19–2.09 (3H, m, H_{16a}, H_{22b}, H_{26}), 1.89–1.79 (1H, m, H_{16b}), 1.77–1.66 (2H, m, H_8, H_{24}), 1.65–1.58 (1H, m, H_{17}), 1.50 (3H, s, Me_{14}), 1.56–1.32 (7H, m, H_{10}, H_{11} x 2, H_{12} x 2, H_{18} x 2), 1.04 (3H, d, *J* = 7.2 Hz, Me_{24}), 1.00–0.93 (30H, m, Me_{26}, SiCH$_2$C<u>H</u>$_3$ x 9), 0.89–0.84 (9H, m, Me_8, Me_{10}, Me_{17}), 0.68 (6H, q, *J* = 7.8 Hz, SiC<u>H</u>$_2$CH$_3$ x 3), 0.60 (6H, q, *J* = 7.8 Hz, SiC<u>H</u>$_2$CH$_3$ x 3), 0.58 (6H, q, *J* = 7.8 Hz, SiC<u>H</u>$_2$CH$_3$ x 3); **^{13}C NMR** (125 MHz, $CDCl_3$): δ_C 171.6, 155.1, 146.8, 143.1, 135.0, 133.2, 131.6, 130.3, 130.0, 127.8, 118.9, 118.7, 88.4, 80.9, 79.8, 77.2, 74.3, 70.4, 70.1, 68.4, 55.8, 55.6, 42.6, 41.4, 39.0, 37.8, 36.9, 36.8, 36.4, 34.9, 31.9, 29.9, 28.3, 19.9, 15.8, 14.4, 11.2, 10.3, 10.2, 7.1, 7.0, 6.9, 5.6, 5.2 x 2; **HRMS** calculated for $C_{57}H_{112}NO_{11}Si_3$ $[M+NH_4]^+$ 1070.7538, found 1070.7544.

Macrolactone 165

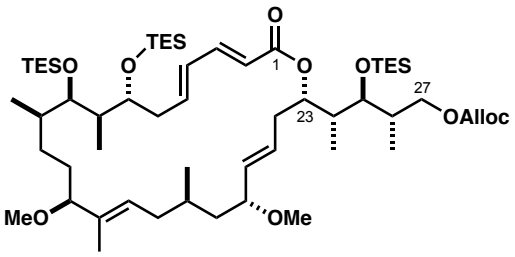

Et_3N (59 μL, 0.759 mmol) was added to a solution of *seco*-acid **164** (20.0 mg, 19.0 μmol) in THF (0.55 mL), followed by dropwise addition of TCBC (103 μL, 0.38 mmol). The mixture was stirred at rt for 1 h, then diluted with PhMe (2.2 mL) and the resulting cloudy orange solution added *via* syringe pump at a rate of 0.2 mL/h to a mixture of DMAP (139 mg, 1.14 mmol) and PhMe (3.4 mL). Upon completion, the reaction mixture was stirred for a further 3 h before being quenched with NH_4Cl solution (5 mL) and diluted with H_2O (3 mL). The organic layer was washed with NH_4Cl solution (3 x 5 mL), the combined organic phases dried (Na_2SO_4) and concentrated *in vacuo*. Crude residue was purified by flash column chromatography (gradient elution: EtOAc/40–60 PE, 1:15 → 1:8) to give macrolactone **165** (14.0 mg, 13.5 mmol, 70%) as a colourless oil.

R_f 0.50 (EtOAc/40–60 PE, 1:5); **$[\alpha]_{20}^{D}$** = +46.8 (*c* 0.5, $CHCl_3$); **IR** (thin film, ν_{max} / cm^{-1}): 2948, 2885, 1748, 1713, 1641, 1459, 1300, 1259, 1235, 1084, 1054, 1039, 1003, 967, 791, 753; **^{1}H NMR** (500 MHz, $CDCl_3$): δ_H 7.23 (1H, dd, *J* = 15.4, 10.8 Hz, H_3), 6.25 (1H, ddd, *J* = 14.5, 9.6, 4.4 Hz, H_5), 6.16 (1H, dd, *J* = 15.3, 10.8 Hz, H_4), 5.96 (1H, ddt, *J* = 16.5, 10.7, 5.8 Hz, C<u>H</u>=CH_2), 5.85 (1H, d, *J* = 15.3 Hz, H_2), 5.57 (1H, ddd, *J* = 14.9, 9.1, 6.1 Hz, H_{21}), 5.38 (1H, ddt, *J* = 17.2, 2.8, 1.6 Hz, CH=C<u>H_a</u>H_b), 5.31–5.27 (2H, m, CH=CH_a<u>H_b</u>, H_{23}), 5.06 (1H, dd, *J* = 15.5, 9.1 Hz, H_{20}), 5.05–5.02 (1H, m, H_{15}), 4.67–4.61 (2H, m, OC<u>H_2</u>), 4.30 (1H, dd, *J* = 10.6, 3.9 Hz, H_{27a}), 4.02 (1H, dd, *J* = 10.6, 7.5 Hz, H_{27b}), 3.65–3.62 (1H, m, H_7), 3.59 (1H, dd, *J* = 5.1, 5.1 Hz, H_{25}), 3.52 (1H, dt, *J* = 10.2, 4.2 Hz, H_{19}), 3.42–3.38 (2H, m, H_9, H_{13}), 3.22 (3H, s, OMe_{19}), 3.19 (3H, s, OMe_{13}), 2.40–2.33 (2H, m, H_{22} x 2), 2.31–2.25 (1H, m, H_{6a}), 2.19–2.12 (1H, m, H_{26}), 2.00–1.93 (2H, m, H_{6b}, H_{16a}), 1.86–1.80 (1H, m, H_{24}), 1.75–1.46 (6H, m, H_8, H_{10}, H_{12} x 2, H_{16b}, H_{18a}), 1.45 (3H, s, Me_{14}), 1.28–1.21 (2H, m, H_{17}, H_{18b}), 1.13–1.07 (2H, m, H_{11} x 2), 1.04 (3H, d, *J* = 7.1 Hz, Me_{24}), 1.03 (3H, d, *J* = 6.9 Hz, Me_{26}), 0.99–0.95 (30H, m, Me_{10}, $SiCH_2C$<u>H_3</u> x 9), 0.92 (3H, d, *J* = 7.0 Hz, Me_8), 0.82 (3H, d, *J* = 5.6 Hz, Me_{17}), 0.68–0.56 (18H, m, SiC<u>H_2</u>CH_3 x 9); **^{13}C NMR** (125 MHz, $CDCl_3$): δ_C 166.0, 155.1, 144.3, 142.1, 134.0, 132.9, 131.6, 131.2, 129.6, 129.4, 120.2, 118.7, 87.4, 81.5, 79.0, 77.1, 72.4, 71.4, 70.1, 68.2, 55.5 x 2, 42.5, 42.2, 40.2, 39.0, 38.2, 36.7, 36.2, 35.9, 30.8, 29.5, 27.7, 19.9, 15.4, 14.2, 11.9, 11.4, 9.5, 6.9 x 3, 5.2 x 2, 5.1; **HRMS** calculated for $C_{57}H_{110}NO_{10}Si_3$ $[M+NH_4]^+$ 1052.7432, found 1052.7430.

Macrocyclic alcohol 159

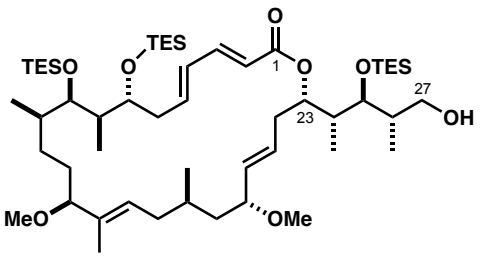

A solution of macrolactone **165** (18.0 mg, 17.4 μmol) in THF (2 mL) was added *via* cannula to a flask containing tetrakis(triphenylphosphine)palladium(0) (2.0 mg, 1.7 μmol) and dimedone (24.0 mg, 0.174 mmol) at rt. The mixture was stirred for 1 h until completion, then quenched with $NaHCO_3$ solution (10 mL) and extracted with EtOAc (2 x 20 mL). Combined organic extracts were dried (Na_2SO_4), concentrated *in vacuo* and the yellow residue was purified by flash column chromatography (gradient elution: EtOAc/40–60 PE, 1:15 → 1:5). Macrocyclic alcohol **159** (16.4 mg, 0.124 mmol, 99%) was obtained as a pale yellow oil.

R_f 0.20 (EtOAc/40–60 PE, 1:5); **^{1}H NMR** (500 MHz, $CDCl_3$): δ_H 7.25 (1H, dd, *J* = 15.2, 10.7 Hz, H_3), 6.27 (1H, ddd, *J* = 15.0, 10.2, 4.8 Hz, H_5), 6.17 (1H, dd, *J* = 14.9, 10.9 Hz, H_4), 5.85 (1H, d, *J* = 15.3 Hz, H_2), 5.58 (1H, ddd, *J* = 14.7, 10.2, 4.0 Hz, H_{21}), 5.26 (1H, ddd, *J* = 10.7, 4.9, 1.7 Hz, H_{23}), 5.08 (1H, dd, *J* = 15.2, 9.0 Hz, H_{20}), 5.04 (1H, dd, *J* = 10.5, 3.2 Hz, H_{15}), 3.72 (1H, ddd, *J* = 11.0, 5.5, 4.1 Hz, H_{27a}), 3.69 (1H, dd, *J* = 4.8, 4.8 Hz, H_{25}), 3.65–3.60 (2H, m, H_7, H_{27b}), 3.52 (1H, dt, *J* = 9.8, 4.1 Hz, H_{19}), 3.44–3.38 (2H, m, H_9, H_{13}), 3.22 (3H, s, OMe_{19}), 3.19 (3H, s, OMe_{13}), 2.53 (1H, t, *J* = 5.7 Hz, O<u>H</u>), 2.45–2.41 (1H, m, H_{22a}), 2.35 (1H, t, *J* = 10.7 Hz, H_{22b}), 2.33–2.26 (1H, m, H_{6a}), 2.02–1.92 (3H, m, H_{6b}, H_{16a}, H_{26}), 1.91–1.87 (1H, m, H_{24}), 1.76–1.46 (6H, m, H_8, H_{10}, H_{12} x 2, H_{16b}, H_{18a}), 1.45 (3H, s, Me_{14}), 1.26–1.21 (2H, m, H_{17}, H_{18b}), 1.14–1.07 (2H, obs m, H_{11} x 2), 1.05 (3H, d, *J* = 6.2 Hz, Me_{24}), 1.04 (3H, d, *J* = 6.2 Hz, Me_{26}), 0.99–0.95 (30H, m, Me_{10}, $SiCH_2C\underline{H}_3$ x 9), 0.92 (3H, d, *J* = 6.4 Hz, Me_8), 0.82 (3H, d, *J* = 5.8 Hz, Me_{17}), 0.73–0.67 (6H, m, $SiC\underline{H}_2CH_3$ x 3), 0.62 (6H, q, *J* = 7.8 Hz, $SiC\underline{H}_2CH_3$ x 3), 0.59 (6H, q, *J* = 7.8 Hz, $SiC\underline{H}_2CH_3$ x 3).

Data in agreement with that presented by Paterson.[108]

6.6. Experimental Procedures for Chapter 5

Alcohol 275

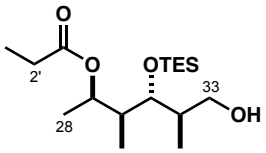

DDQ (4.81 g, 21.2 mmol) was added portionwise to a rapidly stirring biphasic mixture of PMB ether **274** (4.20 g, 9.28 mmol) in CH_2Cl_2/pH 7 buffer (4:1, 125 mL) at 0 °C. The resulting dark blue mixture was stirred at this temperature for 75 min, during which a colour change to murky red occurred. The reaction was quenched by addition of $NaHCO_3$ solution (100 mL), warmed to rt and diluted with H_2O (500 mL). The aqueous phase was extracted with CH_2Cl_2 (5 x 200 mL), the combined organic extracts dried (Na_2SO_4) and concentrated *in vacuo*. The crude product was purified by flash column chromatography (gradient elution: EtOAc/PhMe, 1:20 → 1:10) to yield alcohol **275** (2.84 g, 8.54 mmol, 92%) as a colourless oil.

R_f 0.39 (EtOAc/40–60 PE, 1:4); **^{1}H NMR** (500 MHz, $CDCl_3$): δ_H 5.03 (1H, qd, *J* = 6.2, 3.9 Hz, H_{29}), 3.81 (1H, ddd, *J* = 11.1, 4.3, 4.2 Hz, H_{33a}), 3.68 (1H, dd, *J* = 7.0, 3.5 Hz, H_{31}), 3.60 (1H, ddd, *J* = 11.5, 6.8, 4.9 Hz, H_{33b}), 2.67 (1H, dd, *J* = 6.8, 4.4 Hz, O<u>H</u>), 2.32 (1H, q, *J* = 7.6 Hz, $H_{2'}$ x 2), 1.92–1.85 (1H, m, H_{30}), 1.81 (1H, app dqd, *J* = 7.0, 7.0, 4.1 Hz, H_{32}), 1.28 (3H, d, *J* = 6.4 Hz, Me_{28}), 1.15 (3H, t, *J* = 7.6 Hz, $Me_{3'}$), 1.08 (3H, d, *J* = 7.0 Hz, Me_{32}), 1.00 (9H, t, *J* = 8.0 Hz, $SiCH_2C\underline{H}_3$ x 3), 0.99 (3H, d, *J* = 7.1 Hz, Me_{30}), 0.68 (6H, q, *J* = 7.9 Hz, $SiC\underline{H}_2CH_3$ x 3).

Data in agreement with that presented by Paterson.[108]

Diol 151

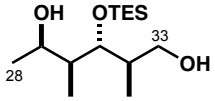

DIBALH (25.6 mL, 1.0 M in hexane, 25.6 mmol) was added dropwise to a solution of ester **275** (2.84 g, 8.54 mmol) in CH_2Cl_2 (150 mL) at −78 °C and the mixture stirred at this temperature for 2.5 h. The reaction was quenched by addition of Na^+/K^+ tartrate solution (250 mL), warmed to rt and stirred for 16 h. The phases were separated, the organic layer extracted with EtOAc (3 x 150 mL). Combined organic phases were dried (Na_2SO_4) and concentrated *in vacuo*. The crude was purified by flash column chromatography (gradient elution: EtOAc/40–60 PE, 1:10 → 1:7) to give diol **151** (2.21 g, 7.99 mmol,

94%) as a colourless oil.

R_f 0.16 (EtOAc/40–60 PE, 1:4); **^{1}H NMR** (400 MHz, $CDCl_3$): δ_H 4.25 (1H, br q, *J* = 6.3 Hz, H_{29}), 3.74 (1H, dd, *J* = 7.0, 3.4 Hz, H_{31}), 3.67 (1H, app t, *J* = 3.9 Hz, H_{33}), 2.91 (1H, br s, O<u>H</u>$_{29}$), 2.02–1.93 (1H, m, H_{32}), 1.83 (1H, app t, *J* = 5.4 Hz, O<u>H</u>$_{33}$), 1.65–1.58 (1H, m, H_{30}), 1.15 (3H, d, *J* = 6.5 Hz, Me_{28}), 1.02 (3H, d, *J* = 7.0 Hz, Me_{30}), 1.00 (9H, t, *J* = 8.0 Hz, $SiCH_2C\underline{H}_3$ x 3), 0.98 (3H, d, *J* = 7.0 Hz, Me_{32}), 0.71 (6H, q, *J* = 7.8 Hz, $SiC\underline{H}_2CH_3$ x 3).

Data in agreement with that presented by Paterson.[108]

Aldehyde 277

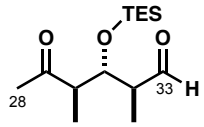

DMSO (2.59 mL, 36.5 mmol) was added dropwise to a solution of oxalyl chloride (1.54 mL, 18.3 mmol) in CH_2Cl_2 (100 mL) at −78 °C and stirred for 15 min. A solution of diol **151** (1.68 g, 6.08 mmol) in CH_2Cl_2 (25 mL) was added *via* cannula and the mixture stirred for further 15 min before dropwise addition of Et_3N (10.1 mL, 73.0 mmol). The reaction was kept at this temperature for an additional 1 h before removing the cooling bath and stirring for 10 min until completion. The mixture was quenched with NH_4Cl solution (100 mL), the layers separated and the aqueous phase extracted with CH_2Cl_2 (50 mL). Combined organic extracts were sequentially washed with 0.5 M HCl (100 mL), H_2O (100 mL) and $NaHCO_3$ solution (100 mL), dried (Na_2SO_4) and concentrated *in vacuo*. Due to risk of epimerisation, crude aldehyde **277** was used in the subsequent step without further purification.

(*Z*)-vinylformamide 152

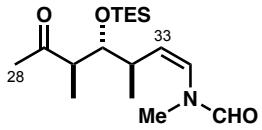

Freshly prepared LiHDMS (8.51 mL, 1.0 M in THF, 8.51 mmol) was added dropwise to a suspension of phosphonium salt **150** (3.37 g, 9.12 mmol) in THF (30 mL) at −78 °C. The mixture was warmed to 0 °C and stirred for 45 min before the resulting yellow suspension was cooled back to −78 °C. A solution of crude aldehyde **277** (1.63 g, *ca.* 5.98 mmol, dried over CaH_2 in THF for 20 min before use) in THF (15 mL) was then added slowly *via* cannula and the reaction was stirred for 1.5 h until completion. The mixture was quenched with NH_4Cl solution (50 mL), warmed to rt and extracted with EtOAc (3 x 30 mL). Combined organic phases were dried ($MgSO_4$), concentrated *in vacuo* and purified by flash column

chromatography (gradient elution: EtOAc/CH_2Cl_2, 1:30 → 1:20) to yield (*Z*)-vinylformamide **152** (1.38 g, 4.21 mmol, 70% over 2 steps, 4.3:1 *Z*/*E*) as a colourless oil.

Data for the (*Z*)-isomer:

R_f 0.46 (EtOAc/ 40–60 PE, 1:1); **^{1}H NMR** (400 MHz, $CDCl_3$): δ_H 8.18 (0.83H, s, NC<u>H</u>O), [8.06] (0.17H, s, NC<u>H</u>O*), [6.26] (0.17H, s, NC<u>H</u>O*), 5.96 (1H, d, *J* = 8.8 Hz, H_{34}), 5.35 (0.83H, dd, *J* = 10.7, 8.8 Hz, H_{33}), [5.12] (0.17H, dd, *J* = 10.7, 8.8 Hz, H_{33}*), 3.86 (1H, dd, *J* = 8.0, 2.9 Hz, H_{31}), [3.16] (0.51H, s, NMe*), 3.02 (2.49H, s, NMe), 2.75–2.59 (2H, m, H_{30}, H_{32}), 2.16 (3H, s, Me_{28}), [1.07] (0.51H, d, *J* = 6.9 Hz, Me_{30}*), 1.07 (2.49H, d, *J* = 6.9 Hz, Me_{30}), 0.96 (9H, t, *J* = 8.1 Hz, $SiCH_2C\underline{H}_3$ x 3), 0.92 (3H, d, *J* = 7.1 Hz, Me_{32}), 0.61 (6H, q, *J* = 7.9 Hz, $SiC\underline{H}_2CH_3$ x 3).

Distinguishable resonances of the minor rotamer (4.7:1 ratio) are given in brackets and marked with an asterisk. Data in agreement with that presented by Paterson.[108]

Alcohol 278

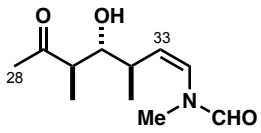

Distilled acetic acid (1.01 mL) was added to a solution of TBAF (22.3 mL, 1.0 M in THF, 22.3 mmol) at 0 °C and stirred for 30 min. The mixture was added *via* cannula to a flask containing TES ether **152** (1.05 g, 3.21 mmol) at 0 °C and stirred for 4 h until completion. The reaction mixture was poured into a solution of $NaHCO_3$ (100 mL) at 0 °C, stirred for 30 min then extracted with EtOAc (5 x 50 mL). Combined organic phases were dried (Na_2SO_4), concentrated *in vacuo* and purified by flash column chromatography (gradient elution: EtOAc/40–60 PE, 1:5 → 1:0). Alcohol **278** (684 mg, 3.20 mmol, 99%) was obtained as a colourless oil.

Data for the (*Z*)-isomer:

R_f 0.12 (EtOAc/40–60 PE, 3:2); **^{1}H NMR** (400 MHz, $CDCl_3$): δ_H 8.18 (0.83H, s, NC<u>H</u>O), [8.04] (0.17H, s, NC<u>H</u>O*), 6.00 (1H, d, *J* = 8.8 Hz, H_{34}), 5.32 (1H, dd, *J* = 10.7, 9.1 Hz, H_{33}), 3.62 (0.83H, dd, *J* = 7.2, 3.5 Hz, H_{31}), [3.56–3.52] (0.17H, m, H_{31}*), [3.13] (0.51H, s, NMe*), 3.04 (2.49H, s, NMe), 2.84 (1H, br s, O<u>H</u>), 2.72–2.65 (1H, m, H_{32}), 2.60 (1H, dq, *J* = 7.4, 7.4 Hz, H_{30}), [2.21] (0.51H, s, Me_{28}*), 2.20 (2.49H, s, Me_{28}), [1.18] (0.51H, obs, Me_{32}*), 1.16 (2.49H, d, *J* = 6.8 Hz, Me_{32}), [1.08] (0.51H, obs, Me_{30}*), 1.06 (2.49H, d, *J* = 7.4 Hz, Me_{30}).

Distinguishable resonances of the minor rotamer (4.7:1 ratio) are given in brackets and marked with an asterisk. Data in agreement with that presented by Paterson.[108]

Acetate 279

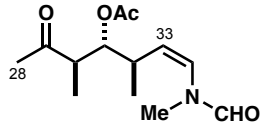

Et_3N (1.20 mL, 16.3 mmol), Ac_2O (1.40 mL, 14.9 mmol) and DMAP (1 crystal) were added sequentially to a stirring mixture of alcohol **278** (634 mg, 2.97 mmol) in CH_2Cl_2 (15 mL) at 0 °C and the reaction was stirred at this temperature for 1 h. Upon completion, the mixture was quenched by addition of $NaHCO_3$ solution (20 mL), warmed to room temperature and the aqueous phase extracted with CH_2Cl_2 (3 x 10 mL). Combined organic layers were dried ($MgSO_4$), concentrated *in vacuo* and filtered through a short silica plug, eluting with EtOAc/40–60 PE (3:2). The filtrate was concentrated *in vacuo* and submitted directly to the subsequent isomerisation reaction.

Data for the (*Z*)-isomer:

R_f 0.31 (EtOAc/CH_2Cl_2, 1:1); **^{1}H NMR** (400 MHz, $CDCl_3$): δ_H 8.19 (0.83H, s, NC<u>H</u>O), [8.09] (0.17H, s, NC<u>H</u>O*), [6.29] (0.17H, d, *J* = 8.8 Hz, H_{34}*), 6.03 (0.83H, d, *J* = 8.9 Hz, H_{34}), 5.18 (1H, dd, *J* = 9.3 Hz, H_{33}), 5.13 (1H, dd, *J* = 10.8 Hz, H_{31}), [3.19] (0.51H, s, NMe*), 3.06 (2.49H, s, NMe), 2.92–2.83 (1H, m, H_{32}), 2.75 (1H, dq, *J* = 7.6, 7.1 Hz, H_{30}), 2.16 (3H, s, Me_{28}), 2.06 (3H, s, OC(O)Me), 1.07 (3H, d, *J* = 7.1 Hz, Me_{32}), 1.07 (3H, d, *J* = 6.8 Hz, Me_{30}).

Distinguishable resonances of the minor rotamer (4.7:1 ratio) are given in brackets and marked with an asterisk. Data in agreement with that presented by Paterson.[108]

(*E*)-enamide 118

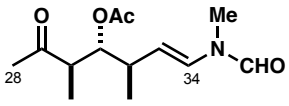

Iodine (1.13 g, 4.46 mmol) was added in one portion to a solution of (Z)-enamide **279** (*ca*. 759 mg, 2.97 mmol, 4.3:1 *Z*/*E*) in CH_2Cl_2 (200 mL) in the dark and stirred at rt for 22 h before quenching with $Na_2S_2O_3$ solution (100 mL). The biphasic mixture was rapidly stirred for 30 min during which a colour change from dark red to pale yellow was observed. The phases were separated and the aqueous layer was extracted with CH_2Cl_2 (3 x 100 mL). Combined organic phases were dried ($MgSO_4$), concentrated *in*

vacuo and the crude product was purified by flash column chromatography (gradient elution: EtOAc/40–60 PE, 1:2 → 3:2) to give the (*E*)-enamide **118** (724 mg, 2.84 mmol, 95% over 2 steps) as a pale yellow oil.

R_f 0.31 (EtOAc/CH_2Cl_2, 1:1); **^{1}H NMR** (500 MHz, $CDCl_3$): δ_H **^{1}H NMR** (500 MHz, $CDCl_3$): δ_H 8.31 (0.65H, s, NC<u>H</u>O), [8.10] (0.35H, s, NC<u>H</u>O*), [7.19] (0.35H, d, *J* = 14.5 Hz, H_{34}*), 6.52 (0.65H, d, *J* = 14.2 Hz, H_{34}), 5.14 (1H, dd, *J* = 8.8, 4.2 Hz, H_{31}), [5.02] (0.35H, obs, H_{33}*), 4.99 (0.65H, dd, *J* = 14.1, 9.4 Hz, H_{33}), [3.09] (1.05H, s, NMe*), 3.05 (1.95H, s, NMe), 2.79 (0.65H, dq, *J* = 8.0, 7.0 Hz, H_{30}), [2.74] (0.35H, dq, *J* = 8.2, 7.0 Hz, H_{30}*) 2.58–2.49 (1H, m, H_{32}, H_{32}*), 2.17 (1.95H, s, Me_{28}*), [2.16] (1.05H, s, Me_{28}*), 2.06 (1.95H, s, OC(O)Me), [2.05] (1.05H, s, OC(O)Me*), 1.13 (1.95H, d, *J* = 7.2 Hz, Me_{30}), [1.12] (1.05H, d, *J* = 7.2 Hz, Me_{30}*), 1.08 (1.95H, d, *J* = 7.0 Hz, Me_{32}), [1.07] (1.05H, d, *J* = 6.8 Hz, Me_{32}*).

Distinguishable resonances of the minor rotamer (1.8:1 ratio) are given in brackets and marked with an asterisk. Data in agreement with that presented by Paterson.[108]

Aldehyde 120

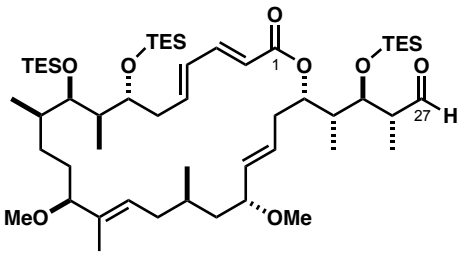

Oxalyl chloride (8 μL, 94.6 mol) was added to a solution of DMSO (13 μL, 189 μmol) in CH_2Cl_2 (2 mL) at −78 °C and stirred for 30 min before a solution of alcohol **159** (30.0 mg, 31.5 μmol) in CH_2Cl_2 (1.5 mL) was added *via* cannula. The resulting mixture was stirred for 30 min, followed by the addition of Et_3N (38 μL, 284 μmol). The reaction was stirred at this temperature for 30 min, then warmed up to 0 °C for a further 15 min. Upon completion, the mixture was quenched with NH_4Cl solution (2 mL), warmed to rt and the phases separated. The aqueous phase was extracted with Et_2O (3 x 5 mL), the combined organic layers dried ($MgSO_4$) and concentrated *in vacuo* to give aldehyde **120** (29.3 mg, 30.9 μmol, 98%) as a pale yellow oil, which was used immediately in the subsequent aldol reaction.

R_f 0.50 (EtOAc/40–60 PE, 1:5); **^{1}H NMR** (500 MHz, $CDCl_3$): δ_H 9.81 (1H, d, *J* = 2.1 Hz, C<u>H</u>O), 7.26 (1H, dd, *J* = 15.2, 10.7 Hz, H_3), 6.28 (1H, ddd, *J* = 15.2, 9.5, 4.7 Hz, H_5), 6.18 (1H, dd, *J* = 15.6, 11.0 Hz, H_4), 5.86 (1H, d, *J* = 15.2 Hz, H_2), 5.59 (1H, ddd, *J* = 14.9, 8.9, 5.1 Hz, H_{21}), 5.32 (1H, dt, *J* = 9.4, 3.7 Hz, H_{23}), 5.08 (1H, dd, *J* = 15.0, 9.0 Hz, H_{20}), 5.07-5.04 (1H, m, H_{15}), 3.95 (1H, dd, *J* = 5.4, 4.0 Hz, H_{25}), 3.64 (1H, dd, *J* = 7.8, 4.1 Hz, H_7), 3.54 (1H, app td, *J* = 10.0, 4.0, H_{19}), 3.45–3.39 (1H, obs, H_{19}), 3.39 (1H, dd, *J* = 10.9, 4.4 Hz, H_{13}), 3.22 (3H, s, OMe_{19}), 3.16 (3H, s, OMe_{13}), 2.69–2.64 (1H, m, H_{26}), 2.43–2.33 (2H, m, H_{22} x 2), 2.32–2.26 (1H, m, H_{6a}), 2.02–1.95 (2H, m, H_{6b}, H_{16a}), 1.88 (1H, qdd, *J* = 7.0, 3.9, 1.7 Hz, H_{24}), 1.77–1.64 (3H, m, H_8, H_{12a}, H_{16b}), 1.62–1.46 (2H, m, H_{10}, H_{12b}), 1.45 (3H, s, Me_{14}), 1.28–1.19 (2H, m, H_{17}, H_{18b}), 1.14 (3H, d, *J* = 7.1 Hz, Me_{26}), 1.13–1.08 (2H, obs, H_{11} x 2), 0.99–0.95 (33H, $SiCH_2C\underline{H}_3$ x 9, Me_{10}, Me_{24}), 0.93 (3H, d, *J* = 6.9 Hz, Me_8), 0.82 (3H, d, *J* = 5.7 Hz, Me_{17}), 0.68-0.57 (18H, m, $SiC\underline{H}_2CH_3$ x 9).

Data in agreement with that presented by Paterson.[108]

Enone 282 *via* aldol adduct 281

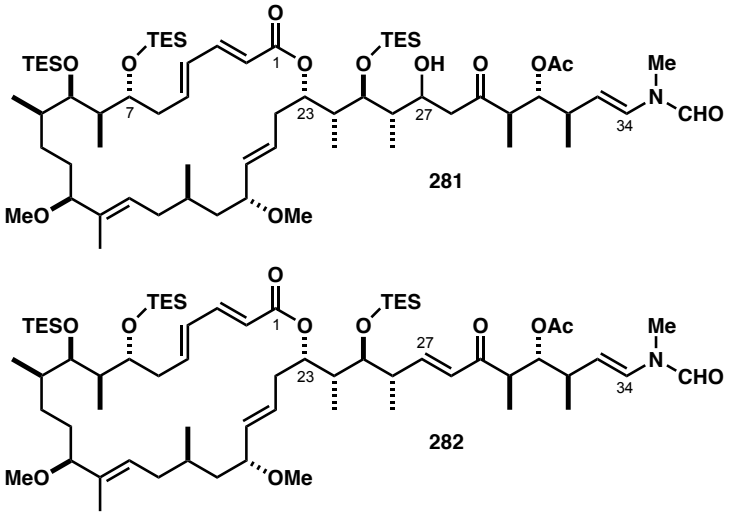

Ketone **118** (38.0 mg, 0.149 mmol) and aldehyde **120** (29.3 mg, 30.8 μmol) were dried azeotropically with PhH and placed under vacuum for 18 h. Ketone **118** was dissolved in Et_2O (0.5 mL), followed by sequential addition of Et_3N (28 μL, 0.201 mmol) and Cy_2BCl (31 μL, 0.150 mmol) at 0 °C. The resulting cloudy yellow solution was stirred for 1 h at this temperature before being cooled to –78 °C and a solution of aldehyde **120** in Et_2O (1.5 mL) was added. The reaction mixture was stirred at –78 °C for 1 h, warmed to –40 °C for an additional 1 h and gradually warmed to –10 °C over 1 h before quenching with pH 7 buffer (2 mL) and MeOH (2 mL). The mixture was stirred for 30 min before being extracted with EtOAc (3 × 10 mL), dried over ($MgSO_4$) and concentrated *in vacuo*. The crude material was purified by flash column chromatography (gradient elution: EtOAc/40–60 PE, 1:5 → 3:1) and all fractions containing

product along with recovered ketone **118** were collected and combined. The resulting mixture was used directly in the subsequent elimination.

Burgess reagent (27.0 mg, 95.0 μmol) was added to a flask containing the mixture of aldol adduct **281** and ketone **118** dissolved in THF (0.5 mL). The reaction mixture was stirred at rt for 16 h before quenching with NH_4Cl solution (3 mL) and the mixture being extracted with EtOAc (5 × 3 mL). The combined organic extracts were dried ($MgSO_4$), concentrated *in vacuo* and the crude product purified by flash column chromatography (gradient elution: EtOAc/40–60 PE, 1:4 → 2:5) to afford enone **282** (22.8 mg, 19.2 μmol, 63% over 2 steps) as a colourless oil.

R_f 0.87 (EtOAc/40–60 PE, 3:2); **^{1}H NMR** (500 MHz, $CDCl_3$) δ_H 8.32 (0.67H, s, C<u>H</u>O), [8.11] (0.33H, s, C<u>H</u>O*), 7.24 (1H, dd, *J* = 15.2, 10.5 Hz, H_3), [7.20] (0.33H, d, *J* = 15.0 Hz, H_{34}*), 7.02 (0.67H, dd, *J* = 15.6, 8.0 Hz, H_{27}), [7.00] (0.33H, dd, *J* = 15.8, 7.8 Hz, H_{27}*), 6.52 (0.67H, d, *J* = 14.0 Hz, H_{34}), 6.27 (1H, ddd, *J* = 15.2, 9.2, 4.1 Hz, H_5), 6.20 (0.67H, d, *J* = 15.7 Hz, H_{28}), [6.19] (0.33H, d, *J* = 15.6 Hz, H_{28}*), 6.15 (1H, dd, *J* = 15.6, 10.6 Hz, H_4), 5.85 (1H, d, *J* = 15.3 Hz, H_2), 5.62–5.56 (1H, m, H_{21}), 5.31–5.27 (1H, m, H_{23}), 5.21 (0.67H, dd, *J* = 8.8, 3.7 Hz, H_{31}), [5.20] (0.33H, dd, *J* = 8.5, 3.6 Hz, H_{31}*), 5.10–5.02 (2H, m, H_{33}, H_{20}), 5.02 (1H, dd, *J* = 13.9, 9.3 Hz, H_{15}), 3.66–3.61 (2H, m, H_7, H_{25}), 3.53 (1H, ddd, *J* = 13.0, 9.9, 4.0 Hz, H_{19}), 3.40 (1H, obs, H_9), 3.40 (1H, dd, *J* = 11.0, 4.3 Hz, H_{13}), 3.22 (3H, s, OMe_{19}), 3.19 (3H, s, OMe_{13}), [3.10] (1H, s, NMe*), 3.06 (2H, s, NMe), 3.01 (0.67H, dq, *J* = 8.5, 7.2 Hz, H_{32}), [2.97] (0.33H, dq, *J* = 8.8, 7.0 Hz, H_{32}*), 2.67–2.51 (2H, m, H_{26}, H_{30}), 2.38–2.27 (3H, m, H_{6a}, H_{22} x 2), 2.01 (2H, s, COC<u>H</u>$_3$), [2.00] (1H, s, COC<u>H</u>$_3$*), 2.02–1.95 (2H, m, H_{6b}, H_{16a}), 1.80–1.63 (4H, m, H_8, H_{12a}, H_{16b}, H_{24}), 1.63–1.43 (3H, m, H_{10}, H_{12b}, H_{18a}), 1.45 (3H, s, Me_{14}), 1.26–1.19 (2H, m, H_{18b}, H_{17}), 1.11–1.07 (8H, m, H_{11} x 2, Me_{26}, Me_{32}), 1.00 (3H, d, *J* = 7.1 Hz, Me_{30}), 0.99–0.95 (30H, m, Me_{10}, $SiCH_2C$<u>H</u>$_3$ x 9), 0.94 (3H, d, *J* = 6.7 Hz, Me_{24}), 0.93 (3H, d, *J* = 6.7 Hz, Me_8), 0.82 (3H, d, *J* = 5.5 Hz, Me_{17}), 0.68–0.57 (18H, m, SiC<u>H</u>$_2CH_3$ x 9).

Distinguishable resonances of the minor rotamer (2:1 ratio) are given in brackets and marked with an asterisk.

References

(1) Masamune, S.; Ali, S. A.; Snitman, D. L.; Garvey, D. S. *Angew. Chem. Int. Ed.* **1980**, *19*, 557.

(2) Yamada, K.; Makoto, O.; Ishigaki, T.; Yoshida, Y. *J. Am. Chem. Soc.* **1993**, *115*, 11020.

(3) Williams, D. H.; Stone, M. J.; Hauck, P. R.; Rahman, S. K. *J. Nat. Prod.* **1989**, *52*, 1189.

(4) Skropeta, D.; Wei, L. *Nat. Prod. Rep.* **2014**, *31*, 999.

(5) Blunt, J. W.; Copp, B. R.; Keyzers, R. A.; Munro, M. H. G.; Prinsep, M. R. *Nat. Prod. Rep.* **2014**, *31*, 160.

(6) Zhang, G.; Li, J.; Zhu, T.; Gu, Q.; Li, D. *Curr. Opin. Biotechnol.* **2016**, *42*, 13.

(7) Brahmachari, G. *Bioactive Natural Products*, Wiley, Germany, 2014.

(8) Gerwick, W. H.; Moore, B. S. *Chem. Biol.* **2012**, *19*, 85.

(9) Monciardini, P.; Iorio, M.; Maffioli, S.; Sosio, M.; Donadio, S. *Microb. Biotechnol.* **2014**, *7*, 209.

(10) Malik, S.; Cusidó, R. M.; Mirjalili, M. H.; Moyano, E.; Palazón, J.; Bonfill, M. *Process Biochem.* **2011**, *46*, 23.

(11) Kingston, D. G. I. *Chem. Commun.* **2001**, No. 10, 867.

(12) Allred, T. K.; Manoni, F.; Harran, P. G. *Chem. Rev.* **2017**, DOI: 10.1021/acs. chemrev.7b00126.

(13) Newman, D. J. *Pharmacol. Ther.* **2016**, *162*, 1.

(14) Smith, A. B.; Beauchamp, T. J.; LaMarche, M. J.; Kaufman, M. D.; Qiu, Y.; Arimoto, H.; Jones, D. R.; Kobayashi, K. *J. Am. Chem. Soc.* **2000**, *122*, 8654.

(15) Paterson, I.; Florence, G. J.; Gerlach, K.; Scott, J. P. *Angew. Chem. Int. Ed.* **2000**, *39*, 377.

(16) Mickel, S. J.; Sedelmeier, G. H.; Niederer, D.; Schuerch, F.; Seger, M.; Schreiner, K.; Daeffler, R.; Osmani, A.; Bixel, D.; Loiseleur, O.; Cercus, J.; Stettler, H.; Schaer, K.; Gamboni, R.; Bach, A.; Chen, G.-P.; Chen, W.; Geng, P.; Lee, G. T.; Loeser, E.; McKenna, J.; Kinder, F. R.; Konigsberger, K.; Prasad, K.; Ramsey, T. M.; Reel, N.; Repič, O.; Rogers, L.; Shieh, W.-C.; Wang, R.-M.; Waykole, L.; Xue, S.; Florence, G.; Paterson, I. *Org. Process Res. Dev.* **2004**, *8*, 113.

(17) Mickel, S. J.; Sedelmeier, G. H.; Niederer, D.; Schuerch, F.; Grimler, D.; Koch, G.; Daeffler, R.; Osmani, A.; Hirni, A.; Schaer, K.; Gamboni, R.; Bach, A.; Chaudhary, A.; Chen, S.; Chen, W.; Hu, B.; Jagoe, C. T.; Kim, H.-Y.; Kinder, F. R.; Liu, Y.; Lu, Y.; McKenna, J.; Prashad, M.; Ramsey, T. M.; Repič, O.; Rogers, L.; Shieh, W.-C.; Wang, R.-M.; Waykole, L. *Org. Process Res.*

Dev. **2004**, *8*, 101.

(18) Mickel, S. J.; Niederer, D.; Daeffler, R.; Osmani, A.; Kuesters, E.; Schmid, E.; Schaer, K.; Gamboni, R.; Chen, W.; Loeser, E.; Kinder, F. R.; Konigsberger, K.; Prasad, K.; Ramsey, T. M.; Repič, O.; Wang, R.-M.; Florence, G.; Lyothier, I.; Paterson, I. *Org. Process Res. Dev.* **2004**, *8*, 122.

(19) Mickel, S. J.; Sedelmeier, G. H.; Niederer, D.; Daeffler, R.; Osmani, A.; Schreiner, K.; Seeger-Weibel, M.; Bérod, B.; Schaer, K.; Gamboni, R.; Chen, S.; Chen, W.; Jagoe, C. T.; Kinder, F. R.; Loo, M.; Prasad, K.; Repič, O.; Shieh, W.-C.; Wang, R.-M.; Waykole, L.; Xu, D. D.; Xue, S. *Org. Process Res. Dev.* **2004**, *8*, 92.

(20) Mickel, S. J.; Sedelmeier, G. H.; Niederer, D.; Schuerch, F.; Koch, G.; Kuesters, E.; Daeffler, R.; Osmani, A.; Seeger-Weibel, M.; Schmid, E.; Hirni, A.; Schaer, K.; Gamboni, R.; Bach, A.; Chen, S.; Chen, W.; Geng, P.; Jagoe, C. T.; Kinder, F. R.; Lee, G. T.; McKenna, J.; Ramsey, T. M.; Repič, O.; Rogers, L.; Shieh, W.-C.; Wang, R.-M.; Waykole, L. *Org. Process Res. Dev.* **2004**, *8*, 107.

(21) Yu, M. J.; Zheng, W.; Seletsky, B. M. *Nat. Prod. Rep.* **2013**, *30*, 1158.

(22) Aicher, T. D.; Buszek, K. R.; Fang, F. G.; Forsyth, C. J.; Jung, S. H.; Kishi, Y.; Matelich, M. C.; Scola, P. M.; Spero, D. M.; Yoon, S. K. *J. Am. Chem. Soc.* **1992**, *114*, 3162.

(23) Towle, M. J.; Salvato, K. A.; Budrow, J.; Wels, B. F.; Kuznetsov, G.; Aalfs, K. K.; Welsh, S.; Zheng, W.; Seletsky, B. M.; Palme, M. H.; Habgood, G. J.; Singer, L. A.; DiPietro, L. V.; Wang, Y.; Chen, J. J.; Quincy, D. A.; Davis, A.; Yoshimatsu, K.; Kishi, Y.; Yu, M. J.; Littlefield, B. A. *Cancer Res.* **2001**, *61*, 1013.

(24) Bauer, A. Časar, Z., Ed.; *Synthesis of Heterocycles in Modern Medicinal Chemistry*, Springer, 2016, pp 209–270.

(25) Okude, Y.; Hirano, S.; Hiyama, T.; Nozaki, H. *J. Am. Chem. Soc.* **1977**, *99*, 3179.

(26) Jin, H.; Uenishi, J.; Christ, W. J.; Kishi, Y. *J. Am. Chem. Soc.* **1986**, *108*, 5644.

(27) Harvey, A. L.; Edrada-Ebel, R.; Quinn, R. J. *Nat. Rev. Drug Discov.* **2015**, *14*, 111.

(28) Newman, D. J.; Cragg, G. M. *J. Nat. Prod.* **2016**, *79*, 629.

(29) Cragg, G. M.; Grothaus, P. G.; Newman, D. J. *J. Nat. Prod.* **2014**, *77*, 703.

(30) Scannell, J. W.; Blanckley, A.; Boldon, H.; Warrington, B. *Nat. Rev. Drug Discov.* **2012**, *11*, 191.

(31) Kuttruff, C. A.; Eastgate, M. D.; Baran, P. S. *Nat. Prod. Rep.* **2014**, *31*, 419.

(32) Yamamura, S.; Hirata, Y. *Tetrahedron* **1963**, *19*, 1485.

(33) Kuroda, T.; Kigoshi, H. *Org. Lett.* **2008**, *10*, 489.

(34) Kita, M.; Kawamura, A.; Kigoshi, H. *Tetrahedron Lett.* **2016**, *57*, 858.

(35) Kawamura, A.; Kita, M.; Kigoshi, H. *Angew. Chem. Int. Ed.* **2015**, *54*, 7073.

(36) Yamada, K.; Ojika, M.; Kigoshi, H.; Suenaga, K. *Nat. Prod. Rep.* **2009**, *26*, 27.

(37) Ojika, M.; Kigoshi, H.; Suenaga, K.; Imamura, Y.; Yoshikawa, K.; Ishigaki, T.; Sakakura, A.;

Mutou, T.; Yamada, K. *Tetrahedron* **2012**, *68*, 982.

(38) Ojika, M.; Kigoshi, H.; Ishigaki, T.; Tsukada, I.; Tsuboi, T.; Ogawa, T.; Yamada, K. *J. Am. Chem. Soc.* **1994**, *116*, 7441.

(39) Ojika, M.; Kigoshi, H.; Ishigaki, T.; Yamada, K. *Tetrahedron Lett.* **1993**, *34*, 8501.

(40) Ojika, M.; Kigoshi, H.; Ishigaki, T.; Nisiwaki, M.; Tsukada, I.; Mizuta, K.; Yamada, K. *Tetrahedron Lett.* **1993**, *34*, 8505.

(41) Suenaga, K.; Ishigaki, T.; Sakakura, A.; Kigoshi, H.; Yamada, K. *Tetrahedron Lett.* **1995**, *36*, 5053.

(42) Kigoshi, H.; Ojika, M.; Ishigaki, T.; Suenaga, K.; Mutou, T.; Sakakura, A.; Ogawa, T.; Yamada, K. *J. Am. Chem. Soc.* **1994**, *116*, 7443.

(43) Kigoshi, H.; Suenaga, K.; Mutou, T.; Ishigaki, T.; Atsumi, T.; Ishiwata, H.; Sakakura, A.; Ogawa, T.; Ojika, M.; Yamada, K. *J. Org. Chem.* **1996**, *61*, 5326.

(44) Ojika, M.; Kigoshi, H.; Yoshida, Y.; Ishigaki, T.; Nisiwaki, M.; Tsukada, I.; Arakawa, M.; Ekimoto, H.; Yamada, K. *Tetrahedron* **2007**, *63*, 3138.

(45) Kita, M.; Hirayama, Y.; Sugiyama, M.; Kigoshi, H. *Angew. Chem. Int. Ed.* **2011**, *50*, 9871.

(46) Ohno, O.; Morita, M.; Kitamura, K.; Teruya, T.; Yoneda, K.; Kita, M.; Kigoshi, H.; Suenaga, K. *Bioorg. Med. Chem. Lett.* **2013**, *23*, 1467.

(47) Shoemaker, R. *Nat. Rev. Cancer* **2006**, *6*, 813.

(48) Ciavatta, M. L.; Lefranc, F.; Carbone, M.; Mollo, E.; Gavagnin, M.; Betancourt, T.; Dasari, R.; Kornienko, A.; Kiss, R. *Med. Res. Rev.* **2017**, *37*, 702.

(49) Saito, S.-y.; Watabe, S.; Ozaki, H.; Kigoshi, H.; Yamada, K.; Fusetani, N.; Karaki, H. *J. Biochem.* **1996**, *120*, 552.

(50) Sheterline, P.; Clayton, J.; Sparrow, J. *Actin*, Oxford University Press, 1999.

(51) Pollard, T. D.; Borisy, G. G. *Cell* **2003**, *112*, 453.

(52) Allingham, J. S.; Klenchin, V. A.; Rayment, I. *Cell. Mol. Life Sci. C.* **2006**, *63*, 2119.

(53) Pollard, T. D.; Cooper, J. A. *Science* **2009**, *326*, 1208.

(54) Courtemanche, N.; Pollard, T. D. *Biochemistry* **2013**, *52*, 6456.

(55) Goley, E. D.; Welch, M. D. *Nat. Rev. Mol. Cell Biol.* **2006**, *7*, 713.

(56) Blanchoin, L.; Pollard, T. D.; Hitchcock-DeGregori, S. E. *Curr. Biol.* **2001**, *11*, 1300.

(57) Jordan, M. A.; Wilson, L. *Curr. Opin. Cell Biol.* **1998**, *10*, 123.

(58) Cooper, J. A.; Schafer, D. A. *Curr. Opin. Cell Biol.* **2000**, *12*, 97.

(59) Torres Cleuren, Y.; Boonstra, J. *Actin: Structure, function and disease*, Nova Science Publishers, 2012.

(60) Tanaka, J.; Blain, J. C.; Allingham, J. S. *Chem. Biol.* **2008**, *15*, 205.

(61) Ueoka, R.; Uria, A. R.; Reiter, S.; Mori, T.; Karbaum, P.; Peters, E. E.; Helfrich, E. J. N.; Morinaka, B. I.; Gugger, M.; Takeyama, H.; Matsunaga, S.; Piel, J. *Nat. Chem. Biol.* **2015**, *11*,

705.

(62) Yeung, K.-S.; Paterson, I. *Angew. Chem. Int. Ed.* **2002**, *41*, 4632.

(63) Allingham, J. S.; Zampella, A.; D'Auria, M. V.; Rayment, I. *Proc. Natl. Acad. Sci. USA* **2005**, *102*, 14527.

(64) D'Auria, M. V.; Paloma, L. G.; Minale, L.; Zampella, A.; Verbist, J.-F.; Roussakis, C.; Debitus, C.; Patissou, J. *Tetrahedron* **1994**, *50*, 4829.

(65) Patterson, G. M. L.; Smith, C. D.; Kimura, L. H.; Britton, B. A.; Carmeli, S. *Cell Motil. Cytoskeleton* **1993**, *24*, 39.

(66) Kernan, M. R.; Faulkner, D. J. *Tetrahedron Lett.* **1987**, *28*, 2809.

(67) Matsunaga, S.; Fusetani, N.; Hashimoto, K.; Koseki, K.; Noma, M.; Noguchi, H.; Sankawa, U. *J. Org. Chem.* **1989**, *54*, 1360.

(68) Sasse, F.; Steinmetz, H.; Höfle, G.; Reichenbach, H. *J. Antibiot.* **1993**, *46*, 741.

(69) Hagelueken, G.; Albrecht, S. C.; Steinmetz, H.; Jansen, R.; Heinz, D. W.; Kalesse, M.; Schubert, W.-D. *Angew. Chem. Int. Ed.* **2009**, *48*, 595.

(70) Kitamura, M.; Schupp, P. J.; Nakano, Y.; Uemura, D. *Tetrahedron Lett.* **2009**, *50*, 6606.

(71) Kigoshi, H.; Suenaga, K.; Takagi, M.; Akao, A.; Kanematsu, K.; Kamei, N.; Okugawa, Y.; Yamada, K. *Tetrahedron* **2002**, *58*, 1075.

(72) Suenaga, K.; Kamei, N.; Okugawa, Y.; Takagi, M.; Akao, A.; Kigoshi, H.; Yamada, K. *Bioorg. Med. Chem. Lett.* **1997**, *7*, 269.

(73) Perrins, R. D.; Cecere, G.; Paterson, I.; Marriott, G. *Chem. Biol.* **2008**, *15*, 287.

(74) Pereira, J. H.; Petchprayoon, C.; Hoepker, A. C.; Moriarty, N. W.; Fink, S. J.; Cecere, G.; Paterson, I.; Adams, P. D.; Marriott, G. *ChemMedChem* **2014**, *9*, 2286.

(75) Hirata, K.; Muraoka, S.; Suenaga, K.; Kuroda, T.; Kato, K.; Tanaka, H.; Yamamoto, M.; Takata, M.; Yamada, K.; Kigoshi, H. *J. Mol. Biol.* **2006**, *356*, 945.

(76) Allingham, J. S.; Tanaka, J.; Marriott, G.; Rayment, I. *Org. Lett.* **2004**, *6*, 597.

(77) Klenchin, V. A.; Allingham, J. S.; King, R.; Tanaka, J.; Marriott, G.; Rayment, I. *Nat. Struct. Biol.* **2003**, *10*, 1058.

(78) McLaughlin, P. J.; Gooch, J. T.; Mannherz, H.-G.; Weeds, A. G. *Nature* **1993**, *364*, 685.

(79) Kobayashi, K.; Fujii, Y.; Hirayama, Y.; Kobayashi, S.; Hayakawa, I.; Kigoshi, H. *Org. Lett.* **2012**, *14*, 1290.

(80) Kuroda, T.; Suenaga, K.; Sakakura, A.; Handa, T.; Okamoto, K.; Kigoshi, H. *Bioconjug. Chem.* **2006**, *17*, 524.

(81) Kita, M.; Yoneda, K.; Hirayama, Y.; Yamagishi, K.; Saito, Y.; Sugiyama, Y.; Miwa, Y.; Ohno, O.; Morita, M.; Suenaga, K.; Kigoshi, H. *ChemBioChem* **2012**, *13*, 1754.

(82) Kita, M.; Hirayama, Y.; Yoneda, K.; Yamagishi, K.; Chinen, T.; Usui, T.; Sumiya, E.; Uesugi, M.; Kigoshi, H. *J. Am. Chem. Soc.* **2013**, *135*, 18089.

(83) Hirayama, Y.; Yamagishi, K.; Suzuki, T.; Kawagishi, H.; Kita, M.; Kigoshi, H. *Bioorg. Med. Chem.* **2016**, *24*, 2809.

(84) Jordan, M. A.; Thrower, D.; Wilson, L. *Cancer Res.* **1991**, *51*, 2212.

(85) Jordan, M. A.; Wendell, K.; Gardiner, S.; Brent Derry, W.; Copp, H.; Wilson, L. *Cancer Res.* **1996**, *56*, 816.

(86) Field, J. J.; Kanakkanthara, A.; Miller, J. H. *Bioorg. Med. Chem.* **2014**, *22*, 5050.

(87) van Vuuren, R. J.; Visagie, M. H.; Theron, A. E.; Joubert, A. M. *Cancer Chemother. Pharmacol.* **2015**, *76*, 1101.

(88) Penna, L. S.; Henriques, J. A. P.; Bonatto, D. *Pharmacol. Ther.* **2017**, *173*, 67.

(89) Senter, P. D.; Sievers, E. L. *Nat. Biotechnol.* **2012**, *30*, 631.

(90) Erickson, H. K.; Park, P. U.; Widdison, W. C.; Kovtun, Y. V.; Garrett, L. M.; Hoffman, K.; Lutz, R. J.; Goldmacher, V. S.; Blättler, W. A. *Cancer Res.* **2006**, *66*, 4426.

(91) Beck, A.; Goetsch, L.; Dumontet, C.; Corvaïa, N. *Nat. Rev. Drug Discov.* **2017**, *16*, 315.

(92) Prashad, A. S.; Nolting, B.; Patel, V.; Xu, A.; Arve, B.; Letendre, L. *Org. Process Res. Dev.* **2017**, *21*, 590.

(93) Wang, Y.-J.; Li, Y.-Y.; Liu, X.-Y.; Lu, X.-L.; Cao, X.; Jiao, B.-H. *Mar. Drugs* **2017**, *15*, 18.

(94) Lu, J.; Jiang, F.; Lu, A.; Zhang, G. *Int. J. Mol. Sci.* **2016**, *17*, 561.

(95) Loganzo, F.; Sung, M.; Gerber, H.-P. *Mol. Cancer Ther.* **2016**, *15*, 2825.

(96) Gébleux, R.; Casi, G. *Pharmacol. Ther.* **2016**, *167*, 48.

(97) Newman, D.; Cragg, G. *Planta Med.* **2016**, *82*, 775.

(98) Peters, C.; Brown, S. *Biosci. Rep.* **2015**, *35*, e00225.

(99) Jain, N.; Smith, S. W.; Ghone, S.; Tomczuk, B. *Pharm. Res.* **2015**, *32*, 3526.

(100) Chari, R. V. J.; Miller, M. L.; Widdison, W. C. *Angew. Chem. Int. Ed.* **2014**, *53*, 3796.

(101) Flygare, J. A.; Pillow, T. H.; Aristoff, P. *Chem. Biol. Drug Des.* **2013**, *81*, 113.

(102) Gerber, H.-P.; Koehn, F. E.; Abraham, R. T. *Nat. Prod. Rep.* **2013**, *30*, 625.

(103) Kovtun, Y. V.; Goldmacher, V. S. *Cancer Lett.* **2007**, *255*, 232.

(104) Lyon, R. P.; Bovee, T. D.; Doronina, S. O.; Burke, P. J.; Hunter, J. H.; Neff-LaFord, H. D.; Jonas, M.; Anderson, M. E.; Setter, J. R.; Senter, P. D. *Nat. Biotechnol.* **2015**, *33*, 733.

(105) Lin, K.; Tibbitts, J. *Pharm. Res.* **2012**, *29*, 2354.

(106) Thompson, P.; Bezabeh, B.; Fleming, R.; Pruitt, M.; Mao, S.; Strout, P.; Chen, C.; Cho, S.; Zhong, H.; Wu, H.; Gao, C.; Dimasi, N. *Bioconjug. Chem.* **2015**, *26*, 2085.

(107) Drake, P. M.; Rabuka, D. *Curr. Opin. Chem. Biol.* **2015**, *28*, 174.

(108) Paterson, I.; Fink, S. J.; Lee, L. Y. W.; Atkinson, S. J.; Blakey, S. B. *Org. Lett.* **2013**, *15*, 3118.

(109) Paterson, I.; Cowden, C. J.; Woodrow, M. D. *Tetrahedron Lett.* **1998**, *39*, 6037.

(110) Paterson, I.; Woodrow, M. D.; Cowden, C. J. *Tetrahedron Lett.* **1998**, *39*, 6041.

(111) Williams, S. *PhD thesis*, University of Cambridge, 2015.

(112) Hayakawa, I.; Saito, K.; Matsumoto, S.; Kobayashi, S.; Taniguchi, A.; Kobayashi, K.; Fujii, Y.; Kaneko, T.; Kigoshi, H. *Org. Biomol. Chem.* **2017**, *15*, 124.
(113) Kobayashi, K.; Fujii, Y.; Hayakawa, I.; Kigoshi, H. *Org. Lett.* **2011**, *13*, 900.
(114) Marshall, J. A.; Johns, B. A. *J. Org. Chem.* **2000**, *65*, 1501.
(115) Calter, M. A.; Guo, X. *Tetrahedron* **2002**, *58*, 7093.
(116) Calter, M. A.; Zhou, J. *Tetrahedron Lett.* **2004**, *45*, 4847.
(117) El-Awa, A.; Fuchs, P. *Org. Lett.* **2006**, *8*, 2905.
(118) Noshi, M. N.; El-Awa, A.; Torres, E.; Fuchs, P. L. *J. Am. Chem. Soc.* **2007**, *129*, 11242.
(119) Hong, W. P.; Noshi, M. N.; El-Awa, A.; Fuchs, P. L. *Org. Lett.* **2011**, *13*, 6342.
(120) Evans, D. A.; Ennis, M. D.; Mathre, D. J. *J. Am. Chem. Soc.* **1982**, *104*, 1737.
(121) Evans, D. A.; Bartroli, J.; Shih, T. L. *J. Am. Chem. Soc.* **1981**, *103*, 2127.
(122) Wadsworth, W. S.; Emmons, W. D. *J. Am. Chem. Soc.* **1961**, *83*, 1733.
(123) Katsuki, T.; Sharpless, K. B. *J. Am. Chem. Soc.* **1980**, *102*, 5974.
(124) Julia, M.; Paris, J.-M. *Tetrahedron Lett.* **1973**, *14*, 4833.
(125) Hikota, M.; Sakurai, Y.; Horita, K.; Yonemitsu, O. *Tetrahedron Lett.* **1990**, *31*, 6367.
(126) Kiefel, M. J.; Maddock, J.; Pattenden, G. *Tetrahedron Lett.* **1992**, *33*, 3227.
(127) Boden, E. P.; Keck, G. E. *J. Org. Chem.* **1985**, *50*, 2394.
(128) Marshall, J. A.; Grant, C. M. *J. Org. Chem.* **1999**, *64*, 696.
(129) Marshall, J. A.; Johns, B. A. *J. Org. Chem.* **1998**, *63*, 7885.
(130) Comins, D. L.; Dehghani, A. *Tetrahedron Lett.* **1992**, *33*, 6299.
(131) Anh, N. T. *Organic Chemistry Syntheses and Reactivity*, Springer, 1980, pp 145–162.
(132) Gilbert, J. C.; Weerasooriya, U. *J. Org. Chem.* **1979**, *44*, 4997.
(133) Calter, M. A.; Orr, R. K.; Song, W. *Org. Lett.* **2003**, *5*, 4745.
(134) Calter, M. A. *J. Org. Chem.* **1996**, *61*, 8006.
(135) Calter, M. A.; Guo, X.; Liao, W. *Org. Lett.* **2001**, *3*, 1499.
(136) Bobinski, T. P.; Fuchs, P. L. *Tetrahedron Lett.* **2015**, *56*, 4155.
(137) Jacobsen, E.; Zhang, W.; Muci, A. R.; Ecker, J. R.; Deng, L. *J. Am. Chem. Soc.* **1991**, *113*, 7063.
(138) Torres, E.; Chen, Y.; Kim, I. C.; Fuchs, P. L. *Angew. Chem. Int. Ed.* **2003**, *42*, 3124.
(139) Brocchini, S. J.; Eberle, M.; Lawton, R. G. *J. Am. Chem. Soc.* **1988**, *110*, 5211.
(140) Wan, Z.-K.; Choi, H.; Kang, F.-A.; Nakajima, K.; Demeke, D.; Kishi, Y. *Org. Lett.* **2002**, *4*, 4431.
(141) Müller, S.; Liepold, B.; Roth, G. J.; Bestmann, H. J. *Synlett* **1996**, *1996*, 521.
(142) Abo, M.; Mori, K. *Biosci. Biotechnol. Biochem.* **1993**, *57*, 265.
(143) Roush, W. R.; Palkowitz, A. D.; Ando, K. *J. Am. Chem. Soc.* **1990**, *112*, 6348.
(144) Paterson, I.; Tillyer, R. D. *Tetrahedron Lett.* **1992**, *33*, 4233.
(145) Evans, D. A.; Chapman, K. T.; Carreira, E. M. *J. Am. Chem. Soc.* **1988**, *110*, 3560.
(146) Saksena, A. K.; Mangiaracina, P. *Tetrahedron Lett.* **1983**, *24*, 273.

(147) Takai, K.; Nitta, K.; Utimoto, K. *J. Am. Chem. Soc.* **1986**, *108*, 7408.
(148) Paterson, I.; Blakey, S. B.; Cowden, C. J. *Tetrahedron Lett.* **2002**, *43*, 6005.
(149) Woodrow, M. *PhD thesis*, University of Cambridge, 1998.
(150) Paterson, I.; Yeung, K.-S.; Smaill, J. B. *Synlett* **1993**, *1993*, 774.
(151) Grieco, P. A.; Pogonowski, C. S. *J. Am. Chem. Soc.* **1973**, *95*, 3071.
(152) Rychnovsky, S. D.; Kim, J. *J. Org. Chem.* **1994**, *59*, 2659.
(153) Corey, E. J.; Bakshi, R. K.; Shibata, S. *J. Am. Chem. Soc.* **1987**, *109*, 5551.
(154) Weissman, K. J. *Beilstein J. Org. Chem.* **2017**, *13*, 348.
(155) Zimmerman, H. E.; Traxler, M. D. *J. Am. Chem. Soc.* **1957**, *79*, 1920.
(156) Evans, D. A.; Vogel, E.; Nelson, J. V. *J. Am. Chem. Soc.* **1979**, *101*, 6120.
(157) Paterson, I.; Findlay, A. D.; Noti, C. *Chem. Asian J.* **2009**, *4*, 594.
(158) Paterson, I.; Davies, R. D. M.; Heimann, A. C.; Marquez, R.; Meyer, A. *Org. Lett.* **2003**, *5*, 4477.
(159) Paton, R. S.; Goodman, J. M. *J. Org. Chem.* **2008**, *73*, 1253.
(160) Goodman, J. M.; Paton, R. S. *Chem. Commun.* **2007**, No. 21, 2124.
(161) Evans, D. A.; Hoveyda, A. H. *J. Am. Chem. Soc.* **1990**, *112*, 6447.
(162) Lee, L. Y. W. *PhD thesis*, University of Cambridge, 2010.
(163) Kashem, A.; Anisuzzaman, M.; Whistler, R. L. *Carbohydr. Res.* **1978**, *61*, 511.
(164) Paterson, I.; Cowden, C. J.; Rahn, V. S.; Woodrow, M. D. *Synlett* **1998**, *1998*, 915.
(165) Dess, D. B.; Martin, J. C. *J. Org. Chem.* **1983**, *48*, 4155.
(166) Mohr, P.; Tori, M.; Grossen, P.; Herold, P.; Tamm, C. *Helv. Chim. Acta* **1982**, *65*, 1412.
(167) Corey, E. J.; Kwiatkowski, G. T. *J. Am. Chem. Soc.* **1966**, *88*, 5654.
(168) Corey, E. J.; Bakshi, R. K.; Shibata, S.; Chen, C. P.; Singh, V. K. *J. Am. Chem. Soc.* **1987**, *109*, 7925.
(169) Bal, B. S.; Childers, W. E.; Pinnick, H. W. *Tetrahedron* **1981**, *37*, 2091.
(170) Omura, K.; Swern, D. *Tetrahedron* **1978**, *34*, 1651.
(171) Blanchette, M. A.; Choy, W.; Davis, J. T.; Essenfeld, A. P.; Masamune, S.; Roush, W. R.; Sakai, T. *Tetrahedron Lett.* **1984**, *25*, 2183.
(172) Blakey, S. B. *PhD thesis*, University of Cambridge, 2002.
(173) Paterson, I.; Cowden, C.; Watson, C. *Synlett* **1996**, *1996*, 209.
(174) Burgess, E. M.; Penton, H. R.; Taylor, E. A. *J. Org. Chem.* **1973**, *38*, 26.
(175) Mahoney, W. S.; Brestensky, D. M.; Stryker, J. M. *J. Am. Chem. Soc.* **1988**, *110*, 291.
(176) Lee, D.; Yun, J. *Tetrahedron Lett.* **2005**, *46*, 2037.
(177) Fink, S. J. *PhD thesis*, University of Cambridge, 2012.
(178) Kita, M.; Hirayama, Y.; Yamagishi, K.; Yoneda, K.; Fujisawa, R.; Kigoshi, H. *J. Am. Chem. Soc.* **2012**, *134*, 20314.

(179) Paterson, I.; Yeung, K.-S.; Ward, R. A.; Cumming, J. G.; Smith, J. D. *J. Am. Chem. Soc.* **1994**, *116*, 9391.

(180) Nicolaou, K. C.; Ajito, K.; Patron, A. P.; Khatuya, H.; Richter, P. K.; Bertinato, P. *J. Am. Chem. Soc.* **1996**, *118*, 3059.

(181) Paterson, I.; Doughty, V. A.; McLeod, M. D.; Trieselmann, T. *Angew. Chem. Int. Ed.* **2000**, *39*, 1308.

(182) Paterson, I.; Britton, R.; Delgado, O.; Meyer, A.; Poullennec, K. G. *Angew. Chem. Int. Ed.* **2004**, *43*, 4629.

(183) Paterson, I.; Watson, C.; Yeung, K.-S.; Wallace, P. A.; Ward, R. A. *J. Org. Chem.* **1997**, *62*, 452.

(184) Williams, S. *Unpublished results*, University of Cambridge, 2014

(185) Kocienski, P. J. *Protecting Groups*, Thieme, 2005.

(186) Mukaiyama, T.; Iwasawa, N.; Stevens, R. W.; Haga, T. *Tetrahedron* **1984**, *40*, 1381.

(187) Evans, D. A.; Clark, J. S.; Metternich, R.; Novack, V. J.; Sheppard, G. S. *J. Am. Chem. Soc.* **1990**, *112*, 866.

(188) Evans, D. A.; Allison, B. D.; Yang, M. G.; Masse, C. E. *J. Am. Chem. Soc.* **2001**, *123*, 10840.

(189) Hoffmann, R. W. *Chem. Rev.* **1989**, *89*, 1841.

(190) Heathcock, C. H.; Pirrung, M. C.; Sohn, J. E. *J. Org. Chem.* **1979**, *44*, 4294.

(191) Karplus, M. *J. Chem. Phys.* **1959**, *30*, 11.

(192) Karplus, M. *J. Am. Chem. Soc.* **1963**, *85*, 2870.

(193) Dale, J. A.; Mosher, H. S. *J. Am. Chem. Soc.* **1973**, *95*, 512.

(194) Hoye, T. R.; Jeffrey, C. S.; Shao, F. *Nat. Protoc.* **2007**, *2*, 2451.

(195) Evans, D. A.; Rieger, D. L.; Bilodeau, M. T.; Urpi, F. *J. Am. Chem. Soc.* **1991**, *113*, 1047.

(196) Cież, D.; Pałasz, A.; Trzewik, B. *Eur. J. Org. Chem.* **2016**, *2016*, 1476.

(197) Figueras, S.; Martín, R.; Roméa, P.; Urpí, F.; Vilarrasa, J. *Tetrahedron Lett.* **1997**, *38*, 1637.

(198) Esteve, C.; Ferreró, M.; Roméa, P.; Urpí, F.; Vilarrasa, J. *Tetrahedron Lett.* **1999**, *40*, 5079.

(199) Solsona, J. G.; Roméa, P.; Urpí, F.; Vilarrasa, J. *Org. Lett.* **2003**, *5*, 519.

(200) Solsona, J. G.; Nebot, J.; Roméa, P.; Urpí, F. *J. Org. Chem.* **2005**, *70*, 6533.

(201) Gregg, C.; Perkins, M. V. *Tetrahedron* **2013**, *69*, 6845.

(202) Dias, L. C.; Perez, C. C. *Eur. J. Org. Chem.* **2013**, *2013*, 2930.

(203) Miles, W. H.; Jones, S. T.; George, J. S.; Tang, P.-I.; Hayward, M. D. *Tetrahedron Lett.* **2015**, *56*, 2303.

(204) Zambrana, J.; Roméa, P.; Urpí, F.; Luján, C. *J. Org. Chem.* **2011**, *76*, 8575.

(205) Ralston, K.; Hulme, A. *Synthesis* **2012**, *44*, 2310.

(206) Rychnovsky, S. D.; Rogers, B.; Yang, G. *J. Org. Chem.* **1993**, *58*, 3511.

(207) Evans, D. A.; Rieger, D. L.; Gage, J. R. *Tetrahedron Lett.* **1990**, *31*, 7099.

(208) Oikawa, Y.; Yoshioka, T.; Yonemitsu, O. *Tetrahedron Lett.* **1982**, *23*, 889.

(209) Takano, S.; Akiyama, M.; Sato, S.; Ogasawara, K. *Chem. Lett.* **1983**, No. 10, 1593.
(210) Mohr, P.; Tori, M.; Grossen, P.; Herold, P.; Tamm, C. *Helv. Chim. Acta* **1982**, *65*, 1412.
(211) Lam, P.; Hui, R. A. H. F.; Jones, B. *J. Org. Chem.* **1986**, *51*, 2047.
(212) Chen, C. S.; Fujimoto, Y.; Girdaukas, G.; Sih, C. J. *J. Am. Chem. Soc.* **1982**, *104*, 7294.
(213) Poppe, L.; Novák, L.; Kolonits, P.; Bata, Á.; Szántay, C. *Tetrahedron* **1988**, *44*, 1477.
(214) Lehr, K.; Mariz, R.; Leseurre, L.; Gabor, B.; Fürstner, A. *Angew. Chem. Int. Ed.* **2011**, *50*, 11373.
(215) Herold, P.; Mohr, P.; Tamm, C. *Helv. Chim. Acta* **1983**, *66*, 744.
(216) Dossetter, A. G.; Jamison, T. F.; Jacobsen, E. N. *Angew. Chem. Int. Ed.* **1999**, *38*, 2398.
(217) Gademann, K.; Chavez, D. E.; Jacobsen, E. N. *Angew. Chem. Int. Ed.* **2002**, *41*, 3059.
(218) Casiraghi, G.; Casnati, G.; Puglia, G.; Sartori, G.; Terenghi, G. *J. Chem. Soc. Perkin Trans. 1* **1980**, 1862.
(219) Bergbreiter, D. E.; Hobbs, C.; Hongfa, C. *J. Org. Chem.* **2011**, *76*, 523.
(220) Evans, D. A.; Johnson, J. S.; Olhava, E. J. *J. Am. Chem. Soc.* **2000**, *122*, 1635.
(221) Keller, T. H.; Weiler, L. *J. Am. Chem. Soc.* **1990**, *112*, 450.
(222) Harried, S. S.; Yang, G.; Strawn, M. A.; Myles, D. C. *J. Org. Chem.* **1997**, *62*, 6098.
(223) Freeman, P. K.; Hutchinson, L. L. *J. Org. Chem.* **1980**, *45*, 1924.
(224) Crimmins, M. T.; Zuccarello, J. L.; McDougall, P. J.; Ellis, J. M. *Chem. Eur. J.* **2009**, *15*, 9235.
(225) Rodríguez, A.; Nomen, M.; Spur, B. W.; Godfroid, J. J. *Tetrahedron Lett.* **1999**, *40*, 5161.
(226) Horita, K.; Yoshioka, T.; Tanaka, T.; Oikawa, Y.; Yonemitsu, O. *Tetrahedron* **1986**, *42*, 3021.
(227) MacGregor, C. I. *PhD thesis*, University of Cambridge, 2015.
(228) Parenty, A.; Moreau, X.; Campagne, J.-M. *Chem. Rev.* **2006**, *106*, 911.
(229) Shiina, I.; Kubota, M.; Ibuka, R. *Tetrahedron Lett.* **2002**, *43*, 7535.
(230) Paterson, I.; Ashton, K.; Britton, R.; Cecere, G.; Chouraqui, G.; Florence, G. J.; Stafford, J. *Angew. Chem. Int. Ed.* **2007**, *46*, 6167.
(231) Paterson, I.; Ashton, K.; Britton, R.; Cecere, G.; Chouraqui, G.; Florence, G. J.; Knust, H.; Stafford, J. *Chem. Asian J.* **2008**, *3*, 367.
(232) Cergol, K. M.; Coster, M. J. *Nat. Protoc.* **2007**, *2*, 2568.
(233) Parenty, A.; Moreau, X.; Niel, G.; Campagne, J.-M. *Chem. Rev.* **2013**, *113*, PR1.
(234) Evans, D. A.; Nagorny, P.; McRae, K. J.; Sonntag, L. S.; Reynolds, D. J.; Vounatsos, F. *Angew. Chem. Int. Ed.* **2007**, *46*, 545.
(235) Staben, L. R.; Koenig, S. G.; Lehar, S. M.; Vandlen, R.; Zhang, D.; Chuh, J.; Yu, S.-F.; Ng, C.; Guo, J.; Liu, Y.; Fourie-O'Donohue, A.; Go, M.; Linghu, X.; Segraves, N. L.; Wang, T.; Chen, J.; Wei, B.; Phillips, G. D. L.; Xu, K.; Kozak, K. R.; Mariathasan, S.; Flygare, J. A.; Pillow, T. H. *Nat. Chem.* **2016**.
(236) Girard, P.; Namy, J. L.; Kagan, H. B. *J. Am. Chem. Soc.* **1980**, *102*, 2693.
(237) Imamoto, T.; Ono, M. *Chem. Lett.* **1987**, *16*, 501.

(238) Adkins, H.; Billica, H. R. *J. Am. Chem. Soc.* **1948**, *70*, 695.

(239) Ireland, R. E.; Liu, L. *J. Org. Chem.* **1993**, *58*, 2899.

(240) Hart, D. J.; Kanai, K.; Thomas, D. G.; Yang, T. K. *J. Org. Chem.* **1983**, *48*, 289.

(241) Denmark, S. E.; Fujimori, S. *Org. Lett.* **2002**, *4*, 3473.

(242) Kretschmer, M.; Dieckmann, M.; Li, P.; Rudolph, S.; Herkommer, D.; Troendlin, J.; Menche, D. *Chem. Eur. J.* **2013**, *19*, 15993.

(243) Dieckmann, M.; Menche, D. *Org. Lett.* **2013**, *15*, 228.

(244) Paterson, I.; Anne Lister, M. *Tetrahedron Lett.* **1988**, *29*, 585.

(245) Liu, X.; Lee, C.-S. *Org. Lett.* **2012**, *14*, 2886.

Appendix

Selected ^{1}H and ^{13}C NMR spectra

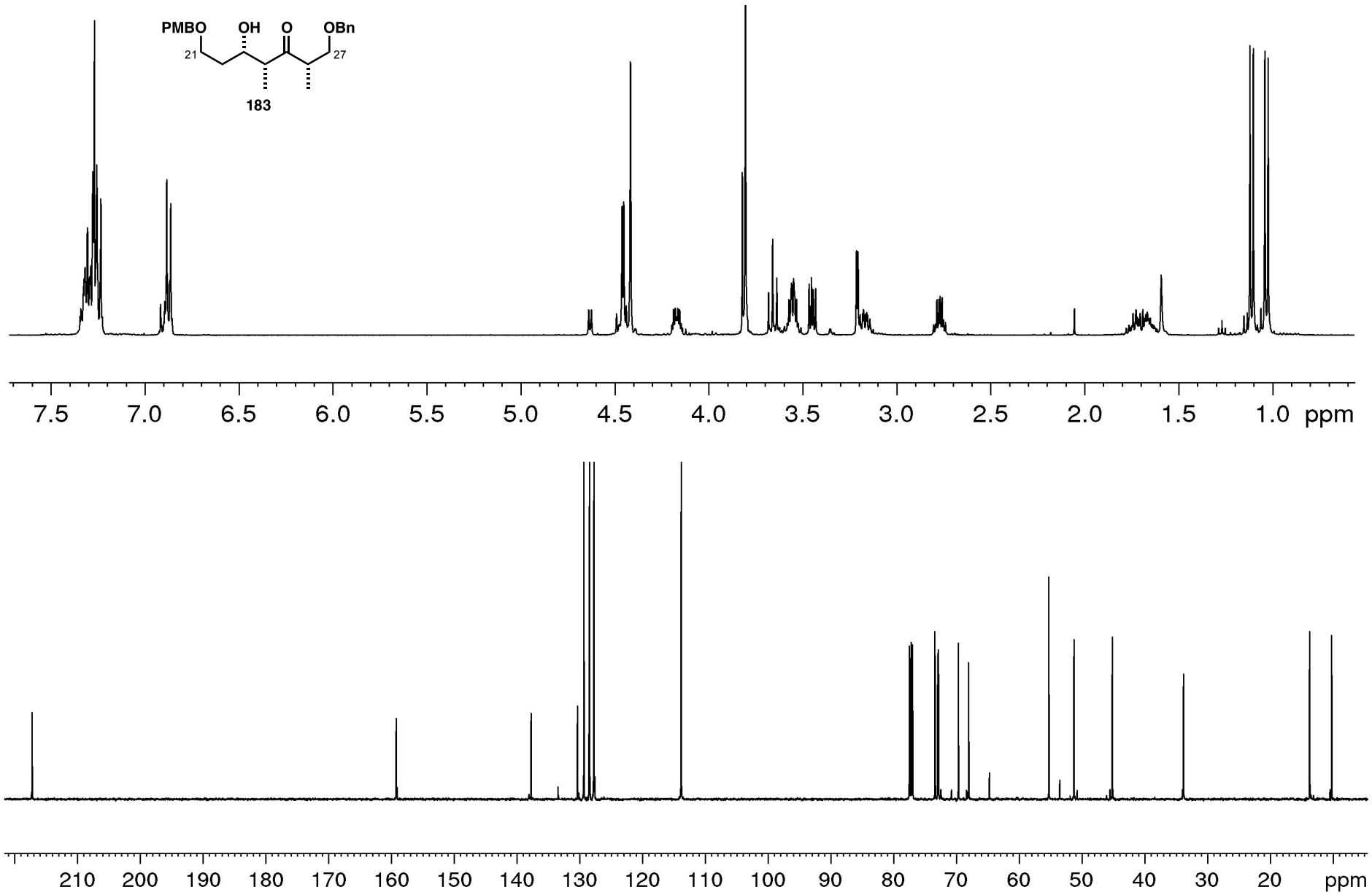
PMBO
OH
O
OBn
21
27
183
7.5
7.0
6.5
6.0
5.5
5.0
4.5
4.0
3.5
3.0
2.5
2.0
1.5
1.0
ppm
210
200
190
180
170
160
150
140
130
120
110
100
90
80
70
60
50
40
30
20
ppm

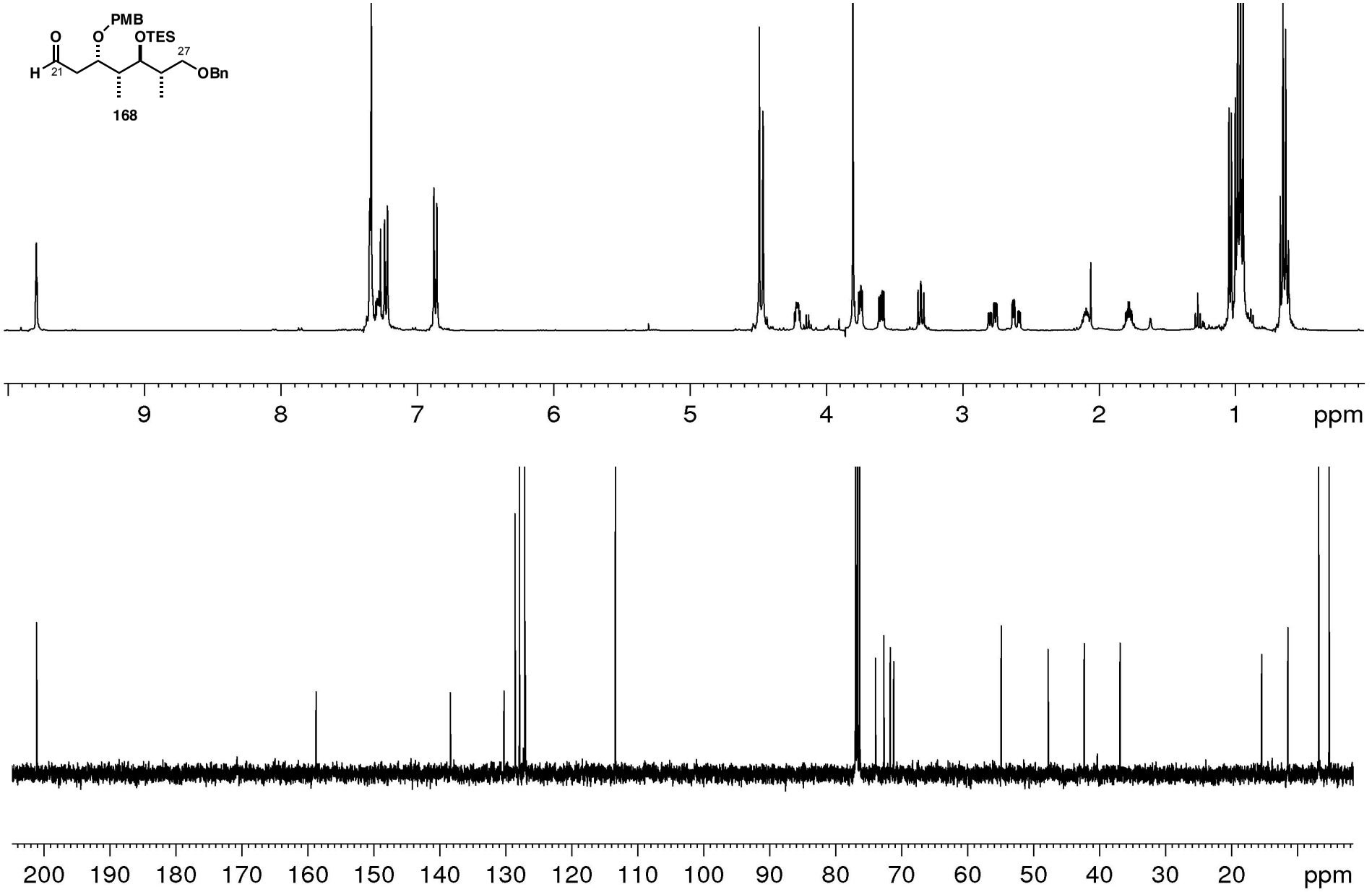
PMB
O
O
OTES
27
H
21
OBn
168
9
8
7
6
5
4
3
2
1
ppm
200
190
180
170
160
150
140
130
120
110
100
90
80
70
60
50
40
30
20
ppm

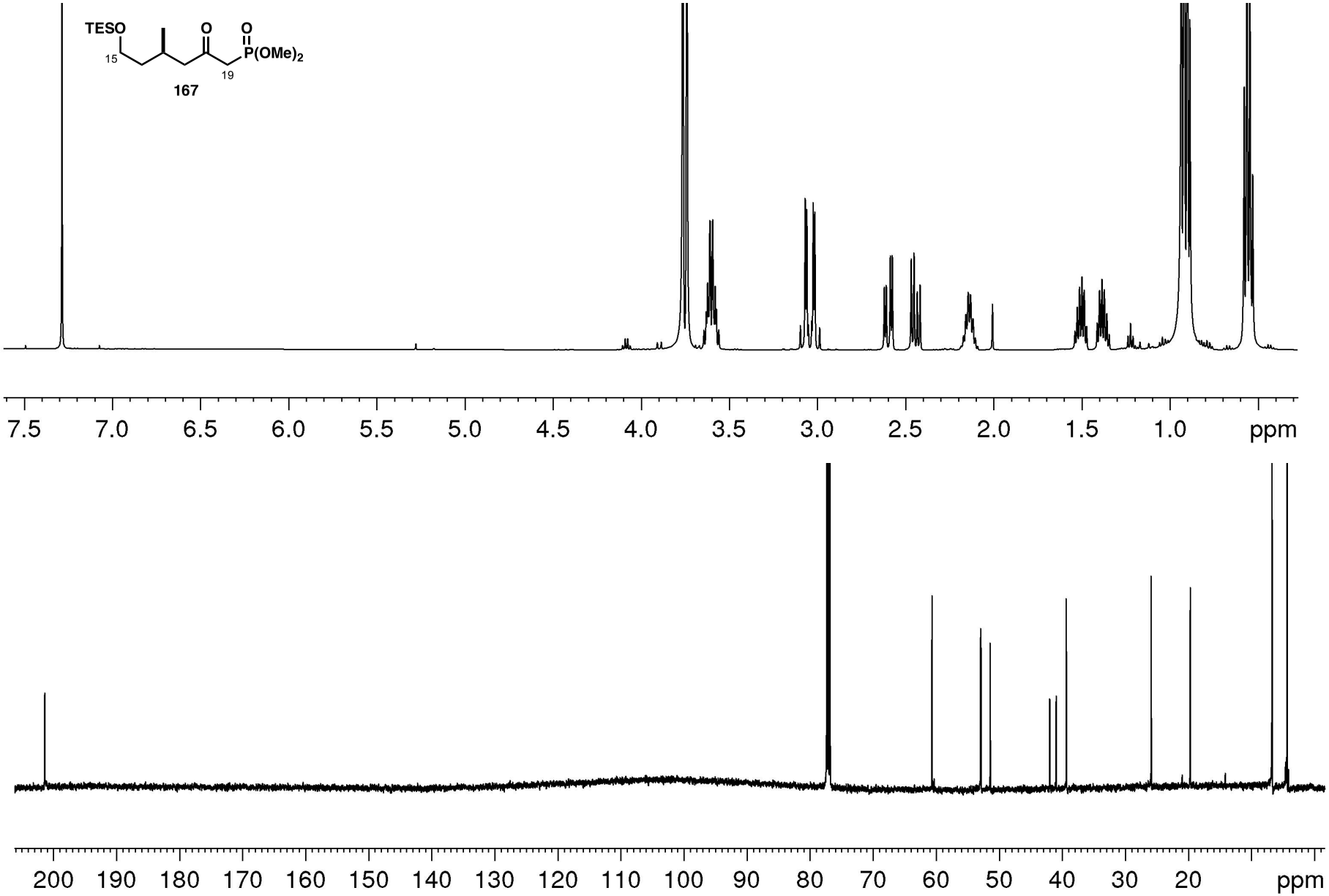
TESO
O
O
P(OMe)2
15
19
167
7.5
7.0
6.5
6.0
5.5
5.0
4.5
4.0
3.5
3.0
2.5
2.0
1.5
1.0
ppm
200
190
180
170
160
150
140
130
120
110
100
90
80
70
60
50
40
30
20
ppm

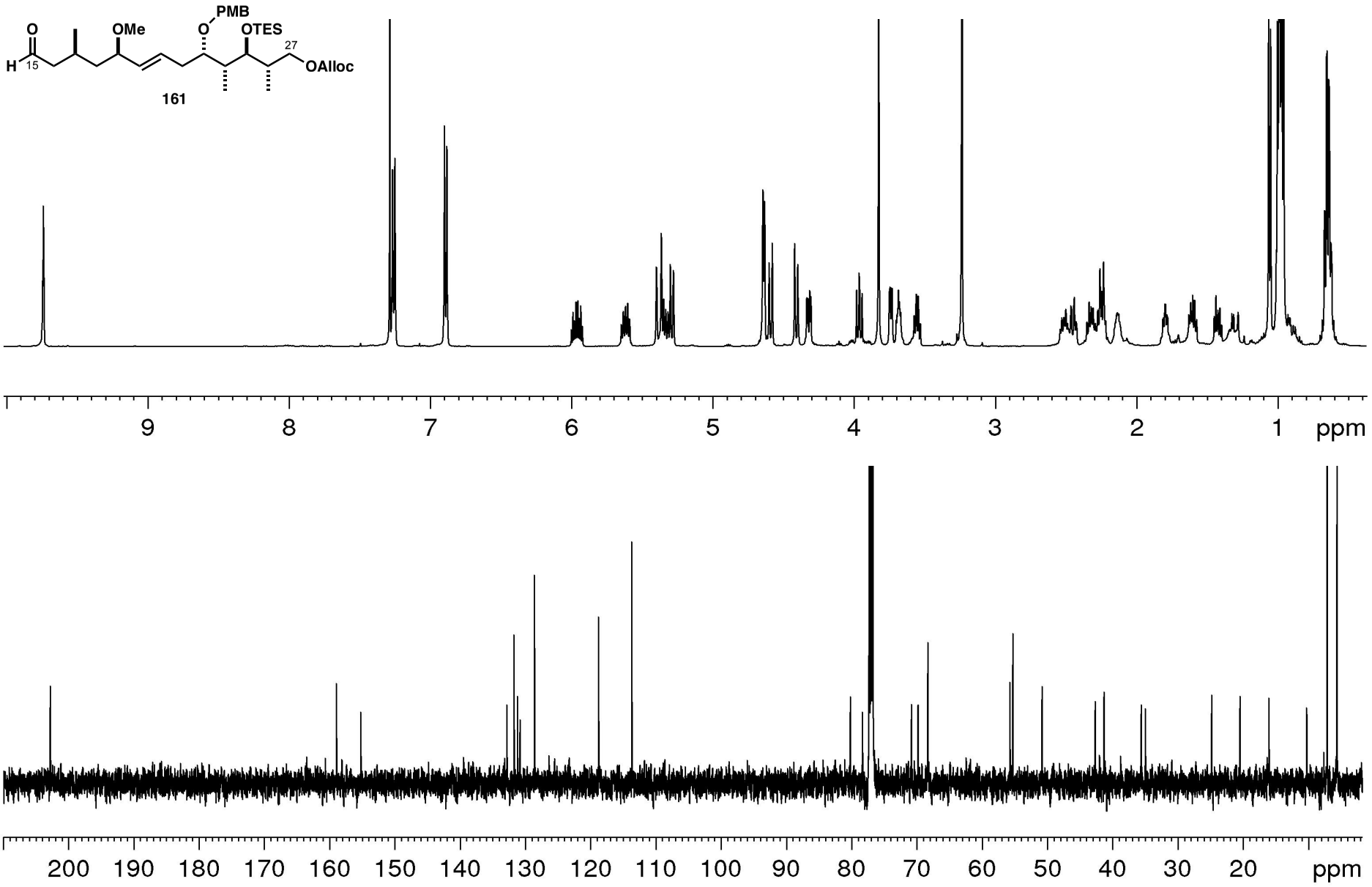
PMB
O
OMe
O
OTES
27
H 15
OAlloc
161
9
8
7
6
5
4
3
2
1
ppm
200
190
180
170
160
150
140
130
120
110
100
90
80
70
60
50
40
30
20
ppm

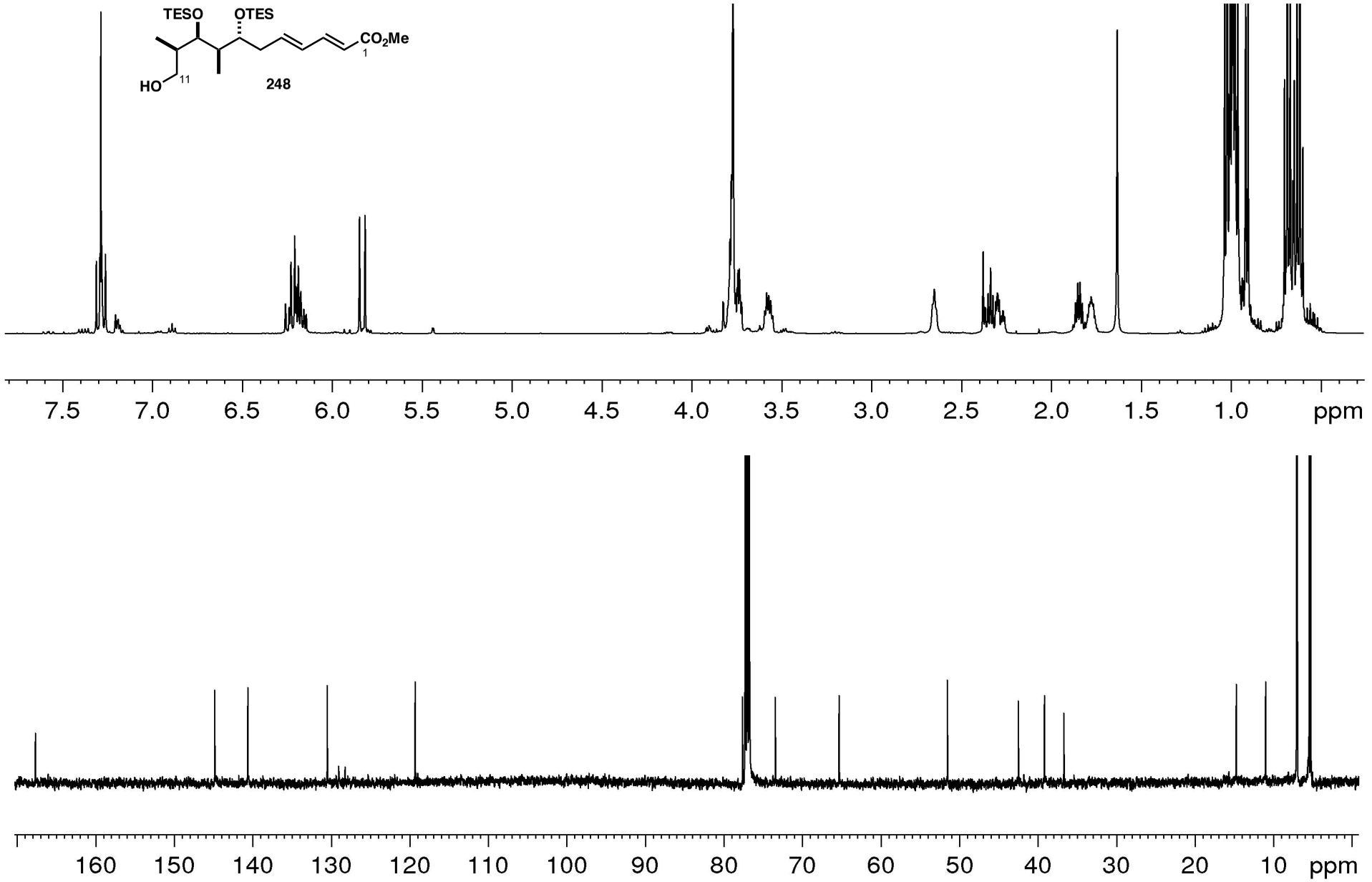
TESO
OTES
CO2Me
1
HO
11
248
7.5
7.0
6.5
6.0
5.5
5.0
4.5
4.0
3.5
3.0
2.5
2.0
1.5
1.0
ppm
160
150
140
130
120
110
100
90
80
70
60
50
40
30
20
10
ppm

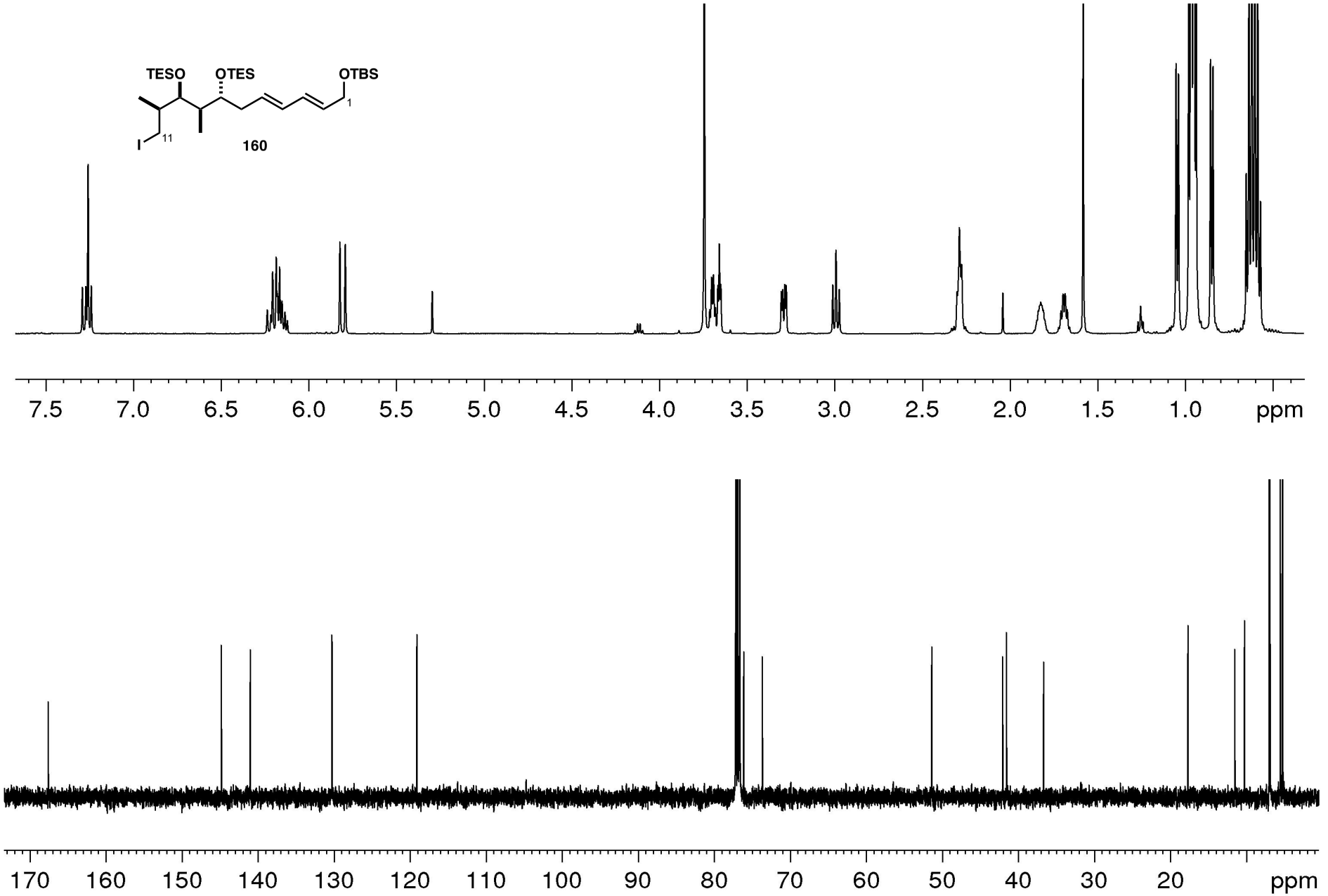
TESO
OTES
OTBS
1
I
11
160
7.5
7.0
6.5
6.0
5.5
5.0
4.5
4.0
3.5
3.0
2.5
2.0
1.5
1.0
ppm
170
160
150
140
130
120
110
100
90
80
70
60
50
40
30
20
ppm

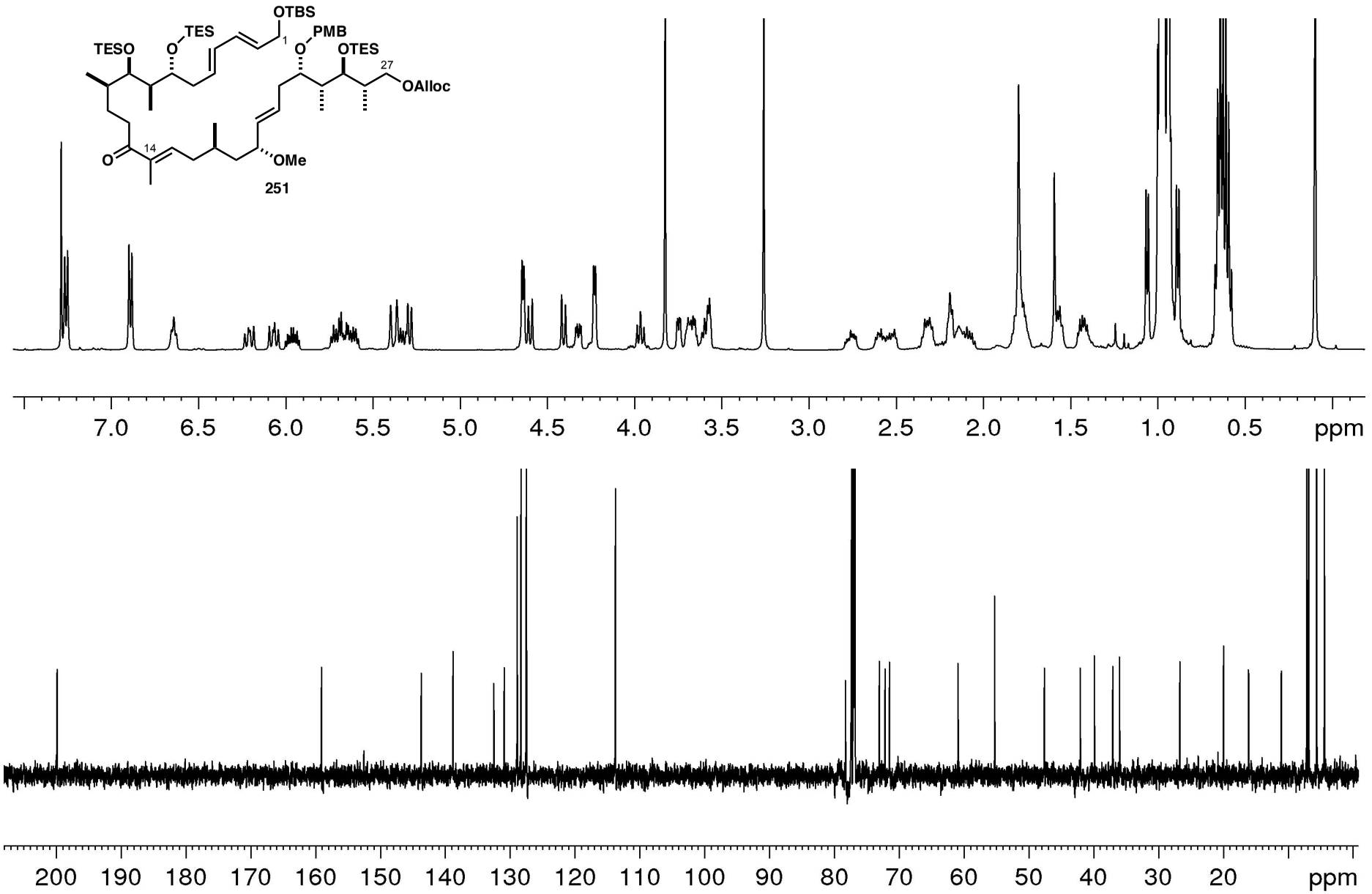
OTBS
TES
PMB
TESO
O
O
OTES
1
27
OAlloc
14
O
OMe
251
7.0
6.5
6.0
5.5
5.0
4.5
4.0
3.5
3.0
2.5
2.0
1.5
1.0
0.5
ppm
200
190
180
170
160
150
140
130
120
110
100
90
80
70
60
50
40
30
20
ppm

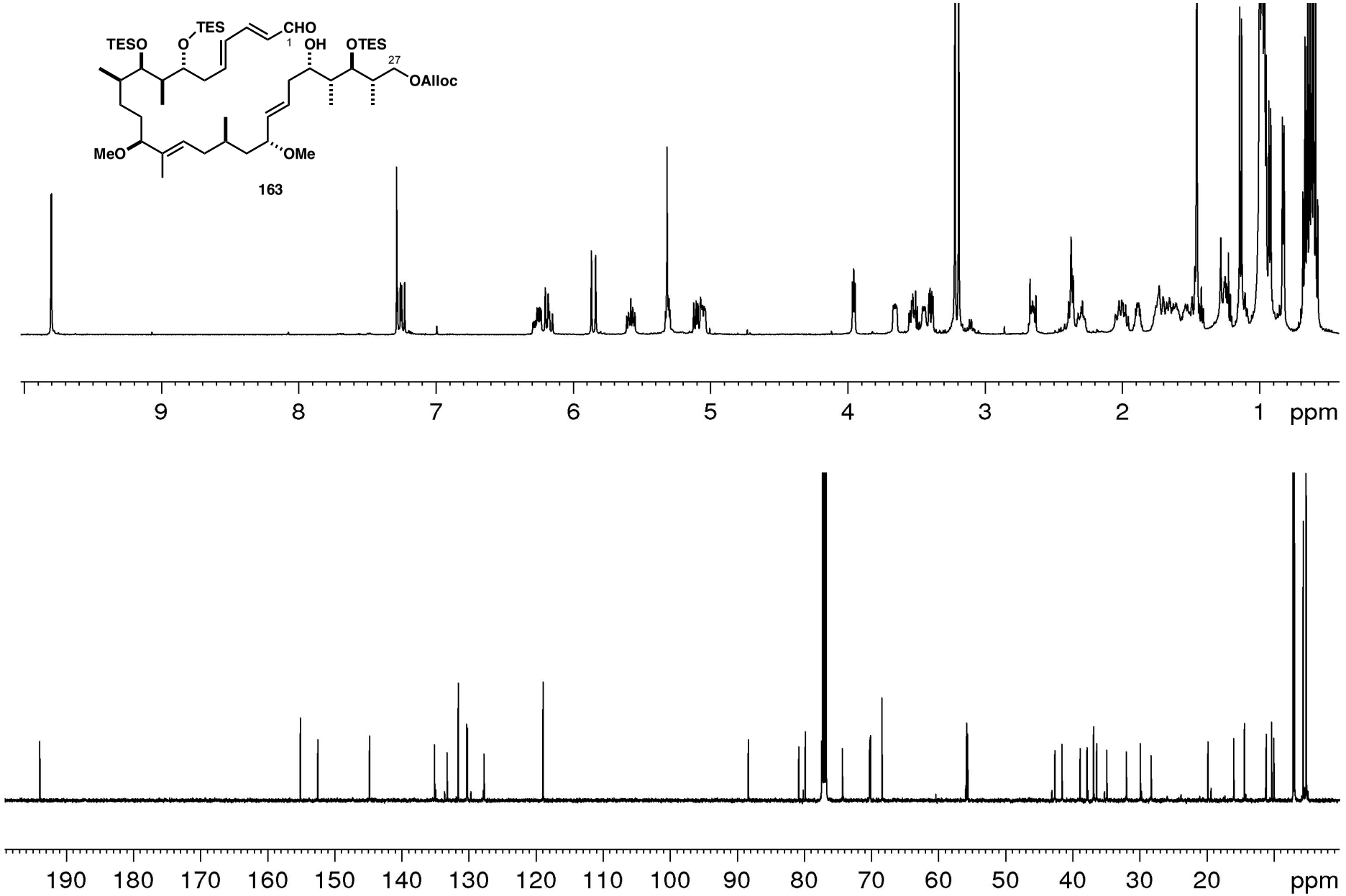
TESO
O
TES
CHO
1
OH
OTES
27
OAlloc
MeO
OMe
163
9
8
7
6
5
4
3
2
1
ppm
190
180
170
160
150
140
130
120
110
100
90
80
70
60
50
40
30
20
ppm

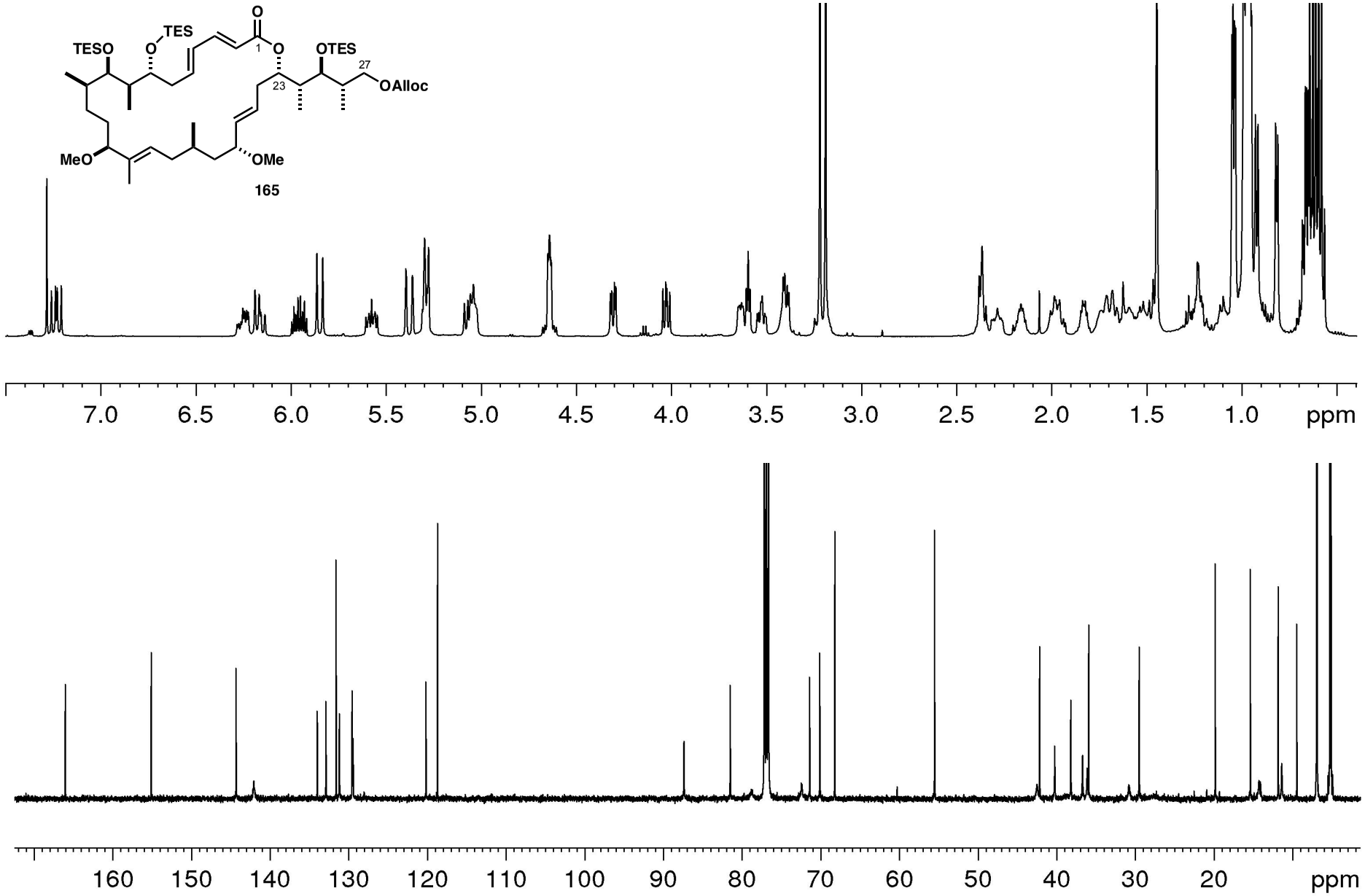
TESO
O
TES
O
1
O
OTES
27
OAlloc
23
MeO
OMe
165
7.0
6.5
6.0
5.5
5.0
4.5
4.0
3.5
3.0
2.5
2.0
1.5
1.0
ppm
160
150
140
130
120
110
100
90
80
70
60
50
40
30
20
ppm